

A Thesis Submitted for the Degree of PhD at the University of Warwick

Permanent WRAP URL:

<http://wrap.warwick.ac.uk/88594>

Copyright and reuse:

This thesis is made available online and is protected by original copyright.

Please scroll down to view the document itself.

Please refer to the repository record for this item for information to help you to cite it.

Our policy information is available from the repository home page.

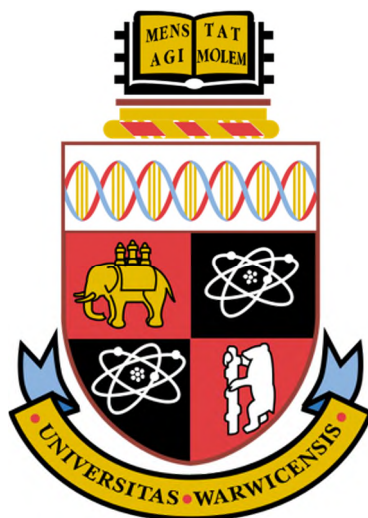
For more information, please contact the WRAP Team at: wrap@warwick.ac.uk

***Polymer synthesis and conjugation
strategies for enhancing the stability of
oxytocin***

Jennifer Collins

***A thesis submitted in partial fulfilment of the requirements for
the degree of***

Doctor of Philosophy in Chemistry



Department of Chemistry

University of Warwick

September 2016

Table of Contents

Table of Contents.....	i
Acknowledgments	ix
Declaration	xii
List of Figures	xiii
List of Schemes.....	xxi
List of Tables.....	xxiii
Abbreviations	xxv
Abstract.....	xxviii
1. Introduction	1
1.1. Oxytocin.....	2
1.1.1. Oxytocin relation of maternal mortality	2
1.1.2. Oxytocin for uterotonic activity	3
1.1.3. Degradation of oxytocin formulations	4
1.1.4. Current solutions for stabilising oxytocin	5
1.1.4.1. Oxytocin analogues: carbetocin and desamino-oxytocin.....	5
1.1.4.2. Disulfide bond engineering on oxytocin.....	6
1.1.4.3. Storage buffers containing metal ions.....	8
1.1.4.4. Dry powder formulations.....	9
1.1.4.5. Previous oxytocin conjugation strategies.....	10
1.2. Site-selective protein/peptide conjugation strategies.....	11
1.2.1. PEGylation	11
1.2.1.1. Current FDA approved PEG conjugates.....	12
1.2.2. Amine targeting strategies.....	14
1.2.2.1. N-Hydroxysuccinimidyl esters (NHS)	15

1.2.2.2. Aldehyde.....	16
1.2.2.3. Carboxylic acid.....	16
1.2.2.4. Other amine reactive groups.....	17
1.2.3. Thiol targeting strategies	17
1.2.3.1. N-Substituted maleimide reagents	18
1.2.3.1. 'Thiol-ene'	19
1.2.3.2. Pyridyl disulfide	19
1.2.4. Disulfide bridging chemistry.....	20
1.2.4.1. Dibromo/dithiophenolmaleimide two-carbon disulfide bridging.....	20
1.2.4.1. Arsenic compounds for disulfide bridging.....	21
1.2.4.2. Vinyl sulfone conjugation/bis-sulfone three-carbon disulfide bridging	22
1.2.5. Other site specific targeting strategies	23
1.3. Reversible-Deactivation Radical Polymerisations techniques (RDRP)	24
1.3.1. Nitroxide mediated polymerisation (NMP)	25
1.3.2. Reversible addition-fragmentation chain-transfer polymerisation (RAFT)	26
1.3.3. Copper mediated polymerisation techniques.....	27
1.3.3.1. Atom transfer radical polymerisation (ATRP)	28
1.3.3.2. SET-LRP – Cu(0) mediated polymerisation.....	29
1.3.3.3. Aqueous Cu(0) mediated polymerisation.....	30
1.4. Controlled radical polymerisations and conjugation chemistry	31
1.4.1. 'Grafting-to'	31
1.4.1.1. Amino targeting.....	32
1.4.1.2. Thiol targeting.....	33
1.4.2. 'Grafting-from'	34
1.5. References	35
2. Amine targeted PEGylation of oxytocin.....	45
2.1. Introduction	46

2.2. Results & Discussion	48
2.2.1. Activated ester linear PEGylation	48
2.2.1.1. Oxytocin conjugation using succinimidyl ester PEG	49
2.2.2. Aldehyde functional linear PEG conjugation.....	52
2.2.2.1. Oxytocin conjugation using aldehyde functional PEG	54
2.2.3. PolyPEGylation strategies	56
2.2.3.1. Activated ester polymer synthesis	57
2.2.3.2. Activated ester functional polymer conjugation.....	61
2.2.3.3. Protected aldehyde polymer synthesis.....	65
2.2.3.4. Aldehyde functional polymer conjugation	72
2.2.4. Potential reversible Schiff base conjugation of oxytocin.....	74
2.2.4.1. Linear PEG reversible conjugation	74
2.2.4.2. Investigation of conjugation with model small aldehydes	77
2.2.4.3. PolyPEG reversible conjugation	89
2.2.5. Reversibility studies of oxytocin Schiff base conjugates	90
2.2.5.1. Butyraldehyde Schiff base conjugate reversibility	91
2.2.5.2. Linear PEG Schiff base conjugate reversibility	92
2.2.5.3. PolyPEG Schiff base conjugate reversibility	95
2.3. Chapter 2 Conclusions.....	96
2.4. Experimental	97
2.4.1. Materials.....	97
2.4.2. Instrumentation & Analysis.....	98
2.4.3. Synthetic procedures for chapter 2.....	100
2.4.3.1. NHS ester linear PEG conjugation onto oxytocin.....	100
2.4.3.2. Aldehyde linear PEG conjugation onto oxytocin.....	100
2.4.3.3. Synthesis of N-hydroxysuccinimide-2-bromo-2-methylpropionate ...	101
2.4.3.4. Cu(0) mediated NHS ester α -functional poly(mPEGA ₄₈₀) synthesis....	101

2.4.3.5. Synthesis of 2-(2,2-dimethoxyethoxy)ethyl-2-bromo-2-methylpropionate.....	102
2.4.3.6. Cu(0) mediated protected α -aldehyde poly(mPEGA ₄₈₀) synthesis	103
2.4.3.7. Deprotection of acetal α -end group	104
2.4.3.8. NHS ester α -functional poly(mPEGA ₄₈₀) conjugation onto oxytocin...	104
2.4.3.9. Aldehyde α -functional poly(mPEGA ₄₈₀) conjugation onto oxytocin....	104
2.4.3.10. Reversible conjugation of aldehyde linear PEG onto oxytocin.....	105
2.4.3.11. Reversible conjugation of butyraldehyde onto oxytocin.....	105
2.4.3.12. Irreversible conjugation of butyraldehyde onto oxytocin	105
2.4.3.13. Reversible and irreversible conjugation of propionaldehyde onto oxytocin	105
2.4.3.14. Reversible conjugation of α -aldehyde poly(mPEGA ₄₈₀) onto oxytocin	106
2.4.3.15. Reversibility experiments of Schiff base conjugated butyraldehyde	106
2.4.3.16. Reversibility experiments of Schiff base conjugated linear PEG	106
2.4.3.17. Reversibility of Schiff base conjugated poly(mPEGA ₄₈₀)	107
2.5. References	107
3. Disulfide bond targeted PEGylation of oxytocin	110
3.1. Introduction	111
3.2. Results & Discussion	112
3.2.1. General considerations for disulfide based chemistry with respect to oxytocin.....	112
3.2.1.1. Reducing the disulfide bond in oxytocin.....	113
3.2.2. Maleimide linear PEG disulfide bridging	115
3.2.2.1. Maleimide linear PEG synthesis.....	116
3.2.2.2. Maleimide linear PEG conjugation.....	120
3.2.3. α -Maleimide polyPEG.....	126
3.2.3.1. Synthesis of α -dithiophenolmaleimide polymers	133
3.2.3.2. Conjugation of α -dithiophenolmaleimide polymers	137

3.2.3.3. Reversibility of dithiophenolmaleimide disulfide bridging	142
3.2.4. Reduced structure targeting (thiol-ene)	145
3.2.4.1. Linear PEG acrylate.....	147
3.2.4.2. PolyPEG acrylate vinyl end group.....	151
3.3. Chapter 3 Conclusions.....	153
3.4. Experimental	154
3.4.1. Materials.....	154
3.4.2. Instrumentation & Analysis.....	155
3.4.3. Synthetic Procedures	157
3.4.3.1. Reduction of disulfide bond of oxytocin.....	157
3.4.3.2. Maleimide linear PEG reagent synthesis & conjugation.....	157
3.4.3.3. DTM-poly(mPEGA ₄₈₀) synthesis & conjugation	160
3.4.3.4. 'Thiol-ene' conjugation onto oxytocin.....	163
3.5. References	164
4. PEGylated oxytocin: Effects of PEGylation on oxytocin activity and stability.	167
4.1. Stability testing	168
4.1.1. Introduction.....	168
4.1.2. Initial oxytocin stability tests.....	169
4.1.3. High temperature thermal assay for non-conjugated excipients	170
4.1.3.1. Oxytocin calibration plot	171
4.1.3.2. Small excipients for stabilisation: The effect of polyols and sugars on oxytocin degradation	173
4.1.3.3. Non-conjugated polymer influence on thermal stability: Non-covalently bound PEG	174
4.1.4. Degradation study on different architectures of oxytocin – PEG conjugates	177
4.1.4.1. Stability of linear oxytocin –PEG conjugates	179
4.1.4.2. Stability of polyPEGylated oxytocin	183
4.1.4.3. Additional oxytocin conjugate stability testing.....	188

4.1.5. Stability testing conclusions.....	189
4.2. Uterotonic Experiments.....	190
4.2.1. Introduction.....	190
4.2.2. Uterotonic testing of oxytocin polymer conjugates Vs. oxytocin.....	191
4.2.2.1. Responses of oxytocin or conjugates upon spontaneous contractile behaviour.....	193
4.2.2.2. Analysis of results of uterotonic testing.....	195
4.2.2.3. Oxytocin receptor antagonist: Atosiban.....	201
4.2.3. Uterotonic testing conclusions.....	202
4.3. Cancer cell-line studies	203
4.3.1. Introduction.....	203
4.3.2. Investigation of oxytocin and polymer conjugates on cancer cell proliferation.....	205
4.3.3. Cancer cell line study conclusions	209
4.4. Chapter 4 Conclusions.....	210
4.5. Experimental	211
4.5.1. High temperature thermal stability tests	211
4.5.1.1. Materials.....	211
4.5.1.2. Instrumentation & Analysis.....	211
4.5.1.3. Heat Stability assay procedure.....	212
4.5.1.4. Synthesis of non-conjugating poly(mPEGA ₄₈₀) ₂₀	213
4.5.2. Uterotonic testing of oxytocin and oxytocin conjugates.....	213
4.5.2.1. Materials.....	214
4.5.2.2. Experimental Procedures.....	214
4.5.3. Cancer cell line study.....	214
4.5.3.1. Materials.....	215
4.5.3.2. Experimental Procedures.....	215
4.6. References	216

5. Synthesis and post-polymerisation peptide conjugation of functional polymers	218
5.1. Potential alternatives to PEG	219
5.1.1. Poly(2-oxazolines): A valuable PEG alternative?	221
5.1.1.1. Synthesis of Poly(OEtOxMA)	222
5.1.1.2. Synthesis of α -aldehyde functional poly(OEtOxMA)	225
5.1.1.3. Peptide conjugation reactions of α -aldehyde poly(OEtOxMA)	228
5.1.1.4. Schiff base reversibility studies of oxytocin-poly(OEtOxMA) conjugates	232
5.1.1.5. Degradation studies on reduced oxytocin-poly(OEtOxMA) conjugates	234
5.1.2. Potential alternatives to PEG conclusions	236
5.2. Thermoresponsive polymers for peptide conjugation	237
5.2.1. Optimisation of reaction conditions and synthesis of thermoresponsive polymers	239
5.2.1.1. Cloud point measurements	246
5.2.2. Dithiophenolmaleimide α -end functional polymers with thermoresponsive behaviour	247
5.2.2.1. Cloud point measurement of dithiophenolmaleimide polymers	251
5.2.3. Disulfide bridging conjugation of thermoresponsive polymers onto oxytocin	252
5.2.3.1. Conjugation of statistical copolymers of mPEGA ₄₈₀ -eDEGA onto a different peptide: Salmon calcitonin	254
5.2.3.2. Further characterisation of oxytocin conjugated thermoresponsive polymers	256
5.2.4. Thermoresponsive polymer conjugates conclusions	259
5.3. Glycopolymers	260
5.3.1. Synthesis of α -end functional glycopolymers	262
5.3.1.1. Synthesis of sugar monomers	262
5.3.1.2. SET-LRP of glycopolymers	263
5.3.2. DTM-poly(mannose) and DTM-poly(mPEGA) disulfide bridging conjugation	267

5.3.3. Glycopolymer conjugates conclusions	271
5.4. Chapter 5 conclusions	272
5.5. Experimental	273
5.5.1. Materials	273
5.5.2. Instrumentation & Analysis.....	273
5.5.3. Synthetic Procedures	275
5.5.3.1. Poly(ethylene glycol) alternatives	275
5.5.3.2. Thermoresponsive polymers for peptide conjugation.....	277
5.5.3.3. Glycopolymers	278
5.6. References	280
6. Overview and outlook.....	284
Publications of results in this thesis	286

Acknowledgments

I would first and foremost like to thank Dave, for allowing me to work within the Haddleton group for the last 5 years. Thank you for all of your support and guidance, particularly when things were not necessarily going the way that we had hoped for. Thanks as well for allowing me the opportunity to pursue such an interesting and easy to discuss project, through which I can at least feel like I am making a difference in the world, even if that is not the case.

Next a huge thanks goes to the 'senior research brotherhood' of Kristian and Paul, the pair of which have contributed more to my work, and general outlook on life in research, in terms of help and advice than I could possibly put in to words, and for which I will be eternally grateful.

I'd like to express gratitude to the members of the group who when I first started were exceptional in helpfulness in taking that fairly incompetent undergraduate and training me into some level of capability. For this in particular I thank Qiang who did so much for me during my master's year and first taught me a lot of the basic knowledge I now take for granted. I definitely wouldn't have stayed on if he hadn't been so understanding, always making time to answer my questions, even though he might not always have appreciated me taking up space in his fume hood.

When I transitioned to starting my PhD there is one person who really made me feel welcome and I still count as one of the best friends I have had at this university. Thanks to Kay, your departure from the group was one of the hardest things I had to overcome during my time here, but thank you for the great times we had in the labs, and out, the many nights of cider, wine, films and food. I'd also like to thank those other people who throughout the first year of my PhD, that even though the chemistry wasn't always working (sialic acid?), ensured I had a lot of fun (and wine/cocktails); I'll always remember that we had a very good year.

I want to thank all members of the extended office C210 family, who have made this last couple of years wholly enjoyable. You guys are the breath of fresh air that anyone fighting their way through completing a doctorate needs to surround themselves with, people I feel I can truly count on, and all the time make me feel part of a team and that you all really care what I have to say. Every day since moving into this office has been entertaining/crazy/(moderately)inappropriate/hilarious/tea-full and always lively. Specifically, Danielle: thanks for making me feel much less clumsy about myself, and your honest and fresh opinions; ‘Captain’ Slowe: for being the ‘old man’ presence in the corner, with all your talk of boats and kilts; Pat: for being the most dedicated and hardworking chemist I have met:- gelukkige donderdag ; Dan: for being my Mr. fix it – you should everyday get the recognition you genuinely deserve for the job that you do, (and thanks for grammar checking my thesis and realising what I actually do); Rachel: For your sensible opinions and level headedness, and always being willing to have a chat; Sam: Thank you for allowing me some entertainment with your forever occurring dramas, and your genuine interest in my opinion on situations, whether sat discussing chemistry in the office or at the pub over a pint.

I would also like to acknowledge the other members of the group, past and present, who have provided me with interesting conversations and time within the lab, and without. Particularly: Jamie, Claudia, Jenny K, Chongyu ‘#ConjugationClub’, Nuttapol, Richard, Joji, Chris S, Chris W, Ed and especially Raj. Thanks as well to the two students I have had the pleasure of helping to look after throughout my time in the group: Jessie and Sacha, the pair of you I am sure will go far in life.

Huge thanks goes to the team at Monash in Australia, especially to Michelle and Betty for providing me with their expertise in a field I did not really have any idea about. Tri for assisting me with acquiring rats and Danielle for running the Cancer cell line studies. Basu, thank you for teaching me how to tie double knots around ridiculously delicate uterine tissue, within solution, under a microscope and occasionally checking I was still alive whilst I was struggling down in the basement dungeon for 12 hour days.

Enormous thanks goes to Mikey, for being great throughout this project, and especially inviting me to come over and work in Melbourne. Thanks for all you've input into maintaining this collaboration, and particularly with finding me somewhere to live, making sure I was alright when I was down under, and being a genuinely great personality to be around.

Thanks to all technical and support staff within the department that have offered advice, allowed me to undertake training or run samples for me on the facilities we have available here at Warwick. I'd also like to thank my four 'extra-special' chromatography instruments, for not deciding to break (irreparably) before I finished writing this thesis.

Large thanks go to my family for these last few months of continually bothering me and asking how my thesis is which, although not always wanted was certainly always appreciated. I am grateful to all my family and friends for always showing me encouragement, and always listening, whether that be to recent successes or general complaints.

Finally, I would like to thank my brand new husband, Tom, for providing me with the ridiculous level of support that he has throughout my 8 years at Warwick. You're always there with a glass of wine and a shoulder to cry on (and potentially a stress relieving cat or two) after the long hard days are over, and I doubt that I could have done any of this without you. I'm so glad that 'thesis-writing, wedding-planning' Jenny has not scared you off forever and I'm so lucky that I can finally call myself your wife; you are truly the better half of me.

Here's to finally starting life in the real world, *'And so it begins'*.

Declaration

Experimental work contained within this thesis is original research carried out by the author, unless otherwise stated, in the Department of Chemistry at the University of Warwick, between October 2012 and September 2016 and at Monash Institute of Pharmaceutical Science, Monash University, Melbourne, Victoria, Australia between February 2015 and May 2015. No material contained herein has been submitted for any other degree, or at any other institution.

Work conducted by other authors are outlined below and labelled throughout the corresponding text.

- 1D & 2D peptide NMR spectra (chapter 2) were acquired by Dr Claudia Blindauer (University of Warwick)
- Vinyl end functional poly(mPEGMA) synthesis by CCTP (chapter 3) was conducted by Samuel Lowe (University of Warwick)
- Cancer cell line studies *via* MTT assay (chapter 4) were conducted by Danielle Senyschyn (Monash University, Australia)
- Poly(OEtOxMA) macromonomer (chapter 5) was synthesised by Dr Kristian Kempe (University of Warwick)

Signed: _____

Jennifer Collins

Date: _____

List of Figures

Figure 1.1. Structure of native oxytocin (cyclic [Cys-Tyr-Ile-Gln-Asn-Cys]-Pro-Leu-Gly-NH ₂).....	2
Figure 1.2. Major disulfide degradation product formation from oxytocin according to Wiśniewski.....	5
Figure 1.3. Structures of oxytocin analogues: desamino-oxytocin and carbetocin.....	6
Figure 1.4. Oxytocin analogues, with disulfide bond replacements investigated for uterotonic activity and plasma stability by Alewood.....	7
Figure 1.5. Structure of mPEG and some functional site-selective conjugating groups.	12
Figure 1.6. Reaction of NHS ester and a model peptide.....	15
Figure 1.7. Two step reductive amination of aldehyde <i>via</i> Schiff base intermediate....	16
Figure 1.8. Carbodiimide mediated reaction between amino group and carboxylic acid reagent.....	17
Figure 1.9. Conjugation reactions of sulfhydryls utilising maleimide (addition) or bromomaleimide (substitution).....	18
Figure 1.10. Thioether bond formation using ‘thiol-ene’ chemistry, and double conjugation at reduced disulfide bond.....	19
Figure 1.11. Disubstituted maleimides for disulfide bridging of peptides.....	21
Figure 1.12. Mechanism of bissulfone three carbon disulfide bridging.....	22
Figure 1.13. NMP polymerisation mechanism.	25
Figure 1.14. RAFT polymerisation mechanism.....	27
Figure 1.15. ATRP polymerisation mechanism.....	28
Figure 1.16. SET-LRP mechanism (as proposed by Percec).....	29
Figure 1.17. Protein polymer conjugation achieved by ‘grafting-to’ or ‘grafting-from’ approaches.....	31
Figure 2.1. RP-HPLC of conjugation of succinimidyl functional linear PEG onto oxytocin.....	50
Figure 2.2. RP-HPLC analysis of purified oxytocin-polymer (NHS) conjugate (2 kDa).....	50
Figure 2.3. MALDI-TOF MS analysis of oxytocin-polymer (NHS) 2 kDa conjugate.....	51
Figure 2.4. Commercially available aldehyde functional PEG reagents.....	53
Figure 2.5. RP-HPLC monitoring of conjugation reaction of aldehyde PEG (2 kDa) onto oxytocin, after stirring for 24 hours at T = 10 °C.....	55
Figure 2.6. RP-HPLC analysis of purified oxytocin-polymer (aldehyde) 2 kDa conjugate.....	55

Figure 2.7. MALDI-TOF MS analysis of oxytocin-polymer (aldehyde) 2 kDa conjugate.	56
Figure 2.8. ^1H NMR (CDCl_3 , 400.05 MHz) of freshly prepared succinimide initiator and 75 % hydrolysed succinimide initiator with a loss of NHS ester functionality.	59
Figure 2.9. ^1H NMR (δ_6 -DMSO) and SEC (DMF) analysis monitoring the polymerisation of NHS-poly(mPEGA ₄₈₀) ₂₀ .	60
Figure 2.10. Kinetic plots for the polymerisation of NHS-poly(mPEG ₄₈₀) ₂₀ .	61
Figure 2.11. RP-HPLC trace of conjugation of NHS-poly(mPEGA) ₂₀ from 'in-situ' conjugation of aliquot of polymerisation solution.	62
Figure 2.12. ^1H NMR (CDCl_3 , 300.13 MHz) of succinimidyl ester functional poly(mPEGA ₄₈₀) ₁₃ .	63
Figure 2.13. RP-HPLC trace monitoring conjugation of NHS-poly(mPEGA) ₁₃ with 1 or 10 equivalences.	64
Figure 2.14. RP-HPLC of oxytocin-poly(mPEGA) conjugate after purification.	65
Figure 2.15. ^1H NMR (CDCl_3 , 300.13 MHz) and ^{13}C NMR (CDCl_3 , 75.47 MHz) of acetal protected aldehyde initiator.	67
Figure 2.16. ^1H NMR (δ_6 -DMSO) and SEC (DMF) analysis of polymerisation of acetal-poly(mPEGA ₄₈₀) ₂₀ .	68
Figure 2.17. Kinetic plots for the polymerisation of acetal-poly(mPEGA ₄₈₀) ₂₀ .	69
Figure 2.18. ^1H NMR (δ_6 -DMSO, 300.13 MHz) of poly(mPEGA ₄₈₀) ₂₁ with acetal protected aldehyde end group functionality.	70
Figure 2.19. NMR and SEC analysis of DP_n 20 & DP_n 50 polymers before and after deprotection.	71
Figure 2.20. ^1H NMR (δ_6 -DMSO, 300.13 MHz) of poly(mPEGA ₄₈₀) ₂₁ after deprotection resulting in α aldehyde end group functionality.	72
Figure 2.21. RP-HPLC trace of aldehyde poly(mPEGA ₄₈₀) ₂₀ polymer conjugation.	73
Figure 2.22. RP-HPLC analysis of conjugation of linear aldehyde PEG (2 kDa) onto oxytocin without the addition of NaCNBH_3 reducing agent.	75
Figure 2.23. RP-HPLC analysis of 2 kDa and 5 k Da linear aldehyde Schiff base conjugation formation at pH 8.0 after 1 and 6 days.	76
Figure 2.24. Rates of formation of conjugates and disappearance of oxytocin in different solvents for both M_w of PEG aldehyde conjugated onto oxytocin.	77
Figure 2.25. Conjugation of butyraldehyde onto oxytocin showing formation of two products.	79
Figure 2.26. HPLC traces of separated butyraldehyde conjugates after $t = 24$ hours and $t = 8$ weeks storage in acidic solutions.	80
Figure 2.27. Conjugation of butyraldehyde with addition of NaCNBH_3 .	82

Figure 2.28. RP-HPLC analysis of reduced butyraldehyde conjugate, non-reduced butyraldehyde conjugate and non-reduced butyraldehyde conjugate upon addition of NaCNBH ₃ .	82
Figure 2.29. RP-HPLC analysis of product distributions with different equivalents of butyraldehyde.	84
Figure 2.30. Small molecule aldehydes conjugated onto oxytocin in a similar manner to PEGs.	86
Figure 2.31. Conjugation of propionaldehyde with and without the addition of NaCNBH ₃ .	86
Figure 2.32. ¹ H NMR analysis of butyraldehyde conjugation reaction mixture (pH 8) with 10 % D ₂ O including a zoom in of the imine region (6 – 9 ppm) and accompanying TOCSY spectra.	88
Figure 2.33. ¹ H NMR analysis of propionaldehyde conjugation reaction mixture (pH 8) with 10 % D ₂ O including a zoom in of the imine region (6 – 9 ppm).	88
Figure 2.34. ¹ H NMR of butyraldehyde and propionaldehyde in CHCl ₃ and D ₂ O showing formation of hydrate under aqueous conditions.	89
Figure 2.35. RP-HPLC trace of Schiff base oxytocin-poly(mPEGA ₄₈₀) ₂₀ conjugate formed without the addition of a reducing agent.	90
Figure 2.36. RP-HPLC trace showing reappearance of oxytocin under reversible conditions, and bar graph highlighting concentration changes of both butyraldehyde conjugates and oxytocin at pH 5.0 and pH 7.4.	92
Figure 2.37. RP-HPLC trace showing reappearance of oxytocin under reversible conditions, and bar graph highlighting concentration changes of both linear PEG conjugates and oxytocin at pH 5 and pH 7.4.	94
Figure 2.38. Concentration changes monitored for oxytocin release from linear PEGylated conjugate across a 2 week period at pH 5 and pH 7.4.	94
Figure 2.39. RP-HPLC traces for polyPEGylated oxytocin release study at pH 5 and pH 7.4.	95
Figure 3.1. RP-HPLC monitoring of oxytocin reduction with TCEP.	114
Figure 3.2. Oxytocin disulfide bond reduction using zinc powder, with and without the addition of TFA additive, and images of the two solutions.	115
Figure 3.3. Different 'N' Substituted maleimides developed over the last 60 years for protein and peptide modification at cysteine residues.	116
Figure 3.4. ¹ H NMR (CDCl ₃) of crude dibromomaleimide PEG and after purification (2 x column chromatography, dialysis, 4 x precipitation) synthesised using Mitsunobu route.	117
Figure 3.5. ¹ H and ¹³ C NMR of synthesis route of DBM PEG.	118
Figure 3.6. ¹ H NMR (CDCl ₃) for final step in synthesis of <i>N</i> -PEG-dithiophenolmaleimide (reaction of <i>N</i> -methoxycarbonyldithiophenolmaleimide with PEG-amine).	120

Figure 3.7. RP-HPLC of maleimide bridging conjugation of DBM PEG onto oxytocin.	121
Figure 3.8. RP-HPLC of maleimide bridging conjugation of DTM PEG onto oxytocin.	122
Figure 3.9. RP-HPLC chromatograms comparing DBM and DTM reagents used for disulfide bridging conjugation of oxytocin analysed under two different HPLC gradients.	123
Figure 3.10. Photographs showing colour change upon addition of DBM PEG to reduced oxytocin.	123
Figure 3.11. UV wavelength shifts of maleimide PEGs with different maleimide functionality.	124
Figure 3.12. Fluorescence spectra of DTM PEG, DBM PEG and maleimide disulfide bridged oxytocin using an excitation wavelength (λ_{ex}) of 314 nm.	125
Figure 3.13. ^1H & ^{13}C NMR (CDCl_3) of dithiophenolmaleimide alkyl halide initiator.	127
Figure 3.14. SEC (DMF) analysis for synthesis of poly(mPEGA) ₂₀ in different solvent combinations and ^1H NMR (D_2O) analysis of polymer synthesised in 80 % DMSO (99 % conv., M_n : 11600, \bar{D} : 1.08) with an expansion of the vinyl peaks showing disappearance of monomer.	130
Figure 3.15. SEC chromatograms for synthesis of EBiB-poly(mPEGA)s with accompanying high conversion NMR, and photograph of polymer phase separation.	132
Figure 3.16. SEC analysis of DP_n 20, 50 and 100 DTM-poly(mPEGA ₄₈₀) ₂₀ and RI/UV overlay of SEC chromatogram.	134
Figure 3.17. Photographs showing the phase separation during polymerisation of DP_n 50 or DP_n 100 poly(mPEGA ₄₈₀) in DMSO:Water (4:1).	135
Figure 3.18. Comparison of ^1H NMR (400.13 MHz, δ_6 -DMSO) individually measured of top and bottom layer within polymerisation, with an expansion of the vinyl/aromatic regions.	136
Figure 3.19. Assigned ^1H NMR (D_2O) of DTM – poly(mPEGA ₄₈₀) ₂₀ after purification.	137
Figure 3.20. RP-HPLC analysis of DTM poly(mPEGA) conjugation onto oxytocin by UV and FLD.	138
Figure 3.21. RP-HPLC of 'in-situ' conjugation of DTM polymers onto oxytocin.	139
Figure 3.22. RP-HPLC analysis of purified oxytocin conjugates showing change in retention time from DTM poly(mPEGA), and newly observed fluorescence.	140
Figure 3.23. UV monitoring of oxytocin, DTM polymer and disulfide bridged oxytocin poly(mPEGA) conjugate for shift in maleimide functionality.	141
Figure 3.24. Fluorescence study of DTM polymers and oxytocin-polymer conjugates, showing an increase in fluorescence.	141
Figure 3.25. RP-HPLC trace of GSH reversal of conjugation with expansion of oxytocin region, showing the regeneration of the native peptide.	143

Figure 3.26. MALDI-TOF analysis of released oxytocin from oxytocin-(mPEGA ₄₈₀) ₂₀ polymer conjugate.	144
Figure 3.27. ABA triblock polymer, containing central peptide block from oxytocin.	146
Figure 3.28. RP-HPLC of conjugation of (mPEGA ₄₈₀) ₂ onto oxytocin through phosphine catalysed thiol-ene Michael addition.	148
Figure 3.29. MALDI-TOF analysis of oxytocin-(mPEG ₄₈₀) ₂ conjugate.	149
Figure 3.30. RP-HPLC monitoring of conjugation of mPEGA (2 kDa and 5 kDa) onto reduced oxytocin <i>via</i> phosphine catalysed thiol-ene Michael addition.	150
Figure 3.31. MALDI-TOF analysis of oxytocin-(mPEG ₂₀₀₀) ₂ conjugate.	150
Figure 3.32. ¹ H NMR (MeOD) of vinyl functional poly(mPEGMA)	152
Figure 3.33. RP-HPLC of conjugation vinyl end functional poly(mPEGMA) onto oxytocin.	153
Figure 4.1. Monitoring the degradation of oxytocin at 50 °C over 28 days by RP-HPLC.	170
Figure 4.2. Calibration plot for different concentrations of oxytocin.	172
Figure 4.3. RP-HPLC chromatogram of oxytocin before and after thermal stressing at 80 °C.	172
Figure 4.4. Thermally stressed stability of oxytocin in the presence of polyol and saccharide excipients at 1 and 100 molar equivalents at 80 °C for 24 hours.	174
Figure 4.5. Evaluation of % of oxytocin remaining after 24 hours of thermal stressing (80 °C) containing different molecular weights of PEG.	175
Figure 4.6. Evaluation of % of oxytocin remaining after 24 hours of thermal stressing (80 °C) containing different molecular weights of PEG after taking 'n' into consideration.	176
Figure 4.7. Calibration plots of peak areas from RP-HPLC for linear and polyPEG conjugates at concentrations used for thermally stressed stability testing.	178
Figure 4.8. Structures of linear PEGylated oxytocin.	179
Figure 4.9. Stability results for all linear PEGylated conjugates (6 kDa) compared to native oxytocin and the peptide solution containing 5 kDa PEG as a non-conjugated additive.	180
Figure 4.10. RP-HPLC chromatograms of succinimide and aldehyde oxytocin polymer conjugates (6 kDa) after 24 hours of storage at 80 °C.	181
Figure 4.11. Diagrams showing different structures of disulfide conjugated polymers and influence on cyclic ring size within oxytocin.	182
Figure 4.12. NMR and GPC of EBiB initiated polymer used as a non-conjugating polyPEG additive in heat stability testing of oxytocin at 80 °C.	184

Figure 4.13. RP-HPLC traces of oxytocin at $t = 0$, oxytocin after 80 °C storage ($t = 0$) and oxytocin after 80 °C storage with addition of a polyPEG additive.	185
Figure 4.14. Structures of polyPEG oxytocin conjugates, and oxytocin with non-conjugated polymer.....	185
Figure 4.15. Stability results for all polyPEGylated conjugates compared to native oxytocin and the peptide solution containing 20 Eq. 350 Da PEG, and DP_n 20 polyPEG as a non-conjugated additive.....	186
Figure 4.16. HPLC traces of degradation of oxytocin polyPEG conjugates (80 °C, 24 h, 25 mM).....	187
Figure 4.17. Stability of oxytocin polymer conjugates at 50 °C across 28 days.....	189
Figure 4.18. Oxytocin mechanism for stimulating contractions and structure of oxytocin highlighting important residues for contraction.....	191
Figure 4.19. Experimental organ bath set-up.	192
Figure 4.20. Example pictures of HiK and oxytocin induced response in uterotonic tissue showing effect on spontaneous contractions.	193
Figure 4.21. Example uterotonic traces for linear aldehyde, polyPEG aldehyde and polyPEG dithiophenolmaleimide conjugates.....	194
Figure 4.22. Observation of contractile responses for linear aldehyde PEG conjugate monitoring the effect of HiK, oxytocin and conjugate upon spontaneous contractions.	195
Figure 4.23. Contractile peak response analysis of data for linear aldehyde PEG and oxytocin PEG conjugate with respect to amplitude, integration, frequency and duration.	196
Figure 4.24. Contractile peak response analysis of data for aldehyde polyPEG and oxytocin polyPEG conjugate with respect to amplitude, integration, frequency and duration.....	198
Figure 4.25. Contractile peak response analysis of data for dithiophenolmaleimide polyPEG and oxytocin polyPEG conjugate with respect to amplitude, integration, frequency and duration.	199
Figure 4.26. Comparison of the structure of oxytocin and oxytocin antagonist atosiban.	201
Figure 4.27. Trace of uterotonic contractions showing the effect of atosiban upon oxytocin uterotonic activity, after initial HiK response.....	202
Figure 4.28. Structure of oxytocin and oxytocin analogue F314 (atosiban).....	204
Figure 4.29. Cell viability after treatment with different concentrations of oxytocin compared to untreated control cells after 144 hours.	206
Figure 4.30. Cell viability on treatment with different oxytocin conjugates for 144 hours.....	207

Figure 4.31. Cell viability of all linear and polyPEG oxytocin conjugates w.r.t untreated control after 72 hours of cell growth.	208
Figure 4.32. Cell viability of all polymers after 72 hours w.r.t untreated control.	209
Figure 5.1. PEG, polyPEG and some different biodegradable and non-biodegradable PEG alternatives.....	220
Figure 5.2. ^1H NMR (CDCl_3) and SEC (CHCl_3) of oligo(2-ethyl-2-oxazoline) methacrylate macromonomer.	223
Figure 5.3. ^1H NMR (CHCl_3 , 400 MHz) and SEC (CHCl_3) of poly(OEtOxMA) at $t = 24$ hours synthesised with WSI ($[\text{I}]:[\text{CuCl}]:[\text{PMDETA}] = 1:0.8:0.8$, $\text{MeOH}/\text{H}_2\text{O}$, 1.6 M NaCl).	225
Figure 5.4. ^1H NMR (CHCl_3 , 400 MHz) and SEC (CHCl_3) of poly(OEtOxMA) at $t = 24$ hours synthesised with PALD initiator ($[\text{I}]:[\text{CuCl}]:[\text{PMDETA}] = 1:0.8:0.8$, $\text{MeOH}/\text{H}_2\text{O}$, 1.6 M NaCl).	225
Figure 5.5. ^1H NMR (δ_6 -DMSO, 400 MHz) of PALD-poly(OEtOxMA) ₁₀ polymer after purification.....	226
Figure 5.6. ^1H NMR (δ_6 -DMSO) and SEC (CHCl_3) after deprotection of acetal protected aldehyde end group functionality.....	227
Figure 5.7. Conjugation reaction of [Gly-Ty] with α -aldehyde poly(OEtOxMA) monitored by RP-HPLC ($\lambda = 280$ nm) and ^1H NMR (δ_6 -DMSO, 300 MHz).	229
Figure 5.8. RP-HPLC of reductive amination of aldehyde functional poly(OEtOxMA) onto oxytocin after addition of NaCNBH_3	230
Figure 5.9. RP-HPLC monitoring of aldehyde functional poly(OEtOxMA) (DP_n 10 and 20) before and after conjugation onto oxytocin.	231
Figure 5.10. RP-HPLC monitoring of the formation of oxytocin-poly(OEtOxMA) ₂₀ Schiff base conjugate.	232
Figure 5.11. RP-HPLC monitoring of reversal of oxytocin-poly(OEtOxMA) ₂₀ conjugates at pH 5 and pH 7.4 after 14 days at ambient temperature or at $T = 37^\circ\text{C}$	233
Figure 5.12. Bar chart and RP-HPLC traces showing degradation of oxytocin-poly(OEtOxMA) conjugates in comparison to native peptide after 24 h at 80°C	234
Figure 5.13. Cloud point measurements of oxytocin –poly(OEtOxMA) conjugates in water (5 mg ml^{-1}) at $\lambda = 500\text{ nm}$	235
Figure 5.14. SEC analysis of poly[(mPEGA) _x (eDEGA) _{1-x}] for $x = 1, 0.1, 0.05$ & 0 and SEC analysis of synthesis of poly(NiPAm) in DMSO/ H_2O	242
Figure 5.15. SEC (DMF) and ^1H NMR (δ_6 -DMSO) at $t = 24$ hours for homopolymerisation of eDEGA in ethanol/water (4:1).	244
Figure 5.16. SEC analysis of different copolymers of mPEGA and eDEGA, and a NiPAm homopolymer synthesised with EBiB in ethanol/water (4:1).	246
Figure 5.17. Transmittance responses of ethyl end functional thermoresponsive polymers in PBS between 20°C and 80°C	246

Figure 5.18. SEC (DMF) analysis of DTM functional thermoresponsive polymers synthesised in EtOH/H ₂ O (4:1).	249
Figure 5.19. ¹ H NMR (δ ₆ – DMSO) of purified DTM- poly[(mPEGA) _{0.2} (eDEGA) _{0.8}] and DTM-poly(NiPAm) ₁₀₀ showing presence of α-DTM functionality.	250
Figure 5.20. Transmittance of thermoresponsive DTM functional polymers between 20 °C and 80 °C, and photographs of polymer solutions below and above cloud point.	251
Figure 5.21. RP-HPLC analysis (UV, λ = 280 nm) of oxytocin conjugation of purified DTM-poly[(mPEGA) _x (eDEGA) _{1-x}] ₁₀₀	253
Figure 5.22. RP-HPLC analysis of oxytocin conjugation of DTM-poly[(mPEG) _x (eDEGA) _{1-x}], specifically focussing on consumption of peptide.	254
Figure 5.23. RP-HPLC analysis of disulfide bridging conjugation of DTM-[(mPEGA) _x (eDEGA) _{1-x}] onto sCT.	255
Figure 5.24. Images showing colour change from the bright yellow of the dithiophenolmaleimide polymer to a less intense colour, observed during the conjugation reaction.	256
Figure 5.25. UV shifts of DTM functional poly[(mPEGA) _x (eDEGA) _{1-x}] and upon addition to reduced sCT and oxytocin.	257
Figure 5.26. SEC analysis of DTM functional thermoresponsive polymers before and after disulfide bridging conjugation of oxytocin.	259
Figure 5.27. ¹ H and ¹³ C NMR (MeOD) of mannose functional glycomonomer.	263
Figure 5.28. SEC (DMF) chromatograms and ¹ H NMR analysis of polymerisation of mannose glycomonomers with dithiophenolmaleimide initiator after 24 hours.	265
Figure 5.29. ¹ H NMR analysis (δ ₆ -DMSO) of purified dithiophenolmaleimide α-end functional poly(mannose).	266
Figure 5.30. ¹ H NMR (δ ₆ DMSO) and SEC (DMF) of purified dithiophenolmaleimide α-end functional poly(mPEGA ₄₈₀) ₅₀	267
Figure 5.31. RP-HPLC analysis of conjugation of dithiophenolmaleimide poly(mannose) onto salmon calcitonin (UV λ= 280 nm; FLD λ _{ex} : 341 nm, λ _{em} : 502 nm).	269
Figure 5.32. RP-HPLC analysis of conjugation of dithiophenolmaleimide poly(mPEGA ₄₈₀) ₅₀ onto salmon calcitonin.	269
Figure 5.33. Fluorescence spectra of sCT-poly(mannose) ₂₀ with excitation at λ _{ex} = 341 nm and λ _{ex} = 410 nm.	270
Figure 5.34. Emission (λ _{ex} = 410 nm) and excitation (λ _{em} = 536 – 547 nm) spectra of sCT polymer conjugates.	271

List of Schemes

Scheme 2.1. Conjugation of NHS ester functional linear PEG onto oxytocin site specifically at <i>N</i> -terminal amine in DMF (containing 1% TEA) at 10 °C.	49
Scheme 2.2. Schiff base formation of reaction between aldehyde and amine followed by reduction by NaCNBH ₃ forming stable secondary amine linkage.....	52
Scheme 2.3. Formation of stable linear PEGylated oxytocin following reaction with aldehyde PEG and subsequent reduction by NaCNBH ₃	54
Scheme 2.4. Synthesis reaction for NHS ester functional initiator.	58
Scheme 2.5. Cu(0) mediated living radical polymerisation of mPEGA ₄₈₀ using NHS initiator resulting in α -succinimidyl ester functionality poly(mPEGA ₄₈₀).....	59
Scheme 2.6. Conjugation of α -succinimide functional poly(mPEGA ₄₈₀) polymer onto oxytocin.	61
Scheme 2.7. Two step synthesis rout for protected aldehyde initiator.	66
Scheme 2.8. Cu(0) mediated polymerisation of mPEGA ₄₈₀ with protected aldehyde initiator.....	67
Scheme 2.9. Deprotection of acetal protecting group yielding aldehyde functional poly(mPEGA ₄₈₀).....	71
Scheme 2.10. Conjugation reaction of poly(mPEGA ₄₈₀) to oxytocin with reduction by NaCNBH ₃	73
Scheme 2.11. Reversible conjugation of butyraldehyde and oxytocin.....	78
Scheme 2.12. Second step for the irreversible conjugation of butyraldehyde onto oxytocin.	81
Scheme 2.13. Double conjugation of butyraldehyde onto oxytocin from second reaction at the secondary amine.....	83
Scheme 3.1. Reduction of oxytocin disulfide bond generating two free thiols.....	112
Scheme 3.2. Mechanism of TCEP disulfide bond reduction.	113
Scheme 3.3. Dithiophenolmaleimide/dibromomaleimide reagent synthesis.....	117
Scheme 3.4. Reaction scheme of dithiophenolmaleimide reagent functionalisation.	119
Scheme 3.5. Disulfide bridging conjugation of oxytocin with linear maleimide PEG.	120
Scheme 3.6. Polymerisation of mPEGA ₄₈₀ with water soluble initiator using [M]:[I]:[CuBr]:[Me ₆ TREN] = 1:20:0.4:0.4 in DMSO/Water.	129
Scheme 3.7. Polymerisation of mPEGA ₄₈₀ with EBiB using [M]:[I]:[CuBr]:[Me ₆ TREN] = 1:20/100:0.4:0.4 in DMSO:Water (4:1).....	131
Scheme 3.8. Polymerisation of mPEGA ₄₈₀ with dithiophenolmaleimide initiator using [M]:[I]:[CuBr]:[Me ₆ TREN] = 1:n:0.4:0.4 in DMSO:Water (4:1).....	133

Scheme 3.9. Conjugation of dithiophenolmaleimide poly(mPEGA) with reduced oxytocin.....	138
Scheme 3.10. Glutathione induced reversal of oxytocin poly(mPEGA) conjugation, releasing the native peptide.....	143
Scheme 3.11. Mechanism of phosphine induced thiol-ene Michael addition of (meth)acrylates.....	146
Scheme 3.12. Double conjugation of mPEG acrylate onto oxytocin of different molecular weight using TCEP as a disulfide bond reduction agent and thiol-ene catalyst.....	147
Scheme 4.1. Copper mediated polymerisation of mPEGA ₄₈₀ with EBiB initiator in DMSO/H ₂ O (4:1) ([I]:[CuBr]:[Me ₆ TREN] = 1:0.4:0.4).	183
Scheme 5.1. Oligo(2-ethyl-2-oxazoline)methacrylate macromonomer synthesis with initiation by methyl tosylate and termination by methacrylic acid.	222
Scheme 5.2. Polymerisation of oligo(2-ethyl-2-oxazoline) in water/methanol containing 1.6 M NaCl salt using two different initiators with [I]:[CuCl]:[PMDETA] = 1:0.8:0.8.....	224
Scheme 5.3. Reductive amination conjugation of aldehyde poly(OEtOxMA) onto oxytocin with addition of NaCNBH ₃	229
Scheme 5.4. Reversible (Schiff base) conjugation of aldehyde poly(OEtOxMA) onto oxytocin.	231
Scheme 5.5. Polymerisation of mPEGA and DEGA with WSI in water – organic solvents.....	241
Scheme 5.6. Copolymerisation of mPEGA /eDEGA and homopolymerisation of NiPAm in ethanol/water (4:1) using EBiB as initiator ([I]:[M]:[CuBr]:[Me ₆ TREN] = 1:100:0.4:0.4).....	245
Scheme 5.7. Polymerisation reactions for synthesis of copolymers of eDGA and mPEGA and a homopolymer of NiPAm using dithiophenolmaleimide initiator in EtOH/H ₂ O (4:1).	248
Scheme 5.8. Synthesis of mannose glycomonomer.	263
Scheme 5.9. Polymerisation of mannose monomer with DTM initiator in DMSO ([I]:[Cu(II)Br ₂]:[Me ₆ TREN] = 1:0.1:0.18, 5 cm Cu(0) wire).....	264
Scheme 5.10. Disulfide bridging conjugation of DTM glycopolymer onto sCT.....	268

List of Tables

Table 1.1. Different FDA approved PEGylated products available on the commercial market.....	13
Table 2.1. Comparison of molecular weights and dispersities of acetal protected and aldehyde (deprotected) DP_n 20 & DP_n 50 polymers.....	72
Table 2.2. Conjugation of 2 kDa and 5 kDa aldehyde PEG onto oxytocin without reduction – decrease in oxytocin and conjugate peak ratios at $t = 6$ days.	76
Table 2.3. HPLC peak area % of oxytocin, monosubstituted product and disubstituted product on increasing equivalents of aldehyde reagent.	84
Table 2.4. RP-HPLC (UV, $\lambda = 280$ nm) peak areas (mAU) for oxytocin and the two conjugate peaks upon reversal at different pHs for butyraldehyde-oxytocin conjugate.	91
Table 2.5. RP-HPLC (UV, $\lambda = 280$ nm) peak areas (mAU) for oxytocin and the two conjugate peaks upon reversal at different pHs for linear PEG-oxytocin conjugate.....	93
Table 2.6. RP-HPLC (UV, $\lambda = 280$ nm) peak areas (mAU) for oxytocin and the singular conjugate peaks upon reversal at different pHs for polyPEG-oxytocin conjugate.....	95
Table 3.1. Overview of characterisation methods for maleimide enhanced PEGylation of oxytocin.	126
Table 3.2. Polymerisation data for the synthesis of poly(mPEGA ₄₈₀) ₂₀ using water soluble initiator with different DMSO/water content.....	129
Table 3.3. Polymerisation data from synthesis of poly(mPEGA ₄₈₀) _n using EBiB.....	131
Table 3.4. Polymerisation data for synthesis of poly(mPEGA ₄₈₀) using DTM initiator.	133
Table 4.1. Thermal stability study (80 °C, 24 h) of oxytocin (assessed in terms of retained % peak area of the peptide) on addition of various polyols and sugars as external additives.....	173
Table 4.2. Results of thermal degradation study for linear oxytocin-polymer conjugates (6 kDa) after 24 hours storage at 80 °C compared to oxytocin, and non-conjugated PEG (5kDa).....	182
Table 4.3. Results of thermal degradation study for oxytocin-polyPEG conjugates after 24 hours storage at 80 °C, compared to relevant non-conjugated polymers.....	187
Table 5.1. Polymerisation data for the synthesis of poly(OEtOxMA) in MeOH/H ₂ O (2:1.5) containing 1.6 M NaCl with CuCl and PMDETA.....	228
Table 5.2. Polymerisation data for synthesis of eDEGA, mPEGA, NiPAm and copolymers of mPEGA and eDEGA using WSI in DMSO/H ₂ O (5:1) using [I]:[CuBr]:[Me ₆ TREN] = 1:0.4:0.4,.....	241

Table 5.3. Polymerisation data for synthesis of eDEGA, NiPAm and one copolymer of mPEGA and eDEGA using WSI in MeOH/H ₂ O (5:1) using [I]:[CuBr]:[Me ₆ TREN] = 1:0.4:0.4.....	243
Table 5.4. Polymerisation data for the synthesis of thermoresponsive polymers in ethanol / water (4:1) using EBiB as initiator.....	245
Table 5.5. Molecular weight data and cloud point measurements for 1 mg ml ⁻¹ solutions of copolymers of eDEGA and mPEGA and polyNiPAm.....	247
Table 5.6. Polymerisation data for synthesis of thermoresponsive dithiophenolmaleimide polymers.....	249
Table 5.7. Cloud point measurements of DTM α-end functional thermoresponsive polymers.	252
Table 5.8. Molecular weight and conversion data for dithiophenolmaleimide end functional poly(mannose)	265

Abbreviations

ACN	Acetonitrile
ALD	Aldehyde
ATRP	Atom transfer radical polymerisation
CDCl ₃	Deuterated chloroform
CHCA	α -cyano-4-hydroxycinnamic acid
CRP	Controlled radical polymerisation
CTA	Chain transfer agent
Đ	Dispersity
D ₂ O	Deuterated water
δ_6 -dmsO	Deuterated dimethylsulfoxide
Da	Daltons
DBM	Dibromomaleimide
DCM	Dichloromethane
DHB	2,5-Dihydroxybenzoic acid
DMF	Dimethylformamide
DMSO	Dimethylsulfoxide
DP_n	Degree of polymerisation
DTM	Dithiophenolmaleimide
EBiB	Ethyl α -bromoisobutyrate
eDEGA	Di(ethylene glycol) ethyl ether acrylate
Eq.	Equivalents
ESI-MS	Electrospray ionisation mass spectrometry
EtOAc	Ethyl acetate
EtOH	Ethanol
FDA	Food and drug administration
FLD	Fluorescence detection
FT-IR	Fourier transform infrared spectroscopy
k_p	Propagation rate constant
λ_{em}	Emission wavelength
λ_{ex}	Excitation wavelength
LCST	Lower critical solution temperature
LRP	Living radical polymerisation
M	Molar

MALDI-TOF	Matrix assisted laser desorption ionisation time of flight
mAU	Milli absorbance units
Me ₆ TREN	N,N,N',N',N'',N''-hexamethyl-[tris(aminoethyl)amine]
MeOD	Deuterated methanol
MeOH	Methanol
MHz	Megahertz
M _n	Number average molecular weight
mPEGA	Poly(ethylene glycol) methyl ethyl acrylate
mPEGMA	Poly(ethylene glycol) methyl ethyl methacrylate
M _w	Weight average molecular weight
MW	Molecular weight; molar mass
MWCO	Molecular weight cut off
n	Number of monomer repeat units
NaCNBH ₃	Sodium cyanoborohydride
NHS	N-hydroxysuccinimide
NiPAm	N-isopropylacrylamide
NMP	Nitroxide mediated polymerisation
NMR	Nuclear magnetic resonance
OEtOxMA	Oligo(2-ethyl-2-oxazoline)methacrylate
PALD	Protected aldehyde
PBS	Phosphate buffered saline
PEG	Poly(ethylene glycol)
PMDETA	N,N,N',N'',N''-pentamethyldiethylenetriamine
PMMA	Poly(methylmethacrylate)
Poly(mPEGA)	Poly(poly(ethylene glycol) methyl ether acrylate)
Poly(mPEGMA)	Poly(poly(ethylene glycol) methyl ether methacrylate)
Poly(NiPAm)	Poly(N-isopropylacrylamide)
Poly(OEtOXMA)	Poly(oligo(2-ethyl-2-oxazoline)methacrylate)
POx	Poly(2-R-oxazoline)
ppm	Parts per million
RAFT	Reversible addition-fragmentation chain-transfer polymerisation
RDRP	Reversible deactivation radical polymerisation
RI	Refractive Index
ROP	Ring-opening polymerisation

RP-HPLC	Reverse phase high performance liquid chromatography
sCT	Salmon calcitonin
SD	Sprague-Dawley
SEC	Size exclusion chromatography
TCEP	<i>Tris</i> (2-carboxyethyl)phosphine
TEA	Triethylamine
THF	Tetrahydrofuran
TOCSY	Total correlation spectroscopy
UCST	Upper critical solution temperature
UV-Vis	Ultraviolet-visible
WSI	Water soluble initiator

Abstract

The aim of this work was to investigate different methods for the covalent attachment of poly(ethylene glycol) onto the therapeutic peptide oxytocin, a highly important, but thermally unstable therapeutic used globally. This peptide is the WHO recommended therapeutic for prevention of postpartum haemorrhaging, sitting on the WHO list of essential medicines. Tackling the currently unacceptable maternal mortality rate, particularly in developing countries is of paramount importance and is currently one of the WHO's main priorities. Within this project it was speculated that by attachment of PEG to the peptide there would hopefully be an increase in stability, particularly for aqueous formulations at elevated temperatures.

Chapter one gives a brief outline of the problem that the world is facing with respect to maternal mortality, and particularly the gap between developed and developing countries and previous strategies that have looked into improving the stability of oxytocin. Additionally the various different site-specific conjugation approaches available for peptide modification are discussed, alongside how these can be implemented with controlled radical polymerisation techniques for the synthesis of alternative polymer architectures.

Chapter two discusses two particular targeting chemistries for site-selectively targeting the *N*-terminal amine (the only amino group on the peptide structure). Some commercially applicable linear PEGylation reagents (such as utilising NHS esters) were utilised for the conjugation of polymers onto oxytocin in this manner. PolyPEGs were synthesised to contain similar α -end group functionality as for the linear polymers and reacted with oxytocin in similar manners. The reversible nature of one of these chemistries was also investigated, and the potential release of the native peptide dependence on conjugate architecture and pH were evaluated.

In Chapter 3 the potential for conjugation techniques targeting the sulfhydryl groups arising from a reduction of the disulfide bond were approached in two different manners. Disubstituted maleimide chemistry is particularly useful in this case as it allows the rebridging of the disulfide bond, one of the main degradation sites on the peptide, with a stronger 2-carbon bond. Dithiophenolmaleimide α -end functional polyPEGs were synthesised and conjugated onto the peptide via an in-situ approach alongside traditional conjugations with both polyPEGs and linear PEGs. Another approach was evaluated for the conjugation at the disulfide bond that treats both free cysteine residues for separate conjugations utilising phosphine mediated thiol-ene chemistry. The facile synthesis of ABA block copolymers containing a central 'oxytocin' block, however results in a loss of the cyclic structure on the peptide, and likely complete suppression of biological activity.

Chapter 4 reports the investigation of the various conjugation strategies raised in chapters 2 & 3 for how the properties of the peptide might have changed post-conjugation comparing linear PEG and polyPEG site selectively added at either position in comparison to the native peptide. This is evaluated for the thermal stability, where oxytocin shows high levels of degradation in aqueous solutions, particularly at elevated temperatures. Also investigated is the potential retention of uterotonic activity, *via ex-vivo* electrophysiology studies, as well as some previously investigated effects on the inhibition of cell proliferation of the breast cancer cell line MDA-MB231.

Chapter 5 focusses on the conjugation to oxytocin, and another small disulfide containing peptide of some different (non-PEG) polymers synthesised in similar manners to those discussed in chapters 2 and 3. These few examples show that there is a large scope within this polymer synthesis and conjugation chemistry for utilising these techniques for a wide range of different monomer classes. Those described include the synthesis of a promising PEG alternative, two different thermoresponsive polymers and polymers containing pendant sugar functionality followed by the subsequent peptide conjugations.

Chapter 1

1. Introduction

“Every day, approximately 830 women die from preventable causes related to pregnancy and childbirth.”

- World Health Organisation, November 2015

1.1. Oxytocin

Oxytocin is a cyclic neurohypophyseal nonapeptide (cyclic [Cys-Tyr-Ile-Gln-Asn-Cys]-Pro-Leu-Gly-NH₂) naturally produced in the hypothalamus (figure 1.1). The uterine contracting properties of oxytocin were first discovered in 1906 by Sir Henry Hallett Dale, on observing the subsequent contractions caused from delivery of extractions from the pituitary.¹ It was not until the 1950s and the pioneering work of Vincent du Vigneaud that the structure of oxytocin was elucidated² and soon after biochemically synthesised,³ making it the first polypeptide to be sequenced and synthesised, winning du Vigneaud the 1955 Nobel prize in Chemistry.⁴

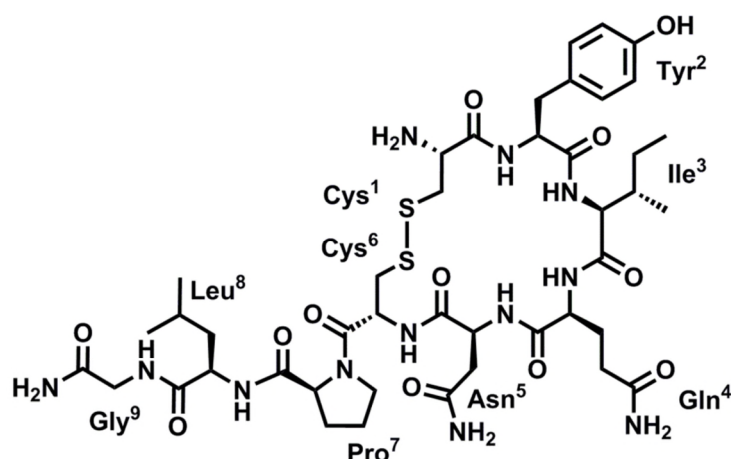


Figure 1.1. Structure of native oxytocin (cyclic [Cys-Tyr-Ile-Gln-Asn-Cys]-Pro-Leu-Gly-NH₂).

1.1.1. Oxytocin relation of maternal mortality

Approximately 300,000 women globally die every year from pregnancy or childbirth related problems.^{5,6} This is particularly prevalent in communities within the developing world, such as in Africa, Asia and Latin America, where tropical climates often have daytime temperatures exceeding 40 °C and reliable cold chain transportation and storage is not always achievable due to economic or social reasons. In developing countries there is

also less access to well-resourced healthcare facilities and particularly medical professionals, which cause large increases in maternal deaths. The global differences in the amount of women dying during childbirth are very high with maternal deaths occurring far too commonly within the developing world (approximately 14 times more incidences than developed countries). As a result the World Health Organisation (WHO) expect 99 % of maternal deaths occurring in 2016 to be within less economically developed regions.^{7,8} The UN has currently been focusing on reducing maternal mortality, with a goal of reducing the maternal mortality rate to less than 70 deaths per 100,000 live births by 2030 (UN sustainable development goal 3).

On consideration of maternal death statistics, at least 25% of these deaths are due to excessive or uncontrolled bleeding after birth: postpartum haemorrhaging (PPH). This usually results in haemorrhaging in excess of 500ml blood after delivery and occurs in 10% of all births. This is mainly due to the atonicity of the uterus post birth (failure to adequately contract). Oxytocin is the World Health Organisation (WHO) recommended drug currently used globally as a uterotonic for the prevention of PPH⁹⁻¹² and is on the WHO list of essential medicines.¹³

1.1.2. Oxytocin for uterotonic activity

Oxytocin receptors are expressed on the cell surfaces of a variety of cells, not only specifically at the uterus.¹⁴ The oxytocin receptor is a G protein-coupled receptor (GPCR), a transmembrane receptor that works as a cell-signalling powerhouse, sensing molecules outside cells and exhibiting cellular responses. When oxytocin binds into this receptor, this elicits a response from the G-protein, with which it is coupled inside the cell. The mechanism of action involves a combination of MLC kinase (activated by an influx of Ca^{2+}), alongside prostaglandin $\text{F}_{2\alpha}$ (derived enzymatically inside the cell), ultimately causing a

contraction of the uterus.^{15,16} Although the exact binding mechanism of oxytocin to the oxytocin receptor is still unknown, the amino acids on the oxytocin structure important for retaining activity have been determined. For receptor binding Ile³, Gln⁴, Pro⁷ and Leu⁸ are all important whereas Asn⁵ and Tyr² are key moieties required for stimulating activity and proper function upon binding to the receptor.^{17,18} Any changes in the structure of the peptide in general, but more specifically to these residues can lead to a loss of biological activity, or the ability to bind into the receptor.

1.1.3. Degradation of oxytocin formulations

A major problem with the administration of oxytocin as a therapeutic is that it possesses a very limited stability in aqueous solutions, particularly at elevated temperatures, such as those found in tropical climates, which leads to a loss of activity of the drug.¹⁸⁻²⁰ Injectable (aqueous) oxytocin formulations therefore require refrigeration (2 – 8 °C) to ensure quality and limit the degradation. The recommended shelf life for refrigerated oxytocin (<8 °C) is 2 years and for non-refrigerated oxytocin (< 25 °C) is less than 6 months.

There have been many investigations into the degradation profiles of oxytocin, in particular to establish at which position on the peptide structure this degradation is occurring.^{18,19,21} Tyr² can readily undergo oxidation, and the amides located at Gln⁴, Asn⁵ and C-terminal Gly⁹ are all susceptible to deamidation under acidic conditions by acid hydrolysis and at neutral / basic conditions *via* the formation of cyclic intermediates.^{22,23}

The major position of degradation, however, was found to be the Cys¹-Cys⁶ disulfide bond where a large amount of degradation processes can occur following β -elimination at Cys¹, generating an *N*-terminal enamine and a cysteine persulfide. This facilitates the formation

of trisulfide and tetrasulfide oxytocin, and can also promote formation of oxytocin dimers and larger aggregation products (figure 1.2).¹⁹

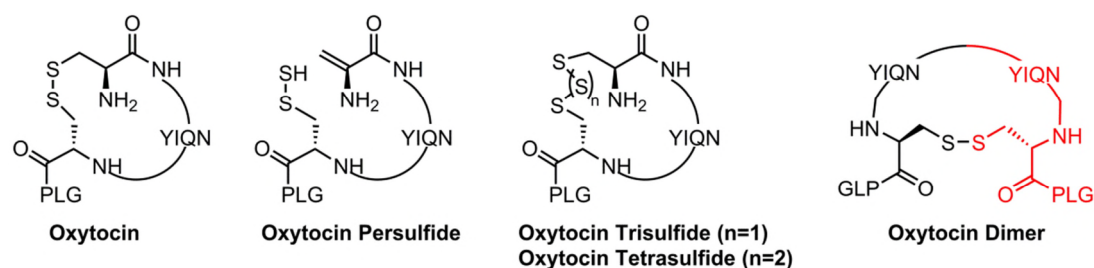


Figure 1.2. Major disulfide degradation product formation from oxytocin according to Wiśniewski.¹⁹

1.1.4. Current solutions for stabilising oxytocin

Previous research in this area has established several methods that may improve the stability of solutions of oxytocin at higher temperatures, to further accommodate the storage facilities in developing countries. Several methods are available, including changes to the peptide structure, as in oxytocin analogues, however, this might not always be desirable as can lead to a loss of affinity in receptor binding or a decrease in biological activity. Another area that has received interest is in changing the storage conditions of the peptide to suppress degradation. Some of these current approaches to improving oxytocin stability are discussed in the following sub-chapters.

1.1.4.1. Oxytocin analogues: carbetocin and desamino-oxytocin

Different analogues of oxytocin have been evaluated with respect to retaining uterotonic activity whilst increasing stability.^{16,24–26} The most well-known oxytocin receptor agonists are desamino-oxytocin and carbetocin, two synthetic peptides exhibiting similar receptor

affinities to oxytocin and which induce contractions via the same mechanism. Both carbetocin and desamino oxytocin exhibit much higher plasma half-lives than oxytocin due to structural changes.^{27–29} Desamino-oxytocin and carbetocin differ from oxytocin by lacking the free amino group at the *N*-terminus, although carbetocin also contains other structural modifications, including replacement of one of the sulphurs at the disulfide bridge with a CH₂ group (figure 1.3).

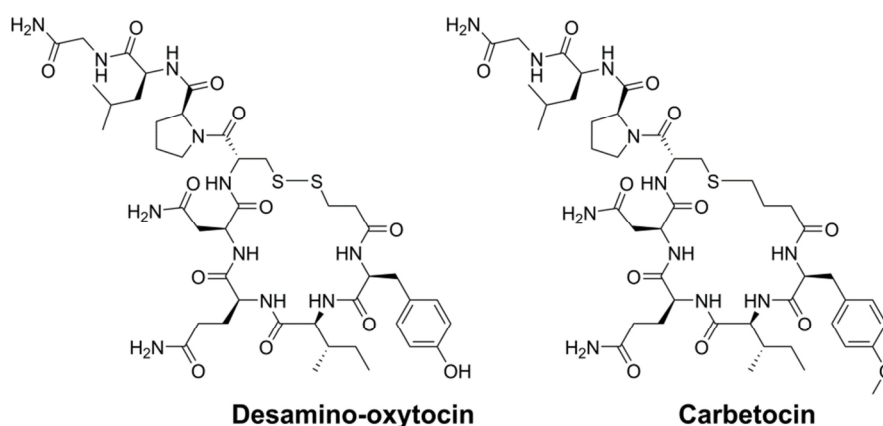


Figure 1.3. Structures of oxytocin analogues: desamino-oxytocin and carbetocin.

Both these oxytocin analogues show a prolonged half-life, with the retention of some uterotonic activity maintained, suggesting that the amino group in oxytocin is not required for biological activity. For carbetocin the increase in half-life is 4- 10 times that of oxytocin, resulting in administration as a single injection rather than a long infusion, and has resulted in carbetocin being approved for medical and veterinary use in many different countries as an effective oxytocin receptor agonist.³⁰

1.1.4.2. Disulfide bond engineering on oxytocin

As the major position of degradation on the peptide is known to be at the disulfide bond a significant amount of research has evolved around different oxytocin analogues where the disulfide bond is replaced in part with other heteroatoms. This is with an aim to avoiding β-

elimination at Cys¹, and as the Cys¹-Cys⁶ disulfide bond is not one of the positions that is directly involved in receptor binding or action it was envisaged that not all biological activity would be lost.

This was initially investigated in the 1960s and 1970s, to establish whether activity was maintained if either one or both thiols within the disulfide bond were altered to CH₂ groups, as in carbetocin.^{31–33} It was found that activity was still observed, although this was moderately suppressed, particularly on altering the ring size of the peptide, but that overall the presence of a disulfide bridge was not a prerequisite for biological activity to be maintained.

Recent studies by Alewood and co-workers have focussed on the replacement of the disulfide with thioether, selenysulfide, diselenide and ditelluride bridges, and the synthesis of a variety of oxytocin analogues containing altered disulfide bonds (figure 1.4). The resulting binding and activity at the human oxytocin receptor was investigated alongside any changes to the metabolic stability in human plasma.^{34,35}

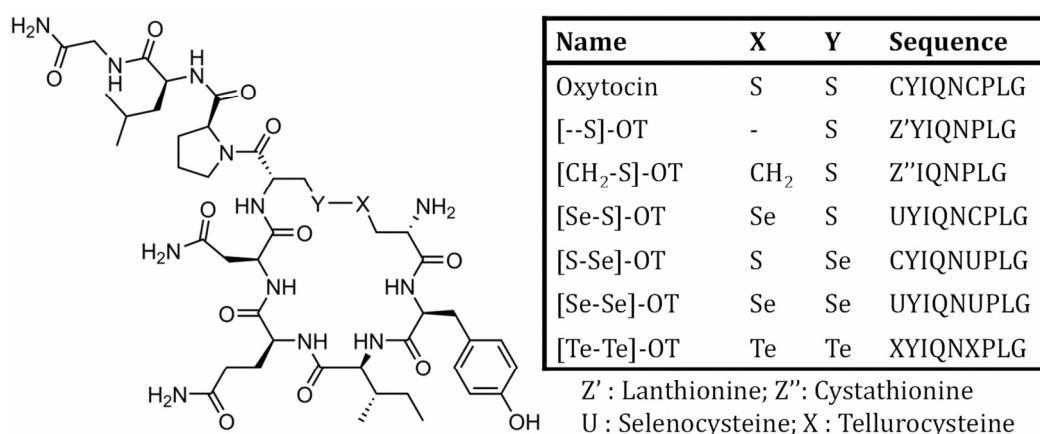


Figure 1.4. Oxytocin analogues, with disulfide bond replacements investigated for uterotonic activity and plasma stability by Alewood.³⁴

They found that a reduction in ring size ([--S]-OT) cause a dramatic (1000-fold) loss of binding affinity and biological activity, although replacement of the S atom in cysteine with a CH₂ group ([CH₂-S]-OT) retained binding affinity and activity. The replacement of cysteine with selenocysteine or tellurocysteine did not have a large effect on the functional activity, although a 10-fold decrease in binding affinity was observed upon replacement of both cysteines (although not when only replacing one cysteine). It was also discovered that by replacing the disulfide bridge (-S-S-) with non-reducible selenoether bonds (-Se-CH₂-), large improvements (1.5 – 3-fold) can be observed in the stability in human plasma, as well as under high thermal stressing (55 °C), as observed by RP-HPLC and LC-MS.

1.1.4.3. Storage buffers containing metal ions

Oxytocin is well-known to be most stable at slightly acidic pH (pH ~ 4.5). At highly acidic pHs (pHs < 3) the peptide can undergo hydrolysis, while at neutral or basic pHs the dimerisation or formation of aggregates around the disulfide bond result in deactivation of the peptide.^{18,36} Work was carried out by Avanti *et al.* on the stabilisation of aqueous solutions of oxytocin by using different storage buffers (citrate, acetate or aspartate, pH 4.5) in combination with various monovalent (Na⁺ and K⁺) or divalent (Ca²⁺, Mg²⁺ and Zn²⁺) metal ions.^{37–40}

Upon storage of oxytocin in unbuffered solutions containing Ca²⁺ (50 mM) and Zn²⁺ (2–50 mM), recovery was promoted from ~ 60 % to ~ 100 % on storage at 4 °C, however, the improvement at higher temperatures were not significant. The combination of divalent metal ions and citrate buffer, however, vastly improved the stability to high temperatures (55 °C), at metal ion concentrations as low as 2 mM.⁴⁰ Similar results were achieved when the metal ions were used in combination with aspartate buffer, where Zn²⁺ ions were shown to be the most effective in increasing solution stability.^{38,39}

It was also proven that after high temperature stressing at 70 °C the degradation products arising from the disulfide bond (trisulfide and tetrasulfide) were severely suppressed by the addition of zinc metal ions in citrate buffer by 20 – 70 %. NMR studies confirmed that the Cys¹-Cys⁶ disulfide bond was being more efficiently protected, by minor conformational changes, suppressing intermolecular interactions at this position.³⁸

1.1.4.4. Dry powder formulations

A further approach that has been evaluated for providing heat stability to oxytocin is the formulation of oxytocin as a dry powder for potential use *via* an inhalation administration technique as opposed to the more common parenteral delivery route. Oxytocin can be spray-dried as an ultrafine powder or in particle form, and is adsorbed very rapidly on delivery to the lungs and counteracts the need for aqueous solutions. Work carried out by McIntosh *et al.* formulated oxytocin particles using a carrier mixture of 1:1:1 glycine: leucine: mannitol resulting in particles with a size of 1–5 µm.⁴¹

The formulations proved effective in *ex-vivo* isolated tissue contractility studies (human and bovine uterine samples), with similar results for the spray dried formulation compared to the native peptide, and no contractility response observed for tracheal tissue. *In-vivo* activity was monitored by electromyographic activity and was found to mimic that of the normal parenteral route, with significantly faster onset of contractions. Importantly, these formulations should remain stable even under extreme environmental conditions (including temperatures up to 50 °C).⁴²

1.1.4.5. Previous oxytocin conjugation strategies

To the best of our knowledge, upon commencing this project we could only find three incidences of conjugation strategies focused upon attachment of macromolecules and oxytocin, none with an aim to improving the solution stability of this vital therapeutic.

Due to the overexpression of cell-surface oxytocin receptors on specific cancer cells, Cavallaro *et al.* used oxytocin as a targeting moiety for a macromolecular conjugate containing the well-known antitumor agent paclitaxel.⁴³ *N*-succinyl-oxytocin was functionalised at the *N*-terminal amine with α,β -poly(*N*-2-hydroxyethyl)-DL-aspartamide-poly(ethylene glycol)₂₀₀₀ (PHEA-PEG₂₀₀₀) followed by introduction of 2'-*O*-succinylpaclitaxel resulting in PHEA-PEG₂₀₀₀-succinyloxytocin-succinylpaclitaxel. *In-vitro* hydrolysis studies revealed that the conjugates were stable at pH 7.4 and in plasma, and *in-vitro* cell activity testing suggested that the incorporation of oxytocin slightly improved the activity compared to paclitaxel and the carrier without the peptide.

In a further study, β -cyclodextrin, a water soluble cyclic oligosaccharide, was successfully employed in the functionalisation of oxytocin using carboxy coupling chemistry (activated using 1-hydroxybenzotriazole and dicyclohexylcarbodiimide).⁴⁴ The β -CD-OT conjugate was evaluated for contractile potency and, although this was found to be less than the native peptide, contractions were still evident at $<\mu\text{M}$ concentrations. It was further believed that this hydrophilic targeted carrier could form a host-guest complex with prostaglandins used as labour inducers, or with anticancer drugs.

Hudnut and Cook filed a patent in 2004 for the incorporation of oxytocin (and some oxytocin analogues) into poly(lactic-co-glycolide) microcapsules, and their subsequent *in vitro* release.⁴⁵ This was for the application of potential therapeutic treatment of a variety of social and behaviour conditions, under which oxytocin plays a role.

1.2. Site-selective protein/peptide conjugation strategies

1.2.1. PEGylation

The most commonly utilised polymer for protein or peptide conjugation is poly(ethylene glycol) (PEG) usually in the form of monomethoxy PEG (mPEG), synthesised by anionic ring opening polymerisation. PEG has many advantages which have inspired use within the polymer therapeutics and drug delivery fields, particularly for covalent attachment to peptides and proteins (PEGylation) (figure 1.5). PEGylation was first achieved in 1977 by Abuchowski *et al.* for the covalent attachment of 2 kDa and 5 kDa PEGs using cyanuric chloride coupling.^{46,47}

PEG has a high solubility in both aqueous and organic solvents, making modifications simple. The hydrophilicity of PEG is not observed for similar structured polymers (*e.g.* poly(methylene oxide) or poly(propylene oxide)).⁴⁸ PEG is classified as a Generally Regarded As Safe (GRAS) chemical, with toxicity only observed at high doses and overall very high biocompatibility.⁴⁹ PEGylation can have beneficial properties on stability, protecting against enzyme degradation and prolonging *in-vivo* half-lives of the conjugate, providing shielding of the protein or peptide, and thus reduce dosage requirements.^{50,51} The addition of this multi-functional polymer can also improve water solubility and shield potential charges thereby creating a 'stealth' effect.⁵²

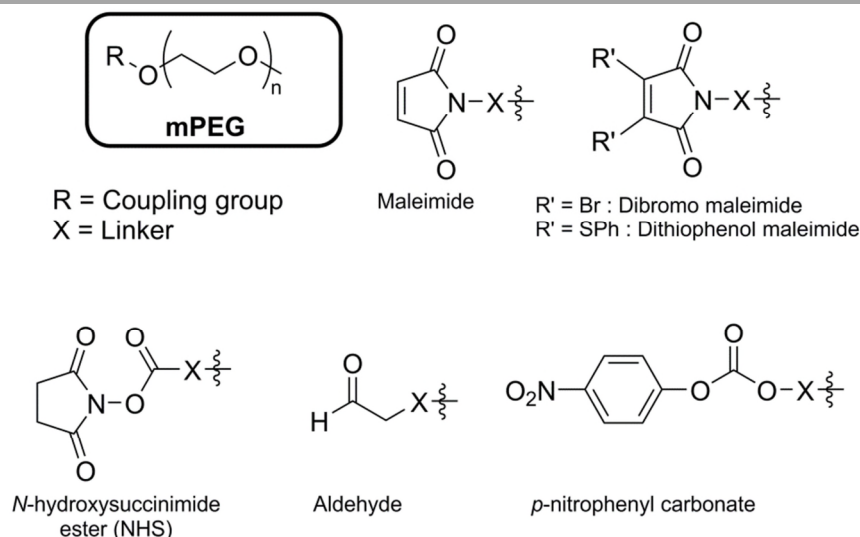


Figure 1.5. Structure of mPEG and some functional site-selective conjugating groups.

PEGylation, however, is not completely without disadvantages, with PEGylated products often leading to the suppression of biological activity post-conjugation due to a shielding of the active residues on the biomolecule, by the polymer.^{53–55} Additionally, PEG does not biodegrade in the body, and this can lead to accumulation and vacuolisation in the liver, kidneys and other vital organs, particularly at molar masses above 20 kDa, alongside the potential for containing toxic side-products if non-pharmaceutical grade PEG is used.^{52,56} A further major problem is that PEG products can cause an immunological response by activation of the immune system.⁵²

Even with these disadvantages PEG is still the number one polymer utilised in polymer therapeutics and drug formulations, and the gold standard for conjugation of proteins and polymers.

1.2.1.1. Current FDA approved PEG conjugates

Since the introduction of covalent attachment of PEG to proteins, there have been various reports on the attachment of PEG to proteins, peptides and therapeutics. It has been

demonstrated that PEGylation can improve a variety of characteristics for the biomolecule including pharmacological properties. This has resulted in several PEGylated proteins receiving Food and Drug Administration (FDA) approval. Many others, including some peptide polymer conjugates, are currently in clinical trials seeking approval. In 2011, Alconcel, Baas and Maynard reviewed the current FDA approved PEGylated products available on the market, and the possible outlooks for the protein PEGylation field.⁵⁷

Table 1.1. Different FDA approved PEGylated products available on the commercial market.⁵⁷

#	Protein	PEG Size	Drug Name	Site of attachment	Drug Use
1	Adenosine deaminase	5 kDa	Adagen	Lys, Ser, Tyr or His	Enzyme- treat severe combined immunodeficiency disease
2	Anti-TNG α Fab'	40 kDa	Cimzia	C-Terminal Cys	Monoclonal antibody drug- treat Crohn's disease and rheumatoid arthritis
3	Anti-VEGF	40 kDa	Pegaptanib /Macugen	Lys	Anti-angiogenic – Treat age-related macular degeneration
4	L-Asparaginase	5 kDa	Oncaspar	Lys, Ser, Tyr or His	Antineoplastic drug- treat lymphoblastic leukemia
5	Continuous erythropoietin receptor activator	30 kDa	Mircera	Lys ⁵² or Lys ⁴⁶	Treat renal anemia in patients with chronic kidney disease
6	G-CSF	20 kDa	Neulasta	N-Terminal Met	Growth factor – manage febrile neutropenia
7	hGH antagonist B2036	5 kDa	Somavert	Lys or N-Terminal Phe	Growth hormone receptor antagonist – treat acromegaly
8	Interferon α -2a	40 kDa	PEGASYS	Lys ³¹ , Lys ¹²¹ , Lys ¹³¹ or Lys ¹³⁴	Treat chronic hepatitis C

9	Interferon α -2b	12 kDa	PEGINTRON	His ³⁴	Treat chronic hepatitis C
10	Mammalian urate oxidase	10 k Da	Krystexxa	Lys	Treat chronic gout refractory

A variety of different conjugation chemistries are used for PEG attachment to the protein of interest including *N*-hydroxy succinimidyl ester (NHS): (**1,4,5,7,8,9**), maleimide (**2**), aldehyde (**6**) and *p*-nitrophenol (**10**). Overall the attachment of PEG can reduce clearance of drugs, shield drugs from the immune system and slow enzymatic degradation; however, most of these FDA approved drug conjugates show multisite attachment, which can lead to reductions in remaining biological activity and heterogeneity in the product distribution.

A wide variety of different functional PEGs are available for conjugation at site-selective positions on proteins or peptides using different coupling chemistries, including at amino and thiol functionalities found naturally within peptide structures. There are various different strategies which have been developed over the last 40 years that can be used for selective conjugation.

1.2.2. Amine targeting strategies

The most common strategy for site selective targeting within peptides or proteins is the targeting of amino groups located either on lysine side chains or at the *N*-terminal amine. Most proteins usually have ~ 10 % lysine within the amino acid sequences, and therefore this gives a convenient target for attachment of several side chains. Multiple attachments, however, may not always be desirable as this can lead to more complicated characterisation of conjugation and potentially high losses of biological activity. Conjugations are also able to take advantage of the difference in pK_a between the α -amino

residue of the *N*-terminus ($pK_a = 7.6 - 8$) and ϵ -amino residue of lysine chains ($pK_a = 9.3 - 9.5$) for more selective couplings to occur.⁵⁸

1.2.2.1. *N*-Hydroxysuccinimidyl esters (NHS)

One of the most utilised conjugation strategies for conjugation of amino groups is the use of activated esters, of which *N*-hydroxysuccinimide (NHS) activated esters have been commonly employed, as acylating reagents, since their introduction to peptide conjugation in the 1960s.⁵⁹ NHS ester reagents react with nucleophiles (such as nucleophilic amines), with the release of *N*-hydroxy succinimide resulting in a stable amide linkage to the peptide or protein (figure 1.6).

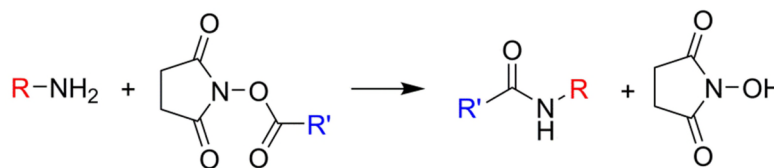


Figure 1.6. Reaction of NHS ester and a model peptide.

The NHS reagent, however, undergoes rapid hydrolysis in water resulting in a loss of the succinimidyl ester conjugating group, with half-life decreasing dramatically upon increasing pH.⁶⁰⁻⁶² Sulfonated-NHS esters add a charged sulfonate group, for which molecules undergo hydrolysis more gradually, as well as improving water solubility, allowing coupling reactions to be carried out in aqueous conditions. It has also been reported that succinimidyl reagents may not react site-specifically with amines, exhibiting reactivity to other nucleophilic amino acids residues such as tyrosine, histidine and serine, although generally at a slower rate to amino coupling.

1.2.2.2. Aldehyde

Aldehyde reagents readily react with amino groups, initially *via* the formation of imine (Schiff base) products. These reversible Schiff bases are readily reduced into stable secondary amines by the addition of a reducing agent such as sodium borohydride (NaBH_4) or sodium cyanoborohydride (NaCNBH_3), in a process referred to as reductive amination (figure 1.7). NaCNBH_3 is generally preferred for the reductions as it is a milder reducing agent, thus selectively reducing the Schiff base product without also reducing the aldehyde or other less reactive carbonyls present in the reaction.^{63,64}

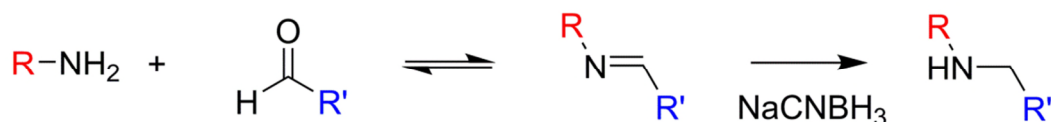


Figure 1.7. Two step reductive amination of aldehyde *via* Schiff base intermediate.

pH is highly important in aldehyde couplings, where reductive amination proceeds fastest at pH 6.5-8.5, although manipulating the pH to slightly acidic conditions can also allow for selective coupling of the *N*-terminus over more basic lysine residues.⁶⁵⁻⁶⁷

1.2.2.3. Carboxylic acid

The coupling of carboxylate groups with amines has been well reported, leading to the formation of amide linkages.⁶⁸ This is generally performed through the use of coupling reagents including carbodiimides such as 1-ethyl-3-(3-dimethylaminopropyl)carbodiimide.HCl (EDC) or dicyclohexylcarbodiimide (DCC), which activate the carboxyl groups for substitution by reactive amines (figure 1.8).^{69,70}

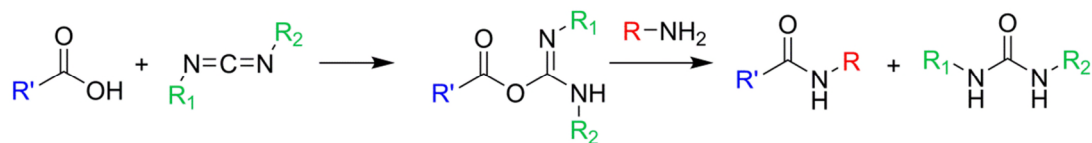


Figure 1.8. Carbodiimide mediated reaction between amino group and carboxylic acid reagent.

1.2.2.4. Other amine reactive groups

Other than those already discussed, there are a variety of other functional groups which can be utilised for conjugation to amino groups on peptides or proteins *via* alkylation or acylation reactions. These include cyanuric chloride,^{46,47} isocyanate,⁷¹ imidoester,⁷² epoxide,⁷³ and several activated ester routes such as *p*-nitrophenyl carbonates,⁷⁴ trichlorophenyl carbonate,⁷⁴ imidazole carbamate^{75–77} and pentafluorophenyl ester.⁷⁸

1.2.3. Thiol targeting strategies

An alternative approach for the conjugation of polymers onto peptides or proteins is the site specific targeting of thiol groups presented by free cysteine residues, or from the reduction of disulfide bonds. This can be beneficial as often there are fewer thiol functionalities (particularly as free cysteines) present on peptide or protein structures compared to amino groups allowing a more site-specific modification. The thiol side chain acts as a mild nucleophile, which can be exploited in the chemical modification of proteins, usually *via* alkylation reactions with a variety of reagents, although intra- and/or intermolecular formation of disulfides is also possible.^{79,80}

1.2.3.1. *N*-Substituted maleimide reagents

One of the most widely used reactive groups for selective cysteine modification within conjugation chemistry are maleimides.⁸¹ There are several *N*-functionalised maleimide reagents available for the selective alkylation reaction to thiols using the maleimide double bond in an irreversible manner. This occurs by an irreversible thiol-Michael addition reaction, changing the nature of the conjugating reagent by removing the double bond (where the product becomes a substituted succinimide). Maleimides may also react with amino groups, but the reaction can be pH controlled to be selective towards the sulfhydryl groups (pH 6.5 -7.5).^{82,83}

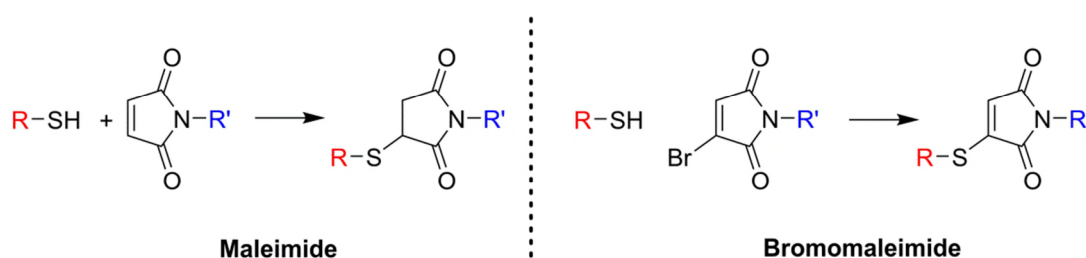


Figure 1.9. Conjugation reactions of sulfhydryls utilising maleimide (addition) or bromomaleimide (substitution).

In 2009-2010 Baker *et al.* reported the use of a new bromomaleimide reagent, similar to maleimides, for selective and rapid conjugation to cysteine residues (figure 1.9).^{84,85} Utilising bromomaleimide allowed reversible conjugations, *via* a substitution reaction, to occur for temporary cysteine modification, which could allow protein/peptide release upon the addition of phosphines, or excess thiols, thereby restoring activity to the protein or peptide of interest. Competitive reactions for the conjugation of cysteine between maleimide and bromomaleimide also show that bromomaleimide reacts more rapidly than maleimides.⁸⁴

1.2.3.1. 'Thiol-ene'

It is well known that thiol groups can undergo hydrothiolation reactions with unsaturated bonds (alkenes or alkynes), called 'thiol-ene' or 'thiol-yne', which can be exploited for bioconjugation at cysteine residues within peptides or proteins (figure 1.10).⁸⁶⁻⁹⁰ Thiol-ene reactions are able to proceed *via* anti-Markovnikov, *via* light- and/or initiator induced radical addition, or alternatively by nucleophile or base catalysed Michael addition to activated alkenes.^{91,92}

In research conducted by Jones *et al.* the disulfide bond of a peptide could be reduced and modified *in situ* through the α,β -unsaturated vinyl group of PEG acrylate, utilising a water-soluble phosphine for the reduction of the disulfide and subsequent catalyst for thiol-ene Michael addition.⁹³ This resulted in the PEGylation of both sulfhydryl residues and was further expanded upon for the synthesis of a peptide macroinitiator for a grafting-from approach.⁹⁴ Overall this provides an accessible route to non-bridging thiol reactive chemistry, with quantitative modifications and short reaction times, alongside aqueous compatibility and mild reaction conditions.

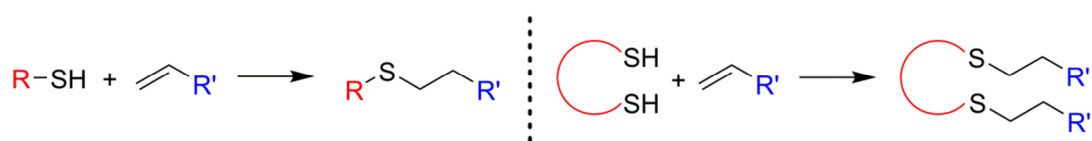


Figure 1.10. Thioether bond formation using 'thiol-ene' chemistry, and double conjugation at reduced disulfide bond.

1.2.3.2. Pyridyl disulfide

An alternative strategy which takes advantage of the synthesis of a disulfide linkage between the polymer and protein is the use of pyridyl disulfide functional groups, which

readily undergo disulfide exchange reactions.⁹⁵ The resulting disulfide bonds are biochemically labile, thus *in-vivo* regeneration of active biomolecules is possible using this methodology, and as such provides a valuable releasable conjugation approach.^{96–98}

1.2.4. Disulfide bridging chemistry

Alongside the addition to cysteines, it may not always be advantageous to reduce the disulfide bond within proteins or peptides, as this could be vital for maintaining tertiary/quaternary structure and/or biological activity.^{99–101} Recently some conjugation strategies have been reported to circumvent these problems by allowing rebridging of reduced disulfide bonds with 2 or 3 carbon disulfide bridges, thereby causing less disruption to the native structure.

1.2.4.1. Dibromo/dithiophenolmaleimide two-carbon disulfide bridging

Following on from their work on bromomaleimide as a cysteine conjugating reagent, Baker and Caddick reported that dibromomaleimides could function as potential disulfide bridging agents, that can insert into a reduced disulfide bond, introducing a two carbon maleimide linkage.⁸⁵ The maleimide insertion is still reversible under a high excess of thiol reagents, and the dibromomaleimide reagent can easily be modified for the addition of desired functionality to the peptide in a reversible manner.¹⁰² Jones *et al.* reported the use of PEGylated dibromomaleimide as a convenient (and reversible) reagent for disulfide bridging PEGylation of peptides.¹⁰³

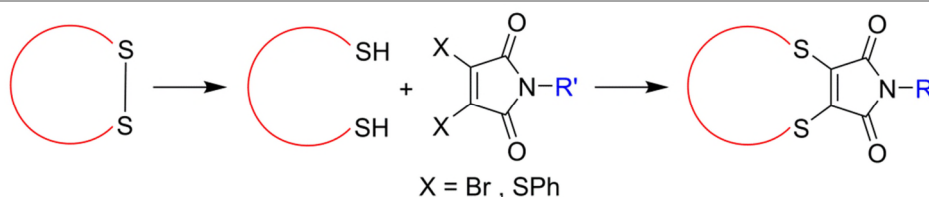


Figure 1.11. Disubstituted maleimides for disulfide bridging of peptides.

Maleimide disulfide bridging chemistry was then expanded upon with the introduction of dithiomaleimides, which were able to undergo disulfide bridging reactions in a similar manner to dibromomaleimide (figure 1.11).^{104,105} In 2013 O'Reilly and coworkers reported that when disubstituted maleimides are used for peptide conjugations, fluorescence is induced within the peptide conjugate structure.¹⁰⁶ This fluorescence is quenched prior to conjugation (as in dithiophenolmaleimide), with fluorescence being exhibited on dithioalkylmaleimides (in the case of peptide conjugation, the peptide acts as a long alkyl group). This provides a convenient method for confirming peptide conjugation as well as fluorescently labelling biomolecules of interest.^{107,108}

1.2.4.1. Arsenic compounds for disulfide bridging

A more recent and elegant strategy that has been developed by Wilson and coworkers is the use of arsenic containing molecules as disulfide bridging agents.¹⁰⁹ The reactions exploit the affinity of the As(III) group for closely spaced chelating thiols (such as those derived from reduced disulfide bonds). This allows the efficient rebridging of reduced disulfide bonds to be realised as an alternative to dibromo/dithiophenolmaleimide bridging. The arsenic conjugates were found to be reversible in the presence of stringer chelating dithiols, such as reduced lipoic acid, allowing a release mechanism to be realised.

1.2.4.2. Vinyl sulfone conjugation/bis-sulfone three-carbon disulfide bridging

Vinyl sulfones are a class of reagents which site-specifically react *via* sequential Michael-type addition of sulfhydryl groups at slightly alkaline pHs, to yield stable β -thioether linkages.^{110–112} In 2006 Brocchini *et al.* suggested a selective method for targeting and rebridging disulfide bonds, *via* a three carbon bond linker based on the reactions of thiols with vinyl sulfone (figure 1.12).^{113–117}

A bis-sulfone reagent was synthesised which can be used for site-specific peptide modification, and in particular the rebridging of reduced disulfide bonds, in a similar manner to dibromo/dithiophenolmaleimides. After reduction of the disulfide bond using standard procedures, an addition elimination of the α,β -unsaturated β' -monosulfone is undertaken with the first thiol. This in turn generates a second double bond which can undergo another addition with the second thiol. The conjugation yields a three-carbon bridge across the previous position of the disulfide retaining the structure of the peptide, and potentially preventing a complete loss of activity.¹¹³

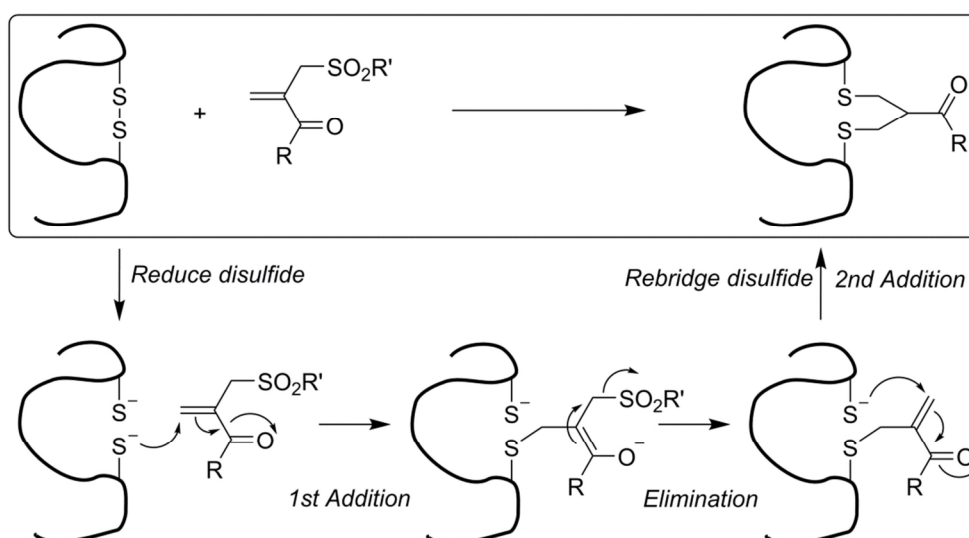


Figure 1.12. Mechanism of bis-sulfone three carbon disulfide bridging.

1.2.5. Other site specific targeting strategies

As well as the conjugation at amino and thiol functionalities on peptides or proteins, which will be discussed throughout this thesis, other amino acids can be presented as target sites for selective conjugation. These include specific conjugations at tyrosine, tryptophan and histidine amongst other natural amino acids.¹¹⁸

Tyrosine is another amino acid that is only moderately represented within peptides, where modifications have been reported via iodination,^{119,120} diazonium reagents,^{121–123} Mannich-type modifications^{124,125} and dicarboxylates/dicarboxamides.^{126,127} Tryptophan residues have a low natural abundance (~ 1 %) and accessibility of the residues is often limited. As such, residue specific modifications have been reported for the indole nitrogen of the Trp side chain by the use of malondialdehydes¹²⁸ and metallocarbenoids, such as rhodium carbenoids.^{129,130} Histidine possesses a pK_a in the physiological range, meaning both acid and basic forms are present at physiological pH and is therefore vital in several enzyme mechanisms as abstraction or donation of protons can occur. Histidine modifications have previously been reported including the use of aldehydes¹³¹ or epoxides,^{132,133} although reactions are not always site-specific, and other amino acid sidechains will often react preferentially. Histidine modifications are also possible with the use of an engineered polyhistidine-tag amino acid motif (His-tag) of at least 6 histidine residues which can be targeted.^{134,135} Arginine is another amino acid that has previously been targeted, including with phenylglyoxal analogues,¹³⁶ geminal diones¹³⁷ and α -oxo-aldehydegroups.¹³⁸ Arginine conjugation strategies however can be limited by the accessibility of amino acids or expression on the surface, alongside protonation generally occurring at physiological pHs, with less reactivity observed than with lysine residues.

Alongside the targeting of natural amino acids, unnatural amino acids can be introduced thereby incorporating unique chemistries for a fully site-selective approach and dramatically expanding the field of potential conjugation reactions.^{139–141}

Overall the most popular method for the targeting of sites on peptides or proteins is through using amine groups, advantageous due to the high natural abundance on structures. Virtually all proteins contain easily accessible primary amino groups in their structures, and the reactions are particularly ideal for the conjugation at multiple sites. Cysteine modifications are preferential to some other amino acid selective approaches, due to the convenience of a high reactivity coupled with general rarity. Even in proteins containing multiple cysteine residues there is usually a small amount of free sulfhydryls which are accessible on the protein surface, which is ideal if a more site-specific approach is required than could be delivered with amino targeting.¹¹⁸

1.3. Reversible-Deactivation Radical Polymerisations techniques (RDRP)

Following the development of ‘living’ anionic polymerisations by Szwarc in 1956¹⁴², many polymerisation techniques have been developed which maintain living characteristics coupled with robustness of conventional free radical polymerisations. These so called ‘living’ radical or controlled radical polymerisation techniques are often referred to as reversible-deactivation radical polymerisation (RDRP), and achieve control by establishing equilibrium between active radical species and dormant chains.

In RDRP techniques it is assumed that radical concentrations remain low, as the dormant species is favoured which limits termination events and ensures that all polymer chains are growing at similar rates. The field of polymer chemistry has been revolutionised by the

precise control over molecular weight, the molecular weight distribution, or dispersity (\bar{D}), and the high end group fidelities these polymerisation techniques.

1.3.1. Nitroxide mediated polymerisation (NMP)

One of the first examples of RDRP techniques to be explored, nitroxide mediated polymerisation (NMP), relies on a nitroxide free-radical to establish an equilibrium between active and dormant species.^{143,144} The propagating polymer chain is reversibly end capped by a stable alkoxyamine radical, such as that generated by 2,2,6,6-tetramethylpiperidynyl-*N*-oxy (TEMPO) (figure 1.13). The equilibrium is controlled by the strong bond formation between the alkoxyamine radical and the polymeric radical chain end, stabilising the dormant species resulting in a low concentration of the propagating radical.

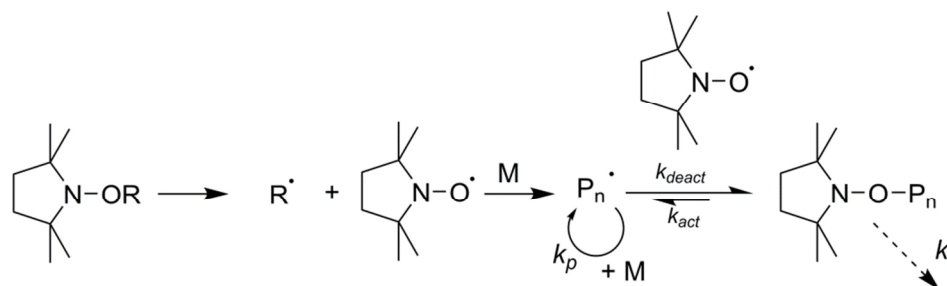


Figure 1.13. NMP polymerisation mechanism.

An advantage of NMP is that it can result in polymers that are not contaminated with metals halides or sulphur, allowing simple purifications. However, disadvantages include the high temperatures required to activate the dormant species (120 – 150 °C) and long reaction times (> 48 hours) required for high yields to be achieved. Since the development of NMP, the technique has been expanded to different monomers, with access to styrene, acrylate, methacrylate and acrylamide polymers, alongside the synthesis of copolymers (block and random), stars and other structures.¹⁴⁵

1.3.2. Reversible addition-fragmentation chain-transfer polymerisation (RAFT)

A polymerisation technique that has more recently been heavily utilised for the controlled synthesis of a wide range of polymeric materials for a variety of purposes is reversible addition-fragmentation chain-transfer polymerisation (RAFT). RAFT was developed in the 1990s by Moad, Rizzardo and Thang, and utilises thiocarbonyl thio species as reversible chain transfer agents (CTAs) to control the polymerisation.¹⁴⁶ A simplified mechanism is displayed in figure 1.14, where initially radicals are generated, *e.g.* thermally from azo- or peroxide compounds, after which these initiate a polymer chain which can add to the CTA. Fragmentation occurs, releasing a radical which can reinitiate polymerisation. Control is maintained by having a smaller number of 'active' chains, compared to 'dormant' CTA end capped chains.

RAFT is particularly useful for its tolerance to a wide range of functional monomers for which it has been previously been applied. These include some monomers less susceptible to polymerisation under other controlled radical polymerisation techniques (for example less activated monomers like vinyl acetate, and *N*-vinyl pyrrolidone).¹⁴⁷

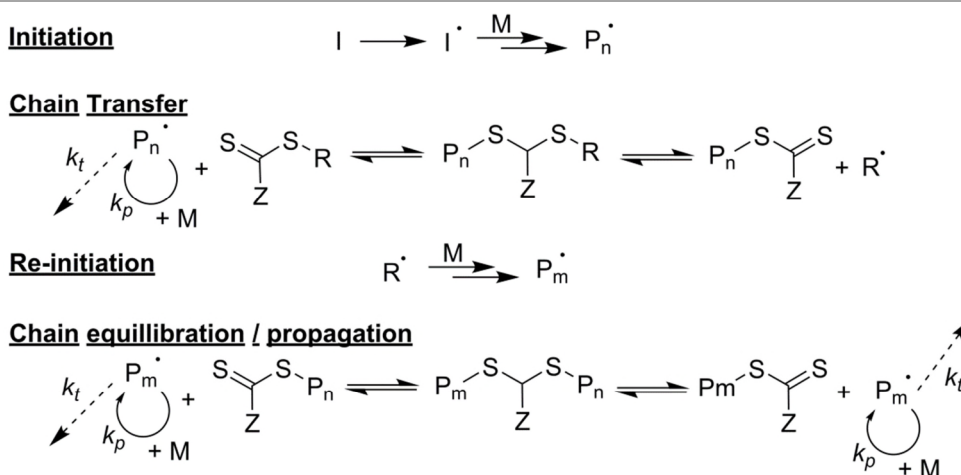


Figure 1.14. RAFT polymerisation mechanism.

The polymerisation system can be tuned to better suit specific monomers or reaction conditions, by careful selection of an appropriate RAFT agent.^{148,149} The introduction of redox RAFT, means there is no longer a requirement for high temperatures to decompose the azo or peroxide initiator, which is useful for a variety of polymers including those exhibiting LCST (lower critical solution temperature) transitions.^{150–152}

1.3.3. Copper mediated polymerisation techniques

Several different techniques have been exploited which utilise transition metals as tools for controlling polymerisation. Transition metal mediated living radical polymerisation (TMMLRP) and atom transfer radical polymerisation (ATRP) were developed by Sawamoto and Matyjaszewski independently in 1995, using ruthenium and copper halide complexes.^{153,154} In the last 20 years the synthesis of polymers utilising various copper salts has generated a high amount of interest alongside a high level of controversy regarding the mechanisms of polymerisation.

1.3.3.1. Atom transfer radical polymerisation (ATRP)

Polymerisations by ATRP generally occur when a copper halide (either Cl or Br) complexed with a nitrogen based ligand $[\text{Cu(I)}(\text{L})\text{X}]$ extracts a halogen from an alkyl halide initiator (or dormant polymer chain) forming the oxidised complex, $[\text{Cu(II)}(\text{L})\text{X}]\text{X}$ and a radical (either on the initiator or polymer chain) (figure 1.15). The radical formed is able to react with monomer thereby adding to the propagating chain (in an active state) until the chain is reversibly deactivated by the re-addition of the halogen (dormant state) from the $[\text{Cu(II)}(\text{L})\text{X}]\text{X}$ complex formed during activation. The equilibrium is highly in favour of the dormant chains, therefore allowing radical concentrations to remain low limiting the amount of termination that is able to occur, resulting in uniform growth of polymer chains.

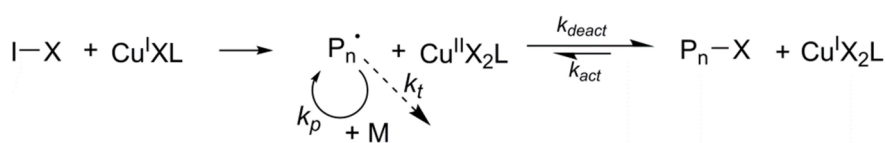


Figure 1.15. ATRP polymerisation mechanism.

In ATRP, at a given monomer conversion assuming 100 % initiator efficiency, molecular weight is predetermined by the ratio between monomer and (alkyl halide) initiator which determines the degree of polymerisation (number of monomer repeat units in the polymer chain). ATRP has been employed for a wide range of monomers including styrenes, (meth)acrylates, acrylonitrile and (meth)acrylamides, and in general polymerisation requires an electron withdrawing group adjacent to the vinyl group. Various polymer architectures can be prepared including linear, star and comb structures. Facile synthesis of block copolymers is also possible, owing to the retention of ω -end group fidelity.¹⁵⁵

1.3.3.2. SET-LRP – Cu(0) mediated polymerisation

In 2006 Percec first reported the synthesis of polymers by single electron transfer living radical polymerisation (SET-LRP) utilising Cu(0) as the active species at 25 °C using nitrogen based ligands and an alkyl halide initiator in polar solvents.¹⁵⁶ Through this work the ‘ultrafast’ polymerisation of ‘ultrahigh’ ($M_n > 10^6$) molecular weight polymers of acrylates, methacrylates and vinyl chloride, with exceptional control ($\bar{D} = 1.1$) was achieved.¹⁵⁷

This polymerisation proceeds in a similar mechanism to ATRP with an equilibrium between an active (propagating polymer chain) and dormant species, however rather than using $[\text{Cu(I)}(\text{L})\text{X}]$, Cu(0) is used and referred to as the activating species, with $[\text{Cu(II)}(\text{L})\text{X}]\text{X}$ still available as the deactivating group (figure 1.16). In this proposed mechanism, the key step is the disproportionation of the $[\text{Cu(I)}(\text{L})\text{X}]$ species into Cu(0) and $[\text{Cu(II)}(\text{L})\text{X}]\text{X}$ required for the polymerisation to occur.

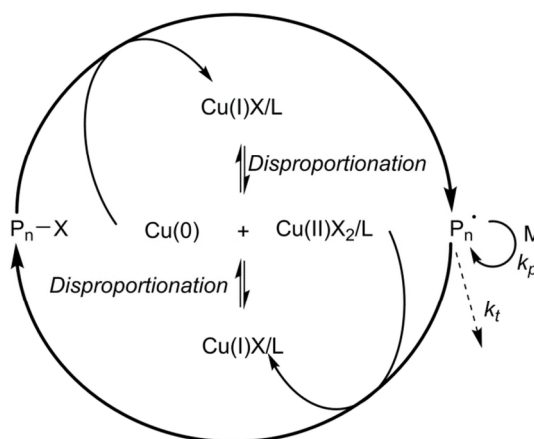


Figure 1.16. SET-LRP mechanism (as proposed by Percec).

Typical ligands used for SET-LRP are nitrogen containing ligands such as Me_6TREN , TREN , PMDETA , and HMTETA , which are able to stabilise Cu^{II} in preference to Cu^{I} . Initiators and monomers utilised for SET-LRP are similar to those for ATRP, with alkyl halide initiators most often being used for the synthesis of poly(meth)acrylates, usually in polar solvents.

Initiator efficiency is generally very high, with molecular weights predetermined as in ATRP by adjusting the ratio between monomer and initiator.¹⁵⁸

SET-LRP is a very useful tool for the designed synthesis of complex polymers and has been used in the synthesis of star polymers^{159,160} and highly sequence controlled multiblock polymers^{161,162} (including glycopolymers)^{163,164} amongst other applications.

1.3.3.3. Aqueous Cu(0) mediated polymerisation

In 2013 members of the Haddleton group reported that efficient polymerisations could be achieved by exploiting the rapid and quantitative disproportionation of Cu(I)Br(L) (L = Me₆TREN) in aqueous solutions into Cu(0) powder and Cu(II)Br₂(L), prior to addition of monomer and initiator.¹⁶⁵ This technique has since been exploited for the controlled polymerisation of acrylates,¹⁶⁶ acrylamides¹⁶⁷ and methacrylates^{168,169} in aqueous, complex,¹⁷⁰ or biologically relevant¹⁷¹ solvent systems.

Polymerisations can achieve high or even quantitative conversions in less than 30 minutes at (or below) ambient temperatures, with controlled chain lengths and narrow molecular weight distributions ($\mathcal{D} < 1.1$). The resulting polymers exhibit high chain-end fidelity and this has further been exploited for the synthesis of multiblock copolymers.¹⁷²

1.4. Controlled radical polymerisations and conjugation

chemistry

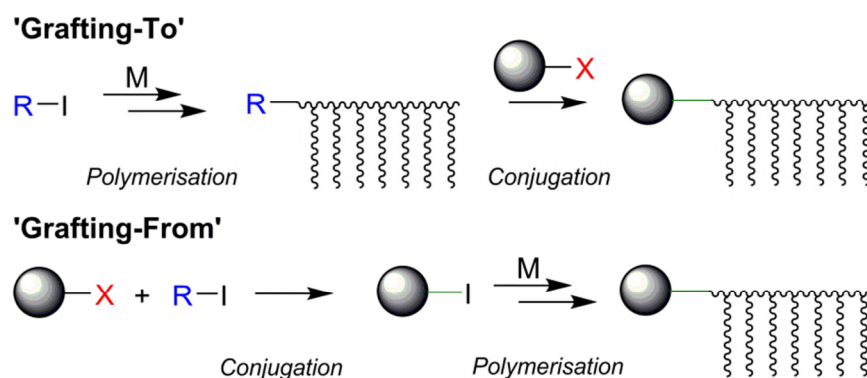


Figure 1.17. Protein polymer conjugation achieved by 'grafting-to' or 'grafting-from' approaches.

With the development of controlled radical polymerisation techniques, the synthesis of innovative bioconjugates has become highly achievable, with a focus on tailoring design to introduce specific and desired properties.^{173,174} There are generally two approaches to polymer-peptide/protein conjugation (figure 1.17). Firstly the synthesis of polymers and subsequent attachment onto the biomolecule of interest, so called 'grafting-to.' Alternatively, polymerisation can occur directly from the peptide/protein with initiating or chain transfer species incorporated, known as 'grafting-from'.

1.4.1. 'Grafting-to'

The simplest way to facilitate post-polymerisation conjugation is *via* the incorporation of functionality on the α - or ω -chain ends of the polymer chain, and then to utilise these for site-directed covalent attachment at complementary amino acid residues present in the target protein/peptide. This is easily incorporated into the ATRP/SET-LRP system by using a functional initiator, and in RAFT with a functional CTA, which can either directly, or after

modification, be used for the conjugation. Side chains can be deprotected during polymerisation, or require post-polymerisation deprotection and work up, if desired functionalities are not compatible with polymerisation techniques. There are a wide variety of different polymers reported in the literature that have been synthesised by RDRP techniques and subsequently attached onto proteins, peptides or other biomolecules.

1.4.1.1. Amino targeting

The incorporation of NHS ester groups into ATRP initiators was used by Lecolley *et al.* for the synthesis of poly(poly(ethylene glycol) methyl ether methacrylate) poly(mPEGMA) using two different *N*-succinimidyl ester functional alkyl halide initiators.⁶² These were subsequently conjugated onto lysozyme with the addition of 6 to 7 polymeric chains. The same initiators were used by Lutz *et al.* for the controlled ATRP synthesis of copolymers of 2-(2-methoxyethoxy)ethyl methacrylate (MEO₂MA) and poly(ethylene glycol) methyl ether methacrylate (mPEGMA) and subsequent conjugation onto trypsin.¹⁷⁵ More recently a PEG alternative, poly(carboxybetaine methacrylate) has been synthesised by ATRP and conjugated onto α -chymotrypsin using the same chemistry.¹⁷⁶ Nicolas *et al.* reported the synthesis of *N*-hydroxysuccinimidyl ester containing alkoxyamines for the synthesis of polyPEGs by NMP and the conjugation onto a model amine, a tripeptide and lysozyme.¹⁷⁷ RAFT has also been utilised for the synthesis and post-polymerisation conjugation of NHS polymers including poly(vinyl pyrrolidone).¹⁷⁸

Aldehyde chemistry can also be utilised for grafting-to approaches and a protected aldehyde ATRP initiator was introduced by Haddleton and co-workers in 2004.¹⁷⁹ This incorporates an acetal protecting group which can easily be removed post-polymerisation for conjugation onto the amino groups within peptides or proteins. Polymers synthesised

in this manner have been described for conjugation onto lysozyme,¹⁷⁹ salmon calcitonin^{65,180} and interferon-alpha.¹⁸¹

1.4.1.2. Thiol targeting

Maynard reported in 2004 the incorporation of a pyridyl disulfide RAFT CTA for the post-polymerisation conjugation of sulfhydryl groups found at cysteine residues.⁹⁸ The same group has recently reported the synthesis of trehalose glycopolymers utilising a different pyridyl disulfide CTA and conjugation to thiolated hen egg white lysozyme as a method for increasing protein stability to lyophilisation or heating.¹⁸² The incorporation of RAFT CTAs within the polymer result in an easy location for post polymerisation modification, wherein the dithioester or trithiocarbonate can easily be reduced to a thiol and subsequently modified such as with divinyl sulfone functionality for post-polymerisation conjugation.¹¹¹

As an alternative approach, Mantovani *et al.* reported the preparation of furan protected maleimide end functional poly(mPEGMA),¹⁸³ multifunctional triblock copolymers¹⁸⁴ and glycopolymers¹⁸⁵ by ATRP, which could be deprotected post polymerisation and conjugated onto BSA by thiol-maleimide coupling. Stenzel *et al.* reported the use of a similar furan protected maleimide CTA for the RAFT synthesis of poly(mPEGMA) and poly(methyl methacrylate) which, after deprotection *via* reflux, were conjugated onto the thiol group of Cys³⁴ on albumin.^{186–188}

Disulfide bridging chemistry has also been exploited using RDRP techniques for the synthesis of polymers containing end groups capable of rebridging reduced disulfide bonds. This was used by Jones and co-workers for two carbon disulfide rebridging of salmon calcitonin using disubstituted maleimide α -end functional polymers synthesised by ATRP.^{103,105} This could be performed by post-polymerisation modification of polymers to

contain dibromomaleimide end group functionality, or by directly using a dithiophenol maleimide initiator which, unlike dibromomaleimide, is compatible with the polymerisation conditions.

Additionally three carbon disulfide bridging has been reported with a bissulfone functional poly(2-methacryloyloxyethyl phosphorylcholine) synthesised by ATRP.¹⁸⁹ Wilson reported the use of an arsenic functional initiator for SET-LRP and subsequent bridging of disulfide bonds with a non-carbon arsenic linker.¹⁰⁹

1.4.2. 'Grafting-from'

As well as employing polymers synthesised in a traditional manner by copper mediated polymerisation or RAFT polymerisation that involve the post-polymerisation conjugation, strategies are available that utilise a peptide macroinitiator (or a macro CTA) in a 'grafting-from' technique. This method of protein/peptide modification can prove highly useful as purification of polymers prior to addition is not required, and the characterisation of the macroinitiator/macro CTA is often simpler than a polymer-conjugate in terms of identification of the specific site of conjugation. Additionally there is no longer any excess polymer present as an impurity within the conjugate solutions, which would generally lead to difficult purification procedures.

This was first reported by Bontempo and Maynard in 2005 where an ATRP initiator incorporating biotin was conjugated onto streptavidin,¹⁹⁰ followed by BSA¹⁹¹ and lysozyme¹⁹¹ using pyridyl disulfide thiol coupling, from which *N*-isopropylacrylamide was polymerised.

Jones reported the utilisation of thiol-ene chemistry for the synthesis of a protein macroinitiator and used this to polymerise ethylene glycol containing monomers using SET-

LRP. The peptide modification for incorporation of RAFT macro CTAs and alternative halide initiators has also been achieved utilising different conjugation chemistries.^{192–194}

1.5. References

- 1 H. H. Dale, *J. Physiol.*, 1906, **34**, 163–206.
- 2 V. Du Vigneaud, C. Ressler and S. Trippett, *J. Biol. Chem.*, 1953, **205**, 949–957.
- 3 V. Du Vigneaud, C. Ressler, J. M. Swan, C. W. Roberts and P. G. Katsoyannis, *J. Am. Chem. Soc.*, 1954, **76**, 3115–3121.
- 4 https://www.nobelprize.org/nobel_prizes/chemistry/laureates/1955/, Accessed June 2016.
- 5 K. S. Khan, D. Wojdyla, L. Say, A. M. Gülmezoglu and P. F. A. Van Look, *Lancet*, 2006, **367**, 1066–1074.
- 6 M. C. Hogan, K. J. Foreman, M. Naghavi, S. Y. Ahn, M. Wang, S. M. Makela, A. D. Lopez, R. Lozano and C. J. L. Murray, *Lancet*, 2010, **375**, 1609–1623.
- 7 <http://www.un.org/sustainabledevelopment/health/>, Accessed June 2016.
- 8 <http://www.who.int/mediacentre/factsheets/fs348/en/>, Accessed June 2016.
- 9 K. L. Maughan, S. W. Heim and S. I. M. S. Galazka, *Am. Fam. Physician*, 2006, **73**, 1025–1028.
- 10 C. Moir, *Proc. R. Soc. Med.*, 1939, **32**, 928–929.
- 11 P. W. Van Dongen, J. Van Roosmalen, C. N. De Boer and J. Van Rooij, *Pharm. Weekbl. Sci.*, 1991, **13**, 238–243.
- 12 *WHO recommendations for the prevention and treatment of postpartum haemorrhage*, World Health Organization, Geneva, 2012.
- 13 <http://www.who.int/medicines/publications/essentialmedicines/en/>, Accessed June 2016.
- 14 H. H. Zingg and S. A. Laporte, *Trends Endocrinol. Metab.*, 2003, **14**, 222–227.
- 15 N. Vrachnis, F. M. Malamas, S. Sifakis, E. Deligeoroglou and Z. Iliodromiti, *Int. J. Endocrinol.*, 2011, **2011**, Article ID 350546.
- 16 M. Manning, A. Misicka, A. Olma, K. Bankowski, S. Stoev, B. Chini, T. Durroux, B. Mouillac, M. Corbani and G. Guillon, *J. Neuroendocrinol.*, 2012, **24**, 609–628.
- 17 R. Walter, I. L. Schwartz, J. H. Darnell and D. W. Urry, *Proc. Natl. Acad. Sci. U. S. A.*, 1971, **68**, 1355–1359.
- 18 A. Hawe, R. Poole, S. Romeijn, P. Kasper, R. Van Der Heijden and W. Jiskoot, *Pharm. Res.*, 2009, **26**, 1679–1688.

-
- 19 K. Wiśniewski, J. Finnman, M. Flipo, R. Galyean and C. D. Schteingart, *Biopolymers*, 2013, **100**, 408–421.
 - 20 J. W. Gard, J. M. Alexander, R. E. Bawdon and J. T. Albrecht, *Am. J. Obstet. Gynecol.*, 2002, **186**, 496–498.
 - 21 V. Kumar, R. Madabushi, H. Derendorf, L. A. Boothby, B. D. Breland, R. C. Hatton and P. L. Doering, *J. Liq. Chromatogr. Relat. Technol.*, 2006, **29**, 2353–2365.
 - 22 M. C. Manning, D. K. Chou, B. M. Murphy, R. W. Payne and D. S. Katayama, *Pharm. Res.*, 2010, **27**, 544–575.
 - 23 M. L. Houchin, K. Heppert and E. M. Topp, *J. Control. Release*, 2006, **112**, 111–119.
 - 24 B. Berde, W. Doepfner and H. Konzett, *Br. J. Pharmacol. Chemother.*, 1957, **12**, 209–214.
 - 25 M. Manturewicz, Z. Grzonka, L. Borovicková and J. Slaninová, *Acta Biochim. Pol.*, 2007, **54**, 805–811.
 - 26 K. Wiśniewski, S. Alagarsamy, R. Galyean, H. Tariga, D. Thompson, B. Ly, H. Wiśniewska, S. Qi, G. Croston, R. Laporte, P. J.-M. Rivière and C. D. Schteingart, *J. Med. Chem.*, 2014, **57**, 5306–5317.
 - 27 D. B. Hope and V. Du Vigneaud, *J. Biol. Chem.*, 1962, **237**, 3146–3150.
 - 28 D. B. Hope, V. V. S. Murti and V. du Vigneaud, *J. Biol. Chem.*, 1962, **237**, 1563–1566.
 - 29 W. Y. Chan and V. Du Vigneaud, *Endocrinology*, 1962, **71**, 977–982.
 - 30 W. Rath, *Eur. J. Obstet. Gynecol. Reprod. Biol.*, 2009, **147**, 15–20.
 - 31 T. Barth, I. Krejčí, B. Kupková and K. Jošt, *Eur. J. Pharmacol.*, 1973, **24**, 183–188.
 - 32 V. Pliska, J. Rudinger, T. Dousa and J. H. Cort, *Am. J. Physiol.*, 1968, **215**, 916–920.
 - 33 C. W. Smith and M. F. Ferger, *J. Med. Chem.*, 1976, **19**, 250–254.
 - 34 M. Muttenthaler, A. Andersson, A. D. de Araujo, Z. Dekan, R. J. Lewis and P. F. Alewood, *J. Med. Chem.*, 2010, **53**, 8585–8596.
 - 35 A. D. de Araujo, M. Mobli, J. Castro, A. M. Harrington, I. Vetter, Z. Dekan, M. Muttenthaler, J. Wan, R. J. Lewis, G. F. King, S. M. Brierley and P. F. Alewood, *Nat. Commun.*, 2014, **5**, 3165.
 - 36 F. A. Chaibva and R. B. Walker, *J. Pharm. Biomed. Anal.*, 2007, **43**, 179–185.
 - 37 C. Avanti, H. P. Permentier, A. Van Dam, R. Poole, W. Jiskoot, H. W. Frijlink and W. L. J. Hinrichs, *Mol. Pharm.*, 2012, **9**, 554–562.
 - 38 C. Avanti, N. A. Oktaviani, W. L. J. Hinrichs, H. W. Frijlink and F. A. A. Mulder, *Int. J. Pharm.*, 2013, **444**, 139–145.
 - 39 C. Avanti, W. L. J. Hinrichs, A. Casini, A. C. Eissens, A. Van Dam, A. Kedrov, A. J. M. Driessen, H. W. Frijlink and H. P. Permentier, *J. Pharm. Sci.*, 2013, **102**, 1734–1741.
-

-
- 40 C. Avanti, J.-P. Amorij, D. Setyaningsih, A. Hawe, W. Jiskoot, J. Visser, A. Kedrov, A. J. M. Driessen, W. L. J. Hinrichs and H. W. Frijlink, *AAPS J.*, 2011, **13**, 284–290.
- 41 R. J. Prankerd, T.-H. Nguyen, J. P. Ibrahim, R. J. Bischof, G. C. Nassta, L. D. Olerile, A. S. Russell, F. Meiser, H. C. Parkinson, H. A. Coleman, D. A. V Morton and M. P. McIntosh, *PLoS One*, 2013, **8**, e82965.
- 42 K. A. Johnson, *Adv. Drug Deliv. Rev.*, 1997, **26**, 3–15.
- 43 G. Cavallaro, L. Maniscalco, M. Campisi, D. Schillaci and G. Giammona, *Eur. J. Pharm. Biopharm.*, 2007, **66**, 182–92.
- 44 C. Bertolla, S. Rolin, B. Evrard, L. Pochet and B. Masereel, *Bioorg. Med. Chem. Lett.*, 2008, **18**, 1855–1858.
- 45 P. S. Hudnut and G. P. Cook, Patent WO2004078147 A2, 2004.
- 46 A. Abuchowski, T. van Es, N. C. Palczuk and F. F. Davis, *J. Biol. Chem.*, 1977, **252**, 3578–3581.
- 47 A. Abuchowski, J. R. McCoy, N. C. Palczuk, T. van Es and F. F. Davis, *J. Biol. Chem.*, 1977, **252**, 3582–3586.
- 48 J. Israelachvili, *Proc. Natl. Acad. Sci. U. S. A.*, 1997, **94**, 8378–8379.
- 49 A. Bendele, J. Seely, C. Richey, G. Sennello and G. Shopp, *Toxicol. Sci.*, 1998, **42**, 152–157.
- 50 P. Caliceti and F. M. Veronese, *Adv. Drug Deliv. Rev.*, 2003, **55**, 1261–1277.
- 51 O. B. Kinstler, D. N. Brems, S. L. Lauren, A. G. Paige, J. B. Hamburger and M. J. Treuheit, *Pharm. Res.*, 1996, **13**, 996–1002.
- 52 K. Knop, R. Hoogenboom, D. Fischer and U. S. Schubert, *Angew. Chemie*, 2010, **49**, 6288–6308.
- 53 F. M. Veronese and A. Mero, *BioDrugs*, 2008, **22**, 315–329.
- 54 A. P. Chapman, *Adv. Drug Deliv. Rev.*, 2002, **54**, 531–545.
- 55 F. M. Veronese, *Biomaterials*, 2001, **22**, 405–417.
- 56 G. Pasut and F. M. Veronese, *Prog. Polym. Sci.*, 2007, **32**, 933–961.
- 57 S. N. S. Alconcel, A. S. Baas and H. D. Maynard, *Polym. Chem.*, 2011, **2**, 1442–1448.
- 58 G. T. Hermanson, *Bioconjugate Techniques*, Elsevier, Third Edit., 2013.
- 59 G. W. Anderson, J. E. Zimmerman and F. M. Callahan, *J. Am. Chem. Soc.*, 1964, **86**, 1839–1842.
- 60 G. W. Cline and S. B. Hanna, *J. Org. Chem.*, 1988, **53**, 3583–3586.
- 61 G. W. Cline and S. B. Hanna, *J. Am. Chem. Soc.*, 1987, **109**, 3087–3091.
- 62 F. Lecolley, L. Tao, G. Mantovani, I. Durkin, S. Lautru and D. M. Haddleton, *Chem. Commun.*, 2004, 2026–2027.
-

-
- 63 R. F. Borch, M. K. Bernstein and H. D. Durst, *J. Am. Chem. Soc.*, 1971, **93**, 2897–2904.
- 64 L. Peng, G. J. Calton and J. W. Burnett, *Appl. Biochem. Biotechnol.*, 1987, **14**, 91–99.
- 65 C. T. Sayers, G. Mantovani, S. M. Ryan, R. K. Randev, O. Keiper, O. I. Leszczyszyn, C. Blindauer, D. J. Brayden and D. M. Haddleton, *Soft Matter*, 2009, **5**, 3038–3046.
- 66 H. A. Klok, *J. Polym. Sci. Part A Polym. Chem.*, 2005, **43**, 1–17.
- 67 O. B. Kinstler, N. E. Gabriel, C. E. Farrar and R. B. DePrince, US Patent 5985265, 1999.
- 68 E. Valeur and M. Bradley, *Chem. Soc. Rev.*, 2009, **38**, 606–631.
- 69 A. B. Lerner, T. E. H. H. Lee, J. C. Sheehan and G. P. Hess, *J. Am. Chem. Soc.*, 1955, **77**, 1067–1068.
- 70 M. Z. Atassi and T. Manshour, *J. Protein Chem.*, 1991, **10**, 623–627.
- 71 A. M. Landel, *Anal. Biochem.*, 1976, **73**, 280–289.
- 72 G. Levesque, P. Arsène, V. Fanneau-Bellenger and T. N. Pham, *Biomacromolecules*, 2000, **1**, 387–399.
- 73 K. Bergstrom, K. Holmberg, A. Safran, A. S. Hoffman, M. J. Edgell, A. Kozlowski, B. A. Hovanes and J. M. Harris, *J. Biomed. Mater. Res.*, 1992, **26**, 779–790.
- 74 F. M. Veronese, R. Largajolli and E. Boccu, *Appl. Biochem. Biotechnol.*, 1985, **11**, 141–152.
- 75 M. González and S. E. Vaillard, *Curr. Org. Chem.*, 2013, **17**, 1–24.
- 76 C. O. Beauchamp, S. L. Gonias, D. P. Menapace and S. V. Pizzo, *Anal. Biochem.*, 1983, **131**, 25–33.
- 77 S. Rajagopalan, S. L. Gonias and S. V. Pizzo, *J. Clin. Invest.*, 1985, **75**, 413–419.
- 78 K. T. Wiss, O. D. Krishna, P. J. Roth, K. L. Kiick and P. Theato, *Macromolecules*, 2009, **42**, 3860–3863.
- 79 P. Thordarson, B. Le Droumaguet and K. Velonia, *Appl. Microbiol. Biotechnol.*, 2006, **73**, 243–254.
- 80 S. B. Gunnoo and A. Madder, *ChemBioChem*, 2016, **17**, 529–553.
- 81 J. E. Moore and W. H. Ward, *J. Am. Chem. Soc.*, 1948, **70**, 2414–2418.
- 82 C. F. Brewer and J. P. Riehm, *Anal. Biochem.*, 1967, **18**, 248–255.
- 83 M. D. Partis, D. G. Griffiths, G. C. Roberts and R. B. Beechey, *J. Protein Chem.*, 1983, **2**, 263–277.
- 84 L. M. Tedaldi, M. E. B. Smith, R. I. Nathani and J. R. Baker, *Chem. Commun.*, 2009, 6583–6585.
-

-
- 85 M. E. B. Smith, F. F. Schumacher, C. P. Ryan, L. M. Tedaldi, D. Papaioannou, G. Waksman, S. Caddick and J. R. Baker, *J. Am. Chem. Soc.*, 2010, **132**, 1960–1965.
- 86 C. E. Hoyle and C. N. Bowman, *Angew. Chemie Int. Ed.*, 2010, **49**, 1540–1573.
- 87 A. Dondoni and A. Marra, *Chem. Soc. Rev.*, 2012, **41**, 573–586.
- 88 A. Massi and D. Nanni, *Org. Biomol. Chem.*, 2012, **10**, 3791–3807.
- 89 Y. Geng, D. E. Discher, J. Juustynska and S. Helmut, *Angew. Chemie Int. Ed.*, 2006, **45**, 7578–7581.
- 90 A. Dondoni, A. Massi, P. Nanni and A. Roda, *Chem. Eur. J.*, 2009, **15**, 11444–11449.
- 91 A. B. Lowe, *Polym. Chem.*, 2010, 17–36.
- 92 M. G. Finn and V. Fokin, *Chem. Soc. Rev.*, 2010, **39**, 1355–1387.
- 93 M. W. Jones, G. Mantovani, S. M. Ryan, X. Wang, D. J. Brayden and D. M. Haddleton, *Chem. Commun.*, 2009, 5272–5274.
- 94 M. W. Jones, M. I. Gibson, G. Mantovani and D. M. Haddleton, *Polym. Chem.*, 2011, **2**, 572–574.
- 95 J. Carlsson, H. Drevin and R. Axén, *Biochem. J.*, 1978, **173**, 723–737.
- 96 G. Saito, J. A. Swanson and K.-D. Lee, *Adv. Drug Deliv. Rev.*, 2003, **55**, 199–215.
- 97 J.-T. Li, J. Carlsson, J.-N. Lin and K. D. Caldwell, *Bioconjug. Chem.*, 1996, **7**, 592–599.
- 98 D. Bontempo, K. L. Heredia, B. A. Fish and H. D. Maynard, *J. Am. Chem. Soc.*, 2004, **126**, 15372–15373.
- 99 K. S. Siddiqui, A. Poljak, M. Guilhaus, G. Feller, S. D. Amico, C. Gerday and R. Cavicchioli, *J. Bacteriol.*, 2005, **187**, 6206–6212.
- 100 S. F. Betz, *Protein Sci.*, 1993, **2**, 1551–1558.
- 101 J. M. Thornton, *J. Mol. Biol.*, 1981, **151**, 261–287.
- 102 L. Castañeda, Z. V.F. Wright, C. Marculescu, T. M. Tran, V. Chudasama, A. Maruani, E. A. Hull, J. P. M. Nunes, R. J. Fitzmaurice, M. E. B. Smith, L. H. Jones, S. Caddick and J. R. Baker, *Tetrahedron Lett.*, 2013, **54**, 3493–3495.
- 103 M. W. Jones, R. A. Strickland, F. F. Schumacher, S. Caddick, J. R. Baker, M. I. Gibson and D. M. Haddleton, *J. Am. Chem. Soc.*, 2012, **134**, 1847–1852.
- 104 F. F. Schumacher, M. Nobles, C. P. Ryan, M. E. B. Smith, A. Tinker, S. Caddick and J. R. Baker, *Bioconjug. Chem.*, 2011, **22**, 132–136.
- 105 M. W. Jones, R. A. Strickland, F. F. Schumacher, S. Caddick, J. R. Baker, M. I. Gibson and D. M. Haddleton, *Chem. Commun.*, 2012, **48**, 4064–4066.
- 106 M. P. Robin, P. Wilson, A. B. Mabire, J. K. Kiviaho, J. E. Raymond, D. M. Haddleton and R. K. O'Reilly, *J. Am. Chem. Soc.*, 2013, **135**, 2875–2878.
-

-
- 107 J.-K. Y. Tan and J. G. Schellinger, *Ther. Deliv.*, 2015, **6**, 1127–1129.
- 108 J. Youziel, A. R. Akhbar, Q. Aziz, M. E. B. Smith, S. Caddick, A. Tinker and J. R. Baker, *Org. Biomol. Chem.*, 2014, **12**, 557–560.
- 109 P. Wilson, A. Anastasaki, M. R. Owen, K. Kempe, D. M. Haddleton, S. K. Mann, A. P. R. Johnston, J. F. Quinn, M. R. Whittaker, P. J. Hogg and T. P. Davis, *J. Am. Chem. Soc.*, 2015, **137**, 4215–4222.
- 110 M. S. Masri and M. Friedman, *J. Protein Chem.*, 1988, **7**, 49–54.
- 111 G. N. Grover, S. N. S. Alconcel, N. M. Matsumoto and H. D. Maynard, *Macromolecules*, 2009, **42**, 7657–7663.
- 112 M. Morpurgo, F. M. Veronese, D. Kachensky and J. M. Harris, *Bioconjug. Chem.*, 1996, **7**, 363–368.
- 113 S. Shaunak, A. Godwin, J.-W. Choi, S. Balan, E. Pedone, D. Vijayarangam, S. Heidelberger, I. Teo, M. Zloh and S. Brocchini, *Nat. Chem. Biol.*, 2006, **2**, 312–313.
- 114 S. Brocchini, A. Godwin, E. Pedone, J.-W. Choi and S. Shaunak, US Patent US2006/0210526 A1, 2006.
- 115 S. Brocchini, A. Godwin, S. Balan, J. Choi, M. Zloh and S. Shaunak, *Adv. Drug Deliv. Rev.*, 2008, **60**, 3–12.
- 116 J. Choi, A. Godwin, S. Balan, P. Bryant, Y. Cong, E. Pawlisz, M. Porssa, N. Rumpf, R. Singh and S. Brocchini, in *PEGylated Protein Drugs: Basic Science and Clinical Applications*, 2009, pp. 47–72.
- 117 S. Balan, J.-W. Choi, A. Godwin, I. Teo, C. M. Laborde, S. Heidelberger, M. Zloh, S. Shaunak and S. Brocchini, *Bioconjug. Chem.*, 2007, **18**, 61–76.
- 118 O. Koniev and A. Wagner, *Chem. Soc. Rev.*, 2015, **44**, 5495–5551.
- 119 G. Espuña, G. Arsequell, G. Valencia, J. Barluenga, M. Pérez and J. M. González, *Chem. Commun.*, 2000, 1307–1308.
- 120 G. Espuña, D. Andreu, J. Barluenga, X. Pérez, A. Planas, G. Arsequell and G. Valencia, *Biochemistry*, 2006, **45**, 5957–5963.
- 121 T. L. Schlick, Z. Ding, E. W. Kovacs and M. B. Francis, *J. Am. Chem. Soc.*, 2005, **127**, 3718–3723.
- 122 J. Gavriluk, H. Ban, M. Nagano, W. Hakamata and C. F. Barbas, *Bioconjug. Chem.*, 2012, **23**, 2321–2328.
- 123 M. W. Jones, G. Mantovani, C. A. Blindauer, S. M. Ryan, X. Wang, D. J. Brayden and D. M. Haddleton, *J. Am. Chem. Soc.*, 2012, **134**, 7406–7413.
- 124 N. S. Joshi, L. R. Whitaker and M. B. Francis, *J. Am. Chem. Soc.*, 2004, **126**, 15942–15943.
- 125 D. W. Romanini and M. B. Francis, *Bioconjug. Chem.*, 2008, **19**, 153–157.
- 126 H. Ban, M. Nagano, J. Gavriluk, W. Hakamata, T. Inokuma and C. F. Barbas, *Bioconjug. Chem.*, 2013, **24**, 520–532.
-

-
- 127 H. Ban, J. Gavriluk and C. F. Barbas, *J. Am. Chem. Soc.*, 2010, **132**, 1523–1525.
- 128 A. Foettinger, M. Melmer, A. Leitner and W. Lindner, *Bioconjug. Chem.*, 2007, **18**, 1678–1683.
- 129 J. M. Antos and M. B. Francis, *J. Am. Chem. Soc.*, 2004, **126**, 10256–10257.
- 130 B. V. Popp and Z. T. Ball, *J. Am. Chem. Soc.*, 2010, **132**, 6660–6662.
- 131 R. Zamora, M. Alaiz and F. J. Hidalgo, *Chem. Res. Toxicol.*, 1999, **5**, 654–660.
- 132 X. Li, H. Ma, S. Dong, X. Duan and S. Liang, *Talanta*, 2004, **62**, 367–371.
- 133 X. Li, H. Ma, L. Nie, M. Sun and S. Xiong, *Anal. Chim. Acta*, 2004, **515**, 255–260.
- 134 E. Hochuli, W. Bannwarth, H. Döbeli, R. Gentz and D. Stüber, *Nat. Biotechnol.*, 1988, **6**, 1321–1325.
- 135 Y. Cong, E. Pawlisz, P. Bryant, S. Balan, E. Laurine, R. Tommasi, R. Singh, S. Dubey, K. Peciak, M. Bird, A. Sivasankar, J. Swierkosz, M. Muroi, S. Heidelberger, M. Farys, F. Khayrabad, J. Edwards, G. Badescu, I. Hodgson, C. Heise, S. Somavarapu, J. Liddell, K. Powell, M. Zloh, J. Choi, A. Godwin and S. Brocchini, *Bioconjug. Chem.*, 2012, **23**, 248–263.
- 136 P. J. Bjerrum, J. O. Weith and C. L. Borders Jr, *J. Gen. Physiol.*, 1983, **81**, 453–484.
- 137 J. F. Riordan, *Biochemistry*, 1973, **12**, 3915–3923.
- 138 M. A. Gauthier and H. A. Klok, *Biomacromolecules*, 2011, **12**, 482–493.
- 139 C. H. Kim, J. Y. Axup and P. G. Schultz, *Curr. Opin. Chem. Biol.*, 2013, **17**, 412–419.
- 140 W. H. Zhang, G. Otting and C. J. Jackson, *Curr. Opin. Struct. Biol.*, 2013, **23**, 581–587.
- 141 J. A. Johnson, Y. Y. Lu, J. A. Van Deventer and D. A. Tirrell, *Curr. Opin. Chem. Biol.*, 2010, **14**, 774–780.
- 142 M. Szwarc, *Nature*, 1956, **178**, 1168–1169.
- 143 M. K. Georges, R. P. N. Veregin, P. M. Kazmaier and G. K. Hamer, *Macromolecules*, 1993, **26**, 2987–2988.
- 144 D. H. Solomon, E. Rizzardo and P. Caciolo, US Patent 4581429, 1986.
- 145 C. J. Hawker, A. W. Bosman and E. Harth, *Chem. Rev.*, 2001, **101**, 3661–3688.
- 146 J. Chiefari, Y. K. B. Chong, F. Ercole, J. Krstina, J. Jeffery, T. P. T. Le, R. T. A. Mayadunne, G. F. Meijs, C. L. Moad, G. Moad, E. Rizzardo, S. H. Thang and C. South, *Macromolecules*, 1998, **31**, 5559–5562.
- 147 M. Benaglia, J. Chiefari, Y. K. Chong, G. Moad, E. Rizzardo and S. H. Thang, *J. Am. Chem. Soc.*, 2009, **131**, 6914–6915.
- 148 D. J. Keddie, G. Moad, E. Rizzardo and S. H. Thang, *Macromolecules*, 2012, **45**, 5321–5342.
- 149 G. Moad, E. Rizzardo and S. H. Thang, *Aust. J. Chem.*, 2012, **65**, 985–1076.
-

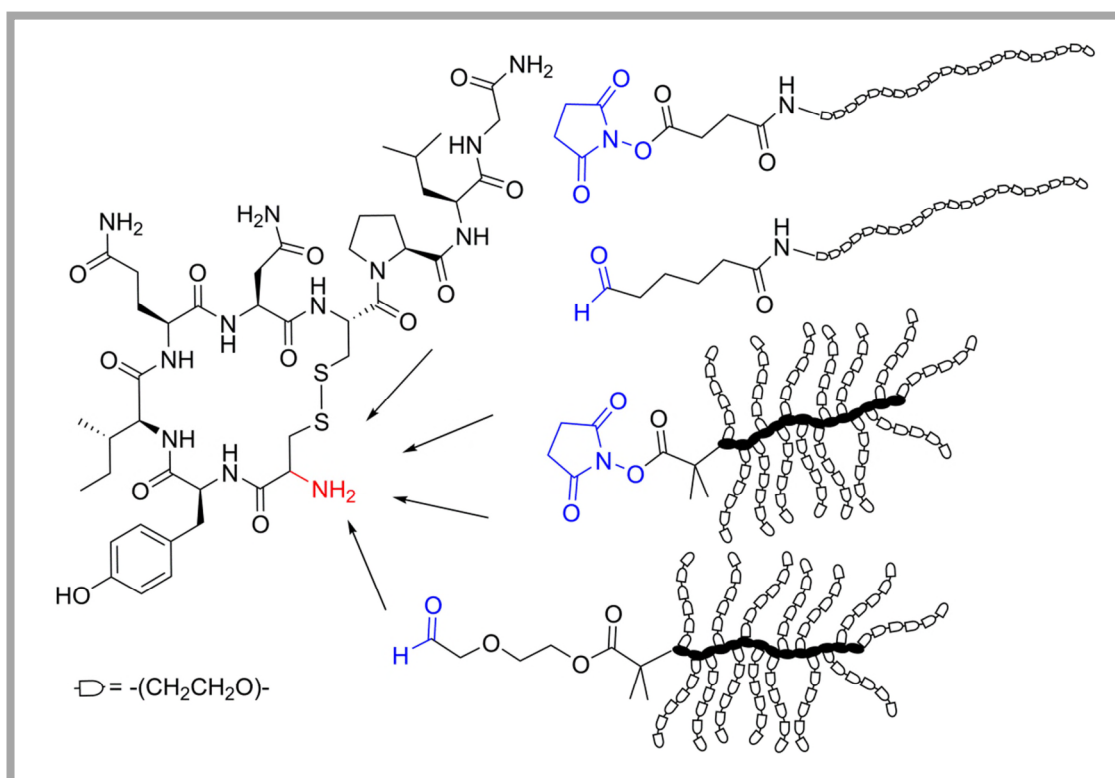
-
- 150 K. Kempe, P. A. J. M. de Jongh, A. Anastasaki, P. Wilson and D. M. Haddleton, *Chem. Commun.*, 2015, **51**, 16213–16216.
- 151 P. A. J. M. de Jongh, A. Mortiboy, G. S. Sulley, M. R. Bennett, A. Anastasaki, P. Wilson, D. M. Haddleton and K. Kempe, *ACS Macro Lett.*, 2016, **5**, 321–325.
- 152 L. Martin, G. Gody and S. Perrier, *Polym. Chem.*, 2015, **6**, 4875–4886.
- 153 M. Kato, M. Kamigaito, M. Sawamoto and T. Higashimuras, *Macromolecules*, 1995, **28**, 1721–1723.
- 154 J. Wang and K. Matyjaszewski, *J. Am. Chem. Soc.*, 1995, **117**, 5614–5615.
- 155 K. Matyjaszewski, *Macromolecules*, 2012, **45**, 4015–4039.
- 156 V. Percec, T. Guliashvili, J. S. Ladislaw, A. Wistrand, A. Stjerndahl, M. J. Sienkowska, M. J. Monteiro and S. Sahoo, *J. Am. Chem. Soc.*, 2006, **128**, 14156–14165.
- 157 B. M. Rosen and V. Percec, *Chem. Rev.*, 2009, **109**, 5069–5119.
- 158 N. H. Nguyen, B. M. Rosen and V. Percec, *J. Polym. Sci. Part A Polym. Chem.*, 2011, **49**, 1235–1247.
- 159 C. Boyer, A. H. Soeriyadi, P. B. Zetterlund and M. R. Whittaker, *Polym. chem*, 2012, **3**, 117–123.
- 160 C. Waldron, A. Anastasaki, R. McHale, P. Wilson, Z. Li, T. Smith and D. M. Haddleton, *Polym. Chem.*, 2014, **5**, 892–898.
- 161 C. Boyer, A. H. Soeriyadi, P. B. Zetterlund and M. R. Whittaker, *Macromolecules*, 2011, **44**, 8028–8033.
- 162 A. Anastasaki, C. Waldron, P. Wilson, C. Boyer, P. Zetterlund, M. R. Whittaker and D. Haddleton, *ACS Macro Lett.*, 2013, **2**, 896–900.
- 163 Q. Zhang, J. Collins, A. Anastasaki, R. Wallis, D. A. Mitchell, C. R. Becer and D. M. Haddleton, *Angew. Chemie Int. Ed.*, 2013, **52**, 4435–4439.
- 164 Q. Zhang, A. Anastasaki, G.-Z. Li, A. J. Haddleton, P. Wilson and D. M. Haddleton, *Polym. Chem.*, 2014, **5**, 3876–3883.
- 165 Q. Zhang, P. Wilson, Z. Li, R. Mchale, J. Godfrey, A. Anastasaki, C. Waldron and D. M. Haddleton, *J. Am. Chem. Soc.*, 2013, **135**, 7355–7363.
- 166 Q. Zhang, P. Wilson, A. Anastasaki, R. McHale and D. M. Haddleton, *ACS Macro Lett.*, 2014, **3**, 491–495.
- 167 G. R. Jones, Z. Li, A. Anastasaki, D. J. Lloyd, P. Wilson, Q. Zhang and D. M. Haddleton, *Macromolecules*, 2016, **49**, 483–489.
- 168 A. Simula, A. Anastasaki and D. M. Haddleton, *Macromol. Rapid Commun.*, 2015, **37**, 356–361.
- 169 A. Simula, V. Nikolaou, F. Alsubaie, A. Anastasaki and D. M. Haddleton, *Polym. Chem.*, 2015, **6**, 5940–5950.
- 170 C. Waldron, Q. Zhang, Z. Li, V. Nikolaou, G. Nurumbetov, J. Godfrey, R. McHale, G.
-

-
- Yilmaz, R. K. Randev, M. Girault, K. McEwan, D. M. Haddleton, M. Droesbeke, A. J. Haddleton, P. Wilson, A. Simula, J. Collins, D. J. Lloyd, J. A. Burns, C. Summers, C. Houben, A. Anastasaki, M. Li, C. R. Becer, J. K. Kiviahho and N. Risangud, *Polym. Chem.*, 2014, **5**, 57–61.
- 171 Q. Zhang, Z. Li, P. Wilson and D. M. Haddleton, *Chem. Commun.*, 2013, **49**, 6608–6610.
- 172 F. Alsubaie, A. Anastasaki, P. Wilson and D. M. Haddleton, *Polym. Chem.*, 2015, **6**, 406–417.
- 173 P. Wilson, J. Nicolas and D. M. Haddleton, in *Chemistry of Organo-Hybrids: Synthesis and Characterization of Functional Nano-Objects*, 2015, pp. 466–502.
- 174 Z. P. Tolstyka and H. D. Maynard, in *Polymer Science: A Comprehensive Reference*, Elsevier B.V., 2012, vol. 9, pp. 317–337.
- 175 Z. Zarafshani, T. Obata and J. F. Lutz, *Biomacromolecules*, 2010, **11**, 2130–2135.
- 176 A. J. Keefe and S. Jiang, *Nat. Chem.*, 2012, **4**, 59–63.
- 177 M. Chenal, C. Boursier, Y. Guillaneuf, M. Taverna, P. Couvreur and J. Nicolas, *Polym. Chem.*, 2011, **2**, 1523–1530.
- 178 L. McDowall, G. Chen and M. H. Stenzel, *Macromol. Rapid Commun.*, 2008, **29**, 1666–1671.
- 179 L. Tao, G. Mantovani, F. Lecolley and D. M. Haddleton, *J. Am. Chem. Soc.*, 2004, **126**, 13220–13221.
- 180 S. M. Ryan, X. Wang, G. Mantovani, C. T. Sayers, D. M. Haddleton and D. J. Brayden, *J. Control. Release*, 2009, **135**, 51–59.
- 181 B. Podobnik, B. Helk, V. Smilović, S. Škrajnar, K. Fidler, S. Jevševar, A. Godwin and P. Williams, *Bioconjug. Chem.*, 2015, **26**, 452–459.
- 182 R. J. Mancini, J. Lee and H. D. Maynard, *J. Am. Chem. Soc.*, 2012, **134**, 8474–8479.
- 183 G. Mantovani, F. Lecolley, L. Tao, D. M. Haddleton, J. Clerx, J. J. L. M. Cornelissen and K. Velonia, *J. Am. Chem. Soc.*, 2005, **127**, 2966–2973.
- 184 B. Le Droumaguet, G. Mantovani, D. M. Haddleton and K. Velonia, *J. Mater. Chem.*, 2007, **17**, 1916–1922.
- 185 J. Geng, G. Mantovani, L. Tao, J. Nicolas, G. Chen, R. Wallis, D. A. Mitchell, B. R. G. Johnson, S. D. Evans and D. M. Haddleton, *J. Am. Chem. Soc.*, 2007, **129**, 15156–15163.
- 186 E. Bays, L. Tao, C. W. Chang and H. D. Maynard, *Biomacromolecules*, 2009, **10**, 1777–1781.
- 187 Y. Jiang, H. Lu, F. Chen, M. Callari, M. Pourgholami, D. L. Morris and M. H. Stenzel, *Biomacromolecules*, 2016, **17**, 808–817.
- 188 Y. Jiang, M. Liang, D. Svejkar, G. Hart-Smith, H. Lu, W. Scarano and M. H. Stenzel, *Chem. Commun.*, 2014, **50**, 6394–6397.
-

-
- 189 A. Lewis, Y. Tang, S. Brocchini, J.-W. Choi and A. Godwin, *Bioconjug. Chem.*, 2008, **19**, 2144–2155.
- 190 D. Bontempo and H. D. Maynard, *J. Am. Chem. Soc.*, 2005, **127**, 6508–6509.
- 191 K. L. Heredia, D. Bontempo, T. Ly, J. T. Byers, S. Halstenberg and H. D. Maynard, *J. Am. Chem. Soc.*, 2005, **127**, 16955–60.
- 192 P. De, M. Li, S. R. Gondi and B. S. Sumerlin, *J. Am. Chem. Soc.*, 2008, **130**, 11288–9.
- 193 C. Boyer, V. Bulmus, J. Liu, T. P. Davis, M. H. Stenzel and C. Barner-Kowollik, *J. Am. Chem. Soc.*, 2007, **129**, 7145–7154.
- 194 J. Liu, V. Bulmus, D. L. Herlambang, C. Barner-Kowollik, M. H. Stenzel and T. P. Davis, *Angew. Chemie*, 2007, **46**, 3099–103.

Chapter 2

2. Amine targeted PEGylation of oxytocin



A common method for the conjugation of polymers onto peptides or proteins is via the reactive amine groups found either on lysine residues or at the N-terminus in an acylation or alkylation reaction. Within the structure of native oxytocin there is only one amine group present at the N-terminus, allowing for site specific amine targeting chemistries. Different conjugation chemistries arising from the use of NHS-ester and aldehyde end functional polymers were used to attach different architectures of PEG onto oxytocin.

2.1. Introduction

Of the large library of potential conjugation routes available for the modification of proteins and peptides, by far the most commonly exploited are those involving conjugation onto amino groups. A large range of different functional groups are available for targeting of lysine or terminal amino groups available on almost all protein or peptide biomolecules. Primarily, these coupling reactions are available *via* acylation or alkylation, with reactions usually occurring efficiently and in high yields to give stable conjugates.¹

The PEGylation of proteins or peptides in this manner is a research area that is constantly expanding, with many PEGylated products undergoing preclinical trials, or going as far as to achieving FDA approval.² This field has also been making progress in the incorporation of different polymer architectures such as branched ‘comb’ PEGs. The development of living radical polymerisation techniques allows for simple and controlled synthesis by implementing (meth)acrylate PEG monomers to generate tailor-made polymers bearing low molar mass PEG side chain ‘teeth’. Comb polymers can provide potential advantages over linear equivalents due to viscosity changes resulting from a change in structure of the polymers in solution with linear PEGs behaving like random coils, and polyPEGs being rigid rods leading to changes in the hydrodynamic volume of polymers.^{3,4} This can lead to reduced polymer crystallisation and subsequent organ vacuolisation.⁵

Modification of the Cys¹ amino terminus of oxytocin could provide a route to the synthesis of PEGylated oxytocin analogues which, due to an absence of any lysine groups or additional amines in the structure of the peptide, would allow site-selective conjugation when selecting appropriate conjugation techniques. Previous amino modifications to oxytocin have had varying levels of success with regard to retained activity or improvements in stability. The amino group has been discovered to not be vital for

oxytocin activity, as its removal (*i.e.* desamino-oxytocin) has still led to high levels of uterine contractility, potentially proving more potent than the native peptide itself.⁶⁻⁸

One of the main degradation sites of oxytocin is focused around the Cys¹-Cys⁶ disulfide bond, where degradation products can include the formation of oxytocin trisulfide or tetrasulfide, as well as leading to dimerisation and the formation of larger aggregates.^{9,10} The amino terminus is sterically close to this disulfide bond, and it was speculated that the addition of polymers at this position could provide some stabilisation or protection to the peptide structure.

In this chapter the use of two different polymer end group functionalities are discussed for potential conjugation onto the small peptide therapeutic oxytocin. Commercial linear monomethoxy PEG (mPEG) polymers are available with a variety of different reactive end groups, including NHS ester and aldehyde functionality for PEGylation at amino groups on peptides and proteins. These polymers, alongside synthetic engineered 'comb' polymer equivalents, will be investigated for the conjugation of different architectures of PEGs onto oxytocin, as well as comparing the different conjugation chemistries employed. For the controlled synthesis of these polymers, copper mediated chemistry provides an ideal route to α -end functional polymers which can undergo post-polymerisation conjugation. The utilisation of aldehyde functional polymers for conjugation is of particular interest as the conjugation reaction can occur reversibly (with the formation of a Schiff base) or irreversibly (by reductive amination). The potential exploitation of the reversible nature of this bond with two different peptide-polymer architectures, alongside a non-polymer conjugated oxytocin analogue, will be explored.

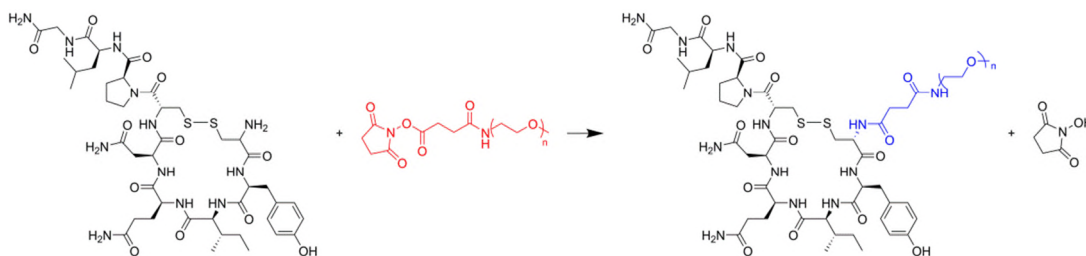
2.2. Results & Discussion

2.2.1. Activated ester linear PEGylation

The use of activated esters, such as *N*-hydroxysuccinimidyl (NHS) esters, for the site selective targeting of peptides or proteins is one of the most commonly used methods for conjugation of polymers to both lysine and terminal amino groups.^{11,12} A large variety of different commercial NHS ester PEGs are available for using in this manner, which react with nucleophilic amines resulting in stable amide linkages.

A large problem associated with using NHS ester functionalised reagents (such as NHS PEG) is that the NHS ester is highly liable to rapid hydrolysis under storage conditions, which leads to a loss of the NHS functionality.¹³ The pH is also found to have a strong impact on the stability and half-life of reagents, with hydrolysis occurring more rapidly on increasing pH causing problems in coupling reactions, with regards to side products, and excess of polymer required.^{14,15} Nevertheless, NHS ester PEG reagents are commonly used for routine PEGylation of peptides and proteins and the majority of FDA approved protein-PEG conjugate drugs are from the use of this type of conjugation chemistry.² Due to the issues resulting from the hydrolysis associated with NHS ester reagents, commercially a large excess of polymer is generally used for conjugations.

2.2.1.1. Oxytocin conjugation using succinimidyl ester PEG



Scheme 2.1. Conjugation of NHS ester functional linear PEG onto oxytocin site specifically at *N*-terminal amine in DMF (containing 1% TEA) at 10 °C.

Two different molecular weights ($M_w = 2$ kDa & $M_w = 5$ kDa) of linear α -methoxy- ω -succinimidyl ester poly(ethylene glycol) (NHS ester PEG) were used for site selective conjugation to oxytocin (scheme 2.1). The reaction was performed in anhydrous DMF (containing 1 % TEA) to prevent hydrolysis of the polymers during the conjugation reaction. A slight excess of polymer (1.5 equivalents) was added to oxytocin and an overnight reaction performed at 10 °C.

After 18 hours an aliquot (equivalent to 0.2 mmol of the peptide) was removed and dissolved in water for analysis by RP-HPLC ($\lambda = 280$ nm). In the chromatogram from the UV detector of the HPLC it was observed that there was a decrease in the peak area of the peak corresponding to oxytocin (retention time $t = 7.8$ minutes), and the appearance of a broad peak at a longer retention time ($t = 14.7$ minutes). The polymer does not exhibit any peaks with high absorptions under the conditions used for RP-HPLC analysis (UV, $\lambda = 280$ nm), suggesting that the new peak observed has arisen from a reaction with the peptide. For the conjugations of both M_w of polymer there was still the presence of some remaining oxytocin observed in the solution after conjugation (figure 2.1). The % yield of the reaction can be calculated by monitoring the disappearance of the native peptide, and after 24 hours this was found to be 70 %.

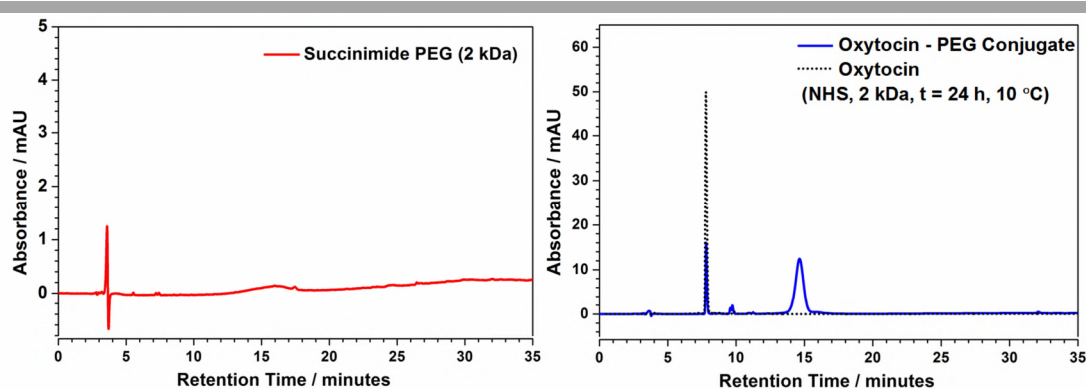


Figure 2.1. RP-HPLC of conjugation of succinimidyl functional linear PEG onto oxytocin.

In order to further confirm the conjugation product, a portion of the 2kDa oxytocin-polymer conjugate was purified by semi preparative RP-HPLC ($\lambda = 280$ nm) to remove any remaining oxytocin as well as excess, or potentially hydrolysed, polymer. In changing to semi preparative RP-HPLC the conditions first had to be optimised for efficient separation to be achieved whilst using the preparative column. The conditions adopted provided good peak separation, and the pure conjugate product was collected. After lyophilisation RP-HPLC analysis of the separated product revealed the appearance of a singular broad peak free of impurities at a retention time of $t = 14.7$ minutes (figure 2.2).

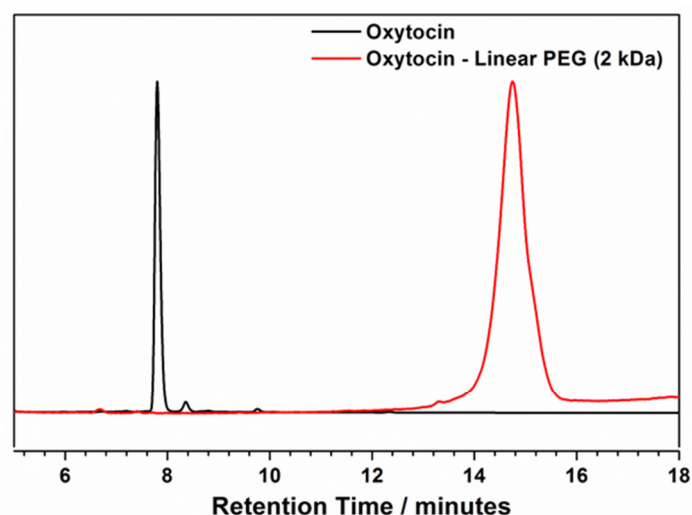


Figure 2.2. RP-HPLC analysis of purified oxytocin-polymer (NHS) conjugate (2 kDa).

The purified 2 kDa oxytocin-polymer sample and the unconjugated polymer were analysed by matrix assisted laser desorption time of flight mass spectrometry (MALDI-TOF MS) using 2,5-dihydroxybenzoic acid (DHB) as the MALDI matrix. MALDI-TOF MS of the commercial polymer contains two major distributions, which are attributable to that of the NHS ester functional polymer and the polymer without the succinimidyl functionality, after hydrolysis. After conjugation only one major distribution remained, with a clear shift in molecular weight of approximately 1 kDa (molar mass of oxytocin is 1007 Da) between the NHS ester polymer and the oxytocin conjugate. A closer inspection of the MALDI-TOF MS spectrum of the oxytocin-polymer conjugate shows good agreement between the theoretical (calculated) values and the experimental values (figure 2.3 for polymer repeat units of $n = 37$ & $n = 38$) and the differences between the peaks correlating to the ethylene glycol repeat unit (44.03 Da).

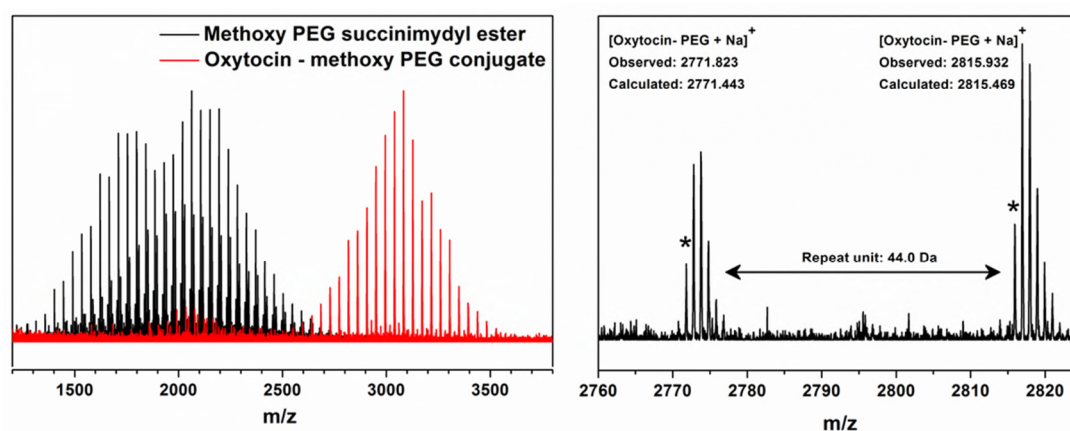


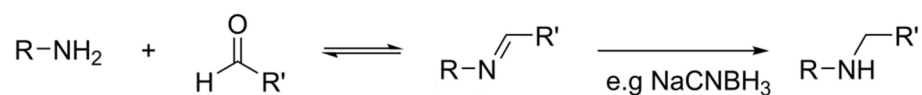
Figure 2.3. MALDI-TOF MS analysis of oxytocin-polymer (NHS) 2 kDa conjugate.

These results indicate that the conjugation of the NHS ester PEG has occurred in the expected singular site specific manner onto oxytocin, resulting in the *N*-terminal amino PEGylated oxytocin conjugate product. This MALDI-TOF MS data provides promising confirmation of the observed conjugate structure, which will be useful for the conjugation

of the 'comb' type polymers, where exact structural characterisation is more difficult due to the repeat unit itself being a macromonomer.

2.2.2. Aldehyde functional linear PEG conjugation

It is reported that amine groups, such as those occurring on lysine residues or at the *N*-terminal amine within a peptide, will react with carbonyl groups such as aldehydes in the presence of suitable reducing agents in a two-step reductive amination process to form stable secondary amines (scheme 2.2). The first step is *via* the formation of a Schiff base / imine linked intermediate which is in equilibrium with the aldehyde and amine. Commonly the intermediate is then reduced by the addition of a reducing agent, which forms a stable secondary amine linkage. Sodium cyanoborohydride is a common reducing agent used in this manner and is preferable to sodium borohydride as the reducing agent.^{16,17} Due to milder reductions being performed, the Schiff base reductions occur efficiently but there is no reduction of any remaining aldehyde, which would potentially prevent higher yields in the reaction. Aldehyde modification of peptide or protein amino groups may also be preferable to NHS reactions, as potential charges can be maintained on the secondary amine product, which are not the case for the amide linkages associated with NHS conjugates.



Scheme 2.2. Schiff base formation of reaction between aldehyde and amine followed by reduction by NaCNBH₃ forming stable secondary amine linkage.

Multiple different chain length spacers between the aldehyde functionality and polymer chain have been used for the reductive amination of biomolecules by aldehyde conjugation, with varying levels of success (figure 2.4). The use of acetaldehyde reagents

have previously been used to couple to peptides, although these can be ineffective due to a limited stability, particularly under basic conditions, and a susceptibility to form undesirable by-products. Functional mPEG-propionaldehyde and mPEG-butyraldehyde contain longer linker chains between the aldehyde functionality and the PEG chain and have proven to have higher stabilities proving more useful under a variety of conditions for reductive amination.¹⁸⁻²⁰

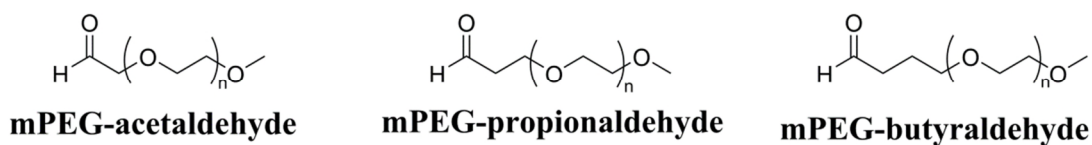
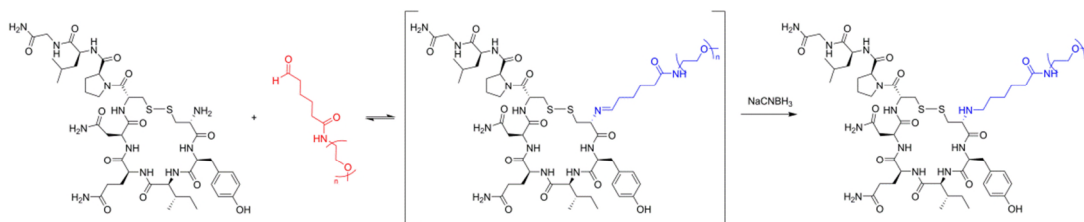


Figure 2.4. Commercially available aldehyde functional PEG reagents.

A further property that is often utilised within these reductive amination conjugation reactions is the tuning of pH for more selective targeting of amine groups on proteins or peptides. As there are two different commonly occurring types of amines that can be presented within peptides and proteins, those found on lysine residues throughout the structure or the singular amine located at the *N*-terminus, it can be beneficial to selectively target the *N*-terminus for a singular attachment.^{1,13,21} The pK_a values for the lysine amines (10 - 10.2) are much higher than for the *N*-Terminus ($pK_a \approx 7$) and under acidic or neutral conditions, the terminal amine can usually be selectively modified.

For the discussion of the conjugation of these polymers onto oxytocin pH controls are not required as there are no lysine groups within the structure, which have associated problems with regards to multiple sites of attachment. In the case of the oxytocin, the singular available amine within the peptide that could potentially react in this manner is that located at the *N*-Terminus and will lead to a site specific attachment.

2.2.2.1. Oxytocin conjugation using aldehyde functional PEG



Scheme 2.3. Formation of stable linear PEGylated oxytocin following reaction with aldehyde PEG and subsequent reduction by NaCNBH₃.

Two different molecular weights ($M_w = 2$ kDa & $M_w = 5$ kDa) of α -methoxy- ω -formyl poly(ethylene glycol) (aldehyde PEG) were conjugated onto oxytocin with reduction by NaCNBH₃ (scheme 2.3). Oxytocin was dissolved in sodium phosphate buffer (pH 7.5, 100 mM) and reacted with 1 equivalent of the PEG reagent and a freshly prepared 25 mM solution of NaCNBH₃ (2.5 eq.) added before the reaction proceeded at 10 °C overnight.

After the conjugation an aliquot of the solution (equivalent to 0.2 mM oxytocin) was removed and diluted in water for RP-HPLC monitoring of the reaction. The HPLC UV coupled ($\lambda = 280$ nm) chromatogram revealed the appearance of a newly formed broad peak at a longer retention time ($t = 14.0$ minutes) to oxytocin ($t = 7.4$ minutes) alongside and approximate 60 % decrease in the native peptide remaining in the solution. RP-HPLC analysis of the unconjugated (aldehyde functional) polymer showed the appearance of one narrow peak at a retention time of $t = 5.2$ minutes. Post conjugation analysis of the reaction solution revealed that the presence of this peak is still observed alongside evidence of unreacted peptide for both M_w of PEGs conjugated (figure 2.5).

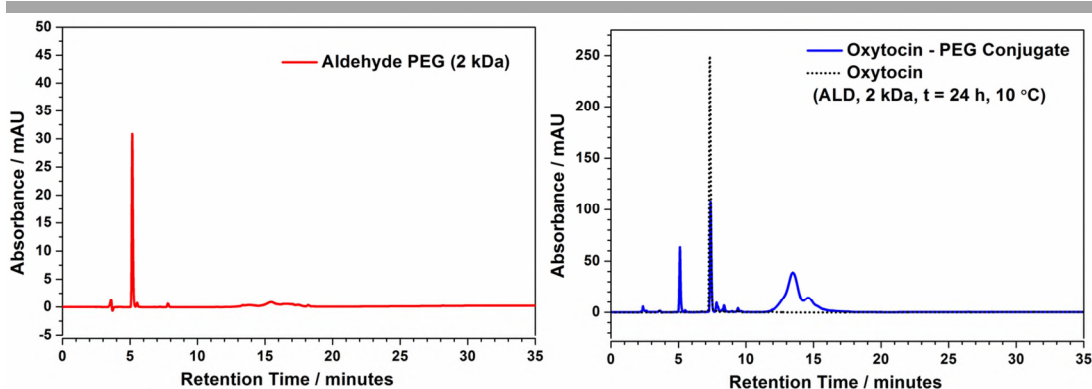


Figure 2.5. RP-HPLC monitoring of conjugation reaction of aldehyde PEG (2 kDa) onto oxytocin, after stirring for 24 hours at $T = 10\text{ }^{\circ}\text{C}$.

In the same method as the succinimydyl conjugated oxytocin, a portion of this newly formed aldehyde conjugated oxytocin was removed and purified by semi-preparative RP-HPLC. The gradient of the semi-preparative system was optimised for efficient peak separation allowing efficient purification of the product. After lyophilisation, analysis of the purified polymer conjugate by analytical RP-HPLC revealed the appearance of a single broad peak (figure 2.6). There is some peak tailing leading to a shoulder appearing on the RP-HPLC chromatogram for the purified conjugate, potentially due to side reactions occurring, leading to the formation of additional products, which will be discussed later in this chapter.

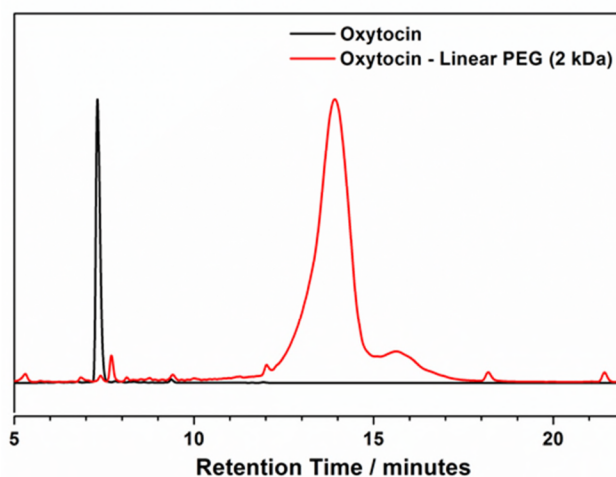


Figure 2.6. RP-HPLC analysis of purified oxytocin-polymer (aldehyde) 2 kDa conjugate.

MALDI-TOF MS analysis was performed on this oxytocin-polymer conjugate using DHB as the MALDI matrix and compared to the native aldehyde functional polymer. Similarly to the other linear (succinimidyl ester) conjugate, the peaks observed by MALDI-TOF MS were in good agreement with those expected for the stable (reduced with NaCNBH_3) aldehyde PEG – oxytocin conjugate. The peaks in the MALDI-TOF MS show very similar calculated (theoretical) and observed (experimental) values (figure 2.7 for $n = 43$ and $n = 44$ for the PEG_n chain) and the ethylene glycol difference between the peaks is maintained (44.03 Da). There is a clear shift in molecular weight from the unconjugated aldehyde polymer to the peptide-polymer conjugate corresponding to the molecular weight of the peptide (1007 Da).

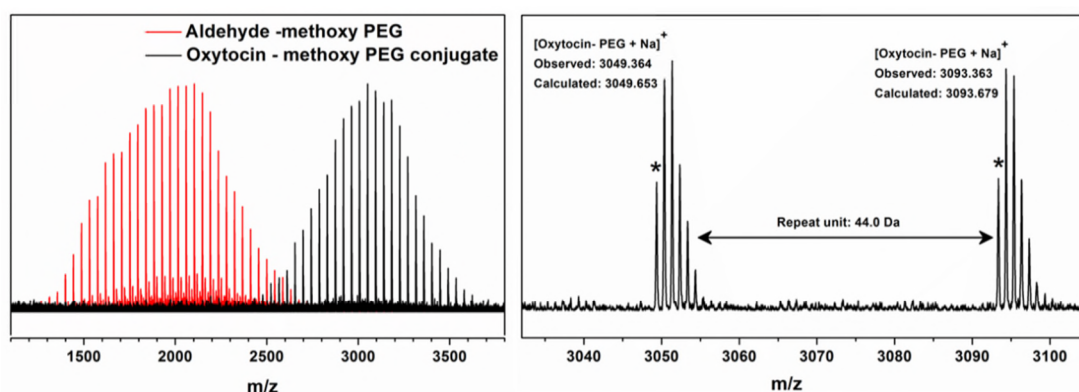


Figure 2.7. MALDI-TOF MS analysis of oxytocin-polymer (aldehyde) 2 kDa conjugate.

These results assist in confirmation of the conjugate structure, ensuring that covalent attachment of the polymer onto oxytocin was in a site-specific manner with only one unit of polymer per peptide (mono-addition).

2.2.3. PolyPEGylation strategies

Along with the more commonly commercially utilised linear PEGylation strategies, various methods are being established for the synthesis of branched (comb) PEG and conjugation

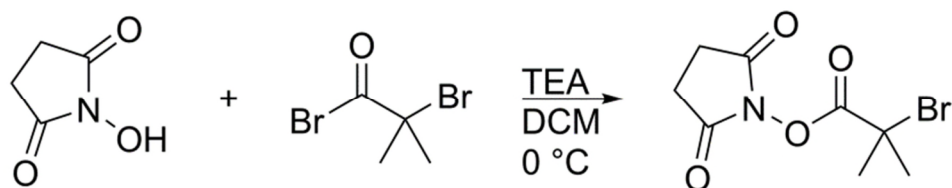
to peptides and proteins resulting in a higher PEG density in the conjugates. The arrival of controlled radical polymerisations has rendered the synthesis of polymers with PEG side chains highly accessible.^{22,23} Functional initiators that contain conjugatable groups can be utilised for the synthesis of α end functional polymers containing short PEG side chains, which can post-polymerisation be grafted onto the desired peptide or protein.^{24,25} The use of polyPEGs compared to linear equivalents presents a few advantages, which include a decreased viscosity compared to linear equivalents, due to acting as rigid rods within solution as opposed to random coils.³ Other advantages include longer circulation times,^{26,27} and reduced polymer crystallisation and subsequent organ vacuolisation,^{5,28} as well as the opportunity to tailor polymers as desired for specific applications.

Conjugations were performed onto oxytocin in a similar method to the linear equivalents by using 'grafting-to' chemistry, where the polymer is first synthesised with α end group conjugating functionality followed by conjugation yielding the poly(mPEGA) – peptide conjugate.

2.2.3.1. Activated ester polymer synthesis

Previously Haddleton *et al.* has successfully employed activated ester (NHS ester) based initiators for the synthesis of polyPEG polymers and subsequently conjugated these onto lysozyme.²⁴ The polymers were synthesised in a controlled manner and after conjugation the multisite attachment of 6-7 polymeric chains per protein was confirmed. Within the literature the same initiator has been successful in the synthesis of a variety of polymers and the attachment of these to proteins.^{29,30} This NHS ester initiator has also previously been utilised in the synthesis of lysozyme protein macroinitiator, from which polymers can be grown in a 'grafting-from' type manner.³¹

The NHS ester functional initiator *N*-succinimidyl 2-bromo-2-methylpropionate was synthesised in a high yielding, one-step reaction as previously described in the literature (scheme 2.4).²⁴ *N*-Hydroxysuccinimide was reacted with 2-bromoisobutyryl bromide in anhydrous DCM with triethylamine at 0 °C for 4 hours. The white crystals were purified by recrystallisation in diethyl ether resulting in an overall yield of 83 %.



Scheme 2.4. Synthesis reaction for NHS ester functional initiator.

The activated ester group, as described earlier in this chapter with reference to the linear succinimidyl ester PEGs is still very prone to hydrolysis.¹³ Consequently care must be taken to minimise water content within storage and particularly storage time, where long storage times prior to use are not ideal. Figure 2.8 shows the ¹H NMR spectra of the NHS ester initiator after fresh preparation and subsequent storage for 12 months in a closed container. The hydrolysis of the NHS functionality can clearly be recognised leading to the loss of 75 % of NHS ester functionality. The products released as a result of hydrolysis, bromoisobutyryl acid and *N*-hydroxysuccinimide can clearly be identified highlighting the need to ensure storage times are kept to a minimal level.

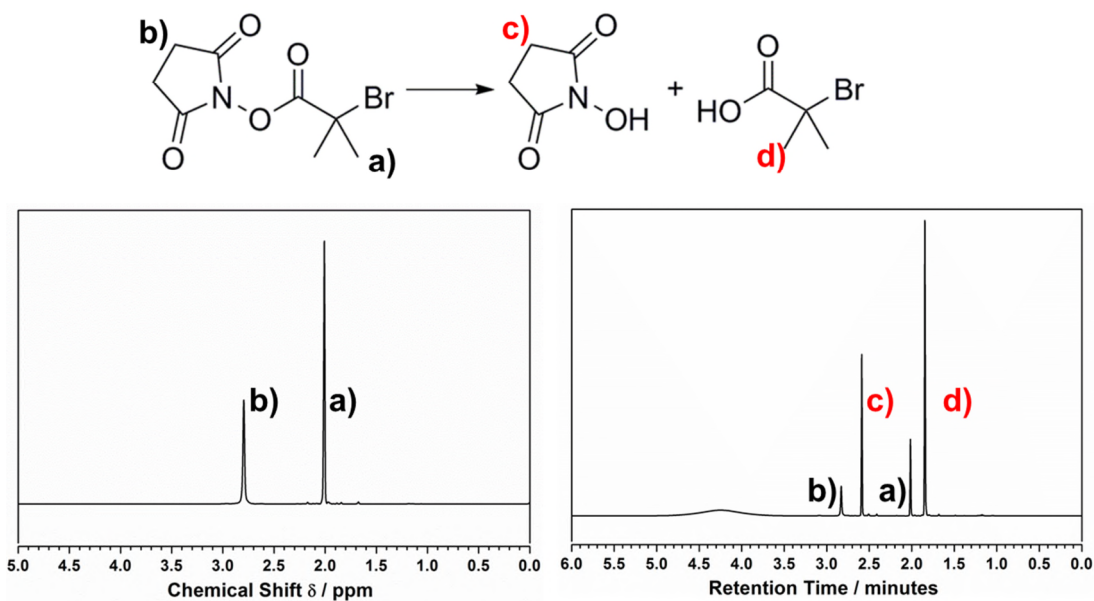
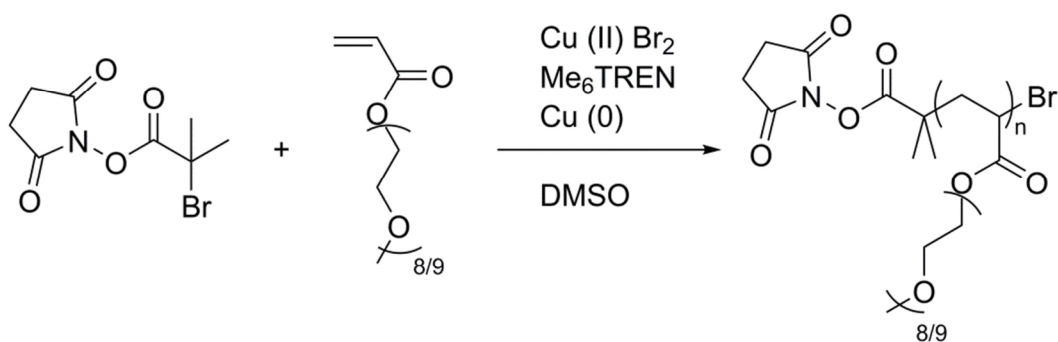


Figure 2.8. ^1H NMR (CDCl_3 , 400.05 MHz) of freshly prepared succinimide initiator and 75 % hydrolysed succinimide initiator with a loss of NHS ester functionality.

Using this NHS ester functional initiator, controlled living radical polymerisation of poly(ethylene glycol) methyl ether acrylate (av. $M_n = 480 \text{ g mol}^{-1}$, mPEGA₄₈₀) was carried out in anhydrous DMSO using Cu(II)Br_2 , Cu(0) wire and tris[2-(dimethylamino)ethyl]amine (Me_6TREN) as a ligand ($[\text{I}]:[\text{M}]:[\text{Me}_6\text{TREN}]:[\text{CuBr}_2] = 1:20:0.18:0.05$ and 5 cm Cu(0) wire) (scheme 2.5).



Scheme 2.5. Cu(0) mediated living radical polymerisation of mPEGA₄₈₀ using NHS initiator resulting in α -succinimidyl ester functionality poly(mPEGA₄₈₀).

In order to follow the kinetics of the reaction samples were periodically removed and diluted in DMF for SEC molecular weight data and δ_6 -DMSO for ^1H NMR conversion analysis (figure 2.9). Conversions were measured by comparing the three vinyl protons of the monomer ($\delta = 5.8 - 6.4$ ppm) with the first CH_2 group in the PEG monomer repeat unit within the polymer ($\delta = 4.1$ ppm). After 60 minutes no polymer could be observed by either ^1H NMR or SEC highlighting that there was a potential initial inhibition time to the polymerisation. After 2 hours however, the conversion had risen to 23 %, with an almost quantitative conversion (98 %) attained after 24 hours. Analysis by SEC showed that only mono-modal peaks were obtained with molecular weights increasing throughout the polymerisation as well as low dispersities being maintained ($\text{Đ} < 1.15$).

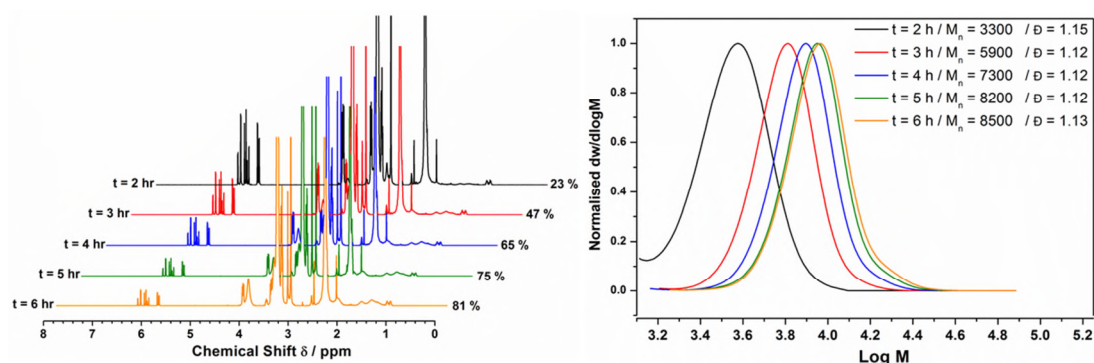


Figure 2.9. ^1H NMR (δ_6 -DMSO) and SEC (DMF) analysis monitoring the polymerisation of NHS-poly(mPEGA₄₈₀)₂₀.

The kinetic experiments revealed a linear increase of $\ln([M]_0/[M])$ with time during the polymerisation (excluding the initial inhibition time) which yields information about the apparent rate for the polymerisation (k_p) ($k_p^{\text{app}} = 4.24 \times 10^{-3} \text{ min}^{-1}$) (figure 2.10). A linear conversion of number average molecular weight (M_n) with conversion (which also correlated well with theoretical molecular weights) gives evidence of the “living” nature of this polymerisation.

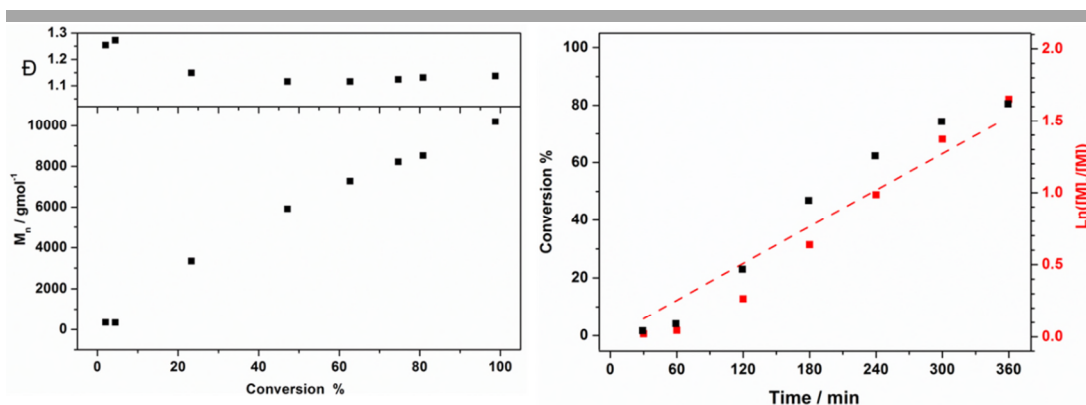
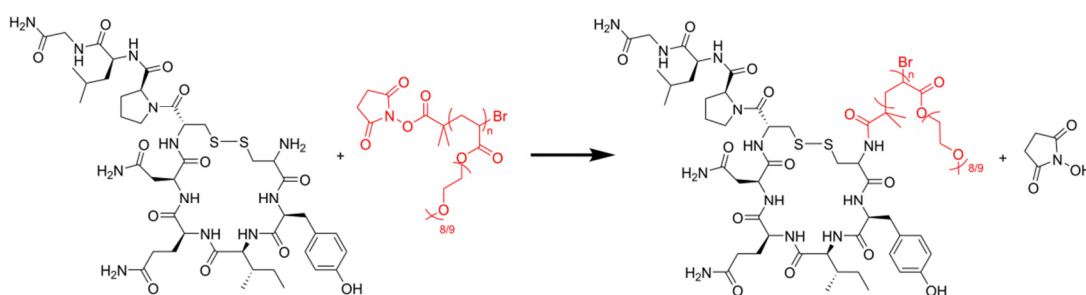


Figure 2.10. Kinetic plots for the polymerisation of NHS-poly(mPEG₄₈₀)₂₀.

2.2.3.2. Activated ester functional polymer conjugation

The conjugation of these synthesised polyPEG ‘comb’ α -succinimide functional polymers could be carried out in a site-specific manner similar to the conjugation carried out for the linear polymers (scheme 2.6). This would again lead to an amide linked oxytocin conjugate, except that with polyPEGylation the PEG density (and ultimately the peptide-polymer architecture) is different to that of the linear example. This difference in structure would likely lead to different properties being observed such as in the potential stability of the peptide, and pharmacokinetic properties or retained biological activity.^{3,32}



Scheme 2.6. Conjugation of α -succinimide functional poly(mPEGA₄₈₀) polymer onto oxytocin.

To prevent the previously observed readily occurring hydrolysis of the polymer end group from occurring before conjugation onto the peptide, an ‘*in-situ*’ method was initially developed to minimise water interaction. An aliquot of the polymerisation solution (with

no purification of the polymer) was added to the peptide in anhydrous solvents, thereby not exposing the conjugatable polymer to an aqueous environment. A colour change was observed during the reaction as the solution changed from a faint green (as within the polymerisation solution) to a brown colour. Monitoring of the conjugation by RP-HPLC analysis ($\lambda = 280$ nm) showed the formation of a number of side products, with minimal concentration changes of the peak on the RP-HPLC chromatogram representing the native peptide (figure 2.11). There is the presence of some potential peptide-polymer conjugate (a broad peak at retention time $t = 26.6$ minutes), however, the number of impurities in the solution mean that purification and further conjugate confirmation would be difficult.

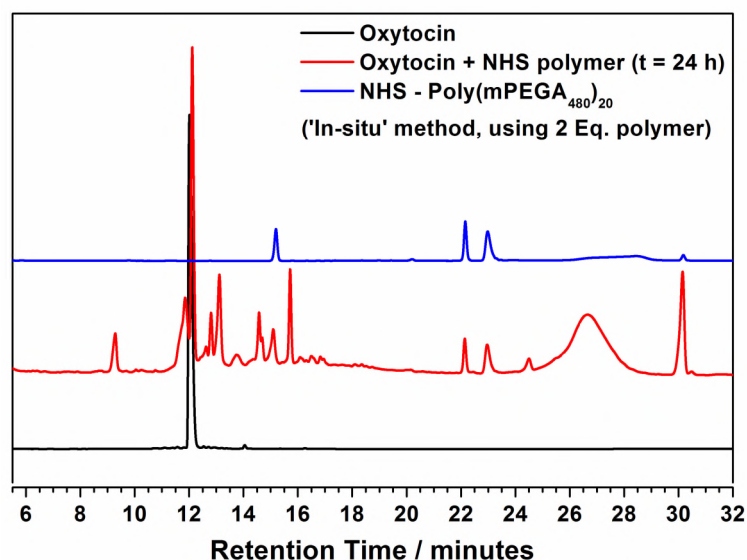


Figure 2.11. RP-HPLC trace of conjugation of NHS-poly(mPEGA)₂₀ from 'in-situ' conjugation of aliquot of polymerisation solution.

An alternative method was established for conducting this conjugation, which involved prior purification of a second batch of succinimide polymer synthesised targeting a molecular weight of 6.5 kDa. This succinimide functional polymer was synthesised using the same conditions for the polymerisation as for the kinetic experiment but with [M]:[I] ratio = 13:1. After polymerisation the removal of residual monomers and purification of the polymer was carried out by repeated precipitation into Et₂O: hexane (1: 1) whilst

carefully minimising the chance of hydrolysis of the succinimide ester end group. The retention of the α -end group succinimide ester functionality was confirmed by ^1H NMR of the purified polymer, where the peak at $\delta = 2.81$ ppm represents the 4 protons in the succinimide ring (figure 2.12). The experimental molecular weight could be calculated by ^1H NMR (CDCl_3) by a comparison between these protons and the protons from the first CH_2 of the PEG repeat unit ($\delta = 4.1$ ppm) yielding an average DP_n of 13 (a molecular weight of 6500 g mol^{-1}). Analysis of the purified polymer by SEC confirmed that the polymer molecular weight distribution remained narrow and mono-modal with final M_n of 6400 g mol^{-1} and dispersity = 1.08.

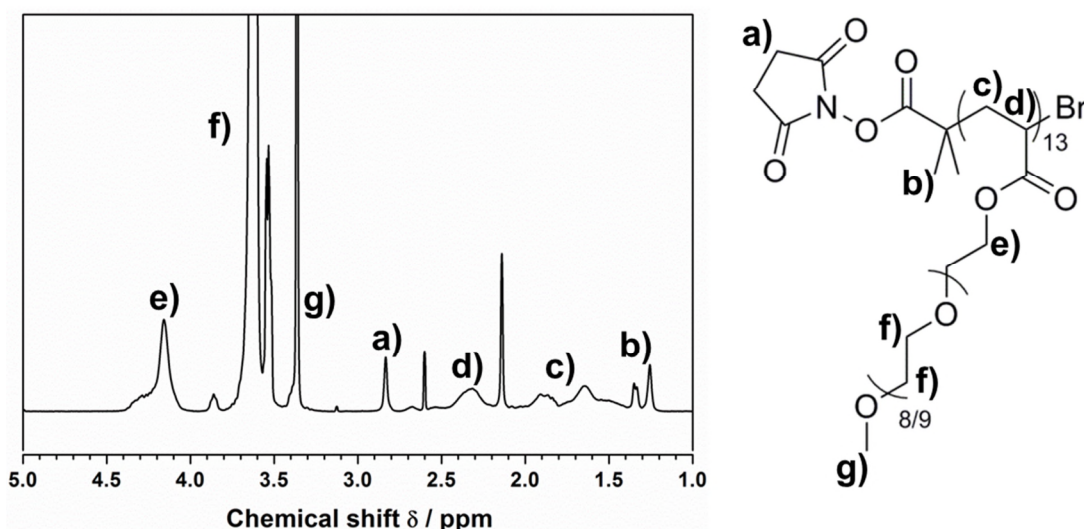


Figure 2.12. ^1H NMR (CDCl_3 , 300.13 MHz) of succinimidyl ester functional poly(mPEGA₄₈₀)₁₃.

Conjugation of purified succinimide – poly(mPEGA)

After confirmation that the α -end group functionality was retained the polymer was subsequently conjugated onto oxytocin using the same conditions as for the linear succinimide ester conjugation (1.5 equivalents of polymer in anhydrous DMF containing 1 % TEA). However, when the reaction was sampled at $t = 24$ hours, or at longer reaction times ($t = 4$ days; $t = 10$ days), analysis by RP-HPLC (UV, $\lambda = 280 \text{ nm}$) did not show the

formation of any desired conjugate product (figure 2.13). It was again believed that this was potentially due to hydrolysis of the succinimide ester end group meaning the functionality required for an efficient conjugation was no longer present.

As the conjugation can only occur at one position on the peptide structure, the addition of a large amount of polymer should have no adverse effect on the conjugation reaction,²⁴ although would lead to a higher amount of the polymer as an impurity in the final product. Therefore, in an alternative procedure, a large excess of the succinimide functional polymer (10 equivalents) was added to oxytocin; it is noted that this is similar to industry used reaction conditions. The high amounts of equivalents were used in order to maintain some level of polymer end functionality and therefore allow conjugation to occur in the expected manner. Although, there is a large excess of polymer, some amount of this is not expected to be reactive with NHS end functionalisation due to hydrolysis.

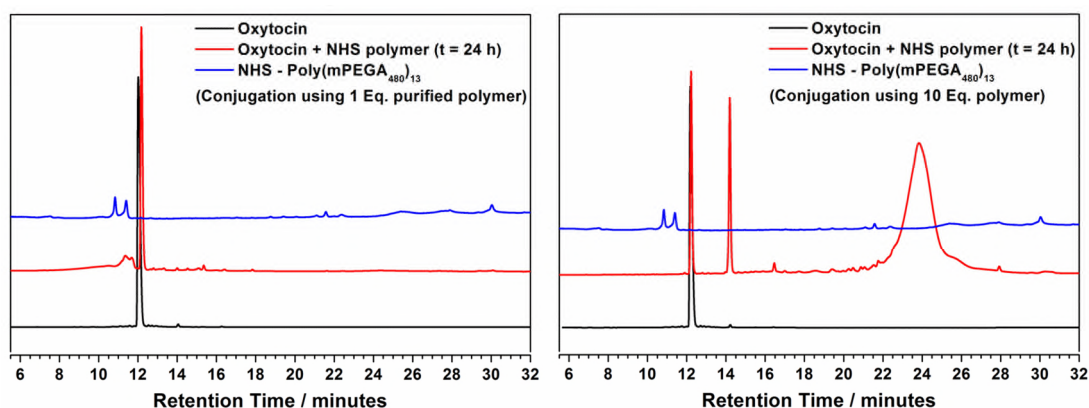


Figure 2.13. RP-HPLC trace monitoring conjugation of NHS-poly(mPEGA)₁₃ with 1 or 10 equivalences.

Analysis of the reaction by RP-HPLC (UV λ = 280 nm) revealed the appearance of a characteristic broad conjugate peak at a longer retention time (t = 23.8 minutes) than the native peptide (t = 12.2 minutes), attributed to the poly(mPEGA)-oxytocin conjugate (figure 2.13). RP-HPLC analysis of the unconjugated polymer did not reveal any peaks with high absorptions, therefore the appearance of a new broad conjugate peak can be attributed to

the desired conjugation occurring. The resulting conjugate was purified by dialysis against water (1 kDa MWCO, 3 days) to remove unreacted peptide and *N*-hydroxysuccinimide released during conjugation, after which RP-HPLC analysis revealed one single broad product (figure 2.14). It must be noted however, that there would still be a significant amount of the polyPEG reagent remaining in the purified conjugate.

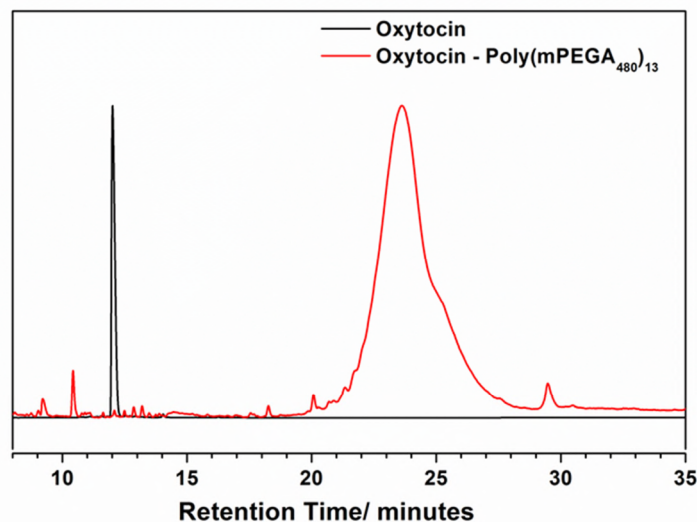


Figure 2.14. RP-HPLC of oxytocin-poly(mPEGA) conjugate after purification.

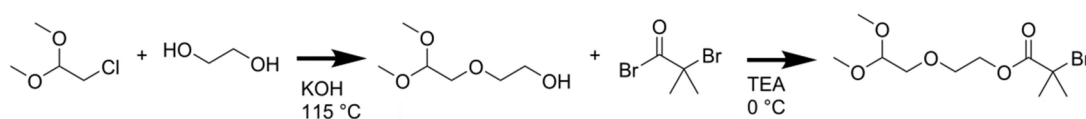
It should be noted that in the original work regarding the synthesis and conjugation of NHS functional poly(mPEGMA) by Haddleton and co-workers, similar issues were raised with the conjugation of polymers wherein no conjugation was observed after 24 hours.²⁴ However, on changing the initiator functionality from that of a methyl propionate group to a propionate, the reactivity was enhanced and the coupling could take place more efficiently.

2.2.3.3. Protected aldehyde polymer synthesis

Previously reported by Haddleton *et al.* has been the use of an acetal-protected aldehyde initiator to synthesise poly(mPEG)methacrylates using copper (I) mediated living radical

polymerisation.²⁵ The deprotected 'comb' poly(mPEG)methacrylates were then successfully conjugated onto lysozyme as a model peptide, resulting in multisite attachments as well as site specifically onto the *N*-terminus of salmon calcitonin.^{21,32} The same polymers have also been used in the preparation of PEGylated interferon and showed a lower increase in viscosity, and longer half-life post conjugation compared to conventional linear reagents.³

The use of a protected aldehyde initiator is particularly beneficial as it ensures that the aldehyde functionality will not undergo undesirable side reactions during polymerisation, but it does involve a post-polymerisation step for the removal of the acetal group. After deprotection the α -aldehyde end functional polymers can undergo identical reactions to that of the linear PEGs with amines either on lysine residues or at the *N*-terminal amine.



Scheme 2.7. Two step synthesis rout for protected aldehyde initiator.

The acetal protected initiator was synthesised in a two-step procedure (scheme 2.7). The first step was carried out by reacting ethylene glycol with chloroacetaldehyde dimethyl acetal in the presence of potassium hydroxide at 115 °C and stirring for 72 hours. This yielded the protected alcohol 2-(2,2-dimethoxy-ethoxy)-ethanol as a yellow oil which was used without purification. To a solution of this alcohol, in the presence of triethylamine, 2-bromo-3-methylpropionyl bromide was added dropwise at 0 °C and left to stir overnight. Purification was carried out by silica column chromatography, yielding the desired acetal functional initiator as a colourless oil (figure 2.15).

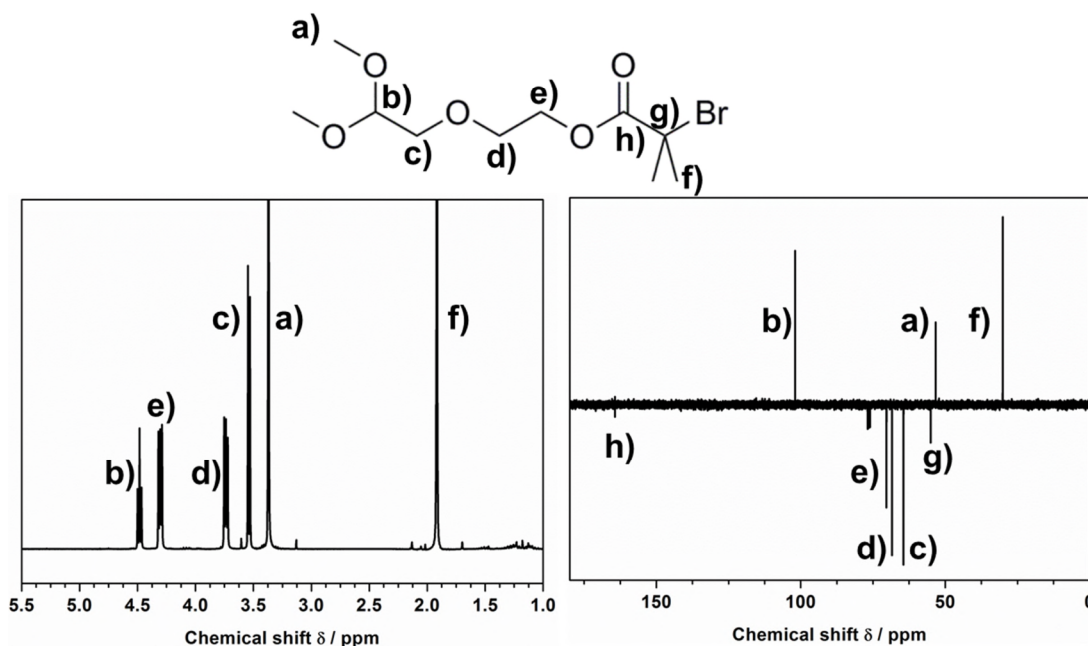
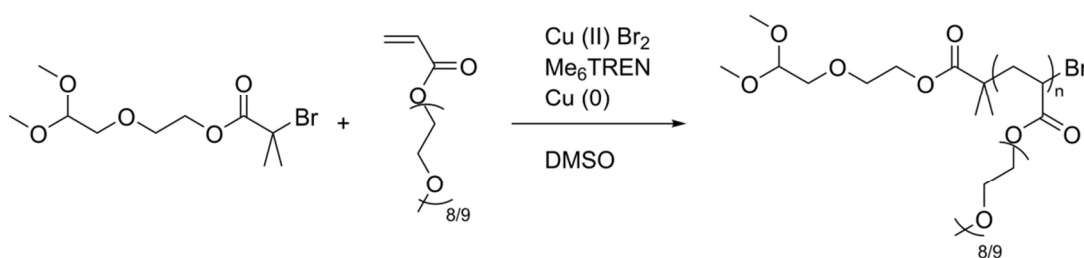


Figure 2.15. ^1H NMR (CDCl_3 , 300.13 MHz) and ^{13}C NMR (CDCl_3 , 75.47 MHz) of acetal protected aldehyde initiator.

Using the same conditions as for the succinimide initiator and targeting a molar mass of 10 kDa, the Cu(0)-mediated polymerisation of poly(ethylene glycol) methyl ether acrylate (av. $M_n = 480 \text{ g mol}^{-1}$, mPEGA₄₈₀) was carried out ($[\text{I}]:[\text{M}]:[\text{Me}_6\text{TREN}]:[\text{CuBr}_2] = 1:20:0.18:0.05$ and 5 cm Cu(0) wire) (scheme 2.8).



Scheme 2.8. Cu(0) mediated polymerisation of mPEGA₄₈₀ with protected aldehyde initiator.

In order to follow the kinetics of the reaction samples were removed periodically and diluted with δ_6 -DMSO for ^1H NMR conversion data and DMF for SEC molecular weight analysis (figure 2.16). Conversions were measured by a comparison of the three vinyl protons of the monomer ($\delta = 5.8 - 6.4 \text{ ppm}$) to the first CH_2 group of the PEG monomer

repeat unit on the polymer ($\delta = 4.1$ ppm). This polymerisation using the acetal functional initiator proceeded at a faster rate (k_p) to that observed with the succinimide initiator and the induction period previously observed was also absent. Analysis by ^1H NMR revealed 33 % conversion after 1 hour, rising to 66 % at $t = 2$ hours and complete conversion being achieved after 24 hours. Molecular weight distributions remained mono-modal and increased throughout the polymerisation whilst dispersities remained low ($\text{Đ} < 1.12$), with good correlation achieved between experimental and theoretical molecular weights throughout.

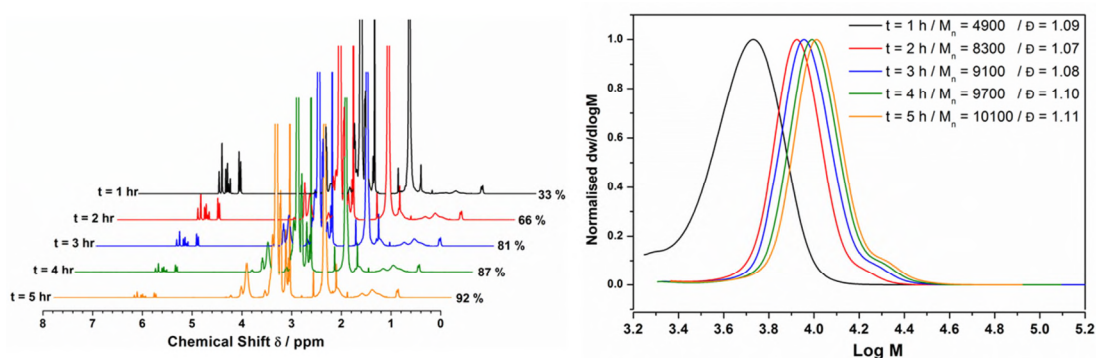


Figure 2.16. ^1H NMR (δ_6 -DMSO) and SEC (DMF) analysis of polymerisation of acetal-poly(mPEGA₄₈₀)₂₀.

The kinetics of the reaction again revealed good ‘living’ characteristics with a linear increase in the evolution of molecular weight (M_n) vs. conversion (figure 2.17). A linear evolution of $\ln([M]_0/[M])$ with time was also observed, which highlights a constant radical concentration. This also showed that the rate of polymerisation for the protected aldehyde initiator ($k_p^{app} = 8.64 \times 10^{-3} \text{ min}^{-1}$) is approximately double that of the succinimide polymerisation ($k_p^{app} = 4.24 \times 10^{-3} \text{ min}^{-1}$). There is high molecular weight tailing observed on the SEC chromatogram, although this is regularly observed for the polymerisation of mPEGA, previously assigned to the possible presence of diacrylate impurities in the monomer reagent.^{33,34}

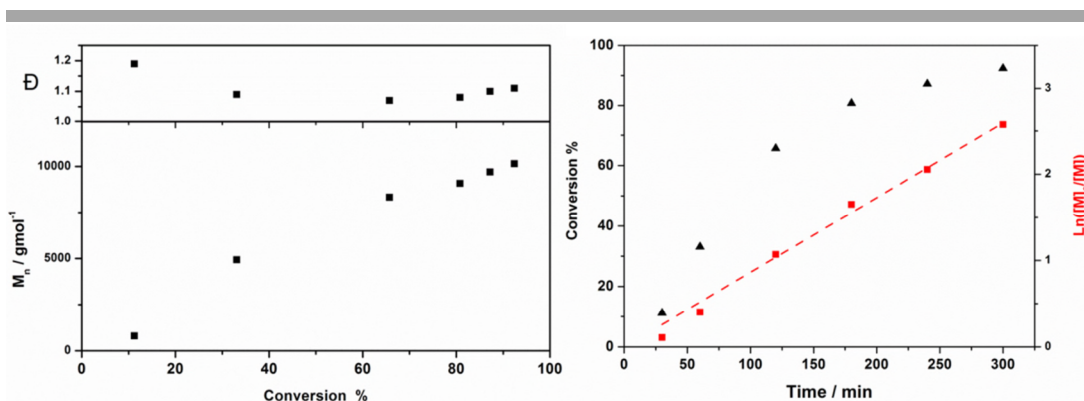


Figure 2.17. Kinetic plots for the polymerisation of acetal-poly(mPEGA₄₈₀)₂₀.

The previously reported polymerisation with this initiator was conducted by ATRP using copper chloride and *N*-(ethyl)-2-pyridylmethanimine ligand in toluene at 80 °C ([I]:[CuCl]:[L] = 1:1:2).²⁵ Although molecular weight dispersities remained low the initiator efficiency was reported as being only 50-60 % which meant molecular weights differed significantly from those anticipated. By performing the polymerisation under SET-LRP conditions, which have previously been reported as having a high initiator efficiency,³⁵ desirably a lower temperature (20 °C), and less equivalences of copper (0.05 Eq.) can be used maintaining controlled polymerisations and more accurate targeted molecular weights.

After well-controlled polymerisations were achieved, two further polymers were synthesised in the same manner to be used for future post-polymerisation conjugation onto oxytocin. Molecular weights were targeted at 10 kDa and 25 kDa (equivalent to [M]:[I] of 20 and 50) with [I]:[Me₆TREN]:[CuBr₂] = 1:0.18:0.05 and 5 cm Cu(0) wire. These polymerisations were performed for 24 hours under a nitrogen atmosphere after which samples were removed for NMR (δ₆-DMSO), which confirmed that quantitative, or near quantitative, conversions had been reached. SEC analysis (DMF) showed that narrow molecular weight distributions were maintained, with final dispersity values of Đ = 1.12 and 1.16.

After the polymerisation the polymers were purified by dialysis against water (1 kDa MWCO, 3 days) and after lyophilisation analysed by ^1H NMR for retained α end functionality (figure 2.18). This revealed the presence of the acetal protecting groups at $\delta = 4.4$ ppm (singular proton of $\text{CH}(\text{OCH}_3)_2$) and $\delta = 3.3$ ppm (6 x methyl groups of $\text{CH}(\text{OCH}_3)_2$). The experimental molecular weight could also be calculated by a comparison between the 6 protons of the isobutyryl group in the α -end group of the polymer ($\delta = 1.07$ ppm) and the first CH_2 group of the PEG repeat unit ($\delta = 4.1$ ppm) giving final DP_n s of 21 and 53, representing molecular weights of 10 kDa and 26 kDa.

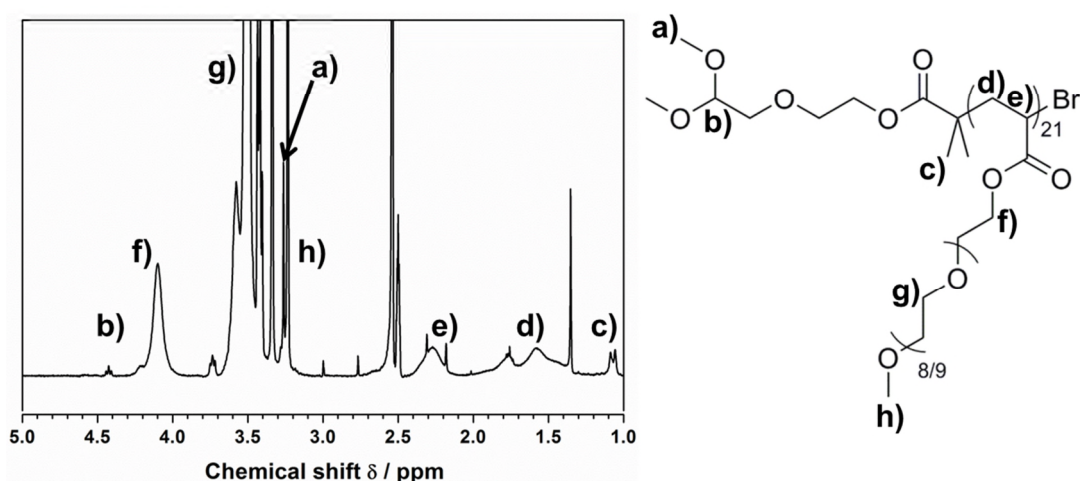
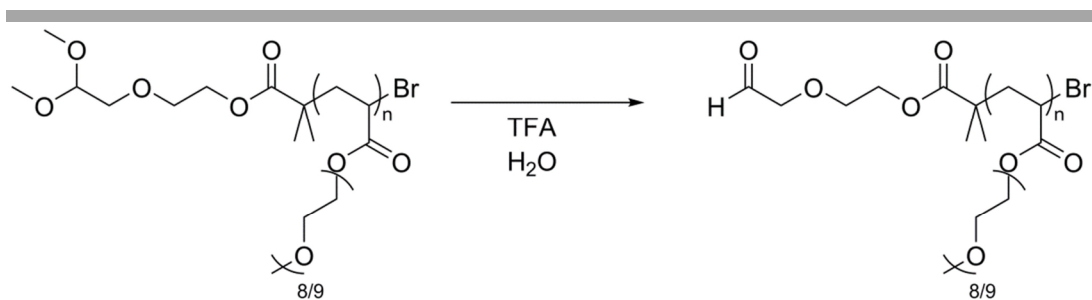


Figure 2.18. ^1H NMR (δ_6 -DMSO, 300.13 MHz) of poly(mPEGA₄₈₀)₂₁ with acetal protected aldehyde end group functionality.

The polymers were then deprotected by addition of aqueous solutions of trifluoroacetic acid (50% v/v), resulting in removal of the acetal protecting group, yielding α -aldehyde functionality on the polymer chains (scheme 2.9).²⁵



Scheme 2.9. Deprotection of acetal protecting group yielding aldehyde functional poly(mPEGA₄₈₀).

The aldehyde functional polymers were purified by dialysis against water (1 kDa MWCO, 3 days) and lyophilised, after which α -end group functionality was confirmed by ^1H NMR (δ_6 -DMSO) (figure 2.19). This was shown by the appearance of a characteristic aldehyde peak at 9.5 ppm and the disappearance of the acetal peaks at 4.4 ppm and 3.3 ppm. After deprotection of the acetal group the polymers were resubmitted for SEC analysis (DMF) which revealed that the molecular weight distributions remained narrow ($\mathcal{D} = 1.15 / 1.18$) and mono-modal, with no cleavage of the PEG chain from the polymer confirmed by only a very small decrease in average molecular weight being observed.

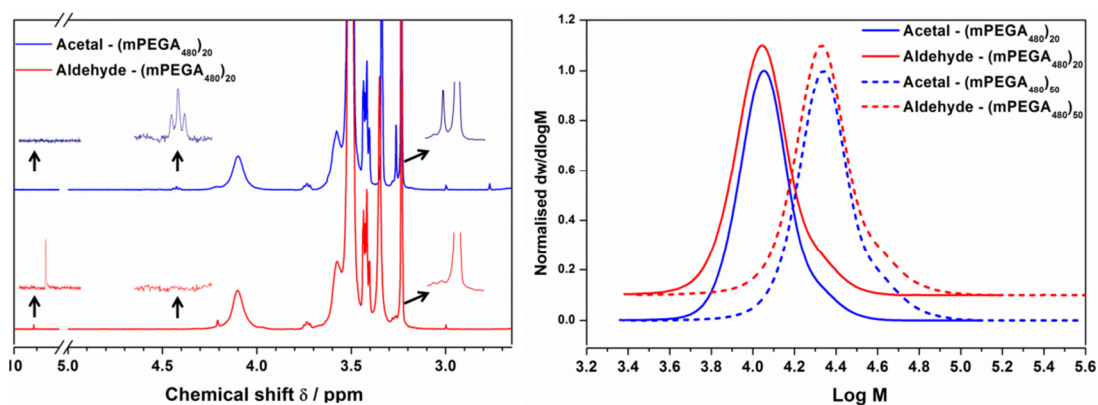


Figure 2.19. NMR and SEC analysis of DP_n 20 & DP_n 50 polymers before and after deprotection.

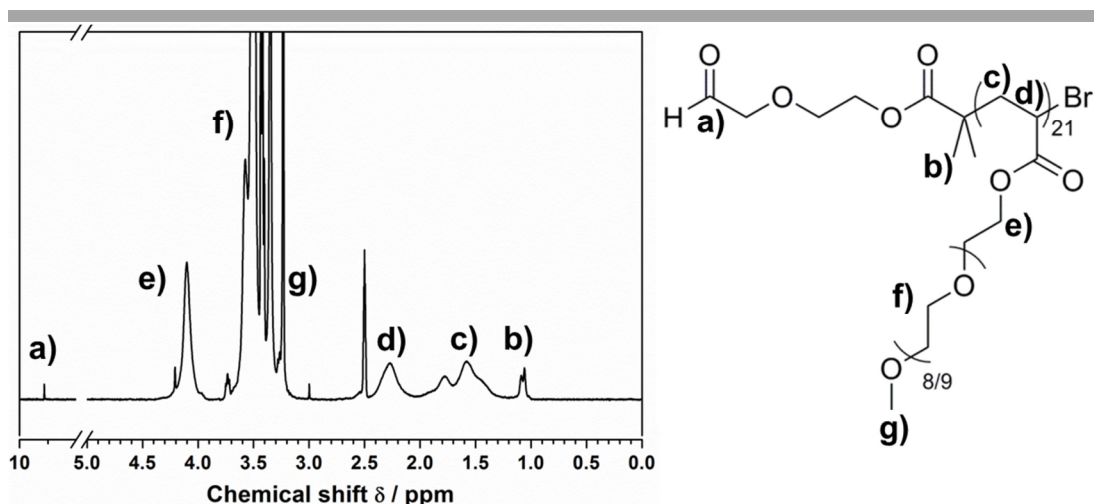


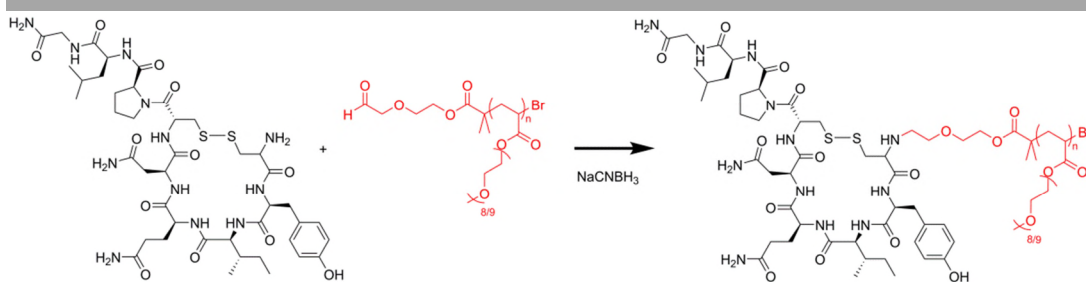
Figure 2.20. ^1H NMR (δ_6 -DMSO, 300.13 MHz) of poly(mPEGA₄₈₀)₂₁ after deprotection resulting in α aldehyde end group functionality.

Table 2.1. Comparison of molecular weights and dispersities of acetal protected and aldehyde (deprotected) DP_n 20 & DP_n 50 polymers.

PolyPEG	Conversion (NMR)	M_n (Da) (SEC)	\bar{D} (SEC)	M_n (Da) (Deprotected) (SEC)	\bar{D} (Deprotected) (SEC)
10 kDa - Acetal	100 %	11000	1.12	10500	1.15
25 kDa - Acetal	99 %	21300	1.16	20500	1.18

2.2.3.4. Aldehyde functional polymer conjugation

The resulting aldehyde functional polymers could then be conjugated onto oxytocin in a similar manner to the linear PEG to result in a secondary amine linked ‘comb’ oxytocin-polymer conjugate (scheme 2.10). 1.5 equivalents of the aldehyde functional polymer were added to oxytocin in phosphate buffer (pH 6.2, 0.1 M) with the addition of a freshly prepared solution of NaCNBH_3 (25 mM).



Scheme 2.10. Conjugation reaction of poly(mPEGA₄₈₀) to oxytocin with reduction by NaCNBH₃.

RP-HPLC analysis of the reaction after 72 hours revealed the appearance of a previously unobserved broad peak at a longer retention time ($t = 20.6$ minutes) compared to the native peptide ($t = 7.1$ minutes), signifying the incorporation of the 'comb' polymer onto the peptide (figure 2.21). Detailed inspection of the RP-HPLC chromatogram revealed a variety of smaller baseline peaks were observed, but these were also present when the purified polymer was analysed by RP-HPLC on its own, suggesting minor impurities in the polymer solution.

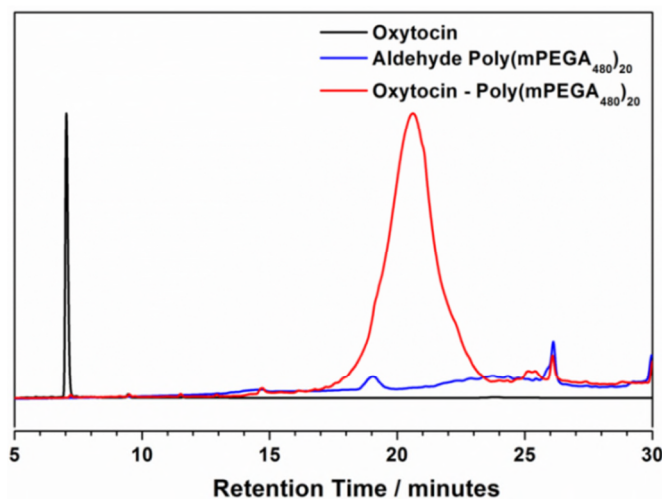


Figure 2.21. RP-HPLC trace of aldehyde poly(mPEGA₄₈₀)₂₀ polymer conjugation.

As with the conjugations of the linear polymers, both molecular weights of aldehyde poly(mPEGA) for conjugation onto oxytocin did not reach completion, resulting in remaining oxytocin in the reaction solution. Recently Maynard *et al.* have reported the importance on the polymer linker length for conjugation yields, which may impact reaction

efficiency.³⁶ However, for this conjugation reaction any residual peptide is removed by dialysis (1 MWCO, 3 days) resulting in a purified sample of oxytocin-polymer conjugate, with a different architecture to that of the linear equivalent.

2.2.4. Potential reversible Schiff base conjugation of oxytocin

The reaction utilised for the conjugation of aldehyde functional polymers onto oxytocin is accessed *via* a two-step reaction including a Schiff base intermediate. The generation of this Schiff base is *via* a reversible equilibrium reaction between the initial aldehyde polymer/ amine peptide and this imine intermediate, with reduction to the non-reversible product only occurring after addition of a reducing agent (such as NaCNBH₃). It was therefore proposed that the Schiff base linkage could be utilised in the formation of reversibly PEGylated oxytocin, whereby the polymer could be completely removed by externally adjusting the pH, allowing the therapeutic to maintain complete activity.

2.2.4.1. Linear PEG reversible conjugation

Initially, the potential for reversible conjugation was investigated with the linear aldehyde PEG, with the conjugation performed under the same conditions (pH 6.2 phosphate buffer, 0.1 M) as for the non-reversible reaction, simply with exclusion of the reducing agent. After 24 hours a sample was removed and submitted for RP-HPLC analysis whereby the RP-HPLC chromatogram (figure 2.22) showed the appearance of a newly formed bimodal peak at a longer retention time ($t = 14.3 / 14.9$ minutes) compared to the native peptide ($t = 7.3$ minutes). This bimodal peak was observed to form with both available linear PEGs, and as this phenomenon was not observed for the conjugation with the addition of NaCNBH₃ as a reducing agent, warranted further inspection.

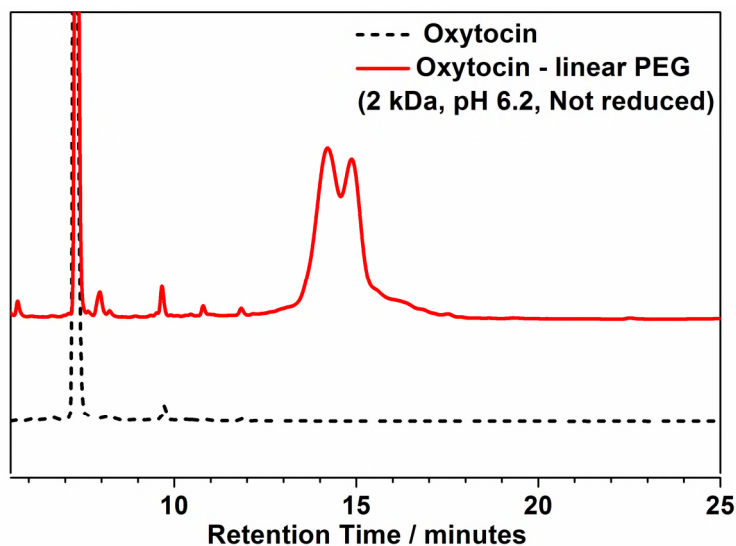


Figure 2.22. RP-HPLC analysis of conjugation of linear aldehyde PEG (2 kDa) onto oxytocin without the addition of NaCNBH_3 reducing agent.

The reaction was subsequently performed at a higher pH to investigate the formation of the bimodal nature of this peak under mildly basic conditions (pH 8.0 phosphate buffer, 0.1 M), where potential acidic hydrolysis would be minimised (figure 2.23). The presence of the bimodal product peak could further be observed suggesting that the potential formation of two distinct conjugate products was occurring. In order to further investigate the formation of these products these conjugation reactions were repeated at these two pHs as well as in an organic solvent (DMF), with samples removed periodically for RP-HPLC monitoring (using an alternative RP-HPLC gradient with a more gradual increase in aqueous content). It was found that the reaction occurred faster at pH 8 than at pH 6, with a more rapid disappearance of the native peptide being observed, theorised to be due to the reverse reaction (back to the native peptide) being favoured under more acidic pHs.

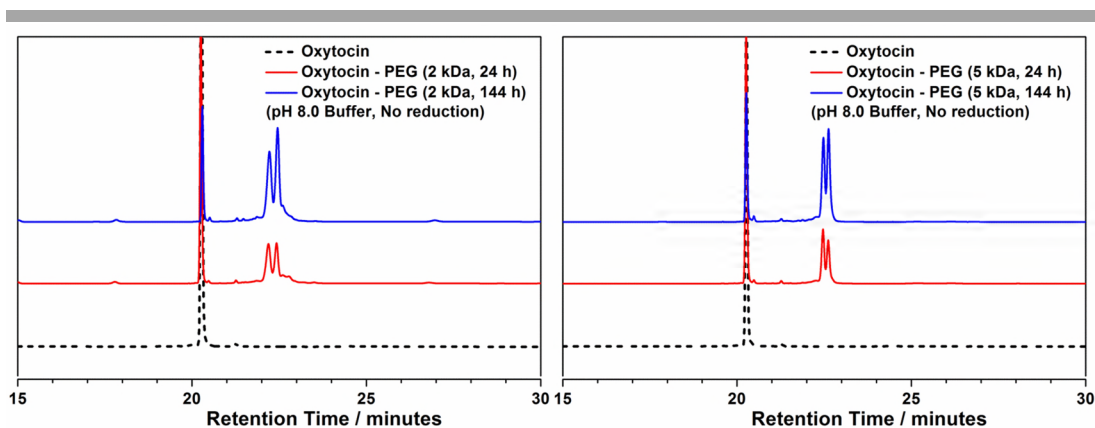


Figure 2.23. RP-HPLC analysis of 2 kDa and 5 kDa linear aldehyde Schiff base conjugation formation at pH 8.0 after 1 and 6 days.

The ratios between the two peaks remained approximately equivalent for the two different buffered pHs, although, after longer reaction monitoring, the second peak became more prominent, particularly in the acidic solution (table 2.2, figure 2.24). However, when the reaction was performed in DMF there was a much larger imbalance between the two peaks throughout the reaction.

Table 2.2. Conjugation of 2 kDa and 5 kDa aldehyde PEG onto oxytocin without reduction – decrease in oxytocin and conjugate peak ratios at t = 6 days.

Solvent	2 kDa PEG conjugation		5 kDa PEG conjugation	
	Oxytocin	Peak 1: Peak 2	Oxytocin	Peak 1: Peak 2
	(% decrease)	Ratio	(% decrease)	Ratio
pH 6.2	53.7	0.45 : 0.55	50.0	0.49 : 0.51
pH 8	78.3	0.43 : 0.58	63.3	0.41 : 0.59
DMF	58.9	0.26 : 0.74	65.7	0.32 : 0.68

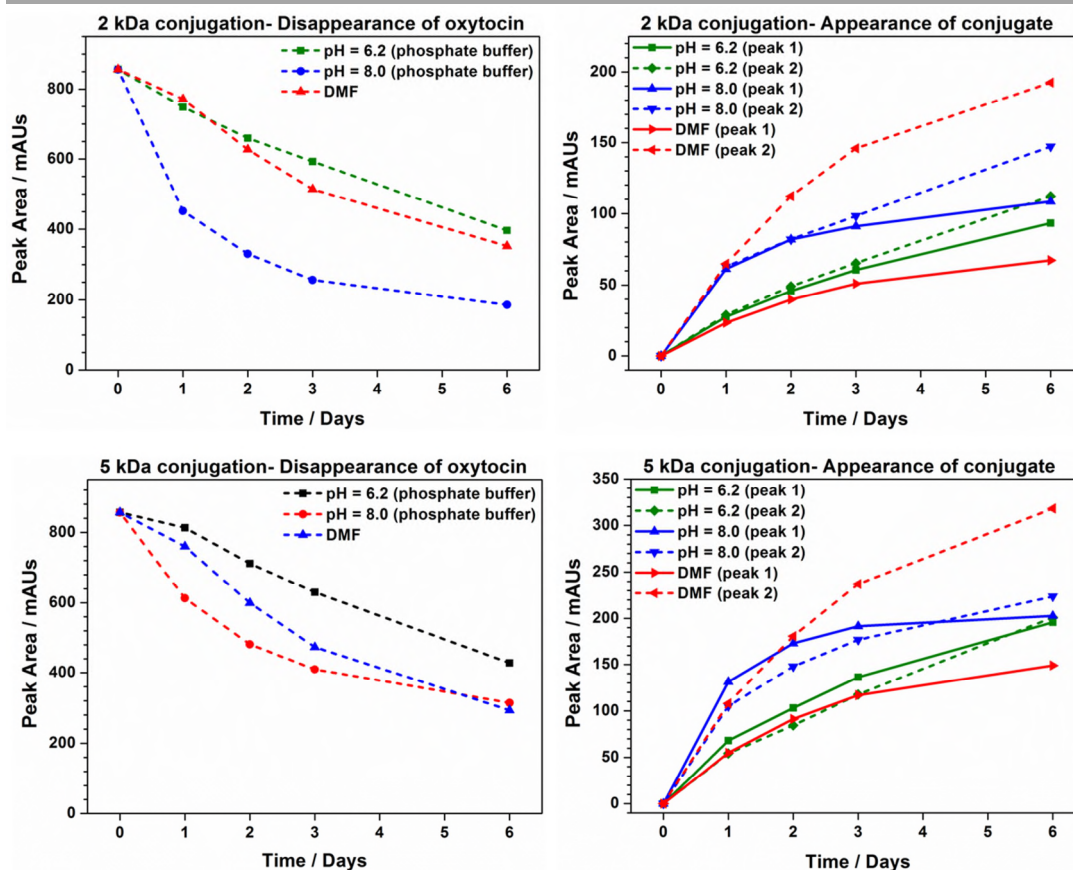


Figure 2.24. Rates of formation of conjugates and disappearance of oxytocin in different solvents for both M_w of PEG aldehyde conjugated onto oxytocin.

A Schiff base is the expected product formed in the reaction; therefore it was proposed that these two peaks could be due to the stereo isomers (E/Z) that could be formed during the reaction.

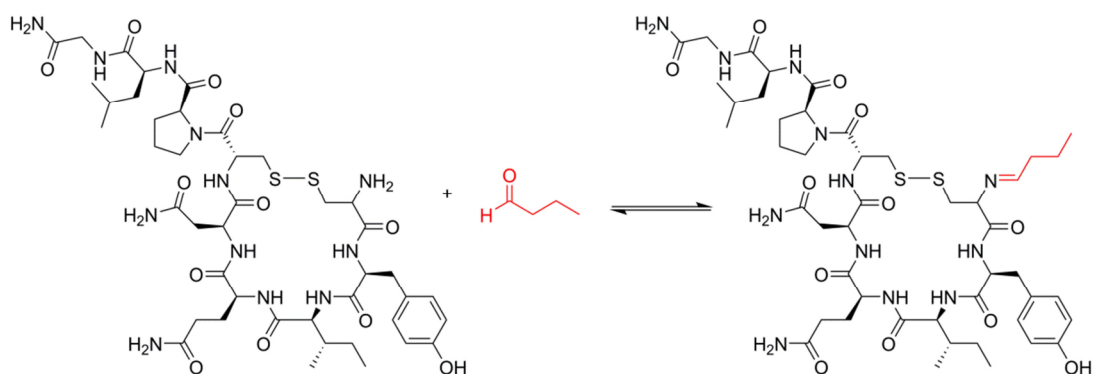
2.2.4.2. Investigation of conjugation with model small aldehydes

Further characterisation of the polymer Schiff base product is challenging due to the nature of the polymer. The products observed by RP-HPLC exist as one bimodal product, rather than two distinct units, making semi-preparative separation problematic. For additional characterisation into the two potential isomers to be undertaken, an

investigation was performed using a small molecule (non-polymer) aldehyde as a model system, under similar conjugation conditions.

Butyraldehyde reversible conjugation

Butyraldehyde, a small, water soluble aldehyde was utilised as a model aldehyde for the reversible conjugation to oxytocin (scheme 2.11). The reaction was performed in phosphate buffer (pH 8, 0.1 M) with a sample removed after 24 hours for analysis by RP-HPLC.



Scheme 2.11. Reversible conjugation of butyraldehyde and oxytocin.

As observed for the PEGylation, the Schiff base reaction showed the formation of two new products with longer retention times ($t = 15.9 / 16.5$ minutes) compared to the native peptide ($t = 11.7$ minutes) upon RP-HPLC analysis (figure 2.25). However, for this reaction it was observed that the appearance of products was that of two distinct sharp peaks after conjugation, with sufficient separation between the products rather than one broad bimodal product, as observed for the aldehyde linear PEG conjugation. Another difference observed for the conjugation of butyraldehyde onto oxytocin in comparison to conjugation of aldehyde PEG was that the reaction had a much higher efficiency, as there was an almost total disappearance of the native peptide after 24 hours. The peaks observed on the RP-HPLC chromatogram for the oxytocin conjugate were also more similar to that of

the native peptide with respect to peak shape, and absorption, compared to the PEGylated products which were much broader, and of a much lower absorbance.

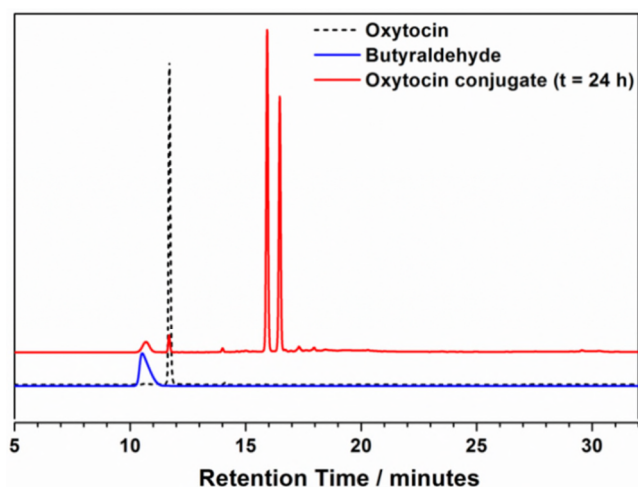


Figure 2.25. Conjugation of butyraldehyde onto oxytocin showing formation of two products.

The two butyraldehyde conjugates were then separated and individually collected using RP-HPLC and analysed by ESI-MS. The major products observed in the two separated samples were confirmed as the expected oxytocin-butyraldehyde Schiff base product $[M+H]^+ = 1061.4$ Da, suggesting that the two peaks formed correspond to two different isomers. Native oxytocin was also observed as a minor product $[M+H]^+ = 1007.3$ Da. The mobile phases used for RP-HPLC (either analytical, or for separation) include TFA as an acidic additive, giving the resting solution of the separation a pH of 2.1. As the reverse reaction is favoured under acidic conditions, some reversibility was observed after the separation, restoring unmodified oxytocin (figure 2.26). The amount of oxytocin released after overnight storage in the acidic solution was evaluated and differed significantly between the two separated peaks with 30.1 % oxytocin released from the first peak ($t = 15.9$ minutes) and 9.3 % released from the second peak ($t = 16.5$ minutes).

A further acidic separation study was carried out, whereby the acidic solutions of the separated conjugates were left for 8 weeks before repeated analysis by ESI-MS and RP-

HPLC (figure 2.26). After this time the majority of quantitative % peak area by RP-HPLC for the separation of conjugate peak 1 had disappeared (0.5 % remaining), with a strong increase in the amount of native peptide present (85.2 %), although some oxytocin degradation products could also be observed (total degradation: 13.9%). Similar behaviour was observed for the separated acidic solution of conjugate peak 2, although for this isomer there was a higher proportion of conjugate left (12.4 % remaining), but still a large increase in reformed oxytocin (75.1 %) accompanied by peptide degradation (total degradation: 12.3 %).

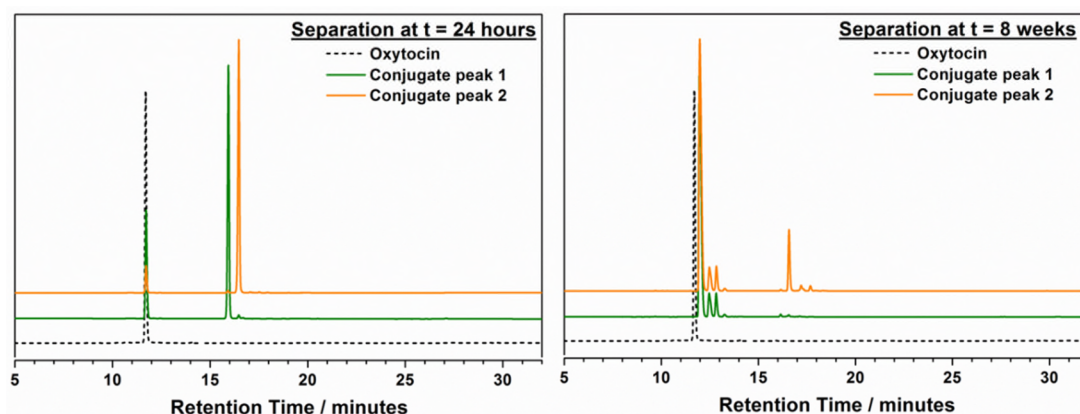


Figure 2.26. HPLC traces of separated butyraldehyde conjugates after $t = 24$ hours and $t = 8$ weeks storage in acidic solutions.

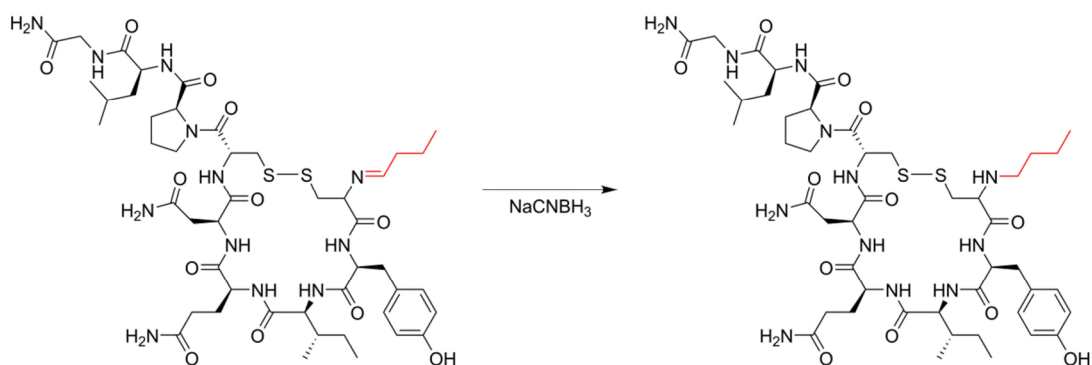
These results suggest that the oxytocin conjugate isomer responsible for the second peak has a higher stability than that observed for the first product and is less prone to reversing allowing restoration of the native peptide. The released oxytocin was confirmed by ESI-MS, where the major peaks observed could only be attributable to reformation of the native peptide $[M+H]^+ = 1007.3$ Da and $[M+Na]^+ = 1029.3$ Da.

This data provides key insights into the reversible nature of this type of conjugation chemistry and will be important for the later investigation of the reversibility of the PEGylated conjugates. It now becomes relatable as to why there might have been a small excess of the second conjugate peak post conjugation. If the PEGylated conjugate is

showing similar stability trends to the butyraldehyde conjugate, the second product is less susceptible to the reverse reaction, and is overall more stable.

Non-reversible conjugation with butyraldehyde

To confirm that the appearance of two different products is a particular characteristic of the reversible conjugate, the conjugation of butyraldehyde was also carried out with the addition of NaCNBH₃ as a reducing agent (scheme 2.12). This would lead to the *in-situ* reduction of the Schiff base resulting in the irreversibly linked stable secondary amine conjugate, previously examined with the aldehyde PEGs.



Scheme 2.12. Second step for the irreversible conjugation of butyraldehyde onto oxytocin.

When the reaction was monitored by RP-HPLC there was an almost complete disappearance of the native peptide and the appearance of one newly formed conjugate peak at a retention time of 13.6 minutes (figure 2.27). This is a lower retention time than either of the peaks monitored for the Schiff base product formation ($t = 15.9 / 16.5$ minutes) and higher than the native peptide ($t = 12.1$ minutes). The reduced butyraldehyde conjugate was confirmed by ESI-MS, where the major product corresponded to that predicted $[M+Na]^+ = 1085.3$ Da.

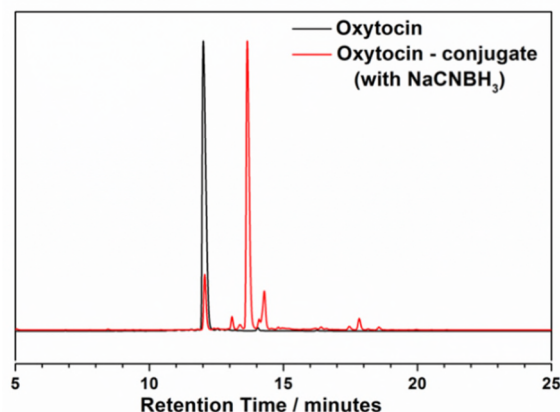


Figure 2.27. Conjugation of butyraldehyde with addition of NaCNBH_3 .

A further experiment was conducted where the reduced and non-reduced conjugations were performed alongside each other. Following the observation of the two isomer peaks by RP-HPLC to have partially formed, NaCNBH_3 was then added. This led to a convergence of both isomer peaks, with the major product peak observed at the end of the reaction being identified as the reduced butyraldehyde conjugate due to occurring at the same retention time in the RP-HPLC chromatogram as for the '*in-situ*' reduction experiment (figure 2.28). This strongly purports that these two peaks are both the Schiff base conjugates, and both can be reduced allowing formation of the singular stable irreversible product.

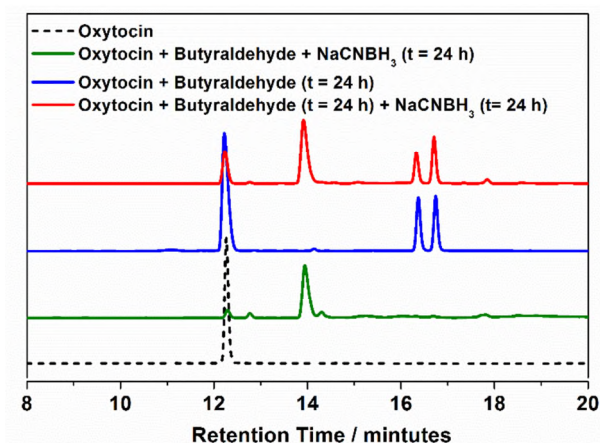
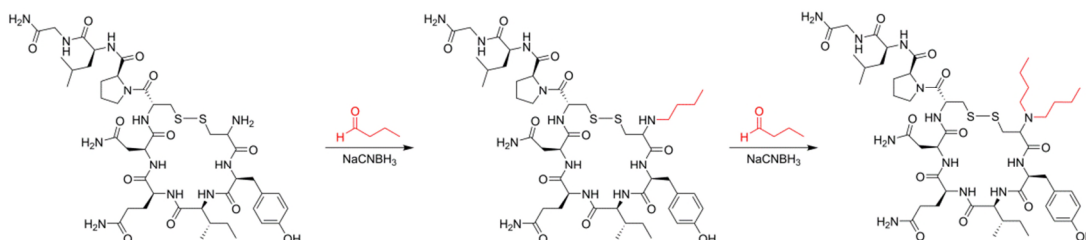


Figure 2.28. RP-HPLC analysis of reduced butyraldehyde conjugate, non-reduced butyraldehyde conjugate and non-reduced butyraldehyde conjugate upon addition of NaCNBH_3 .

Further investigation into the irreversible conjugation of butyraldehyde, with reduction by NaCNBH_3 , revealed that when a greater number of equivalents of the butyraldehyde reagent (5 and 10 equivalents) were used for the reduced conjugate formation, two peaks could be observed on the RP-HPLC. Analysis by ESI-MS showed that the major products appear at $[\text{M}+\text{Na}]^+ = 1085.3 \text{ Da}$ (the expected *N*-butyl oxytocin product) and $[\text{M}+\text{Na}]^+ = 1141.4 \text{ Da}$ (an increase of + 56.1 Da from that of the expected product). This suggests that a second addition of the butyraldehyde ($\text{C}_4\text{H}_8 = 56.06 \text{ Da}$) was able to take place, leading to a doubly conjugated product. The fundamental concept behind the attachment of polymers onto oxytocin *via* the use of amine targeting is that due to the peptide only possessing one conjugatable position (at the *N*-Terminus), only singular, site-specific conjugation could occur. The only position that another possible attachment could therefore take place is at the secondary amine still present after the initial butyraldehyde conjugation, and this explains why this second product is only observed for high equivalents of aldehyde reagent (scheme 2.13).



Scheme 2.13. Double conjugation of butyraldehyde onto oxytocin from second reaction at the secondary amine.

The 'double conjugation' reaction was monitored for several different equivalents of butyraldehyde reagent, investigating differences in % of peak area by RP-HPLC (UV $\lambda = 280 \text{ nm}$) of the two observed products (and the native peptide) (figure 2.29). For all reactions, the only major peaks that could be observed were those of oxytocin (retention time $t =$

12.1 mins), and the two (mono and disubstituted) conjugate products (retention times t_r = 13.6 / 16.3 mins).

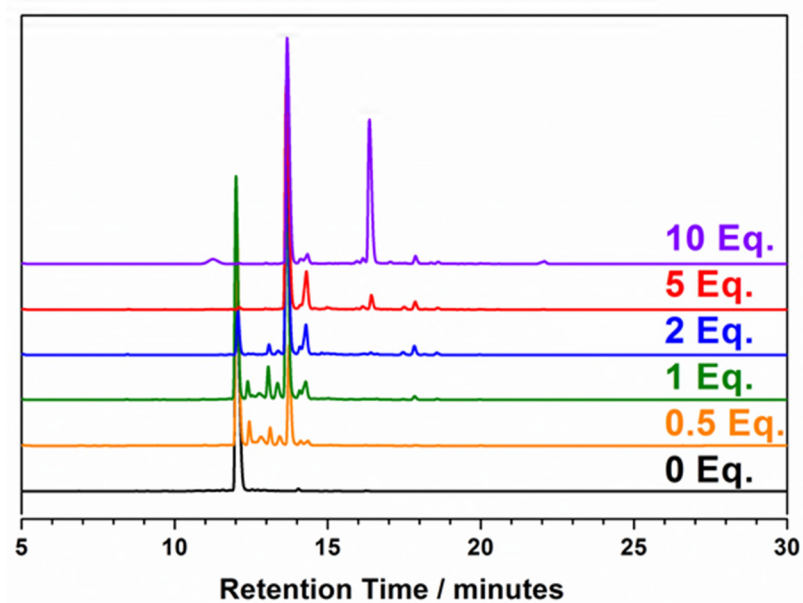


Figure 2.29. RP-HPLC analysis of product distributions with different equivalents of butyraldehyde.

Table 2.3. HPLC peak area % of oxytocin, monosubstituted product and disubstituted product on increasing equivalents of aldehyde reagent.

# Equivalents Butyraldehyde	Oxytocin Peak (%) t_r = 12.1 min	Conjugate Peak 1 (%) t_r = 13.6 min	Conjugate Peak 2 (%) t_r = 16.3 min
0.5	71.1	28.9	-
1	48.5	51.5	-
2	13.9	86.1	-
5	1.0	94.6	4.4
10	0.1	61.4	38.5

These results show that it is possible to acquire the doubly conjugated product, but that this does not become a hindrance for the conjugation until there is a large excess of the aldehyde reagent (table 2.3). The most often used excess in these reactions is 1-2 equivalents, therefore double conjugation should not often be presented as a problem, although it is something that must still be considered.

In the linear aldehyde PEG (reduced) conjugations discussed earlier within this chapter, the conjugate peak showed the presence of a potential second product appearing as a shoulder / peak tailing from the confirmed singular conjugate. This could have arisen from the double conjugation of the aldehyde PEG reagent, as the results for the butyraldehyde conjugation have confirmed that this is a possibility. However, in this case the shoulder peak was present to only a small degree within the overall product, and double conjugation was not evident upon analysis by MALDI-TOF MS.

Conjugations with other small aldehydes

There is a large range of other common aldehyde reagents available, which could be utilised in the same manner as butyraldehyde for conjugation onto peptides or proteins for further characterisation and analysis. The majority of commercially available PEG reagents have small alkyl links, such as propyl or butyl, between the aldehyde functionality and the beginning of the PEG polymer repeat unit. Therefore identical (reduced and non-reduced) conjugation reactions were also performed using propionaldehyde, a small, water soluble aldehyde with similar structure and properties to butyraldehyde (figure 2.30).

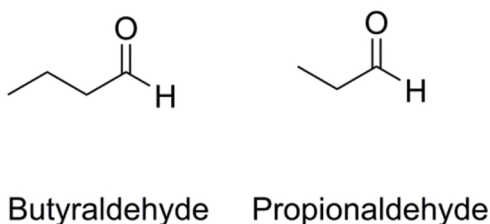


Figure 2.30. Small molecule aldehydes conjugated onto oxytocin in a similar manner to PEGs.

For the reaction of propionaldehyde without addition of a reducing agent, sampling for RP-HPLC (UV $\lambda=280$ nm) after 24 hours revealed the same behaviour as observed for the butyraldehyde equivalent. Two distinct peaks were observed in the RP-HPLC chromatogram at higher retention times ($t = 15.3$ & 15.8 minutes) compared to oxytocin ($t = 12.0$ minutes) alongside an almost complete disappearance of the native peptide, showing again the efficiency of these ‘small aldehyde’ reactions (figure 2.31). The conjugation with the addition of NaCNBH_3 was also very similar to that observed for butyraldehyde with the appearance of a singular major product peak ($t = 12.9$ minutes).

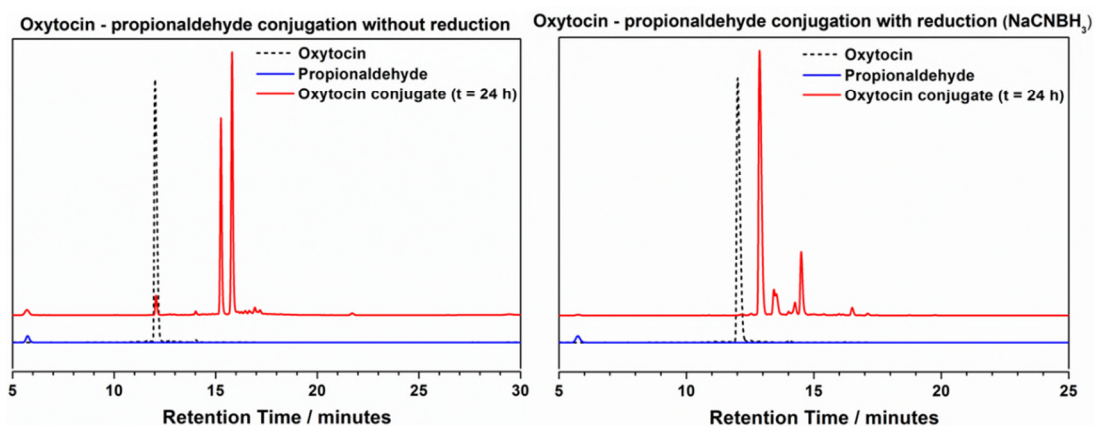


Figure 2.31. Conjugation of propionaldehyde with and without the addition of NaCNBH_3 .

However, when the reactions were repeated with small aromatic aldehydes (2-pyridine carboxaldehyde and 2-hydroxy benzaldehyde), RP-HPLC analysis of the resulting reaction solutions showed either the appearance of a large number of side products, or no

observed conjugation. This is likely due to the aromatic nature of these small molecule aldehydes, preventing efficient conjugation.

Due to the similarities between the results attained for the conjugations of butyraldehyde and propionaldehyde and the linear PEGylations (appearance of two distinct products without addition of NaCNBH₃ and one with the addition of NaCNBH₃), valuable information about the reaction of oxytocin and alkyl aldehydes has been attained. It has become increasingly evidenced that the Schiff base formation occurs in the expected manner leading to the formation of the E and Z isomers, however, further confirmation of the structures would be beneficial.

NMR analysis of small aldehyde conjugates

For further characterisation of the *N*-alkyl oxytocin product, solutions of the reaction mixtures (pH 8, phosphate buffer, 0.1 M) from the reversible conjugations of butyraldehyde and propionaldehyde onto oxytocin (2 mM) were submitted for NMR analysis (10 % D₂O, 600 MHz) (figure 2.32). The native peptide (2 mM) was also analysed under the same conditions, with results correlating well with previous NMR assignments of oxytocin in pH 6.2 phosphate buffer.³⁷

For the butyraldehyde Schiff base conjugate, the presence of two new doublet peaks could clearly be observed within the imine region of the spectra (δ = 7.55 / 7.82 ppm), likely due to the two different isomers formed, although the peak at 7.55 ppm also overlaps with an amide peak on the peptide. Analysis by 2D NMR revealed TOCSY connectives from these imine peaks of two different signals at δ = 4.4 ppm, both assignable to α protons of the Cys¹ residue, which are then coupling to protons at δ = 2.7 ppm, likely the β Cys¹ proton. Additionally, the peaks representing the aromatic groups on the tyrosine residues show a chemical shift post-conjugation (native peptide: δ_H = 7.16, ϵ_H = 6.83 ppm; butyraldehyde

conjugate: $\delta_{\text{H}} = 7.09$, $\epsilon_{\text{H}} = 6.85$ ppm), where Tyr² is the next amino acid from the *N*-terminal amine within the peptide structure.

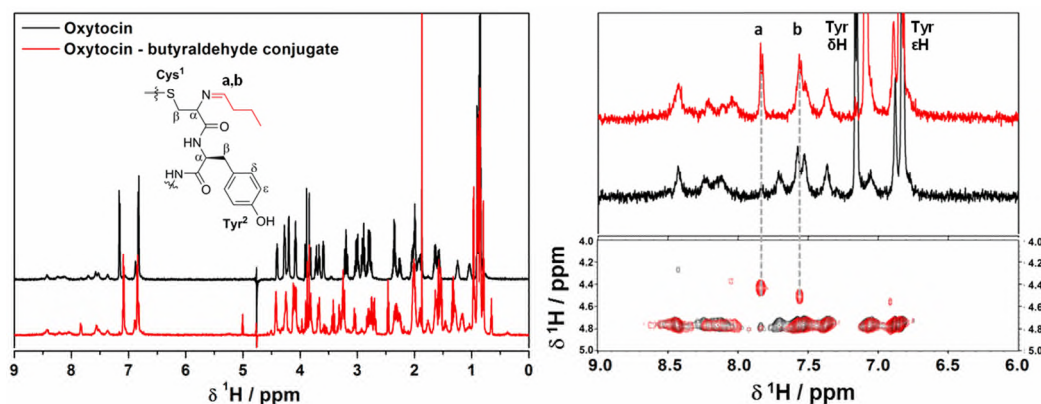


Figure 2.32. ¹H NMR analysis of butyraldehyde conjugation reaction mixture (pH 8) with 10 % D₂O including a zoom in of the imine region (6 – 9 ppm) and accompanying TOCSY spectra.

When the propionaldehyde Schiff base conjugate was investigated in the same manner, very similar behaviour was observed (figure 2.33). There was the presence of the two new imine peaks at similar positions to those found for the butyraldehyde conjugate ($\delta = 7.56$ / 7.83 ppm) and comparable tyrosine shifts were also observed ($\delta_{\text{H}} = 7.08$, $\epsilon_{\text{H}} = 6.82$ ppm).

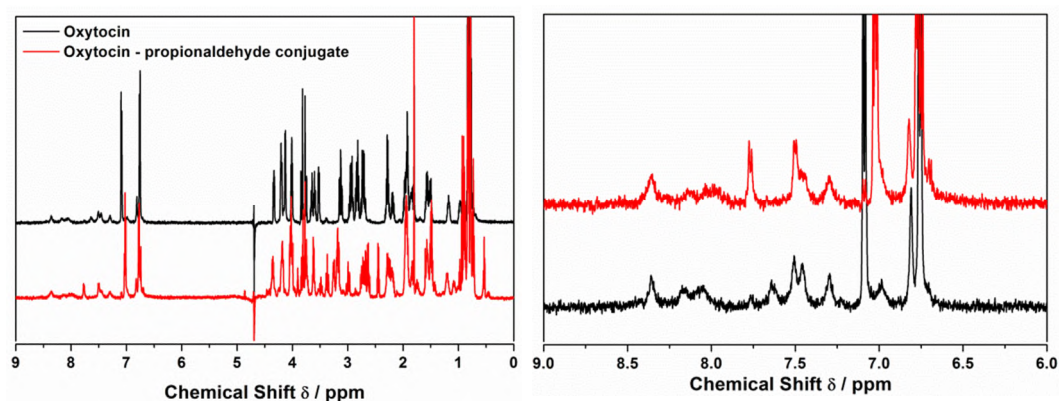


Figure 2.33. ¹H NMR analysis of propionaldehyde conjugation reaction mixture (pH 8) with 10 % D₂O including a zoom in of the imine region (6 – 9 ppm).

As the NMR analysis was taken as a sample of the reaction mixture, the excess aldehyde reagent is still present (figure 2.34). In aqueous solutions (as within the NMR) this aldehyde

reagent undergoes hydrolysis leading to the hydrate product, for which the NMR shows particularly prominent peaks at approximately $\delta = 5.00$ ppm. This can be observed for the reaction mixtures of the aldehyde reagent, in both the propionaldehyde and butyraldehyde samples, as well as in the conjugation mixtures.

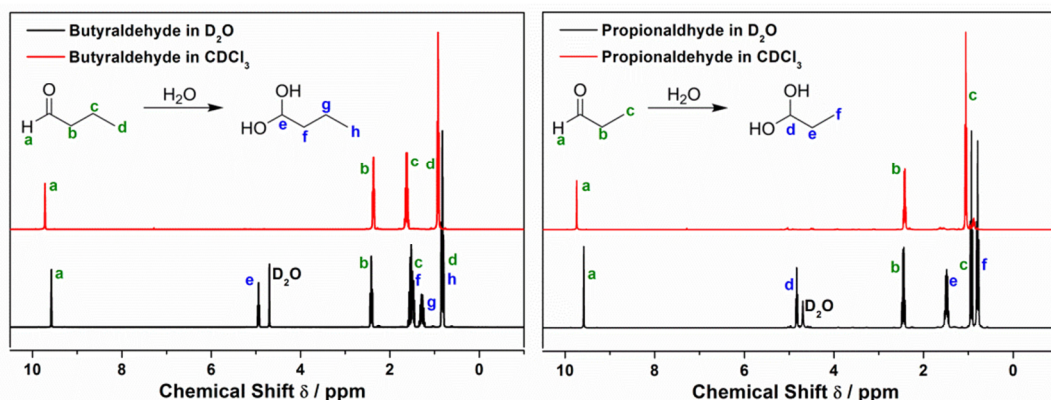


Figure 2.34. ¹H NMR of butyraldehyde and propionaldehyde in CHCl₃ and D₂O showing formation of hydrate under aqueous conditions.

These NMR results support the assignment of the two small aldehyde conjugates as existing as two different imine products predicted during the reaction. From these results however, it is difficult to determine which conjugate product is the E / Z isomer, which, given that one product has a potentially much higher stability, would be beneficial information.

2.2.4.3. PolyPEG reversible conjugation

The aldehyde functional polyPEG (10 kDa) was also conjugated onto oxytocin without the aid of a reducing agent leading to the formation of a Schiff base linked 'comb' polymer-conjugate. This conjugation was carried out in phosphate buffer (0.1 M, pH 8) and sampling by RP-HPLC after 24 hours revealed the presence of a newly formed singular broad peak at a higher retention time ($t = 24.1$ minutes) to the native peptide ($t = 12.1$

minutes) (figure 2.35). The peak observed in the HPLC chromatogram is broader than that observed for the linear polymer or the small molecule studies. It is possible that there could be two distinct isomer peaks observed for the polyPEG, but that only one peak is observed due to disperse nature of the polymer.

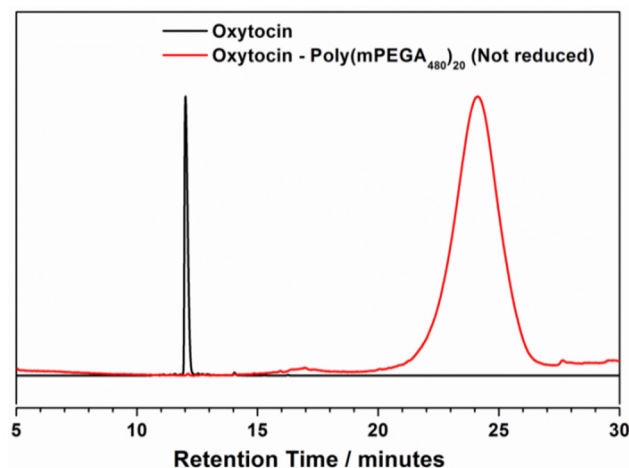


Figure 2.35. RP-HPLC trace of Schiff base oxytocin-poly(mPEGA₄₈₀)₂₀ conjugate formed without the addition of a reducing agent.

2.2.5. Reversibility studies of oxytocin Schiff base conjugates

Following the synthesis and characterisation of the Schiff base linked conjugates; controlled reversibility studies were conducted to ascertain whether the conjugates could be promoted to release a significant amount of native peptide. From the reversibility observed upon storage of the purified butyraldehyde conjugates in acidic solutions, the potential for regeneration of the native peptide is possible, but being able to tune the amount of peptide released would be desirable. In order to investigate oxytocin release, the initial peptide concentration is required to be very low, so that any increases in peptide peak intensity could only be caused by and attributed to the reverse of Schiff base conjugate formation. The samples were monitored by RP-HPLC, tracking the oxytocin

content of the solutions and respective conjugate concentrations over the period of the reversal study.

2.2.5.1. Butyraldehyde Schiff base conjugate reversibility

For reversibility measurements on the butyraldehyde-oxytocin conjugate these were carried out immediately post conjugation, due to the high efficiency of the reaction signifying minimal remaining oxytocin. A sample of the conjugation solution was diluted with two buffers at pH 5.0 (citrate buffer, 0.1 M) and pH 7.4 (phosphate buffer, 0.1 M) to yield overall concentrations of 0.2 mg/ml of peptide. A $t = 0$ sample was submitted to RP-HPLC whereby the oxytocin concentration (RP-HPLC peak area) would be at its lowest point before any potential reversibility of the conjugation. After 4 days of stirring in the buffered solutions there were clear differences observed by RP-HPLC between the two different pHs (table 2.4, figure 2.36).

Table 2.4. RP-HPLC (UV, $\lambda = 280$ nm) peak areas (mAU) for oxytocin and the two conjugate peaks upon reversal at different pHs for butyraldehyde-oxytocin conjugate.

Conjugate	pH	Oxytocin	Oxytocin	Conj	Conj	Conj	Conj
		Peak	Peak	Peak 1	Peak 1	Peak 2	Peak 2
		$t = 0$	$t = 4$ d	$t = 0$	$t = 4$ d	$t = 0$	$t = 4$ d
Butyraldehyde	5.0	68.2	681.8	814.6	402.9	584.8	570.0
Butyraldehyde	7.4	68.2	199.4	814.6	580.5	584.8	710.8

In the pH 5.0 solution, analysing peptide peak area on HPLC revealed a ten-fold increase in oxytocic content. This was accompanied by a decrease in peak area for both conjugate products (overall 30 % decrease in conjugate peaks). Analysis of the two conjugate peaks

revealed that the second peak showed a much smaller decrease in area (-3 %) compared to the first peak (-49 %), signifying that there was not a large change in concentration for this isomer. In the pH 7.4 buffer a moderate three-fold increase in the amount of oxytocin present in solution was observed, but there was not a large accompanying decrease (overall -8%) in the area of the combined conjugate peaks. There was, however, a shift in the ratios observed for the isomers; a decrease in the first peak and an increase in the second peak suggesting the re-formation of the more stable second conjugate product (0.58 : 0.42 to 0.45 : 0.55).

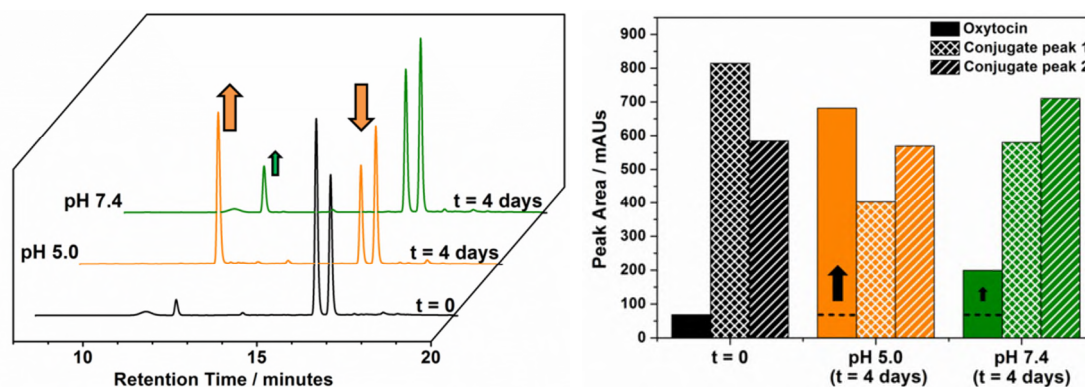


Figure 2.36. RP-HPLC trace showing reappearance of oxytocin under reversible conditions, and bar graph highlighting concentration changes of both butyraldehyde conjugates and oxytocin at pH 5.0 and pH 7.4.

These differences observed at the two pHs are significant in clearly highlighting that the reversal of the conjugation can be partially controlled by using pH as a means to induce release of the native peptide. This highlights the potential for using this system to stimulate oxytocic release, after which the reversible nature of the Schiff base linked PEGylated oxytocin (both linear and polyPEG) were further investigated.

2.2.5.2. Linear PEG Schiff base conjugate reversibility

Prior to investigating the pH-induced reversible nature of the linear PEG, complete removal of any remaining oxytocin was performed by dialysis against pH adjusted water

(pH 8). Immediately post dialysis a sample was submitted for RP-HPLC as a $t = 0$ sample, to assess the minimum level of oxytocin present in the solution before two different pH conditions were examined (pH 5.0 and pH 7.4). For the linear PEGylated conjugate (5 kDa PEG) the oxytocin release was initially monitored by RP-HPLC after storage in the different pH solutions for 18 days (table 2.5, figure 2.37). After this time there is clearly a significant reappearance of native oxytocin stimulated at both pHs in comparison to the $t = 0$ sample.

Table 2.5. RP-HPLC (UV, $\lambda = 280$ nm) peak areas (mAU) for oxytocin and the two conjugate peaks upon reversal at different pHs for linear PEG-oxytocin conjugate.

Conjugate	pH	Oxytocin	Oxytocin	Conj	Conj	Conj	Conj
		Peak	Peak	Peak 1	Peak 1	Peak 2	Peak 2
		$t = 0$	$t = 18$ d	$t = 0$	$t = 18$ d	$t = 0$	$t = 18$ d
Linear PEG	5.0	25	302.3	242.4	97	407.1	338.5
Linear PEG	7.4	25	168.4	242.4	149.9	407.1	423.8

After 18 days the concentration of oxytocin had dramatically increased in the pH 5.0 solution indicating that oxytocin had been released from the conjugate (twelve-fold increase), whilst the pH 7.4 solution showed a more modest release of the native peptide (six-fold increase). This demonstrates that there was some pH control over the release, as observed with the butyraldehyde conjugates. The disappearance of conjugates was also monitored, which further highlighted that the first conjugate peak is much more prone to reversion releasing the native peptide. The loss of conjugates was observed at both pH values but is particularly prominent under acidic conditions (pH 5.0: 60 % decrease; pH 7.4: 38 % decrease).

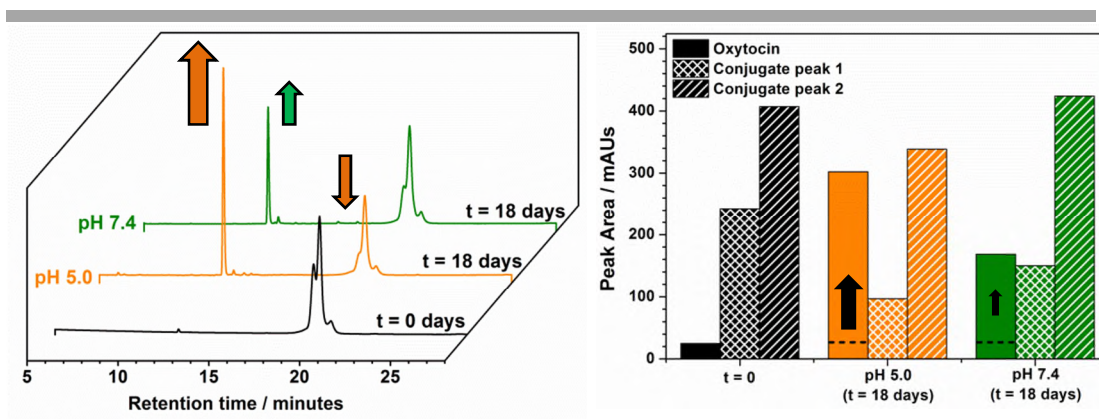


Figure 2.37. RP-HPLC trace showing reappearance of oxytocin under reversible conditions, and bar graph highlighting concentration changes of both linear PEG conjugates and oxytocin at pH 5 and pH 7.4.

The release study was repeated with further monitoring at different time points over a two week period, which revealed interesting characteristics (figure 2.38). Investigations at both pHs show approximately the same initial level of release of oxytocin, however, the release at pH 7.4 reaches a plateau after 4-5 days. The oxytocin concentration however continued to gradually increase in the pH 5 solution across the two week study, showing potential for a prolonged release of oxytocin from the conjugates over time.

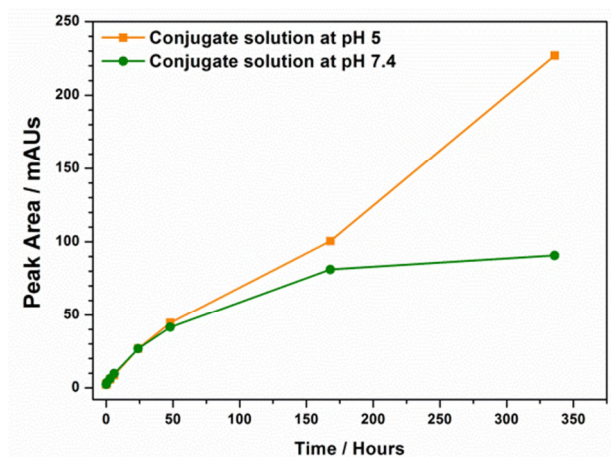


Figure 2.38. Concentration changes monitored for oxytocin release from linear PEGylated conjugate across a 2 week period at pH 5 and pH 7.4.

2.2.5.3. PolyPEG Schiff base conjugate reversibility

For the polyPEG conjugates when the same pH dependant analysis was undertaken there was no change in the peak area for the (singular) conjugate peak. There was an observation of some appearance of oxytocin, but not in an appreciable concentration, particularly in comparison to the linear PEG or butyraldehyde conjugate releases (table 2.6, figure 2.39).

Table 2.6. RP-HPLC (UV, $\lambda = 280$ nm) peak areas (mAU) for oxytocin and the singular conjugate peaks upon reversal at different pHs for polyPEG-oxytocin conjugate.

Conjugate	pH	Oxytocin Peak	Oxytocin Peak	Conjugate Peak	Conjugate Peak
		t = 0	t = 21 d	t = 0	t = 21 d
PolyPEG	5.0	0	6.6	658.4	620.3
PolyPEG	7.4	0	7.5	658.4	619.7.

A peak area of 7 mAU for oxytocin corresponds to a concentration of approximately 2 μmol (0.002 mg ml^{-1}). This suggests that the reverse reaction was not being promoted in this case, or at least not to the same degree as previously observed for the other oxytocin aldehyde conjugates.

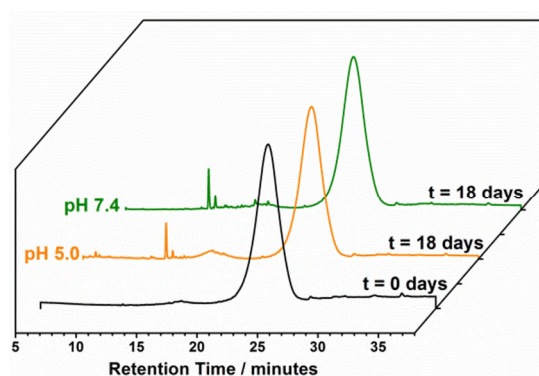


Figure 2.39. RP-HPLC traces for polyPEGylated oxytocin release study at pH 5 and pH 7.4.

This leads to valuable information about the reversible conjugation of these architectures of Schiff base conjugated oxytocin analogues. From the reversibility experiments the smallest (and least branched) Schiff base conjugate released the highest concentration of oxytocin under acidic conditions followed by the linear PEG conjugate, where there was still an appreciable regeneration of the native peptide. On increasing the conjugate size (and structure), the branched 'comb' PEGylated analogue did not show any appreciable conversion of the conjugate back to native oxytocin. It can therefore be assumed that the structural design of the conjugates plays an important role in the ability to reverse the conjugation under stimulated conditions, with larger and more branched polymers proving less prone to reversion.

2.3. Chapter 2 Conclusions

Multiple PEGylation strategies were employed for singularly attaching different polymer architectures to the small peptide oxytocin, site specifically at the *N*-terminal amine. Comb PEG polymers were synthesised by copper (0) mediated controlled radical polymerisation containing succinimide ester end group functionality, with control over molecular weights and low dispersities. The polymers retained their end group functionality and were successfully conjugated onto oxytocin alongside their commercially available linear equivalents.

Comb PEG polymers containing protected aldehyde end group functionality were also synthesised in the same manner, and easily deprotected post-polymerisation, yielding aldehyde end functional polyPEG. These polymers, along with their corresponding linear analogues, were also conjugated onto oxytocin in a two-step reaction *via* a Schiff base intermediate, with the addition of NaCNBH₃, leading to stable peptide-polymer conjugates. The singular attachment of the linear PEG conjugation was confirmed by MALDI-TOF MS,

which shows a good indication that the polyPEG conjugates would react in the same manner. All conjugates were characterised by RP-HPLC, revealing the presence of new peaks at different retention times to the native peptide.

Without the addition of the reducing agent the reaction leads to reversible Schiff base products, and this was evaluated for linear PEG, poly(mPEGA) and one non-polymer small organic aldehyde functional reagent. The use of a non-polymer reagent allowed further characterisation of the Schiff base products formed by ESI-MS and NMR as a model for the polymer reaction. The Schiff base linked peptide-polymer conjugates were envisaged to be able to release the native peptide under certain stimulated conditions therefore the reversibility was evaluated for the oxytocin Schiff bases of linear and polyPEG polymers as well as the small molecule equivalent. This suggested that acidic conditions were able to promote oxytocin release. Furthermore, it was found that the nature of polymer architecture was a highly important factor and, therefore, consideration of the polymers must be undertaken within exploiting these reversible reactions.

2.4. Experimental

2.4.1. Materials

Oxytocin (c- [Cys-Tyr-Ile-Gln-Asn-Cys]-Pro-Leu-Gly-NH₂) was gifted from PolyPeptide laboratories (Hillerød, Denmark) and used as received. Functional poly(ethylene glycol)s: NHS ester functional poly(ethylene glycol) (MW: 2,000 Da / 5,000 Da) and aldehyde functional poly(ethylene glycol) (MW: 2,000 Da / 5,000 Da) were purchased from Rapp Polymere (Germany) and stored in a freezer (-18 °C). Poly(ethylene glycol) methyl ether acrylate (average M_n: 480; containing 100 ppm BHT & 100 ppm MEHQ as inhibitors) was purchased from Sigma Aldrich and stored at 4 °C. Copper (0) wire was pre-treated by

washing in hydrochloric acid (35%) for 20 min, then rinsed with water, and dried under nitrogen immediately prior to use. *N,N,N',N',N'',N''*-Hexamethyl-[tris(aminoethyl)amine] (Me₆-TREN) was synthesised according to a previously reported procedure and stored at -18 °C prior to use.³⁸

2.4.2. Instrumentation & Analysis

Nuclear magnetic resonance (NMR) spectra were acquired with a Bruker DPX-300, Bruker DPX-400, Bruker HD-300 and Bruker HD-400 spectrometers with samples prepared in deuterated solvents (CDCl₃ or δ₆-DMSO) and chemical shifts were reported in parts per million (ppm) with reference to solvent residual peaks. 1D ¹H and 2D ¹H NMR of peptide conjugates were acquired on a Bruker Avance III 600 NMR spectrometer using the reaction mixture (2mM) with 10 % D₂O by Dr Claudia Blindauer.

Size exclusion chromatography (SEC) was performed on an Agilent Polymer Laboratories GPC50 fitted with differential refractive index (RI) detector. Separations were performed on a pair of Agilent Polargel Medium Columns eluting with *N,N* dimethylformamide containing 0.1 M LiBr as an additive at 50 °C with a flow rate of 1 ml/min. Molecular weights were calculated relative to narrow PMMA standards (550 – 955,000 g mol⁻¹) and fitted with a 3rd order polynomial.

Infrared absorption spectra were recorded on a Bruker VECTOR-22 FTIR spectrometer using a Golden Gate diamond attenuated total reflection cell.

Analytical high performance liquid chromatography (HPLC) was performed on Agilent 1260 Infinity series stack equipped with an Agilent 1260 binary pump and degasser. 50 µl samples were injected using Agilent 1260 autosampler with a flow rate of 1 ml/min. The HPLC was fitted with a Phenomenex Luna C18 column (250 x 4.6 mm) with 5 micron

packing (100Å). Detection was achieved using an Agilent 1260 variable wavelength detector monitoring at 280 nm. Mobile phase A consisted of either 100 % water containing 0.04 % TFA as an additive or 90 % water, 10 % acetonitrile containing 0.04 % TFA as an additive. Mobile Phase B consisted of 100 % acetonitrile containing 0.04 % TFA as an additive. The column was equilibrated by washing with the starting % of mobile phase A for 10 minutes prior to injection for all conditions. The method gradient (1) HPLC analysis: 90 % mobile phase A decreasing to 40 % mobile phase A over 27 minutes, and remaining at 40% mobile phase A for 8 minutes, before resetting to the starting conditions in 1 minute and remaining in these conditions for at least 10 minutes to re-equilibrate the column before subsequent injections. The method gradient (2) HPLC analysis: 95 % mobile phase A decreasing to 80 % mobile phase A across 15 minutes, and to 40 % mobile phase A at 22 minutes and remaining at 40% mobile phase A for 5 minutes, before resetting to the starting conditions in 1 minute and remaining in these conditions for at least 10 minutes to re-equilibrate the column before subsequent injections.

Semi-preparative HPLC was performed on the same HPLC system as above fitted with a Phenomenex Jupiter C18 column (250 x 21.2 mm) with 5 micron packing (300Å). Detection was achieved using an Agilent 1260 multiple wavelength detector monitoring at 280 nm and 225 nm. Mobile phase A consisted of 100 % water containing 0.04 % TFA as an additive and Mobile phase B consisted of 100 % acetonitrile containing 0.04 % TFA as an additive. The flow rate was set to 5 ml/min and general gradients were as follows: 81 % mobile phase A for 4 minutes decreasing to 58 % mobile phase A for 30 minutes, and remaining at 58 % mobile phase A for 10 minutes, before decreasing to 50% mobile phase A for 10 minutes and remaining at 50 % mobile phase A for 5 minutes before returning to starting conditions in 1 minute and remaining in these conditions for at least 10 minutes to re-equilibrate the column before subsequent injections.

MALDI-TOF MS was conducted using a Bruker Daltonics Autoflex MALDI-ToF mass spectrometer. MALDI-TOF samples were made by mixing a saturated solution of α -cyano-4-hydroxycinnamic acid (CHCA) in methanol as a matrix (10.8 μ l), sodium iodide in tetrahydrofuran (THF) (1.0 mg/ml) as cationisation agent (4.2 μ l) and sample in THF with 1 drop of water (1.0 mg/ml) (10.8 μ l) and 0.7 μ l of the mixture was applied to target plate. Spectra were recorded in reflector mode calibrating with mPEG 2000 Da. Electrospray ionisation mass spectra (ESI) were recorded on an Agilent 6130B Single-Quad.

2.4.3. Synthetic procedures for chapter 2

2.4.3.1. NHS ester linear PEG conjugation onto oxytocin

Oxytocin (20 mg, 20 μ mol) and NHS-PEG (Rapp-Polymere, 2,000 Da) (60 mg, 30 μ mol) were separately dissolved in 1 ml of DMF and the solutions added together at 10 °C and 20 μ l triethylamine was added. After stirring overnight at T= 10 °C, 20 μ l of the solution was removed and dissolved in 1 ml H₂O for RP-HPLC analysis (λ = 280 nm).

2.4.3.2. Aldehyde linear PEG conjugation onto oxytocin

Aldehyde functional linear PEG (40 mg, 20 μ mol) was dissolved in sodium phosphate buffer (5 ml, pH 6.2, 100 mM) and left at 10 °C for 1 hour. Oxytocin (15 mg, 15 μ mol) was stirred in the same buffer (5 ml) at 10 °C for 15 minutes. Both solutions were added together and a freshly prepared solution of NaCNBH₃ (25 mmol) was added. After stirring overnight at T= 10 °C a 100 μ l aliquot was taken and dissolved in 1 ml H₂O for RP-HPLC analysis.

2.4.3.3. *Synthesis of N-hydroxysuccinimide-2-bromo-2-methylpropionate*

N-Hydroxy succinimide (4.45 g, 38.7 mmol) was dissolved in anhydrous DCM (100 ml) and triethylamine (7.16 ml, 51.5 mmol) was added. The flask was cooled to 0 °C before the addition of α -bromoisobutyryl bromide (5.25 ml, 42.6 mmol) in DCM (20 ml) dropwise under flow of nitrogen. The mixture was stirred at 0 °C for 45 minutes, before warming to room temperature and stirring for a further 3 hours. The reaction mixture was then poured into ice-water (200 ml) and the organic layer was separated and washed with NaHCO₃ (2 x 50 ml) followed by water (2 x 50 ml) and again with NaHCO₃ (2 x 50 ml). The organic layer was dried with MgSO₄ and the solvent removed under reduced pressure. The crude product was purified by recrystallisation with Et₂O to afford the product as an off white powder (8.46 g, 32.0 mmol, 83 %).

¹H NMR (CDCl₃, 400.05 MHz) δ (ppm): 2.06 (6H, s, C(CH₃)₂Br), 2.85 (4H, s, (CH₂CO)₂N). ¹³C NMR (CDCl₃, 100.59 MHz) δ (ppm): 25.54 ((CH₂CO)₂N), 30.59 (C(CH₃)₂Br), 51.17 (C(CH₃)₂Br), 167.40 (NOCO), 168.59 (((CH₂CO)₂N).

2.4.3.4. *Cu(0) mediated NHS ester α -functional poly(mPEGA-₄₈₀) synthesis*

Copper wire (1.25 mm diameter) was activated by washing in hydrochloric acid for 10 minutes, before being rinsed with water and dried under a nitrogen blanket. In a Schlenk tube, Cu(II) bromide (3.73 mg, 0.0167 mmol) was dissolved in DMSO (1.5 ml, anhydrous) and Me₆TREN ligand (16.1 μ l, 0.0602 mmol) was added. NHS-ester functional initiator (88 mg, 0.334 mmol) in DMSO (1 ml, anhydrous) and mPEGA (2.94 ml, 6.68 mmol) in DMSO (1 ml, anhydrous) were added. The solution was degassed by bubbling with nitrogen for 20

minutes before the addition of pre-activated copper wire under a positive nitrogen pressure and the Schlenk tube sealed with a rubber septum. The polymerisation was sampled under a positive pressure of nitrogen for NMR (δ_6 -DMSO) and SEC analysis (DMF).

The polymers were purified by repeated precipitation into diethyl ether / hexane (1:1).

2.4.3.5. Synthesis of 2-(2,2-dimethoxyethoxy)ethyl-2-bromo-2-methylpropionate

The two step protected aldehyde initiator synthesis was adapted from a reported procedure.²⁵ Potassium hydroxide (40 g, 0.71 mol) and ethylene glycol (100 ml, 1.79 mol) were added together and gradually heated to 115 °C with stirring. Chloroacetaldehyde dimethyl acetal was slowly added dropwise and the solution stirred at 115 °C for 48 hours. The solution was cooled to room temperature before the addition of water (200 ml). The solution was then extracted with dichloromethane (2 x 150 ml) and washed with brine (2 x 100 ml) before the organic fractions were dried with MgSO_4 and the solvent removed under reduced pressure yielding 2-(2,2-dimethoxy-ethoxy)-ethanol as a yellow oil (18.12 g, 0.12 mol, 17 %) which was used for the following step without further purification.

^1H NMR (CDCl_3 , 300.13 MHz) δ (ppm): 3.37 (6H, s, $\text{CH}(\text{OCH}_3)_2$), 3.52 (2H, t, $J = 5.09$ Hz, CHCH_2O), 3.56-3.73 (4H, m, $\text{OCH}_2\text{CH}_2\text{OH}$), 4.50 (1H, q, $J = 5.09$ Hz, $\text{CH}(\text{OCH}_3)_2$). ^{13}C NMR (CDCl_3 , 75.47 MHz) δ (ppm): 52.83 ($\text{CH}(\text{CH}_3\text{O})_2$), 61.54 ($\text{CH}_2\text{CH}_2\text{OH}$), 70.51 ($\text{CH}_2\text{CH}_2\text{OH}$), 72.82 (CHCH_2O), 102.47 ($\text{CH}(\text{CH}_3\text{O})_2$).

A solution of 2-(2,2-dimethoxyethoxy)-ethanol (11 g, 73.2 mmol) and triethylamine (12 ml, 86.2 mmol) were dissolved in DCM (150 ml) and cooled to 0 °C under nitrogen. α -Bromoisobutyryl bromide (8.5 ml, 69.7 mmol) in DCM (50 ml) was added dropwise. The solution was stirred for 1 hour at 0 °C and overnight at ambient temperature and the

resulting suspension was filtered. The solution was then washed with saturated NaHCO_3 solution (3 x 100 ml) and dried with MgSO_4 and the solvent removed under reduced pressure yielding a yellow oil (18 g). 6.5 g of this oil was purified by silica column chromatography (petroleum ether: diethyl ether; 19:1 to 3:1) yielding a colourless oil (4.06 g, 12.9 mmol).

^1H NMR (CDCl_3 , 300.13 MHz) δ (ppm): 1.89 (6H, s, $\text{C}(\text{CH}_3)_2\text{Br}$), 3.34 (6H, s, $(\text{OCH}_3)_2\text{CH}$), 3.51 (2H, d, $J = 5.09$ Hz, CHCH_2O), 3.71 (2H, t, $J = 4.71$ Hz, $\text{OCH}_2\text{CH}_2\text{OCO}$), 4.27 (2H, t, $J = 4.71$ Hz, $\text{OCH}_2\text{CH}_2\text{OCO}$), 4.45 (1H, t, $J = 5.09$ Hz, $(\text{OCH}_3)_2\text{CH}$). ^{13}C NMR (CDCl_3 , 75.47 MHz) δ (ppm): 30.09 ($\text{C}(\text{CH}_3)_2\text{Br}$), 53.31 ($(\text{CH}_3\text{O})_2\text{CH}$), 55.00 ($\text{C}(\text{CH}_3)_2\text{Br}$), 64.44 (CH_2O), 68.41 (CH_2O), 70.32 (CH_2O), 101.98 ($(\text{CH}_3\text{O})_2\text{CH}$), 170.85 ($\text{COC}(\text{CH}_3)_2\text{Br}$).

2.4.3.6. *Cu(0) mediated protected α -aldehyde poly(mPEGA₄₈₀)*

synthesis

Copper wire (1.25 mm diameter) was activated by washing in hydrochloric acid for 10 minutes, before being rinsed with water and dried under a nitrogen blanket. In a Schlenk tube, Cu(II) bromide (3.7 mg, 0.0167 mmol) was dissolved in DMSO (1.5 ml) and Me_6TREN ligand (16 μl , 0.0602 mmol) was added. Protected aldehyde initiator (0.1 g, 0.334 mmol) in DMSO (1ml) and mPEGA (2.94 ml, 6.68 mmol) in DMSO (1 ml) were added. The solution was degassed by bubbling with nitrogen for 20 minutes before the addition of pre-activated copper wire under a positive nitrogen pressure and the Schlenk tube sealed with a rubber septum. The polymerisation was sampled under a positive pressure of nitrogen for NMR (δ_6 -DMSO) and SEC analysis (DMF). The polymers were purified by dialysis against water (1 kDa MWCO, 3 days).

2.4.3.7. Deprotection of acetal α -end group

The acetal groups were removed by dissolving polymer (1 g) in a (1:1) solution of TFA: H₂O (30 ml) and stirring for 48 hours. The aldehyde functional deprotected polymer was purified by dialysis against water (regenerated cellulose, 1 kDa MWCO, 3 days).

2.4.3.8. NHS ester α -functional poly(mPEGA₄₈₀) conjugation onto oxytocin

Oxytocin (1 mg, 0.99 μ mol) was dissolved in 1 ml phosphate buffer (pH 6.5, 0.1 M) and added to succinimide functional polyPEG (65 mg, 10 μ mol) dissolved in 1ml of the same buffer. The reaction was stirred overnight at ambient temperature before a sample was removed for RP-HPLC analysis.

2.4.3.9. Aldehyde α -functional poly(mPEGA₄₈₀) conjugation onto oxytocin

Aldehyde functional polyPEG (30 mg, 3 μ mol) was dissolved in sodium phosphate buffer (2.5 ml, pH 6.2, 100 mM) and left at 10 °C for 1 hour. Oxytocin (2 mg, 2 μ mol) was stirred in the same buffer (1 ml) at 10 °C for 15 minutes. Both solutions were added together and a freshly prepared solution of NaCNBH₃ (25 mmol, 0.5 ml) was added. After stirring overnight a sample was taken and dissolved in 1 ml H₂O for RP-HPLC analysis.

2.4.3.10. Reversible conjugation of aldehyde linear PEG onto oxytocin

Aldehyde functional linear PEG (200 mg, 40 μmol) dissolved in phosphate buffer (3 ml, pH 8, 0.1 M) was added to oxytocin (20 mg, 20 μmol) dissolved in the same buffer (2 ml). The reaction was allowed to proceed at ambient temperature overnight before a sample was removed for RP-HPLC analysis.

2.4.3.11. Reversible conjugation of butyraldehyde onto oxytocin

To oxytocin (5 mg, 5 μmol) in H_2O (5 ml) was added butyraldehyde (1.5 μl , 15 μmol). The reaction was stirred at room temperature overnight before a sample was removed for RP-HPLC analysis.

2.4.3.12. Irreversible conjugation of butyraldehyde onto oxytocin

To oxytocin (5 mg, 5 μmol) in H_2O (5 ml) butyraldehyde (1.5 μl , 15 μmol) was added, after which freshly prepared NaCNBH_3 (25 mM, 1 ml) was added. The reaction was stirred at room temperature overnight before a sample was removed for RP-HPLC analysis.

2.4.3.13. Reversible and irreversible conjugation of propionaldehyde onto oxytocin

To two separate solutions of oxytocin (5 mg, 5 μmol) in H_2O (2.5 ml) was added propionaldehyde (1.07 μl , 15 μmol), after which freshly prepared NaCNBH_3 (25 mM, 1 ml)

was added to one of the solutions. The reactions were stirred at room temperature overnight before a sample was removed for RP-HPLC analysis.

2.4.3.14. Reversible conjugation of α -aldehyde

poly(mPEGA₄₈₀) onto oxytocin

Aldehyde functional polyPEG (200 mg, 20 μ mol) dissolved in phosphate buffer (3 ml, pH 8, 0.1 M) was added to oxytocin (10 mg, 10 μ mol) dissolved in the same buffer (2 ml). The reaction was allowed to proceed at room temperature overnight before a sample was removed for RP-HPLC analysis.

2.4.3.15. Reversibility experiments of Schiff base conjugated

butyraldehyde

Butyraldehyde Schiff base conjugated oxytocin solution directly succeeding conjugation (0.5 ml, 4 mM) was diluted with 1.5 ml of different pH solutions (1 mM). After stirring for 96 hours, the samples were analysed by RP-HPLC for any increase in concentration of oxytocin.

2.4.3.16. Reversibility experiments of Schiff base conjugated

linear PEG

Immediately post-conjugation, the conjugation solution was dialysed (3.5 kDa MWCO, 3 days) against water which had been pH adjusted with 0.1 M NaOH to pH 8. After removal from dialysis a sample was submitted for RP-HPLC for minimum oxytocin content. 0.5 ml of

the dialysis solution was diluted with 1.5 ml of pH 5.0 and pH 7.4 buffered solutions, and stirred for 18 days with periodic sampling by RP-HPLC.

2.4.3.17. Reversibility of Schiff base conjugated poly(mPEGA₄₈₀)

Post-conjugation, the solution was dialysed (3.5 kDa MWCO, 3 days) against water which had been pH adjusted NaOH (0.1 M, pH 8). After dialysis a sample was submitted for RP-HPLC minimum oxytocin content. 0.5 ml of the dialysis solution was diluted with buffer (1.5 ml, pH 5.0 & 7.4) and stirred for 18 days with periodic sampling by RP-HPLC.

2.5. References

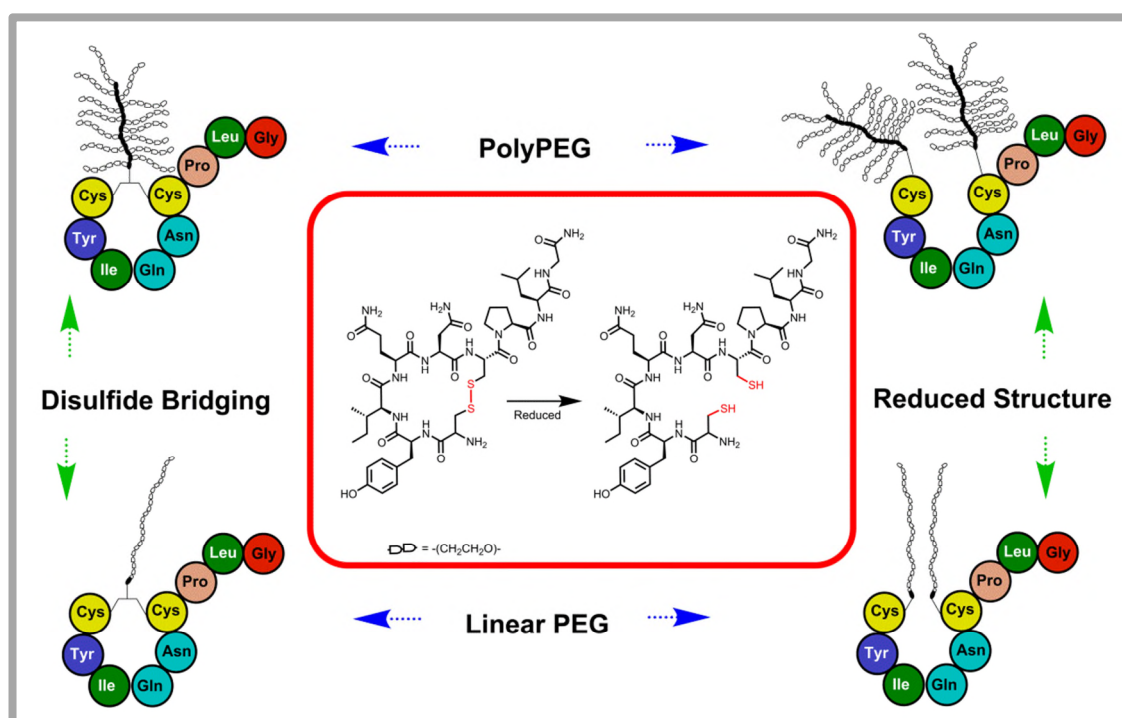
- 1 G. T. Hermanson, *Bioconjugate Techniques*, Elsevier, Third Edit., 2013.
- 2 S. N. S. Alconcel, A. S. Baas and H. D. Maynard, *Polym. Chem.*, 2011, **2**, 1442–1448.
- 3 B. Podobnik, B. Helk, V. Smilović, S. Škrajnar, K. Fidler, S. Jevševar, A. Godwin and P. Williams, *Bioconjug. Chem.*, 2015, **26**, 452–459.
- 4 S. Rathgeber, T. Pakula, A. Wilk, K. Matyjaszewski, H. Lee and K. L. Beers, *Polymer.*, 2006, **47**, 7318–7327.
- 5 A. Bendele, J. Seely, C. Richey, G. Sennello and G. Shopp, *Toxicol. Sci.*, 1998, **42**, 152–157.
- 6 W. Y. Chan and V. Du Vigneaud, *Endocrinology*, 1962, **71**, 977–982.
- 7 D. B. Hope, V. V. S. Murti and V. du Vigneaud, *J. Biol. Chem.*, 1962, **237**, 1563–1566.
- 8 D. B. Hope and V. Du Vigneaud, *J. Biol. Chem.*, 1962, **237**, 3146–3150.
- 9 A. Hawe, R. Poole, S. Romeijn, P. Kasper, R. Van Der Heijden and W. Jiskoot, *Pharm. Res.*, 2009, **26**, 1679–1688.
- 10 K. Wiśniewski, J. Finnman, M. Flipo, R. Galyean and C. D. Schteingart, *Biopolymers*, 2013, **100**, 408–421.
- 11 G. W. Anderson, J. E. Zimmerman and F. M. Callahan, *J. Am. Chem. Soc.*, 1964, **86**, 1839–1842.

- 12 S. Mädler, C. Bich, D. Touboul and R. Zenobi, *J. Mass Spectrom.*, 2009, **44**, 694–706.
- 13 O. Koniev and A. Wagner, *Chem. Soc. Rev.*, 2015, **44**, 5495–5551.
- 14 A. J. Lomant and G. Fairbanks, *J. Mol. Biol.*, 1976, **104**, 243–261.
- 15 P. Cuatrecasas and I. Parikh, *Biochemistry*, 1972, **11**, 2291–2299.
- 16 R. F. Borch, M. K. Bernstein and H. D. Durst, *J. Am. Chem. Soc.*, 1971, **93**, 2897–2904.
- 17 L. Peng, G. J. Calton and J. W. Burnett, *Appl. Biochem. Biotechnol.*, 1987, **14**, 91–99.
- 18 J. M. Harris and M. R. Sedaghat-Herati, US Patent 5252714 A, 1993.
- 19 A. Kozlowski, Patent WO2004022630 A2, 2004.
- 20 P. Rosen and K. Nho, Patent WO03049699 A2, 2003.
- 21 C. T. Sayers, G. Mantovani, S. M. Ryan, R. K. Randev, O. Keiper, O. I. Leszczyszyn, C. Blindauer, D. J. Brayden and D. M. Haddleton, *Soft Matter*, 2009, **5**, 3038–3046.
- 22 P. Wilson, J. Nicolas and D. M. Haddleton, in *Chemistry of Organo-Hybrids: Synthesis and Characterization of Functional Nano-Objects*, 2015, pp. 466–502.
- 23 Z. P. Tolstyka and H. D. Maynard, in *Polymer Science: A Comprehensive Reference*, Elsevier B.V., 2012, vol. 9, pp. 317–337.
- 24 F. Lecolley, L. Tao, G. Mantovani, I. Durkin, S. Lautru and D. M. Haddleton, *Chem. Commun.*, 2004, 2026–2027.
- 25 L. Tao, G. Mantovani, F. Lecolley and D. M. Haddleton, *J. Am. Chem. Soc.*, 2004, **126**, 13220–13221.
- 26 Y. Vugmeyster, C. A. Entrican, A. P. Joyce, R. F. Lawrence-Henderson, B. A. Leary, C. S. Mahoney, H. K. Patel, S. W. Raso, S. H. Olland, M. Hegen and X. Xu, *Bioconjug. Chem.*, 2012, **23**, 1452–1462.
- 27 C. J. Fee, *Biotechnol. Bioeng.*, 2007, **98**, 725–731.
- 28 P. Caliceti and F. M. Veronese, *Adv. Drug Deliv. Rev.*, 2003, **55**, 1261–1277.
- 29 Z. Zarafshani, T. Obata and J. F. Lutz, *Biomacromolecules*, 2010, **11**, 2130–2135.
- 30 A. J. Keefe and S. Jiang, *Nat. Chem.*, 2012, **4**, 59–63.
- 31 J. Nicolas, V. San Miguel, G. Mantovani and D. M. Haddleton, *Chem. Commun.*, 2006, 4697–4699.
- 32 S. M. Ryan, X. Wang, G. Mantovani, C. T. Sayers, D. M. Haddleton and D. J. Brayden, *J. Control. Release*, 2009, **135**, 51–59.
- 33 A. Simula, G. Nurumbetov, A. Anastasaki, P. Wilson and D. M. Haddleton, *Eur. Polym. J.*, 2015, **62**, 294–303.

-
- 34 A. Simula, V. Nikolaou, F. Alsubaie, A. Anastasaki and D. M. Haddleton, *Polym. Chem.*, 2015, **6**, 5940–5950.
- 35 G. Lligadas and V. Percec, *J. Polym. Sci. Part A Polym. Chem.*, 2008, **46**, 4917–4926.
- 36 P. C. Nauka, J. Lee and H. D. Maynard, *Polym. Chem.*, 2016, **7**, 2352–2357.
- 37 A. Ohno, N. Kawasaki, K. Fukuhara, H. Okuda and T. Yamaguchi, *Magn. Reson. Chem.*, 2010, **48**, 168–172.
- 38 M. Ciampolini and N. Nardi, *Inorg. Chem.*, 1966, **5**, 41–44.

Chapter 3

3. Disulfide bond targeted PEGylation of oxytocin



A popular targeting method for the conjugation of polymer onto peptides/proteins is through the use of thiol groups arising from cysteine residues. These often have a less frequent occurrence within the peptide structure, allowing for a more site-specific approach. Conjugation strategies were developed that targeted the pair of thiols arising from the reduction of the Cys¹ – Cys⁶ disulfide bond within oxytocin, either with two separate Michael addition reactions with both of the thiols, or by the rebridging of the disulfide bond using maleimide chemistry, maintaining the cyclic structure.

3.1. Introduction

An approach that is becoming more prevalent in protein/peptide–polymer conjugation strategies is the targeting of thiols found within the protein/peptide structure. Cysteine residues present a convenient target for modifications to take place, due both to the nucleophilicity and reactivity and rarity with peptide and protein structures.¹ The lesser abundance of thiol functionalities (particularly as accessible and free thiols) within the protein/peptide compared to lysine (amine) residues makes site-selective targeting more simple. Often thiols will be generated by reduction of natural disulfide bonds within the structure using reagents such as dithiothreitol (DTT),² 2-mercaptoethanol or *tris*(2-carboxyethyl) phosphine (TCEP).³

One of the major sites where degradation occurs in oxytocin is the Cys¹-Cys⁶ disulfide bond, where a variety of different degradation products can form, including tri/tetrasulfide, dimerization and the formation of larger peptide aggregates.^{4,5} Therefore conjugation strategies with a focus on applying changes to the disulfide bond could be of vital importance for increasing the overall stability of oxytocin.

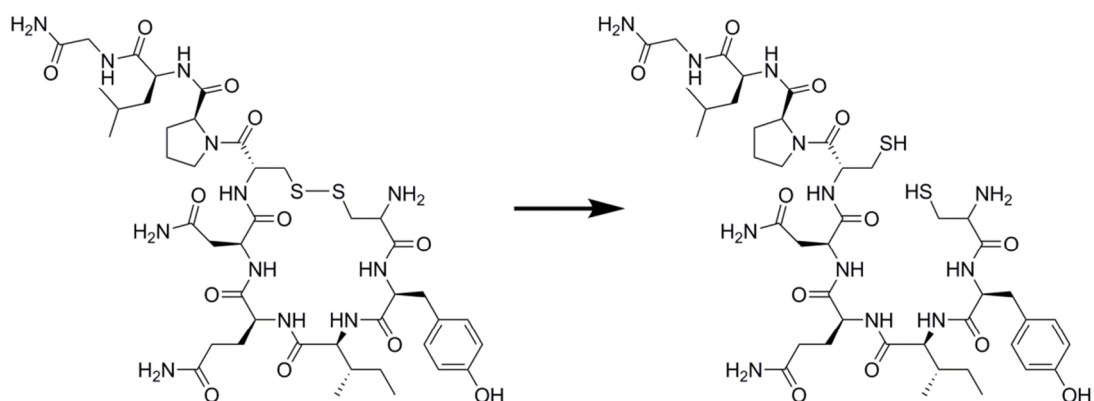
Reports within the literature from the 1970s present alternative oxytocin structures wherein the disulfide bond has been engineered to contain alternative functionality, that may have an effect on the peptide stability or activity.^{6,7} More recent work by Alewood and co-workers reported that by replacing the S-S disulfide bond with CH₂-S, Se-Se, Se-S or Te-Te the stability of the peptide and biological activity could be conserved.^{8,9} This provides further evidence that the disulfide bond is not always required in its native form for biological activity to occur, and thus provides a potentially highly important site for peptide modification.

In this chapter the use of functional PEGs will be described for specific conjugation at the disulfide bond of oxytocin, after reduction leads to two accessible sulfhydryl residues. Polymer conjugation utilising both linear and polyPEG architectures will be explored, as discussed in the previous chapter, as well as the potential for singular conjugation (with disulfide bond rebridging) or double conjugation (with a loss of cyclic structure) of polymers at the peptide disulfide bond.

3.2. Results & Discussion

3.2.1. General considerations for disulfide based chemistry with respect to oxytocin

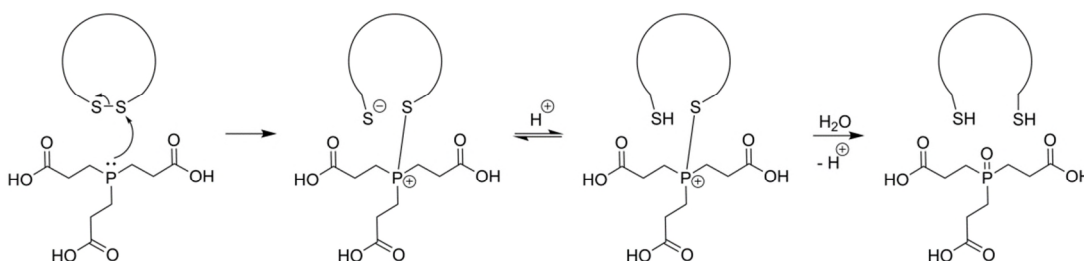
The Cys¹-Cys⁶ disulfide bond of oxytocin presents a convenient alternative approach that can be utilised for the polymeric modification of oxytocin. The conjugation routes utilising this position, however, first require complete reduction of the disulfide bridge (scheme 3.1). This releases two cysteine thiols, each capable of undergoing a large library of sulfhydryl chemical reactions resulting in covalent attachment.



Scheme 3.1. Reduction of oxytocin disulfide bond generating two free thiols.

3.2.1.1. Reducing the disulfide bond in oxytocin

As there is very little literature focused on the chemical modification of the oxytocin disulfide bond (most oxytocin analogues with disulfide changes are synthesised by solid phase protein synthesis (SPPS) techniques to contain desired functional groups),^{6,8-10} the efficiency of the disulfide reduction was investigated initially. Two different routes were investigated for the initial reduction of the disulfide bond in oxytocin resulting in the two reactive sulfhydryl groups which can then be used for subsequent thiol targeted conjugation reactions. The most commonly used reagent for the reduction of disulfide bonds is the commercially available, water-soluble phosphine reagent *tris*(2-carboxyethyl) phosphine (TCEP), which has previously been reported in many incidences for efficient disulfide bond reductions (scheme 3.2).³



Scheme 3.2. Mechanism of TCEP disulfide bond reduction.

In the initial investigation an aqueous solution of oxytocin was treated with 1.5 equivalents of TCEP at ambient temperature. After 2.5 hours the reaction was monitored by RP-HPLC whereby there was a shift in retention time between the peptide (7.3 minutes) and the reduced peptide (7.9 minutes), alongside the appearance of a distinct odour, characteristic of thiol containing compounds. The reduction of the disulfide bond was then monitored over time at three different temperatures, where reduction was much faster at 30 °C (complete reduction after 2 hours) than 20 °C (within 4 hours), and at 10 °C complete reduction was much slower (only 91.2 % reduction after 6 hours) (figure 3.1).

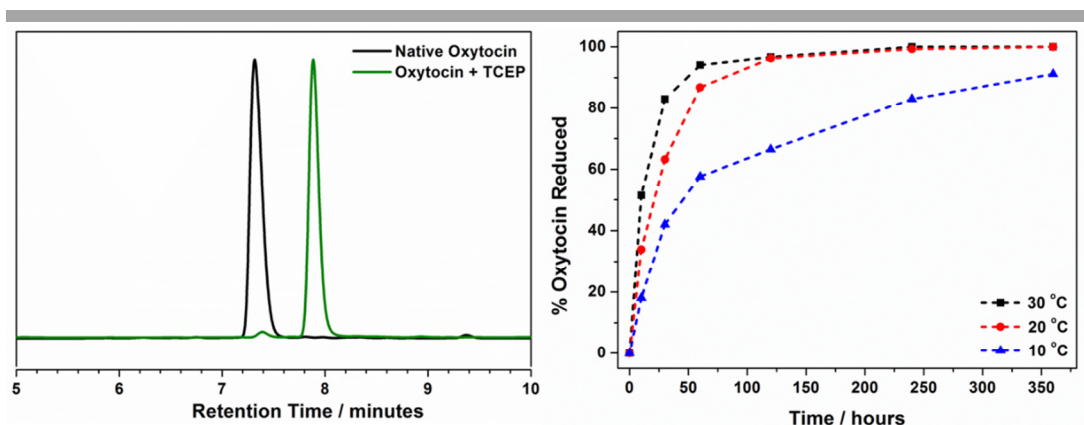


Figure 3.1. RP-HPLC monitoring of oxytocin reduction with TCEP.

An alternative fast, efficient and mild method that can be used to reduce the disulfide bond in peptides is through the use of metallic zinc in acidic solutions.¹¹ The use of zinc dust can offer some advantages over more traditional methods for reducing disulfide bonds, including providing an inexpensive and less hazardous reagent than TCEP, and the reagent can be removed by a simple work up procedure by centrifugation. Furthermore, TCEP has previously been reported to react with maleimides, thus making efficient conjugations after reduction of disulfide bonds more difficult.^{12–14}

The disulfide bond of oxytocin (1 mg) was reduced with zinc dust (< 10 μm , 20 mg) in water containing TFA (1 % v/v). After 60 minutes analysis by RP-HPLC revealed that complete reduction could be obtained (figure 3.2). The reaction was worked up by centrifugation (10,000 G, 5 minutes) after which the peptide solution could be easily removed from the metal zinc pellet. When there was no acid added to the zinc reaction solution, no reduction of the peptide disulfide bond could be observed by RP-HPLC. On visual inspection of the two solutions, the zinc solution not containing any acid became cloudy, whereas for the solution containing TFA, the zinc dust remained highly granular.

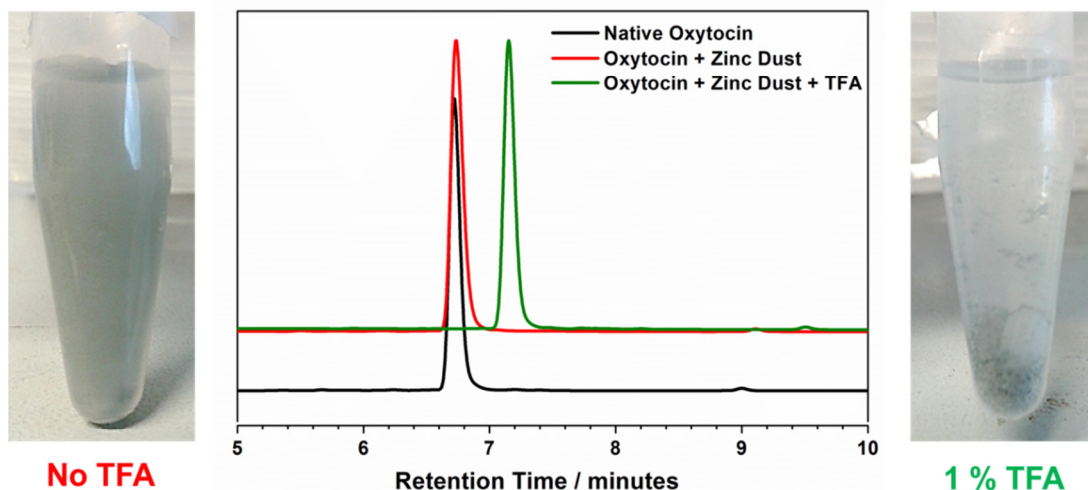


Figure 3.2. Oxytocin disulfide bond reduction using zinc powder, with and without the addition of TFA additive, and images of the two solutions.

The use of zinc as a reducing agent provides a fast and efficient route to dithiol oxytocin; although the addition of acid may lead to challenges if pH control is required for conjugation. Therefore, the route commonly used for the reduction of the disulfide bond of oxytocin throughout this chapter was by a reduction with TCEP, although having an alternative route available is advantageous.

3.2.2. Maleimide linear PEG disulfide bridging

The utilisation of disubstituted *N*-functional maleimides (such as dibromo- or dithiophenolmaleimide) for disulfide bridging addition of polymers to peptides is a relatively new area within protein/peptide modifications. The ability of maleic acid imides (maleimides) to react efficiently and completely with thiol groups, however, have been well known for over 50 years.¹⁵ In that time the development of maleimides for site-specific peptide conjugation has largely evolved, including for the attachment of polymers to biomolecules (figure 3.3).

Following on from the irreversible conjugations of maleimides, more recently bromomaleimide reagents were developed, which first broached the concept of reversible maleimide conjugation for cysteines.^{16,17} The introduction of dibromomaleimide (DBM) reagents in 2010 was particularly beneficial, as this allowed rebridging of previously reduced disulfide bonds in peptides and proteins, through which desired functionality could also be introduced at the *N* substituent.^{17,18}

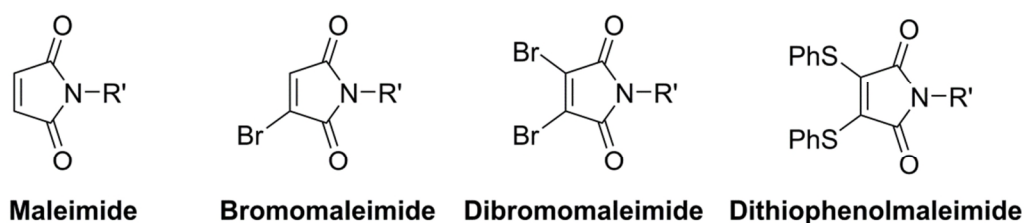


Figure 3.3. Different 'N' Substituted maleimides developed over the last 60 years for protein and peptide modification at cysteine residues.

3.2.2.1. Maleimide linear PEG synthesis

Previously within our group the preparation method for *N*-substituted dibromomaleimide (or dithiophenolmaleimide) with desired functional groups was by using the Mitsunobu reaction. These conditions involve the addition of triphenylphosphine, diisopropyl azodicarboxylate and neopentyl alcohol, to 2,3-dibromomaleimide and the hydroxy substituent to be incorporated, in dry conditions at -78°C . This resulted in very low yields for the synthesis of *N*-PEG-dibromomaleimides (20 %), and several purification steps were required, quite often with the PEG reagents retaining impurities.¹⁸ This synthesis route was initially followed, and figure 3.4 outlines ^1H NMR analysis of the crude reaction mixture and after many purification steps, which shows only the expected PEG peaks. This method for synthesis of the DTM-PEG does result in the polymers able to undergo bioconjugation, but overall requires a long and intense purification procedure resulting in low yields.

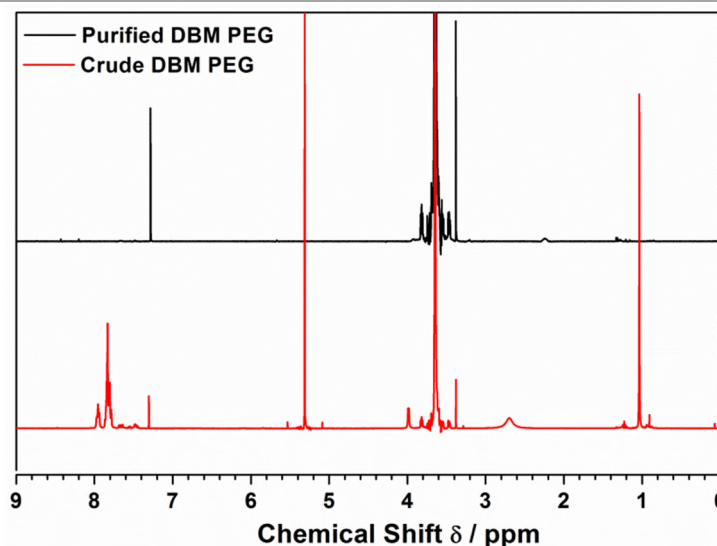
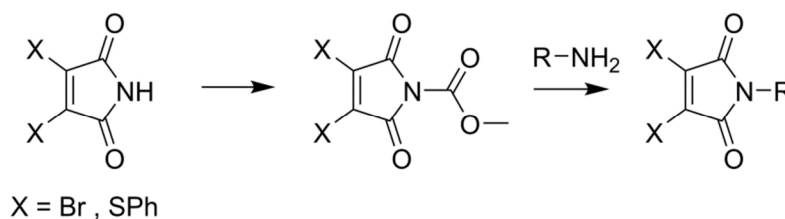


Figure 3.4. ^1H NMR (CDCl_3) of crude dibromomaleimide PEG and after purification (2 x column chromatography, dialysis, 4 x precipitation) synthesised using Mitsunobu route.

Fortunately, in 2013 Caddick and Baker *et al.* reported a method for the relatively simple functionalisation of dibromo- or dithiophenolmaleimides under mild conditions *via* *N*-methoxycarbonylmaleimides.¹⁹ The formation of the *N*-methoxycarbonylmaleimide reagent is simple and quick (less than 30 minutes), resulting in a pink powder in a high yield without further purification required. From the *N*-methoxycarbonylmaleimide, the addition of an amine allows the *N*-functionalisation on the maleimide reagent, and is carried out at ambient temperature (scheme 3.3).



Scheme 3.3. Dithiophenolmaleimide/dibromomaleimide reagent synthesis.

PEG functional dibromomaleimide (DBM-PEG) was synthesised in a simple two step procedure from commercially available 3,4-dibromomaleimide. Firstly *N*-methoxycarbonyl activated dibromomaleimide was synthesised by the reaction of 3,4-dibromomaleimide

with methylchloroformate and *N*-methylmorpholine (NMM). This reaction is very efficient, proceeding to completion within 30 minutes, with little work up or purification required, resulting in a purple-pink powder. The activated dibromomaleimide is then able to undergo a mild reaction with a range of amines at ambient temperature. In this case, α -methoxy ω -amino PEG (5 kDa) was added and stirred at ambient temperature for 24 hours. The DBM PEG reagent was purified by precipitation, resulting in off-white powder in a high yield (76 %). Figure 3.5 shows different steps in the reaction followed by ^1H and ^{13}C NMR.

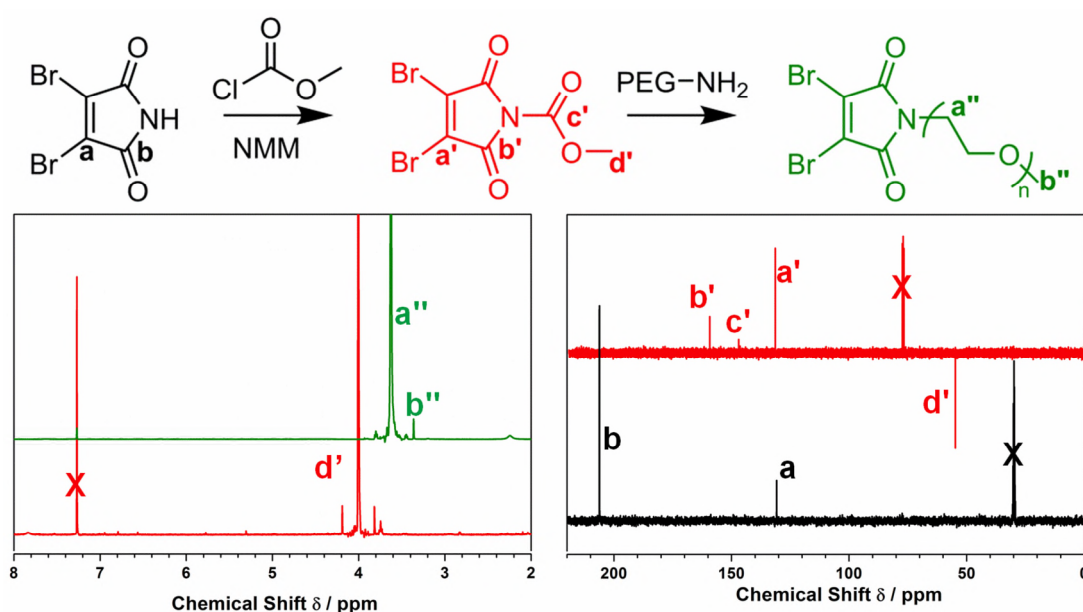
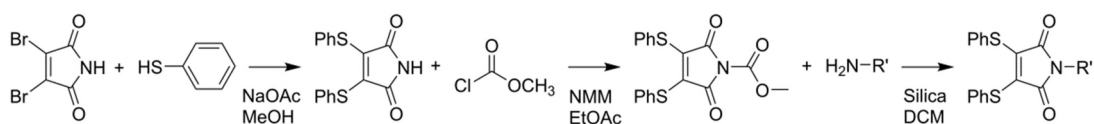


Figure 3.5. ^1H and ^{13}C NMR of synthesis route of DBM PEG.

After the discovery of the ease and efficiency of reactions of dibromomaleimides with thiols, such as on cysteine residues, including for disulfide bridging, Baker investigated this further by employing alternative bis-substituted maleimide reagents.²⁰ Dithiophenolmaleimides (DTM) are in some ways preferential to dibromomaleimides as the reagents are less susceptible to side reactions (such as with TCEP), still maintaining efficient couplings, and acting as disulfide bridging reagents. This also allowed the incorporation of '*in-situ*' protocols for more efficient bridging conjugations, where the retention of cyclisation structure of the protein or peptide during the reaction is vital. This

method can prevent side-reactions and structure unfolding by allowing immediate disulfide bridging with the maleimide reagent.

In a similar manner to DBM functionalisation described, *N*-functional dithiophenolmaleimides, such as *N*-PEG-dithiophenolmaleimide (DTM-PEG), can be synthesised using *N*-methoxycarbonyl activated dithiophenolmaleimide undergoing reactions with different amine functional reagents (scheme 3.4). Dithiophenolmaleimide is easily synthesised from dibromomaleimide by addition of thiophenol in the presence of sodium acetate, resulting in nucleophilic displacement of the bromine atoms. The *N*-methoxycarbonyldithiophenolmaleimide was synthesised in the same manner as the dibromomaleimide analogue, resulting in an orange solid in a high yield. It was reported that for the synthesis of *N*-functional dithiophenolmaleimides *via* the use of this *N*-methoxycarbonyl activated reagent it can be beneficial to add silica, thereby maintaining cyclisation.



Scheme 3.4. Reaction scheme of dithiophenolmaleimide reagent functionalisation.

The PEG functionalisation can clearly be observed after the final step in the synthesis of the PEG reagent by ^1H NMR (figure 3.6). The aromatic groups of the thiophenol substituents on the maleimide can still be clearly identified, however, there is a disappearance of the methoxycarbonyl group ($\delta = 3.9$ ppm) and the appearance of new PEG peaks ($\delta = 3.3 - 3.7$ ppm). This shows that the dithiophenolmaleimide has been functionalised to contain one linear (5 kDa) PEG chain for peptide-polymer modifications.

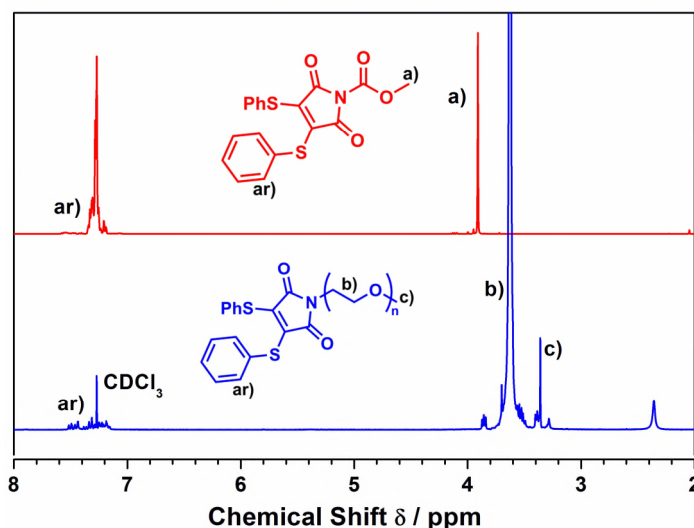
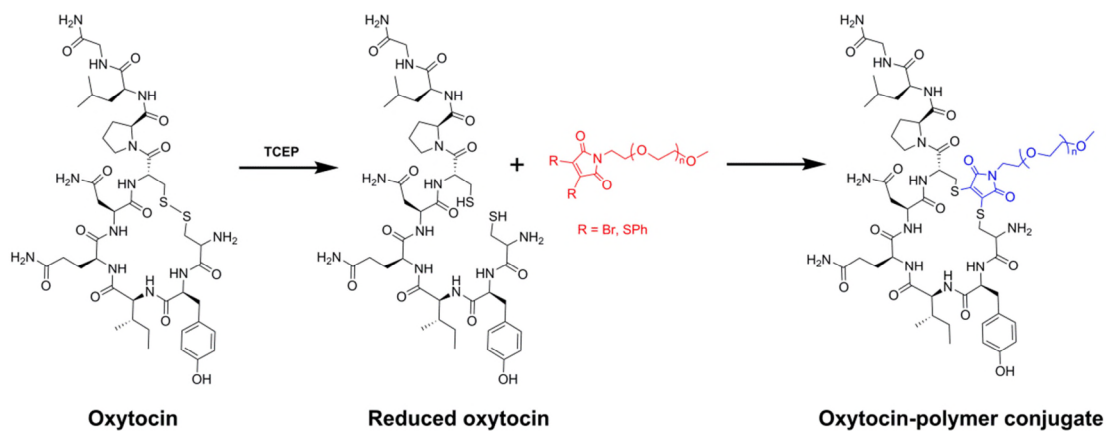


Figure 3.6. ^1H NMR (CDCl_3) for final step in synthesis of *N*-PEG-dithiophenolmaleimide (reaction of *N*-methoxycarbonyldithiophenolmaleimide with PEG-amine).

3.2.2.2. Maleimide linear PEG conjugation

Upon conjugation the dithiophenol or dibromo groups from the maleimide PEGs are substituted by the dithiol- peptide chain of oxytocin, which become covalently bonded onto the maleimide PEG instead. This means that regardless of whether the dibromo or dithiophenolmaleimide-PEG polymers are used, the resulting conjugate will have the same structure (scheme 3.5).



Scheme 3.5. Disulfide bridging conjugation of oxytocin with linear maleimide PEG.

After the disulfide bond of oxytocin had been completely reduced (as confirmed by RP-HPLC), the DBM-PEG or DTM-PEG bridging reagent was added in pH 6.2 phosphate buffer (100 mmol) and stirred at 10 °C for 24 hours. The reactions of dithiophenolmaleimide and dibromomaleimide functional PEGs were monitored by RP-HPLC (figures 3.7 & 3.8). In both reactions a shift in retention time of the major product was observed from the PEG reagents, alongside the appearance of a coincidental fluorescence peak.

There are several impurities observed in both the DBM and DTM PEG reagents as well as in the disulfide-bridging maleimide conjugate, although, in both cases, these are in small amounts compared to the major products. Overall, there is a clear shift in retention time for the major peak observed in both cases, with only one of the peaks in the conjugate product showing a high level of fluorescence.

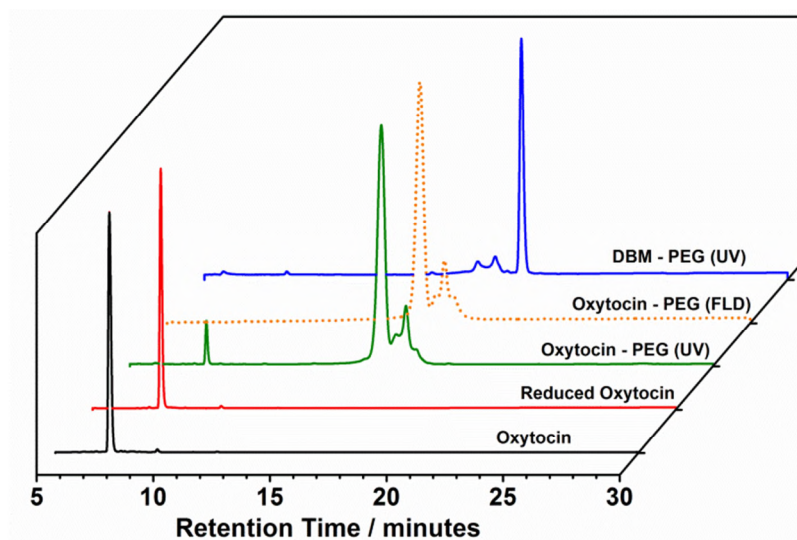


Figure 3.7. RP-HPLC of maleimide bridging conjugation of DBM PEG onto oxytocin.

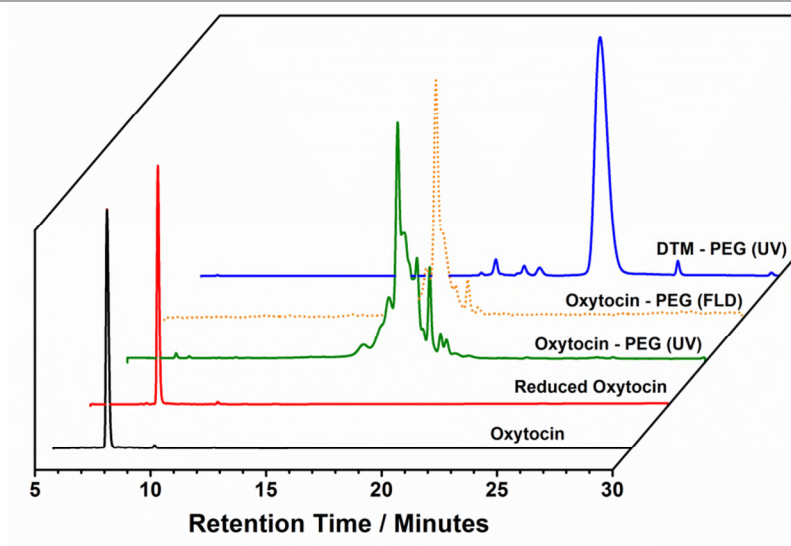


Figure 3.8. RP-HPLC of maleimide bridging conjugation of DTM PEG onto oxytocin.

As the products from the conjugation with dibromo- and dithiophenolmaleimide are expected to give the same product, the RP-HPLC retention times should be precisely the same. The major product for both reactions appears at the same retention time, which shows a shift to shorter retention time than the maleimide reagent (for which each maleimide reagent had a different retention time). An alternative HPLC gradient with a more gradual decrease in aqueous content was used to confirm that the products were eluting at the same retention time when the solvent gradient was elongated (figure 3.9). This adds evidence that the disulfide bridging conjugation of the two different maleimide reagents results in the same product. As with the conjugate observed for the standard HPLC gradient, after purification the conjugation with DBM PEG is cleaner with less side products than the conjugation with DTM.

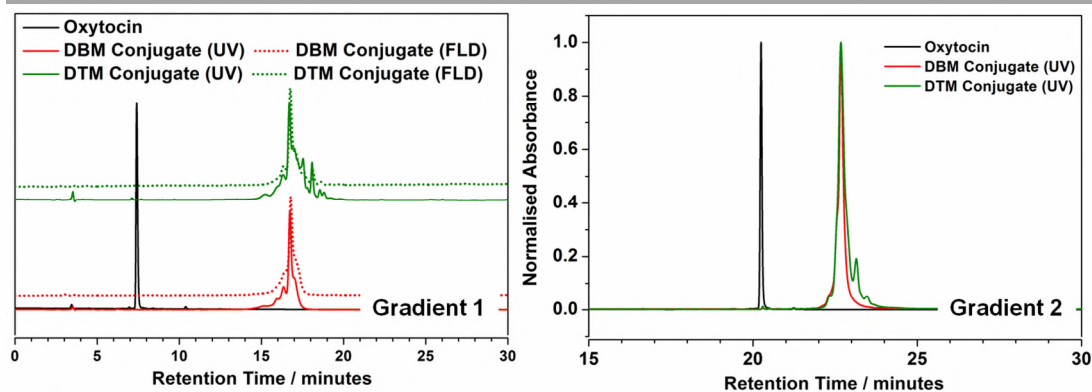


Figure 3.9. RP-HPLC chromatograms comparing DBM and DTM reagents used for disulfide bridging conjugation of oxytocin analysed under two different HPLC gradients.

When the dibromomaleimide PEG was inserted into the disulfide bond of oxytocin, an obvious colour change was observed (figure 3.10). Solutions of dibromomaleimide PEG reagent and the reduced native peptide were not coloured, however, rapidly after addition of the two, a bright yellow colour could be observed.

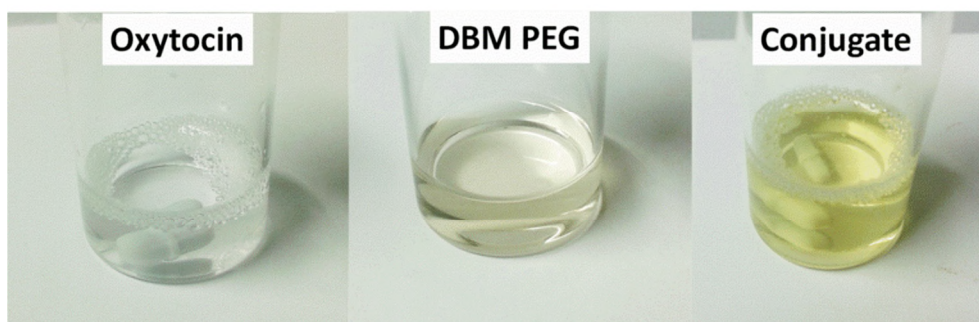


Figure 3.10. Photographs showing colour change upon addition of DBM PEG to reduced oxytocin.

Additional to the change in colour, it has previously been observed that the UV shift for the maleimide functionality changes to reflect the maleimide substituents.²¹ This can be observed for the three different maleimide products investigated: dibromomaleimide PEG, dithiophenolmaleimide PEG and PEG maleimide disulfide bridged oxytocin. Previous studies have suggested that by UV-vis analysis dibromomaleimides absorb at

approximately $\lambda = 320$ nm, with dithioalkylmaleimide (such as maleimide disulfide bridging peptide conjugates) at approximately $\lambda = 390$ nm.²¹ UV-vis analysis (between $\lambda = 300$ nm – 600 nm) was undertaken for the two PEG reagents, and the peptide-polymer conjugate synthesised from both cases. Both of the oxytocin conjugates revealed the same UV response ($\lambda = 380$ nm), consistent with the λ_{max} of previous dithioalkylmaleimides, with no peaks apparent from the dibromo- or dithiophenol- reagents (figure 3.11). The dibromomaleimide reagent has one peak at a smaller wavelength ($\lambda = 321$ nm), whilst the dithiophenolmaleimide reagent shows a major peak with an absorbance at a much higher wavelength ($\lambda = 432$ nm).

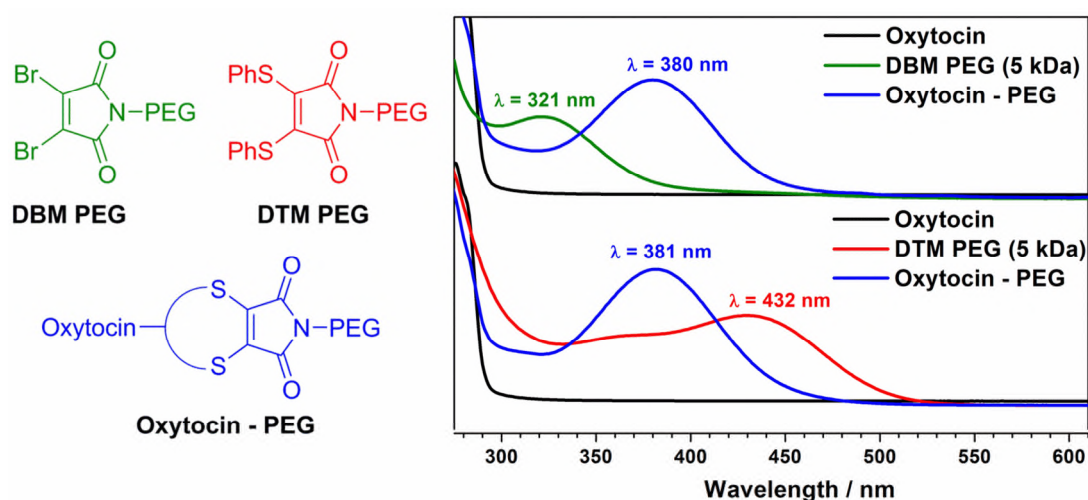


Figure 3.11. UV wavelength shifts of maleimide PEGs with different maleimide functionality.

Additional to providing a shift in the UV spectra of the maleimide functionality, the utilisation of maleimide chemistry can induce fluorescence on the peptide structure due to changing the nature of the maleimide substituents.²² This has previously been observed when analysing the reaction by RP-HPLC equipped with both UV and fluorescence detectors. To further investigate the fluorescence, measurements of the oxytocin polymer conjugates and unconjugated polymers were analysed by a fluorescence spectrophotometer (figure 3.12). The fluorescence excitation wavelengths were set to 314

nm (the same λ_{ex} used for RP-HPLC) and the fluorescence emission region monitored between 400 – 650 nm. For the conjugation with DTM, the polymer exhibits negligible fluorescence under these conditions, however, after peptide conjugation with DTM-PEG fluorescence was increased 20 x ($\lambda_{\text{em}} = 547$ nm). This has previously been ascribed to the fluorescence being quenched by the aromatic groups on the dithiophenolmaleimide reagent.²² In the analysis of the dibromomaleimide polymer, the fluorescence spectra of the polymer showed some evidence of fluorescence before conjugation onto the peptide. This is possibly due to fluorescent impurities within the polymer, such as from undesired nucleophilic substitution of the dibromomaleimide. Regardless, the fluorescence spectrum after conjugation onto oxytocin is very similar to that observed for the DTM conjugation, with one peak observed within the monitored region at $\lambda_{\text{em}} = 535$ nm.

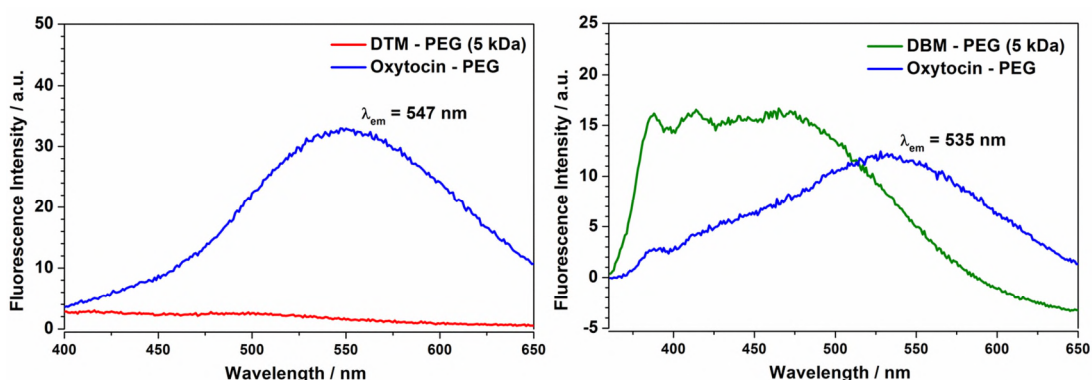


Figure 3.12. Fluorescence spectra of DTM PEG, DBM PEG and maleimide disulfide bridged oxytocin using an excitation wavelength (λ_{ex}) of 314 nm.

The conjugation of dithiophenolmaleimide and dibromomaleimide linear PEGs onto oxytocin provided an efficient route for the PEGylation and enhancement of the peptide disulfide bond, which is prone to degradation. The conjugation can be characterised in a number of different ways, allowing for easy monitoring of the reaction (table 3.1).

Table 3.1. Overview of characterisation methods for maleimide enhanced PEGylation of oxytocin.

	Oxytocin	DBM PEG	DTM PEG	Oxytocin-PEG
RP-HPLC				
Retention time	7.4 min	25.8 min	22.3 min	16.7 min
Colour	Colourless	Colourless	Yellow	Orange/Yellow
UV wavelength	~ 280 nm	321 nm	432 nm	380 nm
Fluorescence	None	(<500 nm)	None	Yes (535-550 nm)

3.2.3. α -Maleimide polyPEG

For the synthesis of comb polymers capable of undergoing post-polymerisation ‘grafting-to’ conjugation, a suitable maleimide initiator must be synthesised, capable of facilitating controlled polymerisations and available for subsequent peptide conjugation. It has previously been established that dibromomaleimide functionality can disrupt the polymerisation characteristics of copper mediated controlled radical polymerisations, as observed by Jones *et al.* for polymerisations using ATRP conditions.¹⁸ Dithiophenolmaleimide alkyl halide initiators have, however, previously proven ‘radical compatible’ and were utilised for the synthesis of poly(poly(ethylene glycol) methyl ether methacrylate) (poly(mPEGMA)) under the same conditions which were unsuccessful for the bromo- substituted maleimide (ATRP, 60 °C, toluene, Cu(I)/pyridine imine catalyst).²³ This allowed the direct incorporation of α -end dithiophenolmaleimide functionality without disrupting the polymerisation. This results in a simple synthesis and peptide

modification of disubstituted maleimide functional polymers without the requirement for any post-polymerisation modifications.

For the maleimide bridging of polyPEGs described in this chapter, a dithiophenolmaleimide initiator was synthesised that was similar to the ATRP initiator described for efficient copper mediated polymerisations by Jones *et al.*²³ This was achieved using the relatively simple functionalisation method described for the synthesis of linear PEG maleimide reagents, *via* the use of *N*-methoxycarbonylmaleimides. Using *N*-methoxycarboxydithiophenolmaleimide, the addition of propargylamine allowed the introduction of alkyne functionality onto the maleimide, as described previously.¹⁹ The incorporation of alkyne functionality onto the maleimide results in an easily modifiable group, and this was used to attach an azide functional alkyl halide initiator by CuAAC chemistry, resulting in the dithiophenolmaleimide initiator (figure 3.13). This initiator is suitable for undergoing copper mediated polymerisations and for subsequent post-polymerisation disulfide bridging within a peptide.

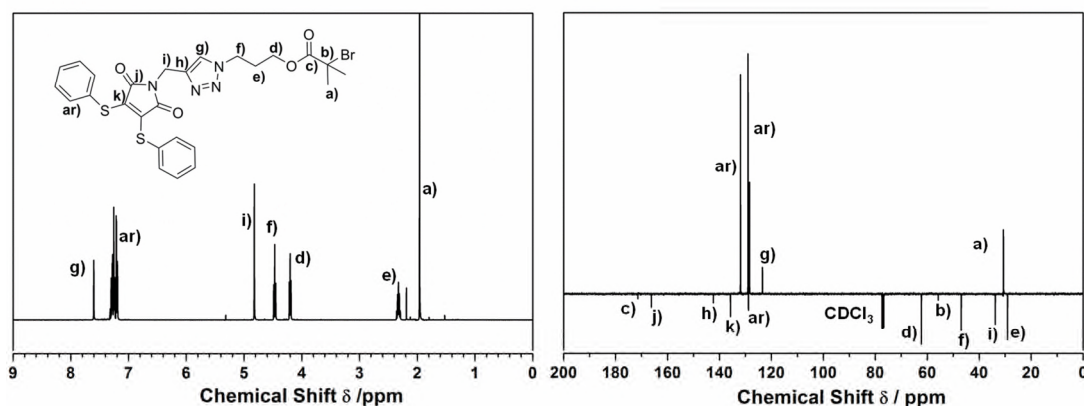


Figure 3.13. ^1H & ^{13}C NMR (CDCl_3) of dithiophenolmaleimide alkyl halide initiator.

During 2012, Haddleton *et al.* reported a new approach for the $\text{Cu}(0)$ mediated polymerisation as an alternative to the $\text{Cu}(0)$ wire method described in the previous chapter.²⁴ This has allowed for controlled polymerisations to be achieved in aqueous

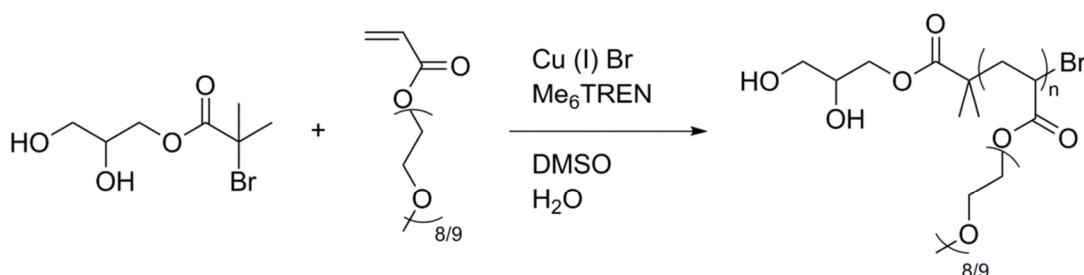
solutions²⁴⁻²⁶ as well as the utilisation of other solvents including; phosphate buffer,²⁴ blood serum²⁷ and commercial mixed water-alcohol systems.²⁸ This utilises an initial rapid disproportionation step wherein Cu(I)Br is allowed to disproportionate in the presence of an *N* containing ligand (Me₆TREN), producing both Cu(0) particles and CuBr₂ as the catalyst system prior to the addition of deoxygenated monomer and initiator. Controlled polymerisations have been achieved for acrylates and acrylamides, and more recently methacrylates,^{29,30} with full conversions reported within 30 minutes at temperatures less than 25 °C, with resulting dispersities reported in many cases of $\bar{D} = 1.1$.

Due to the aromatic nature of the dithiophenolmaleimide initiator it is not soluble in aqueous solutions, therefore a cosolvent mixture is required for efficient polymerisations to occur whilst still utilising the full disproportionation of Cu(I)Br in water with Me₆TREN into Cu(II)Br₂ and Cu(0). The total disproportionation achieved is greatly affected by the addition of co-solvents, and this was investigated by Haddleton and co-workers for a variety of polar organic solvents.³¹ In the tested solvents, methanol reached the highest disproportionation (66 % of [Cu(L)]Br into Cu(0) and [Cu(L)]Br₂), and for DMSO (a popular solvent for organic Cu(0) mediated polymerisation) disproportionation was much lower (~ 30 %). Therefore in order to maintain ideal disproportionation characteristics it is essential to maintain water as the solvent for the initial step wherein Cu(0) and [Cu(L)]Br₂ are generated from [Cu(L)]Br. There is, however, scope to change the solution containing the monomer and initiator before injection into the post-disproportionation generated catalyst solution. This would thereby change the overall water content of the polymerisation, but only after total disproportionation had already occurred.

Solubility studies on the dithiophenolmaleimide initiator found that it was soluble in DMSO-water solutions up to 25 % aqueous content. The aqueous polymerisation system

conditions were adapted to reflect these changes. It was however, predicted that the addition of DMSO was expected to have an adverse effect on the polymerisation control.

To investigate whether this was a viable solvent system for performing the polymerisation, an investigation was carried out using a water soluble initiator (WSI), changing the % of DMSO present in the reaction (table 3.2). The polymerisations of poly(ethylene glycol) methyl ether acrylate (av. $M_n = 480 \text{ g mol}^{-1}$, mPEGA₄₈₀) were carried out using Cu(I)Br, and Tris[2-(dimethylamino)ethyl]amine (Me₆TREN) as ligand ([I]:[M]:[Me₆TREN]:[CuBr] = 1:20:0.4:0.4) (scheme 3.6). The reaction was stirred under nitrogen and a sample was removed after 24 hours for ¹H NMR (D₂O) and SEC (DMF) analysis. For all reactions the disproportionation of Cu(I)Br was always carried out in an 100 % aqueous solution followed by addition of the initiator and monomer in solutions containing the co-solvent (DMSO).



Scheme 3.6. Polymerisation of mPEGA₄₈₀ with water soluble initiator using [M]:[I]:[CuBr]:[Me₆TREN] = 1:20:0.4:0.4 in DMSO/Water.

Table 3.2. Polymerisation data for the synthesis of poly(mPEGA₄₈₀)₂₀ using water soluble initiator with different DMSO/water content.

Water content (%)	Conversion (%) (NMR)	M_n (Da) (SEC)	\bar{D} (SEC)
100	>99	12500	1.30

50	>99	11200	1.12
33	>99	11800	1.30
20	99	11600	1.08

The results showed that in this co-solvent mixture the polymerisation remained viable for different DMSO concentrations in water including up to 80 % organic content (figure 3.14). A sample was removed after 24 hours, which revealed that for the highest organic content almost quantitative conversion had been achieved. Analysis by SEC revealed that the dispersities of polymers remained narrow ($\bar{D} = 1.08$) with a mono-modal chromatogram and good correlation between experimental and theoretical molecular weights.

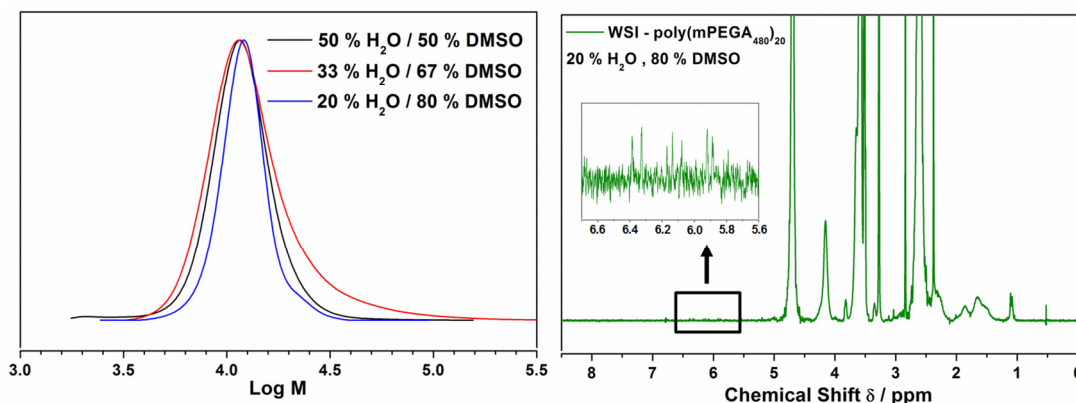
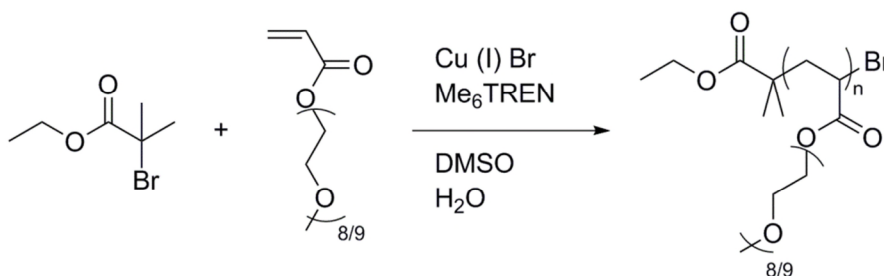


Figure 3.14. SEC (DMF) analysis for synthesis of poly(mPEGA)₂₀ in different solvent combinations and ¹H NMR (D₂O) analysis of polymer synthesised in 80 % DMSO (99 % conv., M_n : 11600, \bar{D} : 1.08) with an expansion of the vinyl peaks showing disappearance of monomer.

Solubility studies on the dithiophenolmaleimide initiator showed that it remained in solution at DMSO content above 75 %, confirming that the 80 % DMSO (20 % aqueous) conditions evaluated are relevant for the synthesis of desired α -end functional polymers. Following on from the results with an initiator soluble in both solvents, a test

polymerisation was conducted using solvent conditions of 80 % DMSO in water with a non-water soluble initiator (ethyl-2-bromoisobutyrate: EBiB) exhibiting similar aqueous solubility to the desired dithiophenolmaleimide initiator (scheme 3.7). Two different sizes of polymers were synthesised using [M]:[I] of 20 & 100 giving predicted molecular weights of 10 kDa and 50 kDa (table 3.3).



Scheme 3.7. Polymerisation of mPEGA₄₈₀ with EBiB using [M]:[I]:[CuBr]:[Me₆TREN] = 1:20/100:0.4:0.4 in DMSO:Water (4:1).

Table 3.3. Polymerisation data from synthesis of poly(mPEGA₄₈₀)_n using EBiB

[M]:[I]	Conversion (%) (NMR)	M _n (Da) (SEC)	Đ (SEC)	Solubility
20	94	12200	1.06	Miscible
100	98	36600	1.25	Immiscible

An interesting observation for the higher molecular weight polymer was the phase separation/polymer precipitation of the larger molecular weight polymer under these conditions (figure 3.15). This led to the appearance of a clear blue solution as the top layer and a colourless bottom layer. This is particularly interesting as polymerisations of mPEGA do not show this behaviour if the polymerisation is carried out in either a purely aqueous or purely DMSO based system.

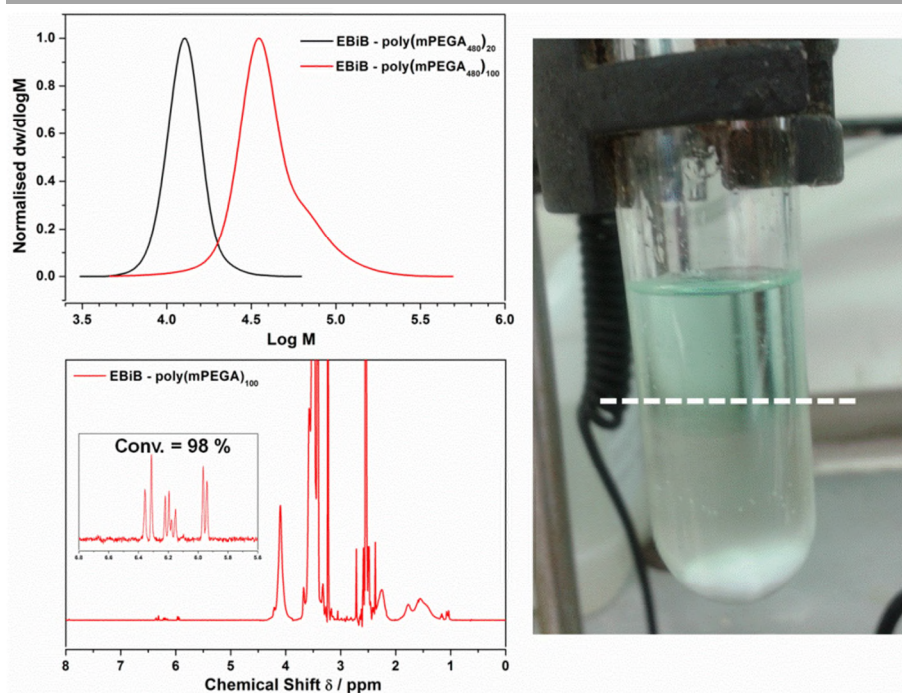


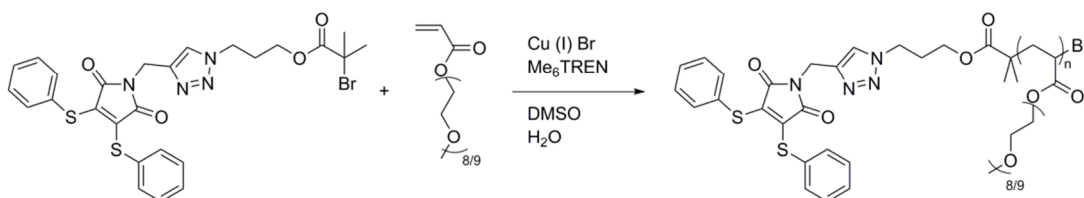
Figure 3.15. SEC chromatograms for synthesis of EBiB-poly(mPEGA)s with accompanying high conversion NMR, and photograph of polymer phase separation.

After 24 hours the polymerisations had reached high conversions whilst retaining narrow mono-modal molecular weight distributions ($\mathcal{D} < 1.3$). This is particularly notable for the phase-separated polymers, as controlled polymerisation was achieved even when the polymer was no longer soluble in the solvent combination used.

These results (using two different initiators) show that it was possible to synthesise controlled polymers using the disproportionation of Cu(I)Br in water, with the addition of a non-disproportionating solvent after generation of the catalyst system. This is promising in providing information towards what might be expected during the polymerisation when an initiator for direct post-polymerisation peptide modification is used (such as the dithiophenolmaleimide initiator previously described).

3.2.3.1. Synthesis of α -dithiophenolmaleimide polymers

The polymerisation was subsequently carried out for the synthesis of α -dithiophenolmaleimide functional poly(mPEGA₄₈₀) polymers using Cu(I)Br with Me₆TREN in water: DMSO (1:4), using ([I]:[CuBr]:[Me₆TREN] = 1:0.4:0.4) (scheme 3.8). Molecular weights were targeting 10 kDa (DP_n 20), 25 kDa (DP_n 50) and 50 kDa (DP_n 100). Cu(I)Br was first allowed to fully disproportionate in water before the addition of a degassed monomer/initiator solution in DMSO.



Scheme 3.8. Polymerisation of mPEGA₄₈₀ with dithiophenolmaleimide initiator using [M]:[I]:[CuBr]:[Me₆TREN] = 1:n:0.4:0.4 in DMSO:Water (4:1).

Table 3.4. Polymerisation data for synthesis of poly(mPEGA₄₈₀) using DTM initiator.

[M]:[I]	Conversion (%) (NMR)	M _n (Da) (SEC)	Đ (SEC)	Solubility
20	90	11600	1.20	Miscible
50	96	22300	1.25	Immiscible
100	97	36000	1.36	Immiscible

Aliquots were removed from the polymerisation solution after 24 hours for ¹H NMR (D₂O) conversion and SEC (DMF) molecular weight data (table 3.4). The polymerisation conversion was calculated by a comparison between the vinyl protons of the monomer

and the CH₂ next to the ester of the PEG repeat unit. This revealed that within 24 hours high conversions (> 90 %) had been achieved for all three polymers.

SEC analysis showed that the polymers still retained low dispersities, although as molecular weight increased the presence of high molecular weight peak tailing was observed. This has previously been ascribed to trace impurities of diacrylate within the monomer reagent.^{30,32} As observed for the polymerisation with EBiB, the molecular weights observed from SEC deviate from the theoretical molecular weights as the DP_n increases. This is most likely due to the SEC calibration being relative to narrow PMMA standards and the difference between the hydrodynamic volume of these poly(mPEGA) 'combs' and the calibration standards. Another notable point for the synthesis of these dithiophenolmaleimide functional polymers is that due to the nature of the α -end group, the polymers are highly UV active, and the UV response on SEC is highly prominent. The RI and UV responses overlay, showing that the DTM functionality is still present on the polymer (figure 3.16).

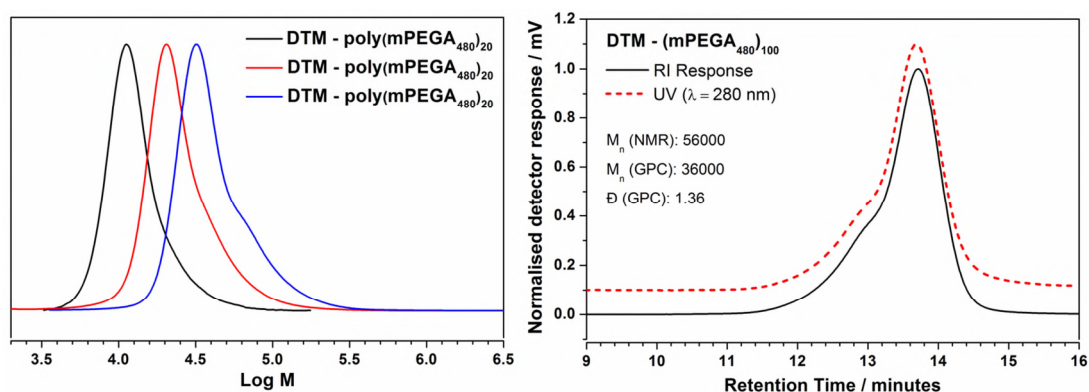


Figure 3.16. SEC analysis of DP_n 20, 50 and 100 DTM-poly(mPEGA₄₈₀)₂₀ and RI/UV overlay of SEC chromatogram.

As with the previous polymerisations using EBiB under the same solvent conditions, phase separation/polymer precipitation was observed, although due to the distinct colour of the polymer the phenomena was more highly visible (figure 3.17). The top layer was a clear

green solution, suggesting that it did not contain any of the dithiophenolmaleimide functional polymer (by ^1H NMR), as this has a distinct orange colour. This suggests that this layer contains a large proportion of the catalyst system, which if true would simplify polymer purification. The bottom layer was bright orange colour suggesting the polymer solution was present in this layer.

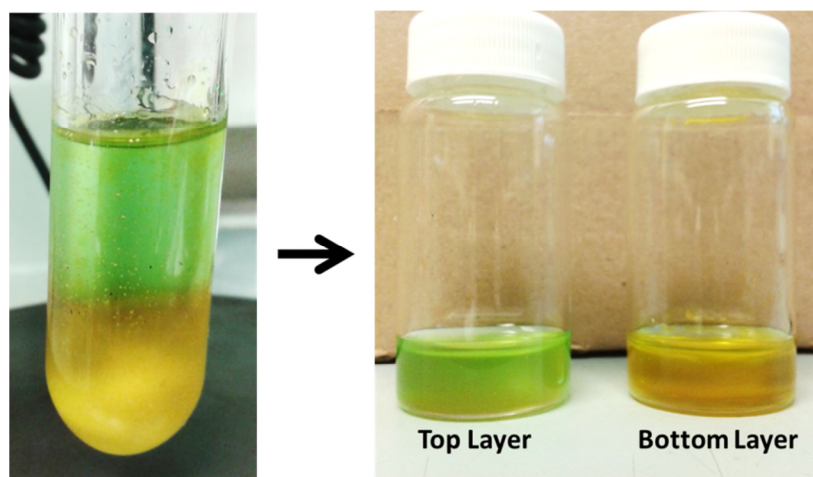


Figure 3.17. Photographs showing the phase separation during polymerisation of DP_n 50 or DP_n 100 poly(mPEGA₄₈₀) in DMSO:Water (4:1).

The two layers were separated and ^1H NMR was carried out which revealed that, although both layers contained residual monomer, only the bottom orange layer contained any polymer (figure 3.18). This was established by the presence of dithiophenolmaleimide groups with peaks at 7.1 – 7.4 ppm corresponding to the aromatic phenol groups, and a peak at 8.0 ppm from the triazole ring within the initiator. The top layer also did not show the presence of the polymer backbone peaks found for acrylate functional polymers (δ = 1.5 – 2.5 ppm), or the broad peak of the first CH_2 from the PEG of the monomer repeat unit on the polymer (δ = 4.2 ppm), although this peak can still be observed within the unreacted monomer.

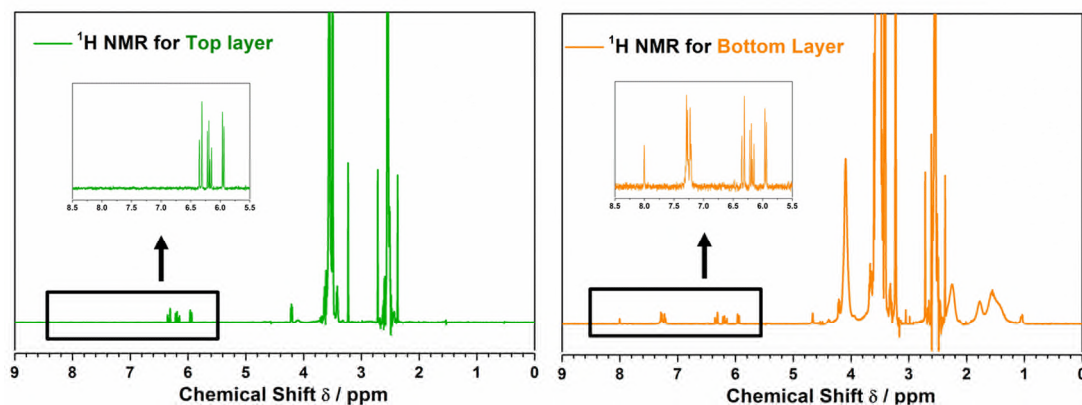


Figure 3.18. Comparison of ¹H NMR (400.13 MHz, δ₆-DMSO) individually measured of top and bottom layer within polymerisation, with an expansion of the vinyl/aromatic regions.

The polymers were purified by dialysis against water (for DP_n 50 and DP_n 100 polymers only the bottom, polymer containing, layer needed to be purified) yielding three α-dithiophenolmaleimide functional polymers, with molecular weights between 10 - 50 kDa. The purified polymers were characterised by ¹H NMR (δ₆-DMSO), where the presence of the aromatic groups on the dithiophenolmaleimide α-end groups are evident at δ = 7 – 7.5 ppm, signifying that the polymers still contains functionality capable of undergoing disulfide bridging conjugation (figure 3.19). From the NMR spectra the experimental molecular weights of polymers could be calculated by a correlation between the 6 protons of the isopropyl group from the initiator (δ = 1.0 ppm) and the CH₂ peak next to the ester on the PEG repeat unit (δ = 4.2 ppm). This gave experimental degrees of polymerisation of 25, 65 & 114, compared to the theoretical values of 20, 50 and 100, implying that the initiator efficiency was ~ 80 – 90 %.

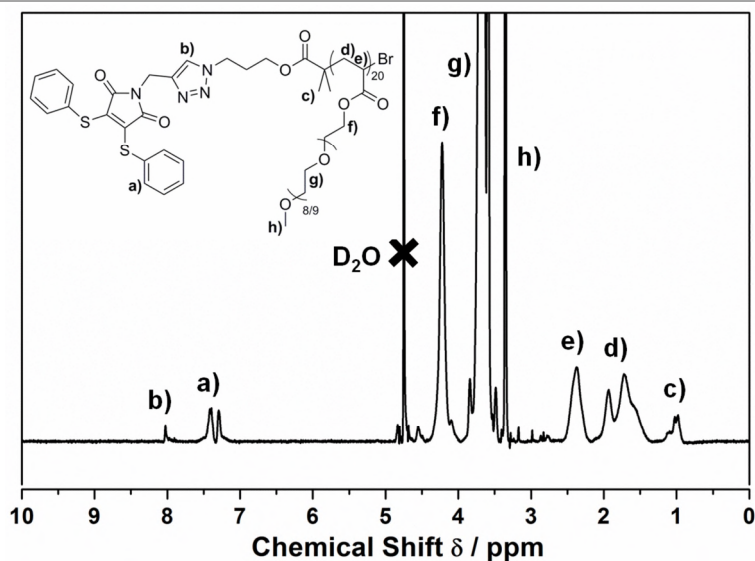
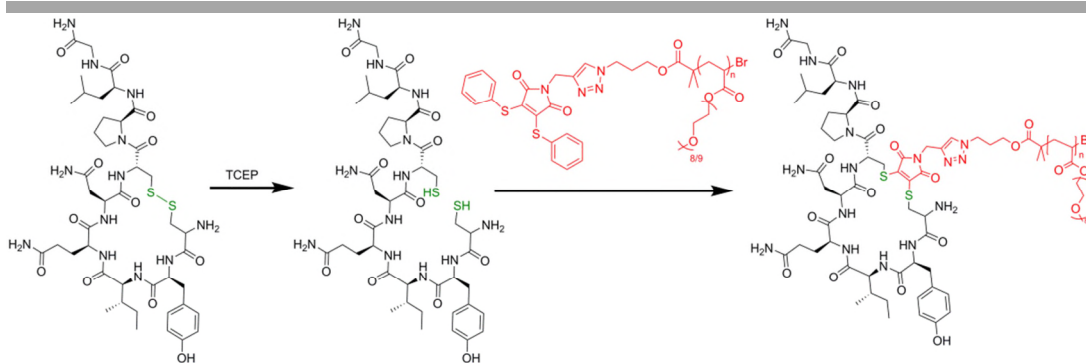


Figure 3.19. Assigned ^1H NMR (D_2O) of DTM – poly(mPEGA₄₈₀)₂₀ after purification.

The DP_n 100 purified polymer was further tested for solubility in water, DMSO and combinations of the two and found to be fully soluble in completely aqueous or DMSO systems. When the water % was below 45 % the polymer was no longer soluble, although solubility was again achieved at less than 15 % aqueous content. The interesting solubility properties of these polymers and synthesis within this narrow region of insolubility mean that initial purification of the polymers can be achieved by simple decantation of the reaction mixture. This results in removal of a significant proportion of polymerisation solution impurities including the catalyst system, although after separation the polymer layer still contains a small amount of unreacted monomer.

3.2.3.2. Conjugation of α -dithiophenolmaleimide polymers

The same conjugation reactions as undertaken with the linear dibromo- and dithiophenolmaleimide PEGs were undertaken with the α -dithiophenolmaleimide poly(mPEGA₄₈₀)s onto oxytocin (scheme 3.9). The disulfide bond was first reduced using TCEP, before addition of the polymers in pH 6.2 buffer and monitoring by RP-HPLC.



Scheme 3.9. Conjugation of dithiophenolmaleimide poly(mPEGA) with reduced oxytocin.

The 'normal' conjugation route with purified dithiophenolmaleimide polymers proceeded as observed for the linear conjugations. There is a retention time shift for the majority of the broad polymer peak after conjugation alongside the appearance of a coincidental fluorescence signal for the conjugate, not observed in the polymer (figure 3.20). Additionally, there is the appearance of a sharp peak at retention time $t = 25.3$ minutes, which represents the thiophenol lost during the conjugation/substitution reaction.

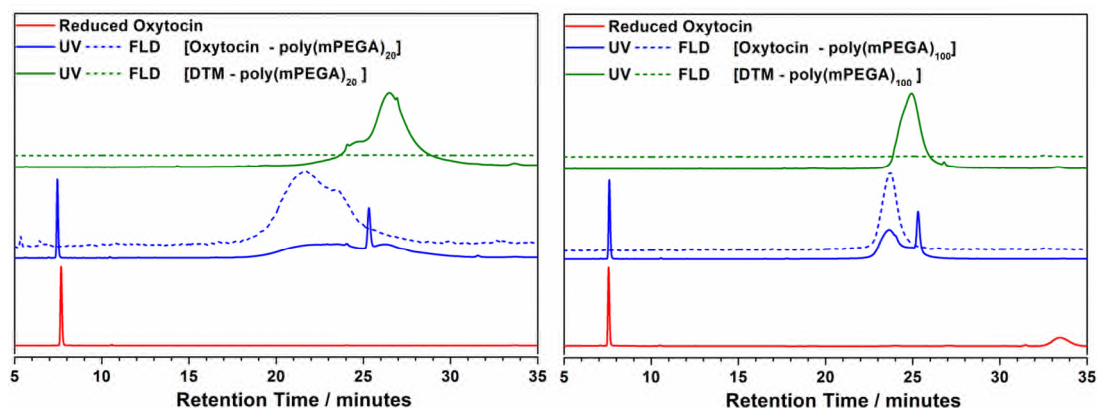


Figure 3.20. RP-HPLC analysis of DTM poly(mPEGA) conjugation onto oxytocin by UV and FLD.

It was speculated that due to specific nature of the maleimide conjugation group and high efficiency of the conjugation reaction, that the conjugation could be conducted without prior purification of the polymer. This results in an '*in-situ*' method for the disulfide

bridging conjugation of oxytocin, where only one purification step is required for the final conjugate product.

For the '*in-situ*' conjugation of the dithiophenolmaleimide polymers onto oxytocin, the same initial conjugation process was used, whereby the disulfide bond of oxytocin was reduced using TCEP (1.5 eq) generating the two free cysteine residues. Conjugation was then performed by direct addition of an aliquot of the polymerisation solution (for the phase separated solutions this was added as a mixture of the two layers). After stirring overnight the reaction was analysed by RP-HPLC, which revealed a shift in retention time from the dithiophenolmaleimide polymer, with the appearance of coincidental fluorescence (figure 3.21). All other minor peaks observed on RP-HPLC are attributed to impurities also observed in the polymerisation solution, except the sharp peak appearing at retention time $t = 25.4$ minutes which corresponds to the thiophenol released from the polymer during conjugation. Overall the HPLC chromatograms from the '*in-situ*' method are in good agreement with the 'standard' conjugation, suggesting the presence of additional impurities does not prevent conjugation occurring.

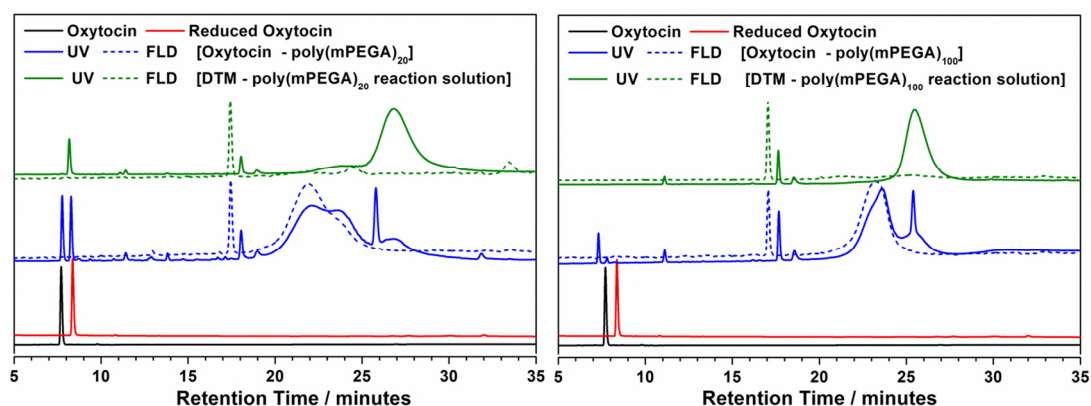


Figure 3.21. RP-HPLC of '*in-situ*' conjugation of DTM polymers onto oxytocin.

The oxytocin-polymer conjugates of the three polymers synthesised in this manner underwent further characterisation after purification by dialysis against water (3.5 kDa

MWCO, 3 days). This removed all impurities observed in the polymerisation solution, resulting in conjugates that were similar to those of the 'standard' conjugation with purification of a functional polymer. This shows that the exclusion of this purification step has no apparent negative effect on peptide-polymer conjugate formation (figure 3.22).

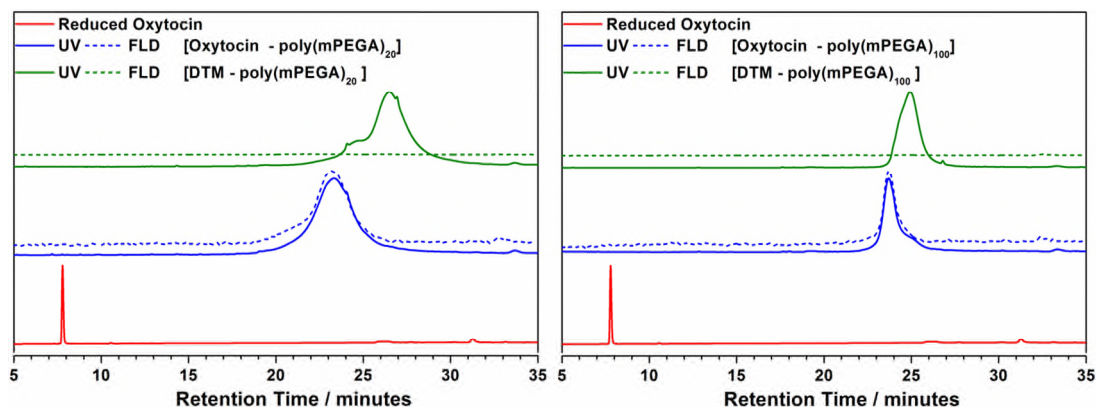


Figure 3.22. RP-HPLC analysis of purified oxytocin conjugates showing change in retention time from DTM poly(mPEGA), and newly observed fluorescence.

Analysis of the polymer and conjugate by UV confirmed that, in a similar manner to that observed during the linear PEG disulfide bridging conjugation, the wavelength for the maleimide functionality had shifted. In this case (DP_n 100 polyPEG conjugate) the λ_{\max} for the maleimide unit changed from 424 nm, when the polymer was end capped with two thiophenol groups, to 377 nm when the polymer was instead substituted with the peptide alkyl chain (figure 3.23). These wavelengths are very similar to the linear *N*-PEG-dithiophenolmaleimide and oxytocin conjugate, and previously reported dithioalkylmaleimide absorbance.²¹ Overall, the maleimide functionality remains very similar, as reflected by the UV λ_{\max} results, however, the *N*- attachment functionality (in this case the polymer architecture) has been changed.

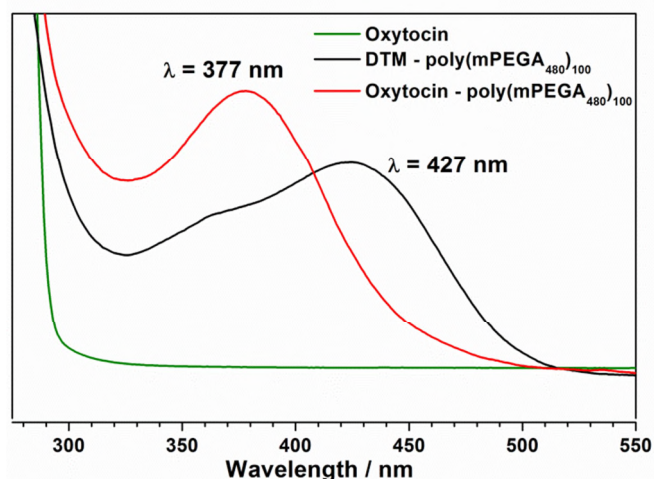


Figure 3.23. UV monitoring of oxytocin, DTM polymer and disulfide bridged oxytocin poly(mPEGA) conjugate for shift in maleimide functionality.

Fluorescence spectroscopy studies were also carried out to investigate the change of fluorescence spectra upon conjugation.²² From RP-HPLC it was known that the polymer does not exhibit fluorescence pre-conjugation, but that a new fluorescence peak appears after conjugation has occurred. This was investigated for both the smallest (DP_n 20) and largest (DP_n 100) polymers and their respective conjugates (figure 3.24). Fluorescence studies were conducted on samples at a concentration of 5 mg ml^{-1} using $\lambda_{\text{ex}} = 341 \text{ nm}$ (the same as λ_{ex} from RP-HPLC), with an analysis of the fluorescence spectra between 400 – 650 nm.

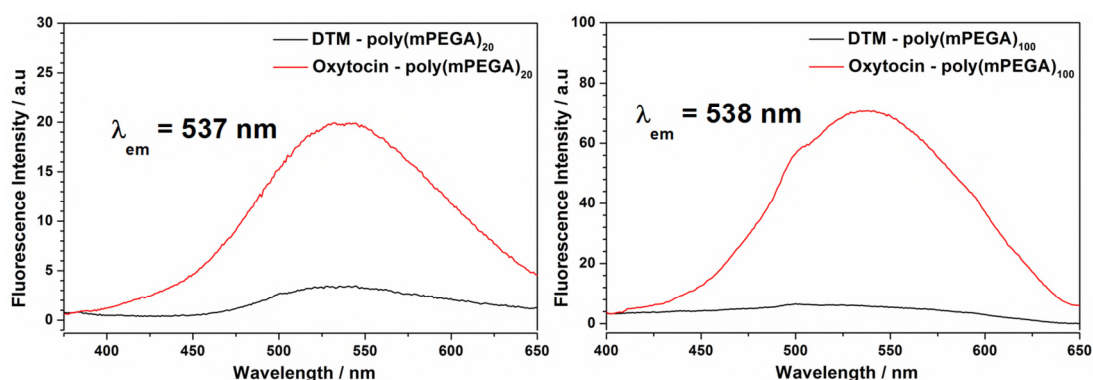


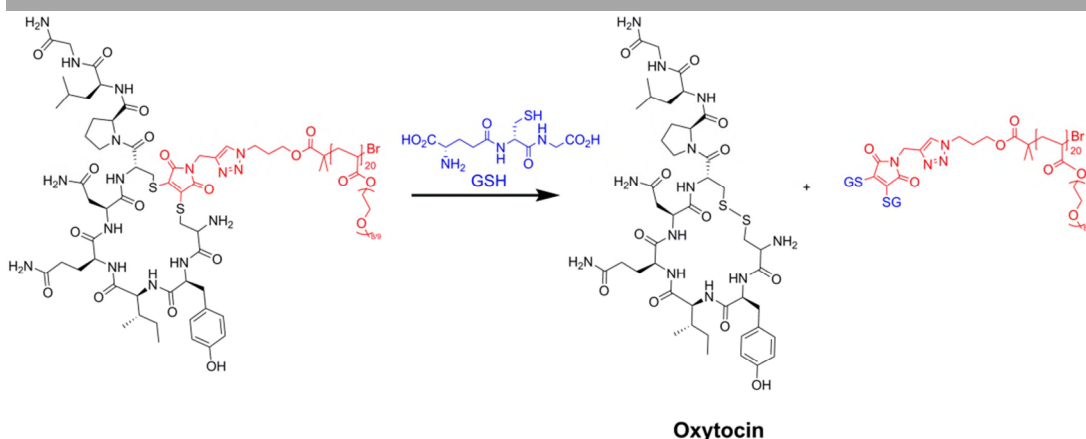
Figure 3.24. Fluorescence study of DTM polymers and oxytocin-polymer conjugates, showing an increase in fluorescence.

These two fluorescence measurements show a large increase in the fluorescence after conjugation for the two different molecular weight polymers conjugated. The emission wavelength (λ_{em}), as expected, was approximately the same for both conjugates. The induction of fluorescence on the peptide structure occurring gives another convenient characterisation handle.

3.2.3.3. Reversibility of dithiophenolmaleimide disulfide bridging

Previous research has found that a large excess of thiols (such as mercaptoethanol) can induce the cleavage of thiol-maleimide linkages *via* thiol exchange, thereby changing the nature of the thiol groups attached to the maleimide.^{16,17} This thiol exchange can therefore be utilised for the release of dithiol- functional maleimides that are conjugated onto peptides or proteins. This in effect changes the thio- functionality of the maleimide polymer with that of the desired thiol, releasing the peptide, which, in the case of oxytocin, can allow for reformation of the disulfide bond.

To investigate the reversibility of dithiophenolmaleimide conjugation under biologically relevant conditions, reversibility studies were carried out using an excess of glutathione (GSH) (scheme 3.10). Glutathione is a small tripeptide containing a cysteine group (source of the thiol) between glutamate and glycine residues. GSH is already well known for reducing disulfide bonds and exists in the cytoplasm of healthy animal cells at concentrations of 0.2 – 10 mM.³³ GSH has also been used previously as an example of a thiol that is capable of reversing maleimide conjugations, and is of particular biological relevance for potential cytoplasm based cleavage.^{17,34–36} In the case of the reversal of oxytocin conjugation, GSH has been used as a model small thiol, and similar thiol exchanges could be performed with different compounds to suit requirements.



Scheme 3.10. Glutathione induced reversal of oxytocin poly(mPEGA) conjugation, releasing the native peptide.

To a solution of the DP_n 20 oxytocin polymer conjugate was added an excess of glutathione equivalent to 6 mM (in the bio-relevant cell concentration range). The reaction was sampled after 4 days and analysis by RP-HPLC revealed the appearance of a sharp peak appearing in a coincidental position to that of the native peptide (figure 3.25). There was also a shift in retention time for the broad fluorescent peak, which is attributable to the formation of the double glutathione substituted maleimide polymer. This polymer retains its fluorescence as, although the substituent has changed from oxytocin to glutathione, the dithiolalkylmaleimide unit is still present with two alkyl thio- substituents.²²

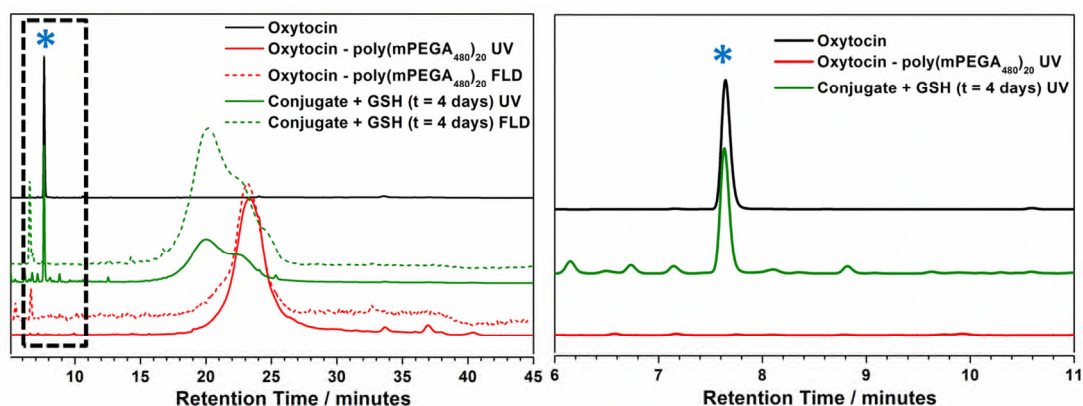


Figure 3.25. RP-HPLC trace of GSH reversal of conjugation with expansion of oxytocin region, showing the regeneration of the native peptide.

The sharp peak (coincidental to native oxytocin observed on the RP-HPLC chromatogram) was separated and collected by RP-HPLC, before MALDI-TOF analysis was undertaken. This confirmed that the native peptide was being released from the polymer conjugate with the appearance of one major mass corresponding to the native peptide at $[M+Na^+] = 1029.6$ (difference of 0.16 Da) (figure 3.26).

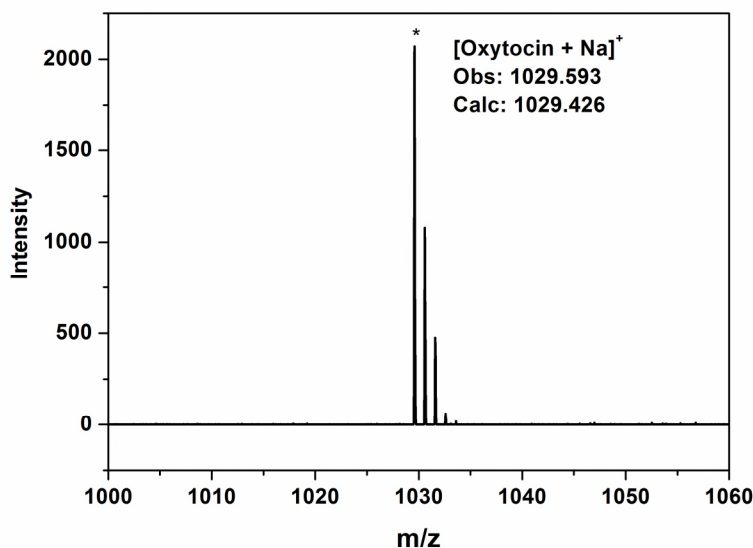


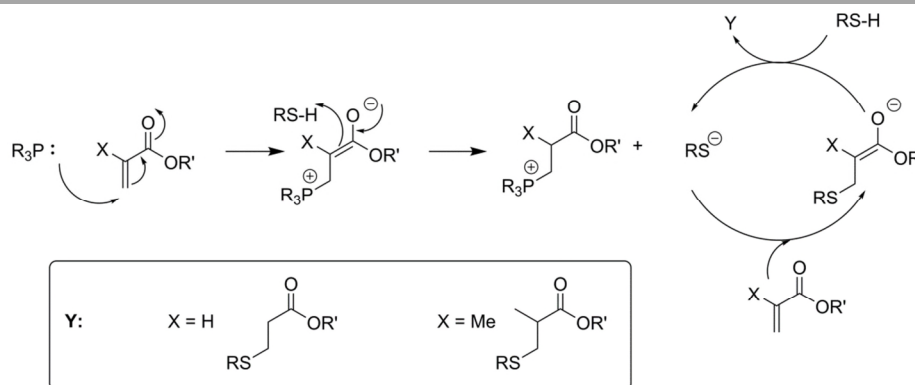
Figure 3.26. MALDI-TOF analysis of released oxytocin from oxytocin-(mPEGA₄₈₀)₂₀ polymer conjugate.

Overall, the dithiophenolmaleimide chemistry provides an interesting route for the PEGylation of oxytocin, whether in the utilisation of linear or 'comb' polyPEG polymers. The resulting conjugates can be characterised by several different methods, with the induction of fluorescence post-conjugation providing a particularly convenient handle. For oxytocin, the disulfide bridging by maleimides is particularly convenient as this is one of the major degradation sites for the peptide.

3.2.4. Reduced structure targeting (thiol-ene)

Another reaction that becomes highly accessible with the reduction of the disulfide bond releasing the two sulfhydryl groups is the reaction between the resultant thiols and an unsaturated double bond. The reactions of thiols with unsaturated carbon-carbon bonds are well known, and commonly referred to as thiol-ene (reaction with a double bond) or thiol-yne (reaction with a triple bond) reactions.^{37–39} Thiol-ene reactions can be promoted by different chemical processes, commonly utilised from light and/or initiator induced radical-based additions or nucleophilic promoted reactions, and have previously been utilised for protein/peptide modification strategies from these different routes.^{40–42}

Jones *et al.* reported the phosphine promoted Michael-type addition of mPEGA (the same reagent described previously as a monomer for polymerisations) for the double functionalisation of the reduced disulfide bond in salmon calcitonin (a 32 amino acid peptide).⁴³ After reduction of the singular disulfide bond on the peptide, two separate thiols are made available that can both react with the unsaturated double bond. This system was expanded utilising a vinyl functional alkyl halide initiator for the synthesis of peptide macroinitiator and subsequent 'grafting-from' polymerisation as an alternative peptide modification approach.⁴⁴ The reaction proceeds *via* a thiol-Michael addition promoted by TCEP (phosphines have previously proven efficient for promoting thiol-ene chemistry of acrylates) (scheme 3.11).⁴⁵ TCEP is a particularly good catalyst for use in the conjugation of vinyl functional polymers to a previously reduced disulfide bond due to providing the initial reduction of the peptide/protein as well as acting as a catalyst for the conjugation.



Scheme 3.11. Mechanism of phosphine induced thiol-ene Michael addition of (meth)acrylates.

For the previously described conjugation of mPEGA onto salmon calcitonin, the activity of the peptide was retained.⁴³ This could in part be due to the structure of this peptide being retained even after reduction of the disulfide bond, due to the presence of additional peptide structure stability *via* an α -helix. With oxytocin, there are no secondary structural features within the peptide, and the conjugation of polymers in this manner would remove cyclisation of the peptide. It is highly likely that the peptide will no longer maintain biological function and activity, but instead allows the synthesis of an ABA triblock copolymer, wherein the middle block is a peptide (figure 3.27). The peptide content of the triblock can be altered by changing the length of the polymer (A) blocks. Although less practical in the sense of synthesising polymer containing oxytocin analogues, this method of polymer conjugation still presents an interesting methodology for the concurrent attachment of two polymer chains to the peptide.

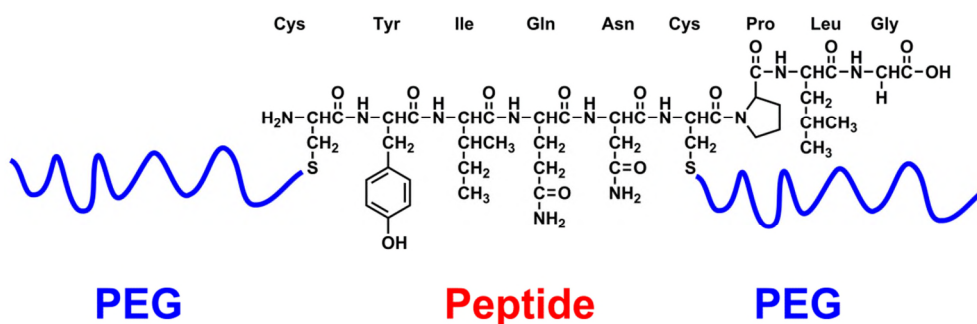
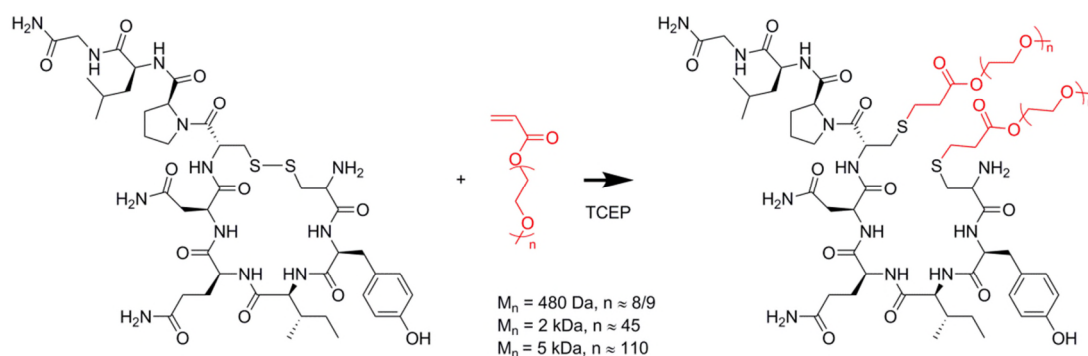


Figure 3.27. ABA triblock polymer, containing central peptide block from oxytocin.

3.2.4.1. Linear PEG acrylate

Michael addition chemistry was utilised for the conjugation of two PEG chains onto each free thiol in oxytocin following reduction of the disulfide bond. An easily accessible and low cost source of α, β –unsaturated PEG chains is through the use of commercially available PEG acrylates. Three different molecular weights of poly(ethylene glycol) methyl ether acrylate polymers ($M_n = 480, 2,000, 5,000$) were used for conjugation to reduced oxytocin *via* phosphine mediated thiol-ene chemistry (scheme 3.12). This would yield the twice PEGylated oxytocin, whereby the molecular weight of the conjugate was expected to increase to 2000, 5,000 and 10,000 Da respectively.

TCEP was selected preferentially over zinc for the reduction of the disulfide bond in this case, as it can reduce the disulfide bond in the first step and act as a catalyst in the subsequent thiol-ene PEGylation. The disulfide bond in oxytocin was firstly treated with 2 equivalents of TCEP and a sample removed after 2.5 hours for RP-HPLC analysis confirmed complete reduction to dithiol oxytocin with a shift in retention time from the native peptide. The acrylate polymers were dissolved in phosphate buffer (pH 6.5, 100 mM) and added to the reduced peptide and left to stir overnight.



Scheme 3.12. Double conjugation of mPEG acrylate onto oxytocin of different molecular weight using TCEP as a disulfide bond reduction agent and thiol-ene catalyst.

The conjugation reaction and reagents were analysed by RP-HPLC. For the mPEGA₄₈₀ reagent a multimodal distribution was evident which was also present in the unpurified conjugate mixture (figure 3.28). This is likely due to the different lengths chains within the mPEGA monomer. After conjugation there is a dramatic reduction in the concentration of oxytocin remaining in solution and the appearance of a broad conjugate peak at a higher retention time ($t = 13.4$ minutes) than either of the reagents.

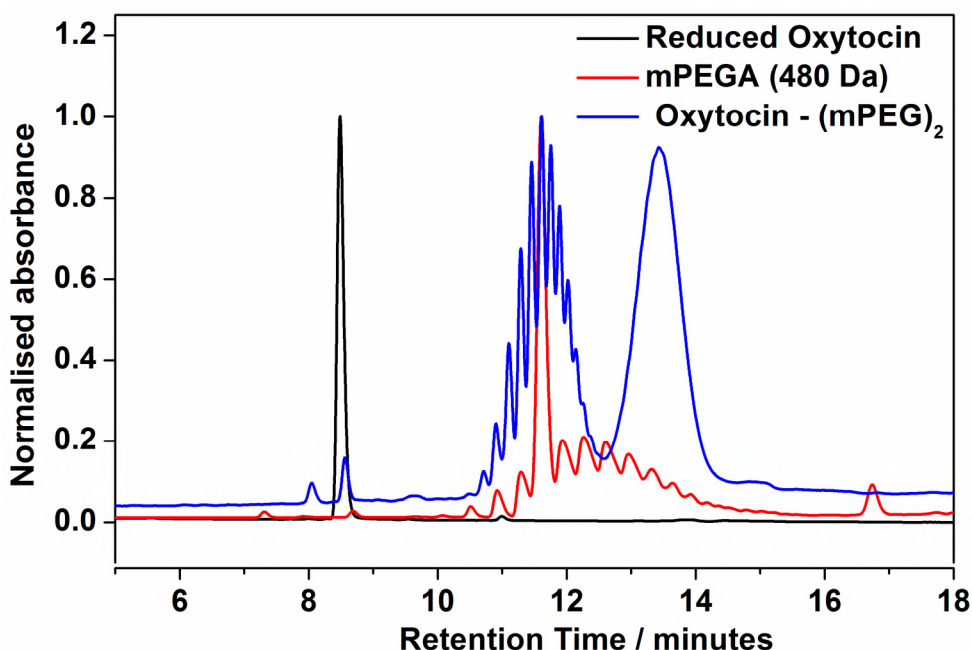


Figure 3.28. RP-HPLC of conjugation of (mPEGA₄₈₀)₂ onto oxytocin through phosphine catalysed thiol-ene Michael addition.

Subsequently the conjugate was purified by semi-preparative RP-HPLC and analysed by MALDI-TOF MS for confirmation that the peptide had undergone two separate conjugations with the acrylate functional PEG polymer (figure 3.29). The MALDI-TOF spectrum revealed the presence of a singular distribution, with a relatively small dispersity of products relating to the doubly conjugated peptide. Each peak is attributable to a different value of n within the PEG polymer, with differences in peaks equivalent to the ethylene glycol repeat unit (44.03 Da). There is no evidence of any monosubstituted

PEGylation product, which would be present at approx. 1500 Da, which could have arisen if only one of the cysteine thiols had undergone the thiol-ene reaction with the acrylate PEG.

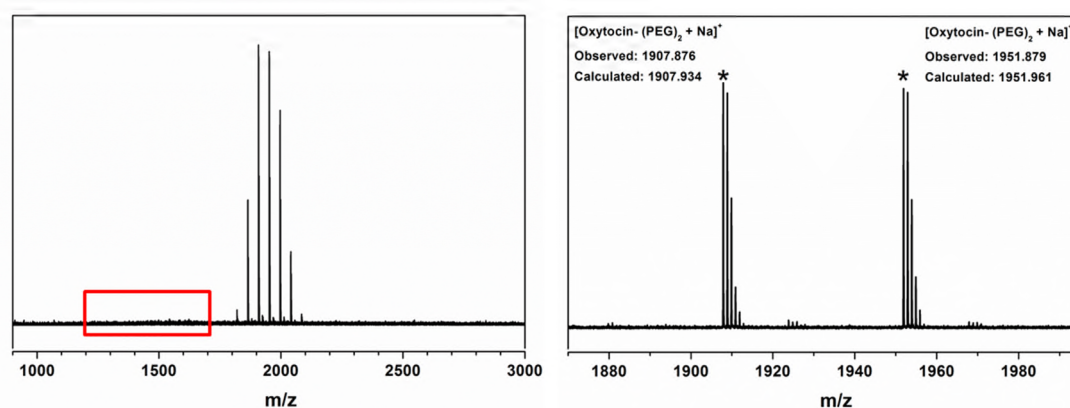


Figure 3.29. MALDI-TOF analysis of oxytocin-(mPEG₄₈₀)₂ conjugate.

Analysis of the two larger molecular weight polymer reagents (mPEGA₂₀₀₀ and mPEGA₅₀₀₀) did not reveal the presence of any polymer peaks, or multimodal distributions (figure 3.30). Alternatively a sharp peak was observed at retention time $t = 14.9$ minutes in both cases. The PEG acrylates are often utilised conventionally as PEG monomers and as such contain inhibitors to prevent auto-polymerisation. The inhibitor added to both of these reagents was 4-Methoxyphenol (MEHQ), and it is likely that this is what is observed in the RP-HPLC chromatogram. On analysis of the two conjugation reaction mixtures, this sharp peak can still be observed, alongside the formation of new peaks, highlighting successful peptide-polymer conjugation.

The 2 kDa conjugate peak appears as mostly one single moiety (retention time $t = 19.3$ minutes), although there is evidence of a minor peak at a slightly lower retention time ($t = 17.8$ minutes). This suggests the formation of one major conjugate product. For the 5 kDa conjugation there is, however, the clear presence of a bimodal peak (maxima at $t = 19.9$ & 20.3 minutes). This suggests that there are two products formed during the reaction and that these are in an approximate 50:50 ratio.

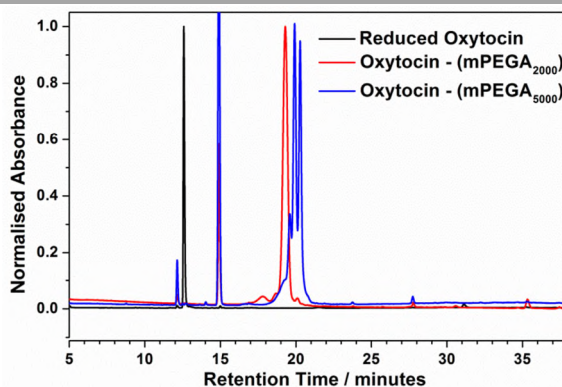


Figure 3.30. RP-HPLC monitoring of conjugation of mPEG (2 kDa and 5 kDa) onto reduced oxytocin *via* phosphine catalysed thiol-ene Michael addition.

The conjugates were purified by dialysis against water (3,500 MWCO, 3 days), for further analysis and confirmation of the disubstituted product. On analysis of the 2kDa conjugate by MALDI-TOF MS, the presence of a singular distribution relating to the doubly conjugated peptide was observed (figure 3.31). There is good agreement between the calculated (theoretical) values and those achieved experimentally, with peak spacing representing the repeat unit appropriately. Further inspection of the area in the MALDI-TOF spectra where the mono-substituted PEGylation product would be present ($\approx 3,000$ Da) reveals some possible peaks with a higher intensity than the baseline. However, these are in such low concentration compared to the major distribution that it would imply mono-substitution occurs to a much smaller degree than di-substitution.

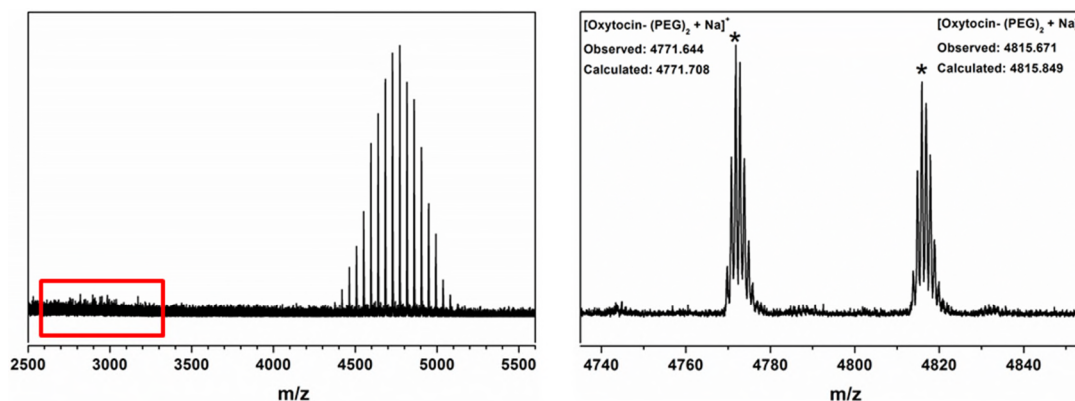


Figure 3.31. MALDI-TOF analysis of oxytocin-(mPEG₂₀₀₀)₂ conjugate.

MALDI-TOF analysis was not achieved for the 5 kDa oxytocin thiol-ene conjugate. It is likely that the double peak observed on the RP-HPLC chromatogram was showing evidence of the occurrence of singular substitution during the reaction. The MALDI-TOF spectrum of the 2 kDa conjugate suggests that this is a possibility. As this has been observed to a small degree for the 2 kDa conjugate and not within the 480 Da conjugated mPEGA it is likely that the size of the polymer plays an important role in the efficiency of the double conjugation.

Overall these results have shown that it is possible to conjugate linear PEG onto oxytocin utilising a phosphine induced thiol-ene Michael addition one-pot process. Three different molecular weights of polymer-conjugates were synthesised, and characterisation by MALDI-TOF MS suggests that the site-selective double attachment of polymers was achieved. The range of molecular weights of the conjugates (and % of oxytocin in the resulting triblock) varies from 2 kDa (50 % oxytocin) to 11 kDa (9 %) oxytocin.

3.2.4.2. PolyPEG acrylate vinyl end group

Following the successful conjugation of acrylate functional linear PEGs onto oxytocin using different molar masses of a PEG acrylate reagent, investigative studies have been undertaken into whether analogous reactions would be possible with the use of a polyPEG reagent. A vinyl end functional polyPEG was synthesised within our group by catalytic chain transfer polymerisation (CCTP), promoted by a cobalt catalyst. This is a free-radical polymerisation technique that uses cobalt macrocycles as catalytic chain transfer agents, and is useful for synthesising polymers with unsaturated double bond end groups, which can be utilised for post-polymerisation modifications. Vinyl end functional polymers synthesised by CCTP have previously been modified utilising thiol-ene Michael addition

resulting in changes to the thermal properties⁴⁶ for the functionalisation of glycopolymers⁴⁷ and for the modification of biological surfaces.⁴⁸

The vinyl end group functionality of the polymers was confirmed by ¹H NMR, and a comparison of vinyl peaks and the CH₂ peaks next to the ester in the PEG repeat unit were used to calculate the experimental molecular weight of 11.5 kDa (figure 3.32).

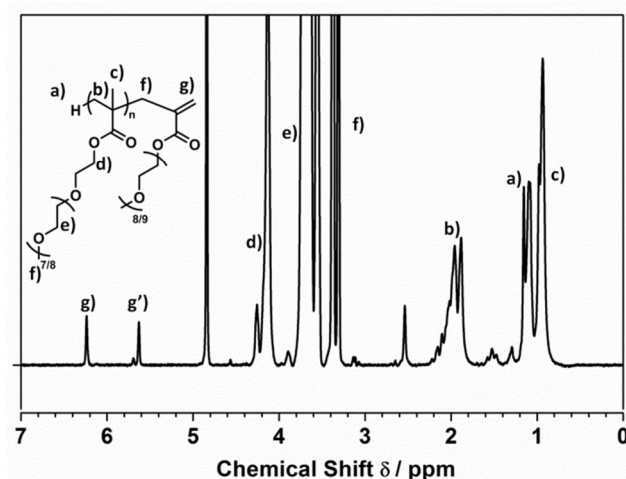


Figure 3.32. ¹H NMR (MeOD) of vinyl functional poly(mPEGMA)

A test reaction was conducted in the same manner as for the conjugation with the different linear PEG acrylates, using TCEP as both a reducing agent and as a catalyst for the two concurrent reactions with the sulfhydryl groups. The reactions were much slower, but RP-HPLC monitoring after several days revealed the formation of a broad peak, possibly signifying conjugate formation (figure 3.33). The vinyl end functional polymer, when analysed by RP-HPLC, did not show any peaks with high absorbance (max peak absorbance 0.5 mAU), even at concentrations up to 20 mg/ml. For the reaction mixture the peak area of the broad peak is 5 x that of the remaining oxytocin in solution, and unlikely to be from unreacted polymer, but potentially arising from the desired peptide-polymer conjugation.

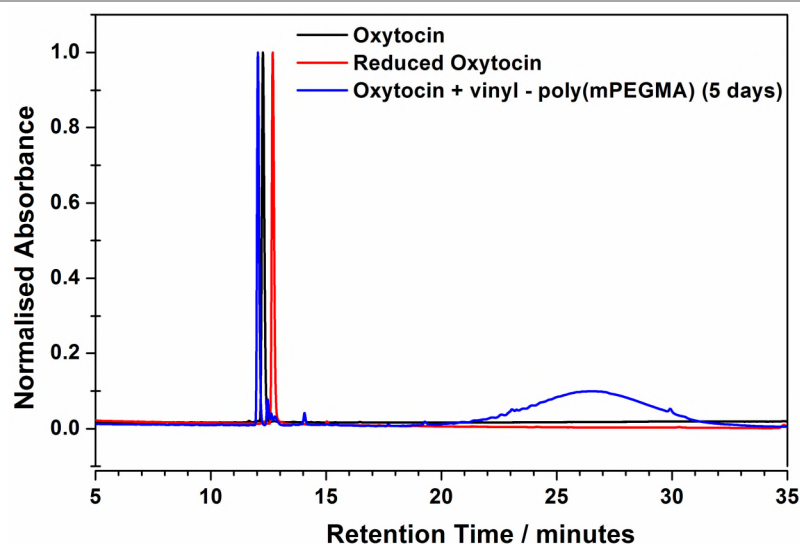


Figure 3.33. RP-HPLC of conjugation vinyl end functional poly(mPEGMA) onto oxytocin.

This initial investigation into the conjugation of polyPEGs onto oxytocin by this method is promising, highlighting an alternative method for polymer conjugation onto oxytocin, and warrants further investigation.

3.3. Chapter 3 Conclusions

There are several methods available for conjugation onto the thiols within peptides and proteins, either at cysteine residues within the structure or from the reduction of a disulfide bond. This can be advantageous compared to amino strategies, as there are likely to be less sulfhydryls available on the peptide or protein structure, allowing a more site specific conjugation.

Two of such approaches have been discussed which lead to the rebridging of the disulfide bond, or the complete removal of cyclic structure. For each strategy linear and polyPEGs can be conjugated as long as the correct conjugatable functionality is retained on the end of the polymer.

The conjugation of polymers at the disulfide bond, particularly by rebridging the disulfide is beneficial as this position is the cause of a large amount of the degradation observed for the native peptide. Whilst not explicitly discussed in this thesis, there are many other disulfide/single cysteine conjugation methods available which could also prove feasible as conjugation methods for the polymeric functionalisation of oxytocin.

3.4. Experimental

3.4.1. Materials

Oxytocin (c- [Cys-Tyr-Ile-Gln-Asn-Cys]-Pro-Leu-Gly-NH₂) was gifted from PolyPeptide laboratories (Hillerød, Denmark) and used as received. *Tris*(2-carboxyethyl) phosphine (TCEP) was purchased from Sigma Aldrich and stored at -18 °C. α-Methoxy ω-amino poly(ethylene glycol) was purchased from Rapp Polymere and stored at - 18 °C. Poly(ethylene glycol) methyl ether acrylate (average M_n: 480; containing 100 ppm BHT & 100 ppm MEHQ as inhibitors) was purchased from Sigma Aldrich and stored at 4 °C. Poly(ethylene glycol) methyl ether acrylate (average M_n: 2,000 Da/5,000 Da ; containing MEHQ as inhibitor) was purchased from Sigma Aldrich and stored at -18 °C. Vinyl end functional poly(poly(ethylene glycol) methyl ether methacrylate) was synthesised within the Haddleton group by Mr Samuel Lowe. Copper (I) Bromide (Cu^IBr, Sigma Aldrich, 98 %) was purified according to the method of Keller. *N,N,N',N',N'',N''*-Hexamethyl-[tris(aminoethyl)amine] (Me₆-TREN) was synthesised according to a reported procedure and stored at -18 °C prior to use. All other reagents were purchased from Sigma Aldrich and used without further purification.

3.4.2. Instrumentation & Analysis

Nuclear magnetic resonance (NMR) spectra were acquired with a Bruker DPX-300 or DPX-400 spectrometer with samples prepared in deuterated solvents (CDCl_3 , MeOD or D_2O). Chemical shifts were reported in parts per million (ppm) with reference to solvent residual peaks.

Size exclusion chromatography (SEC) was performed on either 1) Agilent Polymer Laboratories GPC50 eluting with DMF (0.1 w/v % LiBr) at 50 °C, 1 ml min⁻¹ flow rate, fitted with differential refractive index and UV detectors, 2 x PLgel 5 mm Polargel M columns (300 x 7.5 mm), 1 x Polargel 5 mm guard column (50 x 7.5 mm) and autosampler; 2) Varian 390-LC system using DMF (5 mM NH_4BH_4) eluent at 50 °C, 1 ml min⁻¹ flow rate, equipped with RI, UV, light scattering and viscometry detectors, 2 x PLgel 5 μm mixed D columns (300 x 7.5 mm), 1 x PLgel 5 μm guard column (50 x 7.5 mm) and autosampler.

UV/Vis spectra were recorded on an Agilent Technologies Cary 60 UV-Vis using a quartz cuvette with 10 mm optical length within the range 200 nm – 600 nm, calibrated using water as a blank solution.

Fluorescence studies were carried out on an Agilent Cary Eclipse Fluorescence spectrophotometer using an excitation wavelength $\lambda_{\text{ex}} = 341$ nm and collecting emission spectra between 300 nm and 680 nm. Excitation and emission bandwidths were set to 10 nm and data was collected at a scan speed of 30 nm/min with a 0.5 nm data interval.

Infrared absorption spectra were recorded on a Bruker VECTOR-22 FTIR spectrometer using a Golden Gate diamond attenuated total reflection cell.

Analytical high performance liquid chromatography (HPLC) was performed on an Agilent 1260 infinity series stack equipped with an Agilent 1260 binary pump and degasser. 50 μl

samples were injected using Agilent 1260 autosampler with a flow rate of 1 ml/min. The HPLC was fitted with a phenomenex Luna C18 column (250 x 4.6 mm) with 5 micron packing (100Å). Detection was achieved using an Agilent 1260 variable wavelength detector monitoring at 280 nm. Mobile phase A consisted of either 100 % water containing 0.04 % TFA as an additive or 90 % water, 10 % acetonitrile containing 0.04 % TFA as an additive. Mobile Phase B consisted of 100 % acetonitrile containing 0.04 % TFA as an additive. The column was equilibrated by washing with the starting % of mobile phase A for 10 minutes prior to injection for all conditions. The method gradient for HPLC monitoring of reactions and products was: 90 % mobile phase A decreasing to 40 % mobile phase A for 27 minutes, and remaining at 40% mobile phase A for 8 minutes, before resetting to the starting conditions in 1 minute and remaining in these conditions for at least 10 minutes to re-equilibrate the column before subsequent injections. Fluorescence monitoring of RP-HPLC was achieved using the same system, gradients and column but also equipped with an Agilent 1260 fluorescence detector with fluorescence detection at $\lambda_{\text{ex}} = 341 \text{ nm}$; $\lambda_{\text{em}} = 502 \text{ nm}$. Separation and collection by RP-HPLC was achieved using the same system, gradients and column but also fitted with an Agilent 1260 fraction collector. RP-HPL gradient 2, was carried out on the same system but with a gradient that consisted of 95 % mobile phase A decreasing to 80 % mobile phase A after 15 minutes, followed by decreasing to 40 % mobile phase A after a further 7 minutes and remaining at 40 % mobile phase A for 5 minutes before resetting to 95 % mobile phase A in 1 minute, and a 10 minute column wash with the starting gradient.

MALDI-ToF mass spectrometry was conducted on a Bruker Daltonics Autoflex MALDI-ToF mass spectrometer. MALDI-ToF samples were prepared by mixing a saturated solution of α -Cyano-4-hydroxycinnamic acid (CHCA) in methanol as a matrix (10.8 μl), sodium iodide in tetrahydrofuran (THF) (1.0 mg/ml) as cationisation agent (4.2 μl) and sample in THF with

1 drop of water (1.0 mg/ml) (10.8 μ l) where 0.7 μ l of the mixture was applied to target plate. Spectra were recorded in reflector mode calibrating with mPEG 2000 Da. Electrospray ionisation mass spectra (ESI) were recorded on an Agilent 6130B Single-Quad.

3.4.3. Synthetic Procedures

3.4.3.1. Reduction of disulfide bond of oxytocin

Reduction using TCEP

Oxytocin (5 mg, 4.9 μ mol) and TCEP (2.13 mg, 7.4 μ mol) were dissolved in water (2 ml) and left stirring at ambient temperature for 2.5 hours after which the reaction was sampled by RP-HPLC.

Reduction using zinc

Oxytocin (5 mg, 4.9 μ mol) was dissolved in water (1 ml) (with 1 % TFA) in an Eppendorf tube and zinc dust (100 mg) was added and left stirring at ambient temperature for 1 hour. After centrifugation (5 minutes) the reaction solution was removed from the metal pellet and sampled by RP-HPLC.

3.4.3.2. Maleimide linear PEG reagent synthesis & conjugation

The synthesis of *N*-poly(ethylene glycol)-3,4-dibromomaleimide and *N*-poly(ethylene glycol)-3,4-dithiophenolmaleimide is modified from an existing procedure.¹⁹

3,4-dibromomaleimide-N-PEG synthesis

To a solution of 3,4-dibromomaleimide (2.5 g, 9.8 mmol) and *N*-methylmorpholine (1.08 mL, 9.8 mmol) in THF (90 mL), methylchloroformate (0.75 mL, 9.8 mmol) was added and the mixture was stirred for 20 min at room temperature. DCM (100 mL) was added, and the organic phase was washed with H₂O (2 x 100 mL), and dried with MgSO₄ and the solvent removed *in vacuo*, yielding a pink power (2.32 g, 7.47 mmol, 77 %).

¹H NMR (CDCl₃, 400.03 MHz) δ (ppm): 4.01 (3 H, s, COCH₃); ¹³C NMR (CDCl₃, 75.47 MHz) δ (ppm): 159.2 (C=O), 146.9 (C=OOCH₃), 131.4 (C=C), 54.8 (COCH₃)

Without further purification, *N*-methoxycarbonyl-3,4-dibromomaleimide (31 mg, 0.1 mmol) was dissolved in DCM (25 mL) and amino-PEG (550 mg, 0.11 mmol) was added. The solution was stirred under nitrogen overnight at ambient temperature after which the solvent was removed *in vacuo*. The product was precipitated into hexane: diethyl ether (1:1) yielding a pale off-white solid (440 mg, mmol, 73 %).

¹H NMR (CDCl₃, 400.03 MHz) δ (ppm): 3.80 (4 H, t, J = 5.02 Hz, NCH₂CH₂), 3.63 (480 H, s, OCH₂CH₂), 3.36 (3 H, s, OCH₃)

3,4-dithiophenolmaleimide-N-PEG synthesis

3,4-dibromomaleimide (5 g, 19.6 mmol) was dissolved in methanol (200 mL). NaOAc (2.09 g, 25.5 mmol) and thiophenol (4.55 mL, 44.6 mmol) were added to the solution and stirred overnight at ambient temperature. The methanol was removed *in vacuo* before the addition of EtOAc (100 mL) and the solution extracted with H₂O (3 X 100 mL), dried with MgSO₄ and solvent removed *in vacuo*. The product was recrystallized with hexane/diethyl ether (1:1) yielding a bright yellow powder (3.13 g, 10.0 mmol, 51 %).

^1H NMR (CDCl_3 , 400.05 MHz) δ (ppm): 7.15 – 7.25 (6 H, m, SPh), 7.10 (4 H, d, 7.78 Hz, SPh);

^{13}C NMR (CDCl_3 , 100.59 MHz) δ (ppm): 166.5, (C=O) 136.6 (C=C), 131.8 (SPh), 128.9 (SPh), 128.3 (SPh), 128.6 (SPh).

3,4-dithiophenolmaleimide (2 g, 6.38 mmol) was dissolved in EtOAc (70 ml) and *N*-methylmorpholine (0.70 ml, 6.38 mmol) was added. Methylchloroformate (0.54 ml, 7.02 mmol) was added dropwise and solution stirred for 1 hour. The solution was washed with H_2O (2 x 100 ml) and dried with MgSO_4 before the solvent was removed *in vacuo* yielding a bright orange-yellow powder.

^1H NMR (CDCl_3 , 400.03 MHz) δ (ppm): 7.25-7.35 (10 H, m, SPh), 3.91 (3 H, s, COCH_3); ^{13}C NMR (CDCl_3 , 75.47 MHz) δ (ppm): 161.7 (C=O), 147.7 (C=O), 137.1 (C=C), 132.5 (SPh), 129.1 (SPh), 128.9 (SPh), 128.0 (SPh), 54.3 (COCH_3)

To *N*-methoxycarbonyl-3,4-dithiophenolmaleimide (75 mg, 0.2 mmol), in DCM (5 ml) was added amino-PEG (1.01 g, 0.2 mmol) in DCM (10 ml). After stirring at ambient temperature for 30 minutes silica gel was added and the reaction mixture stirred overnight. The solution was filtered and DTM-PEG precipitated into hexane: diethyl ether (1:1), resulting in a bright yellow powder.

^1H NMR (CDCl_3 , 300.13 MHz) δ (ppm): 7.10-7.55 (10 H, m, SPh), 3.86 (2 H, t, 5.09 Hz, CONCH_3), 3.62 (480 H, s, OCH_2CH_2), 3.36 (3 H, s, OCH_3)

Conjugation of dibromo- or dithiophenolmaleimide

PEGs onto oxytocin

Oxytocin (10 mg, 9.9 μmol) was dissolved in water (2 ml) with TCEP (4.3 mg, 17.2 μmol). After 2.5 hours a sample was removed for RP-HPLC analysis for confirmation of complete

disulfide bond reduction. DBM or DTM PEG (70 mg, 13 μ mol) in water (3 ml) was added to the solution alongside the addition of phosphate buffer (5 ml, 100 mmol. pH 6.2), and the reaction stirred at 10 °C for 24 hours, before further RP-HPLC monitoring.

3.4.3.3. DTM-poly(mPEGA₄₈₀) synthesis & conjugation

3,4-Dithiophenolmaleimide initiator synthesis

N-Methoxycarbonyl-3,4-dithiophenolmaleimide (1.5 g, 4.04 mmol) was dissolved in DCM (100 ml) and propargylamine (0.26 ml, 4.04 mmol) was added. After 30 minutes silica (30 g) was added to the solution and the reaction stirred overnight. The reaction mixture was filtered, and the product purified by column chromatography (ethyl acetate: petroleum ether 1:10).

¹H NMR (CDCl₃, 400.03 MHz) δ (ppm): 7.10-7.25 (10 H, m, SPh); 4.18 (2 H, s, NCH₂); 2.13 (1 H, s, C \equiv CH); ¹³C NMR (CDCl₃, 75.47 MHz) δ (ppm): 165.5 (C=CC=O); 136.0 (SPh); 133.2 (SPh); 129.0 (SPh); 128.5 (SPh); 128.7 (C=C); 76.7 (C \equiv CH); 72.8 (C \equiv CH); 27.7 (NCH₂).

3,4-Dithiophenol-*N*-propynyl-maleimide (4.00 g, 11.4 mmol), 3-azidopropyl 2-bromo-2-methylpropanoate (2.85 g, 11.4 mmol) and Cu(I)Br (163 mg, 1.14 mmol) were dissolved in DMF (40 ml). The mixture was purged with nitrogen for 20 minutes. 2,2 Bipyridine (360 mg, 2.28 mmol) was added to the mixture with stirring and further purged with nitrogen for 20 minutes. The reaction was left stirring at ambient temperature overnight. DMF was removed and a portion of the crude residue was purified twice by silica gel column chromatography (diethyl ether in dichloromethane, 0% -10 %).

¹H NMR (CDCl₃, 400.03 MHz) δ (ppm): 7.57 (s, 1H, C=CH); 7.17- 7.32 (m, 10H, SPh); 4.82 (s, 2H, NCH₂C=CH); 4.47 (t, J = 7.03 Hz, 2H, COOCH₂CH₂CH₂); 4.20 (t, J = 6.02 Hz, 2H,

OCOCH₂CH₂CH₂); 2.33 (qu, J = 6.02 Hz, 7.03 Hz, 2H, OCOCH₂CH₂CH₂); 1.96 (s, 6H, COC(CH₃)₂Br).

¹³C NMR (CDCl₃, 75.47 MHz) δ (ppm): 171.40 (OCOC(CH₃)₂Br; 166.24 (C=CCON); 142.36 (NCH₂C=CH); 135.75 (SPHC=C); 131.90(SPh); 128.99 (SPh); 128.83 (SPh); 128.43 (SPh); 123.43 (C=CHN₃); 62.25 (COOCH₂CH₂CH₂); 55.79 (COC(CH₃)₂Br); 46.91(COOCH₂CH₂CH₂); 33.81(NCH₂C=CH); 30.67 (COC(CH₃)₂Br); 29.08 (COOCH₂CH₂CH₂).

IR: 1159cm⁻¹ (vc-o); 1703 cm⁻¹ (vc=o); 1732 cm⁻¹ (ester vc=o)

HRMS (ESI+): m/z Found: 623.0406, Calc: 623.0393 [C₂₆H₂₅O₄N₄S₂Br + Na]⁺

Example polymerisation using EBiB or DTM

initiator in mixed solvent system

In an oven dried Schlenk tube CuBr (3.6 mg, 24.9 μmol) and water (1 ml) were added and stirred before the addition of Me₆TREN (6.6 μl) upon which there was the immediate formation of Cu(0) powder and blue CuBr₂ solution, which was degassed by nitrogen bubbling for 30 minutes. In a separate vial, initiator (62.2 μmol) and poly(ethylene glycol) methyl ether acrylate (*DP_n* Eq.) were dissolved in DMSO (6 ml) and water (0.5 ml) and degassed by nitrogen bubbling for 30 minutes. The monomer/initiator solution was then added into the catalyst solution by injection (t = 0) and the reaction was stirred at ambient temperature under nitrogen for 20 hours. After this time a sample was removed and diluted with δ₆-DMSO for ¹H NMR analysis and DMF for GPC molecular weight data. Polymers were purified by dialysis (1 kDa MWCO) against water for 3 days.

Oxytocin conjugation with purified polymer

Oxytocin (5 mg, 4.97 μ mol) was dissolved in water (1 ml) and TCEP (2.14 mg, 7.45 μ mol) in water (1 ml) was added. The solution was stirred for 2.5 hours, after which an aliquot was removed (50 μ l) and complete disulfide reduction was confirmed by RP-HPLC. DTM-(mPEGA₄₈₀)₂₀ (71 mg, 5.92 μ mol) was dissolved in water (2 ml) and added to the reduced peptide solution at 10 °C. The reaction was maintained at 10 °C and stirred overnight after which a sample was submitted for RP-HPLC analysis. This revealed the disappearance of the polymer peak and the formation of a new conjugate peak with coincidental fluorescence, and a sharp peak at retention time $t = 25.2$ minutes relating to thiophenol released in the reaction.

In-situ polyPEG conjugation of oxytocin

Oxytocin (5 mg, 4.97 μ mol) was dissolved in water (1 ml) and tris(2-carboxyethyl)phosphine (2.14 mg, 7.45 μ mol) in water (1 ml) was added. The solution was stirred for 2.5 hours, after which an aliquot was removed (50 μ l) and complete disulfide reduction was confirmed by RP-HPLC. The polymerisation solution of DTM-(mPEGA₄₈₀)₂₀ was thoroughly mixed after which an aliquot was removed (0.708 ml, 5.46 μ mol) and diluted in water (1.3 ml) and added to the reduced peptide solution at 10 °C. The reaction was maintained at 10 °C and stirred overnight, after which a sample was taken for RP-HPLC analysis which showed the disappearance of the polymer peak and the formation of a new conjugate peak with coincidental fluorescence and a sharp peak at retention time $t = 25.2$ minutes, attributed to thiophenol released in the reaction. Subsequent conjugates were purified by dialysis (regenerated cellulose dialysis membrane, MWCO 1,000) against water at ambient temperature for a minimum of 3 days with water changes 3 times daily.

Reversibility of peptide-polymer conjugates

Oxytocin – poly(mPEGA₄₈₀)₂₀ (10 mg, 0.769 μ mol) was dissolved in water (2 ml) before the addition of reduced glutathione (3.7 mg, 12 μ mol, 15 equivalents) to the stirred solution at ambient temperature. After four days an aliquot of the reaction solution (0.2 ml) was removed and diluted in water (0.8 ml) for RP-HPLC. This revealed the reappearance of the reduced native peptide, and a shift in retention time from the conjugate peak to a new glutathione substituted polymer, which retains fluorescence.

3.4.3.4. 'Thiol-ene' conjugation onto oxytocin

Oxytocin conjugation with PEG acrylate

Oxytocin (5 mg, 4.96 μ mol) was dissolved in water (2 ml) with TCEP (2.84 mg, 9.93 μ mol). After 2 hours a sample was taken for RP-HPLC (80 μ l) confirming the reduction of the disulfide bridge. pH 6.5 phosphate buffer (10 ml, 100 mM) was added with m-PEG acrylate (Sigma Aldrich, 5,000 Da) (99 mg, 34.72 μ mol) and the reaction stirred overnight at T = 10 °C before analysis by RP-HPLC

Conjugation of vinyl functional poly(mPEGMA)

Oxytocin (4 mg, 3.97 μ mol) was dissolved in water (2 ml) with TCEP (3.4 mg, 11.8 μ mol). After 2 hours a sample was taken for RP-HPLC (100 μ l in 1 ml water) which confirmed reduction of the disulfide bridge. Vinyl end functional poly(mPEGMA) (100 mg, 32 mmol) in pH 7 phosphate buffer (2 ml, 100mM) was added and the reaction stirred overnight at ambient temperature before analysis by RP-HPLC.

3.5. References

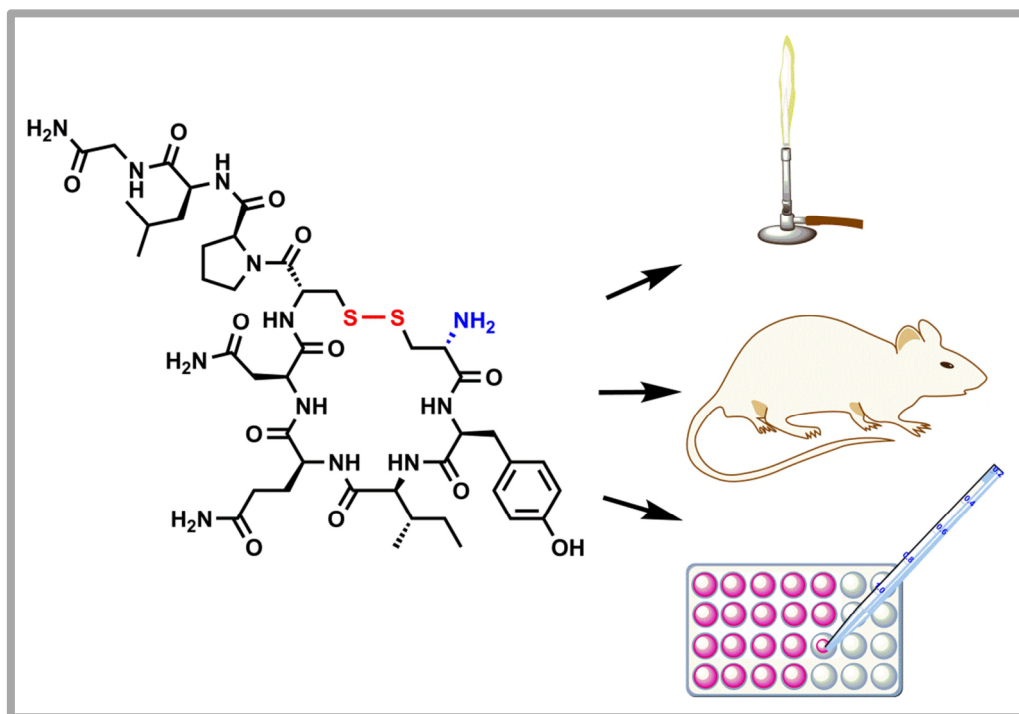
- 1 D. Gilis, S. Massar, N. J. Cerf and M. Rومان, *Genome Biol.*, 2001, **2**, research0049.1–0049.12.
- 2 W. W. Cleland, *Biochemistry*, 1964, **3**, 480–482.
- 3 J. A. Burns, J. C. Butler, J. Moran and G. M. Whitesides, *J. Org. Chem.*, 1991, **56**, 2648–2650.
- 4 A. Hawe, R. Poole, S. Romeijn, P. Kasper, R. Van Der Heijden and W. Jiskoot, *Pharm. Res.*, 2009, **26**, 1679–1688.
- 5 K. Wiśniewski, J. Finnman, M. Flipo, R. Galyean and C. D. Schteingart, *Biopolymers*, 2013, **100**, 408–421.
- 6 C. W. Smith, R. Walter, S. Moore, R. C. Makofske and J. Meienhofer, *J. Med. Chem.*, 1978, **21**, 117–120.
- 7 C. W. Smith and M. F. Ferger, *J. Med. Chem.*, 1976, **19**, 250–254.
- 8 A. D. de Araujo, M. Mobli, J. Castro, A. M. Harrington, I. Vetter, Z. Dekan, M. Muttenthaler, J. Wan, R. J. Lewis, G. F. King, S. M. Brierley and P. F. Alewood, *Nat. Commun.*, 2014, **5**, 3165.
- 9 M. Muttenthaler, A. Andersson, A. D. de Araujo, Z. Dekan, R. J. Lewis and P. F. Alewood, *J. Med. Chem.*, 2010, **53**, 8585–8596.
- 10 J. L. Stymiest, B. F. Mitchell, S. Wong and J. C. Vederas, *Org. Lett.*, 2003, **5**, 47–49.
- 11 M. Erlandsson and M. Hällbrink, *Int. J. Pept. Res. Ther.*, 2005, **11**, 261–265.
- 12 D. E. Shafer, J. K. Inman and A. Lees, *Anal. Biochem.*, 2000, **282**, 161–164.
- 13 K. Tyagarajan, E. Pretzer and J. E. Wiktorowicz, *Electrophoresis*, 2003, **24**, 2348–2358.
- 14 E. B. Getz, M. Xiao, T. Chakrabarty, R. Cooke and P. R. Selvin, *Anal. Biochem.*, 1999, **273**, 73–80.
- 15 E. Friedmann, D. H. Marrian and I. Simon-Reuss, *Br. J. Pharmacol.*, 1949, **4**, 105–108.
- 16 L. M. Tedaldi, M. E. B. Smith, R. I. Nathani and J. R. Baker, *Chem. Commun.*, 2009, 6583–6585.
- 17 M. E. B. Smith, F. F. Schumacher, C. P. Ryan, L. M. Tedaldi, D. Papaioannou, G. Waksman, S. Caddick and J. R. Baker, *J. Am. Chem. Soc.*, 2010, **132**, 1960–1965.
- 18 M. W. Jones, R. A. Strickland, F. F. Schumacher, S. Caddick, J. R. Baker, M. I. Gibson and D. M. Haddleton, *J. Am. Chem. Soc.*, 2012, **134**, 1847–1852.
- 19 L. Castañeda, Z. V. F. Wright, C. Marculescu, T. M. Tran, V. Chudasama, A. Maruani, E. A. Hull, J. P. M. Nunes, R. J. Fitzmaurice, M. E. B. Smith, L. H. Jones, S. Caddick and J. R. Baker, *Tetrahedron Lett.*, 2013, **54**, 3493–3495.

- 20 F. F. Schumacher, M. Nobles, C. P. Ryan, M. E. B. Smith, A. Tinker, S. Caddick and J. R. Baker, *Bioconjug. Chem.*, 2011, **22**, 132–136.
- 21 L. M. Tedaldi, A. E. Aliev and J. R. Baker, *Chem. Commun.*, 2012, **48**, 4725–4727.
- 22 M. P. Robin, P. Wilson, A. B. Mabire, J. K. Kiviaho, J. E. Raymond, D. M. Haddleton and R. K. O'Reilly, *J. Am. Chem. Soc.*, 2013, **135**, 2875–2878.
- 23 M. W. Jones, R. A. Strickland, F. F. Schumacher, S. Caddick, J. R. Baker, M. I. Gibson and D. M. Haddleton, *Chem. Commun.*, 2012, **48**, 4064–4066.
- 24 Q. Zhang, P. Wilson, Z. Li, R. Mchale, J. Godfrey, A. Anastasaki, C. Waldron and D. M. Haddleton, *J. Am. Chem. Soc.*, 2013, **135**, 7355–7363.
- 25 A. Anastasaki, A. J. Haddleton, Q. Zhang, A. Simula, M. Driesbeke, P. Wilson and D. M. Haddleton, *Macromol. Rapid Commun.*, 2014, **35**, 965–970.
- 26 F. Alsubaie, A. Anastasaki, P. Wilson and D. M. Haddleton, *Polym. Chem.*, 2015, **6**, 406–417.
- 27 Q. Zhang, Z. Li, P. Wilson and D. M. Haddleton, *Chem. Commun.*, 2013, **49**, 6608–6610.
- 28 C. Waldron, Q. Zhang, Z. Li, V. Nikolaou, G. Nurumbetov, J. Godfrey, R. McHale, G. Yilmaz, R. K. Randev, M. Girault, K. McEwan, D. M. Haddleton, M. Driesbeke, A. J. Haddleton, P. Wilson, A. Simula, J. Collins, D. J. Lloyd, J. A. Burns, C. Summers, C. Houben, A. Anastasaki, M. Li, C. R. Becer, J. K. Kiviaho and N. Risangud, *Polym. Chem.*, 2014, **5**, 57–61.
- 29 A. Simula, A. Anastasaki and D. M. Haddleton, *Macromol. Rapid Commun.*, 2015, **37**, 356–361.
- 30 A. Simula, V. Nikolaou, F. Alsubaie, A. Anastasaki and D. M. Haddleton, *Polym. Chem.*, 2015, **6**, 5940–5950.
- 31 F. Alsubaie, A. Anastasaki, V. Nikolaou, A. Simula, G. Nurumbetov, P. Wilson, K. Kempe and D. M. Haddleton, *Macromolecules*, 2015, **48**, 6421–6432.
- 32 A. Simula, G. Nurumbetov, A. Anastasaki, P. Wilson and D. M. Haddleton, *Eur. Polym. J.*, 2015, **62**, 294–303.
- 33 M. E. Anderson, *Chem. Biol. Interact.*, 1998, **111-112**, 1–14.
- 34 A. Ross, H. Durmaz, K. Cheng, X. Deng, Y. Liu, J. Oh, Z. Chen and J. Lahann, *Langmuir*, 2015, **31**, 5123–5129.
- 35 Z. Tang, P. Wilson, K. Kempe, H. Chen and D. M. Haddleton, *ACS Macro Lett.*, 2016, **5**, 709–713.
- 36 P. Moody, M. E. B. Smith, C. P. Ryan, V. Chudasama, J. R. Baker, J. Molloy and S. Caddick, *ChemBioChem*, 2012, **13**, 39–41.
- 37 C. E. Hoyle and C. N. Bowman, *Angew. Chemie Int. Ed.*, 2010, **49**, 1540–1573.
- 38 A. B. Lowe, *Polym. Chem.*, 2010, **1**, 17–36.
- 39 A. B. Lowe, *Polym. Chem.*, 2014, **5**, 4820–4870.

- 40 S. Wittrock, T. Becker and H. Kunz, *Angew. Chemie*, 2007, **46**, 5226–5230.
- 41 A. Dondoni, A. Massi, P. Nanni and A. Roda, *Chem. Eur. J.*, 2009, **15**, 11444–11449.
- 42 M. Li, P. De, H. Li and B. S. Sumerlin, *Polym. Chem.*, 2010, **1**, 854–859.
- 43 M. W. Jones, G. Mantovani, S. M. Ryan, X. Wang, D. J. Brayden and D. M. Haddleton, *Chem. Commun.*, 2009, 5272–5274.
- 44 M. W. Jones, M. I. Gibson, G. Mantovani and D. M. Haddleton, *Polym. Chem.*, 2011, **2**, 572–574.
- 45 G.-Z. Li, R. Randev, A. H. Soeriyadi, G. J. Rees, C. Boyer, Z. Tong, C. R. Becer and D. M. Haddleton, *Polym. Chem.*, 2010, **1**, 1196–1204.
- 46 A. H. Soeriyadi, G.-Z. Li, S. Slavin, M. W. Jones, C. M. Amos, C. R. Becer, M. R. Whittaker, D. M. Haddleton, C. Boyer and T. P. Davis, *Polym. Chem.*, 2011, **2**, 815–822.
- 47 Q. Zhang, S. Slavin, M. W. Jones, A. J. Haddleton and D. M. Haddleton, *Polym. Chem.*, 2012, **3**, 1016–1023.
- 48 S. Slavin, E. Khoshdel and D. M. Haddleton, *Polym. Chem.*, 2012, **3**, 1461–1466.

Chapter 4

4. PEGylated oxytocin: Effects of PEGylation on oxytocin activity and stability



The oxytocin-polymer conjugates described in Chapters 2 and 3 were investigated using different techniques and compared to the native peptide. High temperature thermal stability studies were conducted to investigate any improvements in stability after conjugation. Ex vivo organ bath testing was undertaken to investigate the magnitude of retained uterotonic activity for the polymer conjugates with respect to the native peptide. MTT assays were conducted on breast cancer cell line MDA-MB 231 in order to investigate the effect of oxytocin and oxytocin-polymer conjugates on cell proliferation.

4.1. Stability testing

4.1.1. Introduction

Due to the very low thermal stability of oxytocin, the desired effect of polymer conjugation was to reduce, or completely prevent, the thermal degradation that occurs within the native peptide structure. There has been extensive previous research on oxytocin degradation which has largely focussed on investigating the characteristics of degradation.¹⁻⁵ This has involved analysis of the major degradation products, thus highlighting where most of the degradation may be taking place in the peptide structure of native oxytocin, and other oxytocin analogues. Previous degradation studies and analysis by Hawe *et al.* highlighted the formation of trisulfide, tetrasulfide, dimerization and the formation of larger aggregates as the main degradation products, alongside deamidation at Asn⁶, Gln⁴ and Gly⁹.¹ Degradation studies were also carried out by Wiśniewski *et al.* (40 °C, 35 days) which further confirmed the formation of trisulfide and tetrasulfide by-products and dimeric oxytocin.²

These studies (analysed by RP-HPLC and MS) highlight the disulfide bond as one of the main sites that degradation products are known to arise from. The degradation of oxytocin is well known to be a draw-back in the use of the therapeutic, particularly within the developing world where cold-chain supply and storage may not always be achievable for social or economic reasons. This has resulted in guidelines being established for oxytocin storage: (refrigerated, under 10 °C) no more than 24 months; (not refrigerated, under 25 °C) no more than 3 months.⁶ It is vital that the degradation of oxytocin be reduced in order to improve accessibility of the drug for prolonged storage, or easier transportation, particularly within those countries that experience the highest maternal mortality rate.

A large number of therapeutics are well known to undergo degradation *via* chemical and physical pathways during storage or transportation, particularly upon exposure to fluctuating temperatures, often leading to deterioration in activity resulting in a “shelf-life” for each product. Additional to more commonly being used to improve the *in vivo* stability and circulation time of therapeutics, attachment of poly(ethylene glycol) (PEG) has previously been shown to improve the stability of peptide/proteins or other biomolecules and to some level prevent denaturation.⁷

In the first part of this chapter, the aqueous stability of oxytocin will be investigated, and the effect of poly(ethylene glycol) both as a linear polymer and as a ‘comb’ polyPEG is explored. The potential use of PEG as an external non-conjugated excipient will be analysed alongside the library of different conjugation linkages and architectures of oxytocin-polymer conjugates synthesised in chapters 2 and 3. Of particular interest is the effect that the covalent conjugation has on the stability or whether the addition of inexpensive, commercially available polymers to solutions of the peptide leads to similar improvements in stability.

4.1.2. Initial oxytocin stability tests

The stability of oxytocin was initially investigated at 50 °C where solutions of the peptide (1 mM) were dissolved in unbuffered water and left for 28 days (figure 4.1). At regular intervals the peptide samples were removed and analysed by RP-HPLC where the % of oxytocin remaining could be calculated by analysis of the peak area on the chromatogram. It was found that the degradation of oxytocin at this temperature and concentration was very rapid with a 50 % reduction in the amount of peptide after 5 days. After 28 days analysis of the oxytocin levels by RP-HPLC found that only 2.5 % of the peak corresponding to oxytocin (retention time $t = 7.2$ minutes) was observed within the chromatogram,

suggesting that there was an almost complete degradation. After 28 days a variety of other peaks can be observed by RP-HPLC at higher retention times than the native peptide, with the major degradation peaks observed at retention times of $t = 10.6$ minutes and $t = 11.9$ minutes. These results concur with previous stability studies explored for the peptide wherein HPLC analysis has been performed on the degradation products of oxytocin.^{1,2} In the literature it was suggested that the peaks observed are likely from various degradation products centred on the disulfide bond (such as trisulfide/tetrasulfide formation and dimerization or the formation of larger aggregates), as previous studies have shown similar RP-HPLC chromatograms.^{1,2}

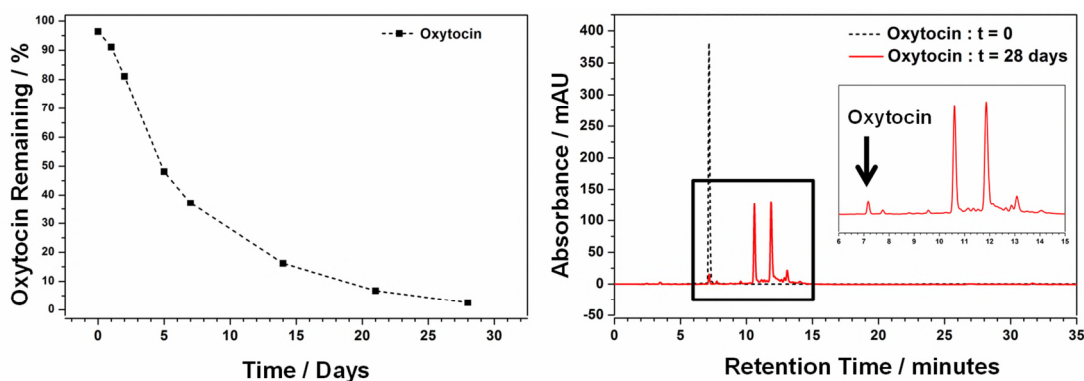


Figure 4.1. Monitoring the degradation of oxytocin at 50 °C over 28 days by RP-HPLC.

The observed rapid and almost complete destruction of the structure highlights the importance of the need for stability enhancements on the peptide.

4.1.3. High temperature thermal assay for non-conjugated excipients

Excipients (inactive chemicals added to formulations) can provide an inexpensive and effective way to enhance protein stabilisation and have previously been shown to provide non-covalent stabilisation, thereby reducing degradation of peptide/protein/drug

formulations.⁸ Commonly used excipients include buffering agents, amino acids, salts, sugars and polyols as well as low molecular weight hydrophilic polymers (such as PEGs and polysaccharides), which aid in preventing aggregation or denaturation of therapeutics and proteins.

Some of these commonly utilised, commercially available excipients (sugars, polyols and polymers) were analysed to ascertain their effects on the stability of oxytocin after high thermal stress at 80 °C. The high temperature was required so that 'normal' oxytocin degradation would be achieved quickly, where only 24 hours was required to attain high % degradation as an accelerated model for degradation at more applicable temperatures. This results in low stability for the native peptide and allows suitable comparisons to be attained between the solutions with and without the addition of external additives. This temperature is also in line with previous high temperature oxytocin degradation carried out by Avanti *et al.*, where a temperature of 70 °C was used to confirm that the addition of metal salts to peptide solutions aided the stability, and hence the recovery, of the active peptide.⁹ An alternative RP-HPLC method was developed with a slower initial gradient. This caused a longer retention time of the native peptide, more similar to the retention time of the oxytocin-polymer conjugates.

4.1.3.1. Oxytocin calibration plot

In order to investigate the amount of oxytocin remaining at the end of the stability study, a calibration plot was made of the native peptide between 1 mM and 0.01 mM (figure 4.2). Oxytocin has a high UV ($\lambda = 280$ nm) absorption even at low concentrations, and the calibration was constructed to ensure the concentration of remaining oxytocin could be reliably calculated, even with residual amounts of peptide still in solution. This linear

calibration plot was used for calculation of the level of oxytocin remaining in all native peptide and non-covalently attached excipient interaction studies.

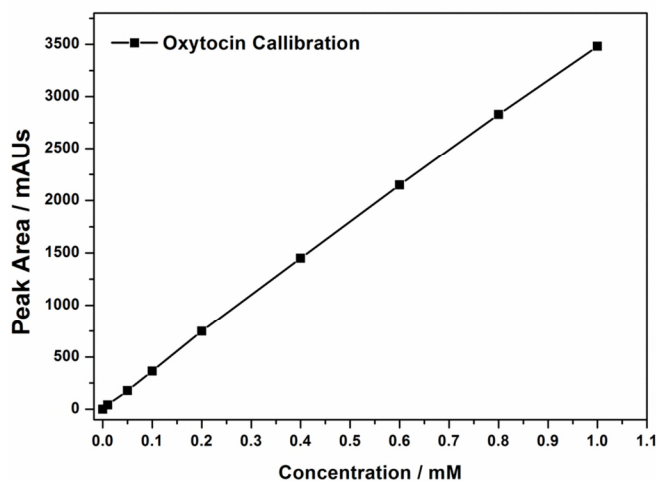


Figure 4.2. Calibration plot for different concentrations of oxytocin.

The degradation of oxytocin (1 mM) monitored after 24 hours storage at 80 °C revealed that oxytocin recovery was low ($19.2 \% \pm 1.10$), suggesting that under these conditions fast degradation of the peptide occurred (Figure 4.3). Similarly to the previously described 28 day (50 °C) study, different degradation peaks are evident, highlighting the highly unstable nature of this peptide.

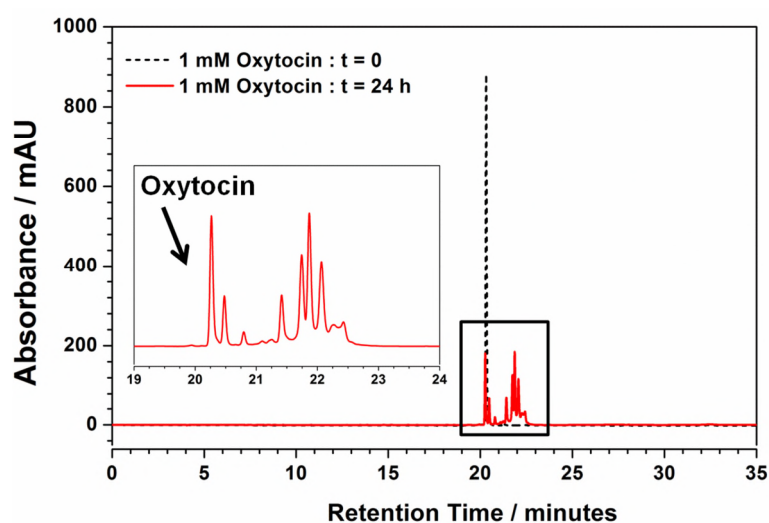


Figure 4.3. RP-HPLC chromatogram of oxytocin before and after thermal stressing at 80 °C.

4.1.3.2. *Small excipients for stabilisation: The effect of polyols and sugars on oxytocin degradation*

Some previously reported sugar and polyol excipients were prepared as 2 mM and 200 mM solutions and added to oxytocin (2 mM), resulting in total concentrations of 1 mM, with 1 x or 100 x molar equivalents of the excipients relative to oxytocin. The samples were then incubated for 24 hours at 80 °C, after which analysis by RP-HPLC (UV, λ = 280 nm) was performed to determine remaining oxytocin content. All samples were investigated in triplicate, with the average peak area for remaining oxytocin used to determine the % of the native peptide remaining (% recovery) (Figure 4.4).

Table 4.1. Thermal stability study (80 °C, 24 h) of oxytocin (assessed in terms of retained % peak area of the peptide) on addition of various polyols and sugars as external additives.

Sample	Sample type	MW (Da)	% Recovery	% Recovery
			1 mM Oxy / Excipient	100 mM Excipient
Oxytocin	Peptide	1007	19.2 (\pm 1.10)	-
Glycerol	Polyol	92.1	16.6 (\pm 0.65)	16.5 (\pm 1.65)
Mannitol	Polyol	182.2	15.6 (\pm 0.14)	14.4 (\pm 0.43)
Sorbitol	Polyol	182.2	18.5 (\pm 0.30)	16.4 (\pm 0.29)
Glucose	Sugar	180.2	14.9 (\pm 0.088)	17.0 (\pm 1.11)
Lactose	Sugar	342.3	14.1 (\pm 0.55)	15.5 (\pm 0.095)
Maltose	Sugar	342.3	14.3 (\pm 1.08)	15.5 (\pm 0.31)
Trehalose	Sugar	342.3	14.3 (\pm 0.37)	13.3 (\pm 0.63)

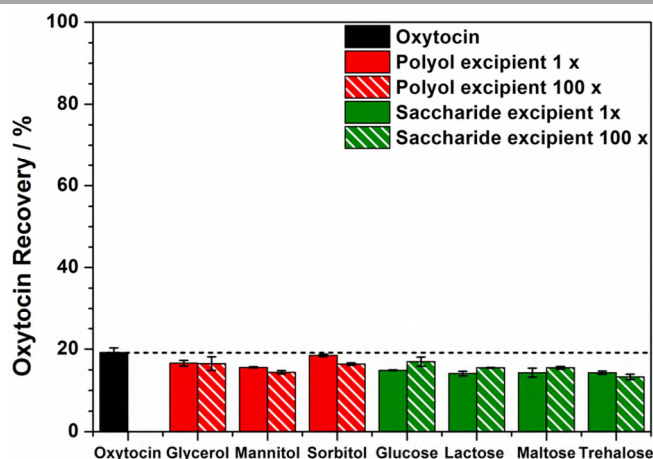


Figure 4.4. Thermally stressed stability of oxytocin in the presence of polyol and saccharide excipients at 1 and 100 molar equivalents at 80 °C for 24 hours.

The results of the stability study show that the use of these small excipients in peptide solutions at the concentrations investigated (1 mM / 100 mM) did not provide any additional stabilisation for oxytocin during thermal stressing. Degradation results in fact showed marginally less stability for the native peptide in all cases, theorised to be due to some small interactions with the peptide, allowing further degradation than for the untreated oxytocin sample.

4.1.3.3. Non-conjugated polymer influence on thermal stability: Non-covalently bound PEG

Polymers are also commonly utilised in peptide or protein therapeutic formulations, most often as solubilising excipients, but can also act to non-specifically provide stability *via* non-covalent interactions. A commonly used polymer in pharmaceutical formulations is poly(ethylene glycol) (PEG), usually accessed at a low molecular weight such as PEG-300 & PEG-400. Various linear PEGs are available commercially at a variety of different molecular weights, as well as containing a variety of different end groups. Some additional polymers to PEG are available which have also proven effective as conjugated or non-conjugated

additives include zwitterionic polymers,¹⁰ non-ionic amphipols^{11,12} and trehalose glycopolymers.^{13,14}

When investigating changes in stability of oxytocin by addition of linear PEG, as an external additive, the molecular weight of the PEG is likely to have an effect on the degradation of the peptide. This was investigated using the same thermal degradation study (80 °C, 24 h) as used for the polyols, where PEG molar masses were between 350 Da – 5 kDa. Firstly the effect of 1 x and 100 x equivalents of α -methoxy- ω -hydroxy PEGs were added to solutions of oxytocin and heated in an oven for 24 hours at 80 °C, and compared to the solutions without any external additives (Figure 4.5). The results showed that that upon the addition of molar masses of PEG above 1 kDa there is no effect on the stability of the peptide, where oxytocin recovery was similar, or equivalent to, when no PEG excipients were present in the solution. However, at low molar masses the PEG was shown to have some stabilising effect on the peptide with less degradation observed and oxytocin recovery levels of up to 44 % (more than twice the 19 % achieved for additive-free native oxytocin recovery). This is consistent with the previous use of low molecular weight PEG (such as PEG₄₀₀) as excipients of pharmaceutical solutions.

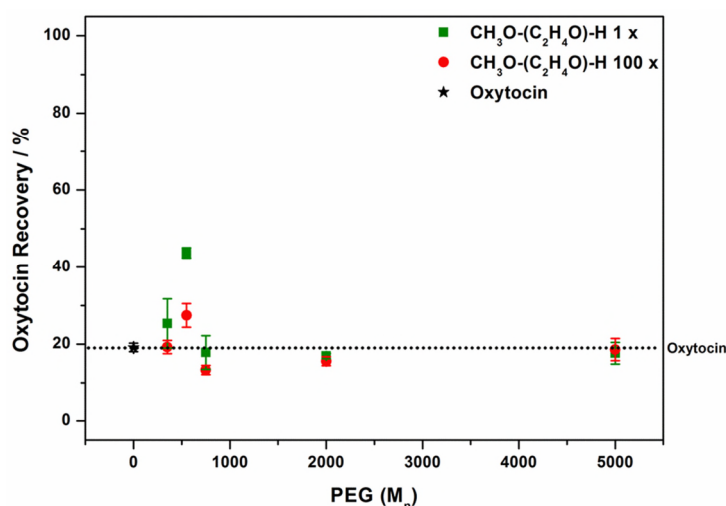


Figure 4.5. Evaluation of % of oxytocin remaining after 24 hours of thermal stressing (80 °C) containing different molecular weights of PEG.

To investigate in more detail the effect of the molecular weight of the PEG, the study was repeated but refocussed into investigating the effect of 'n', the number of ethylene glycol repeat units within each PEG chain $\text{CH}_3\text{O}-(\text{C}_2\text{H}_4\text{O})_n\text{-H}$ compared to the native peptide. Longer PEG chains have a higher number of repeat units in the polymer, increasing the size compared to oxytocin. E.g. it would require 9.5 times the amount of a PEG₅₅₀ ($n \approx 11.8$) to achieve the number 'n' of ethylene glycol repeat units as that of PEG₅₀₀₀ ($n \approx 112.8$). The heat stressed thermal stability assay was therefore performed with respect to the number of ethylene glycol repeat units (figure 4.6).

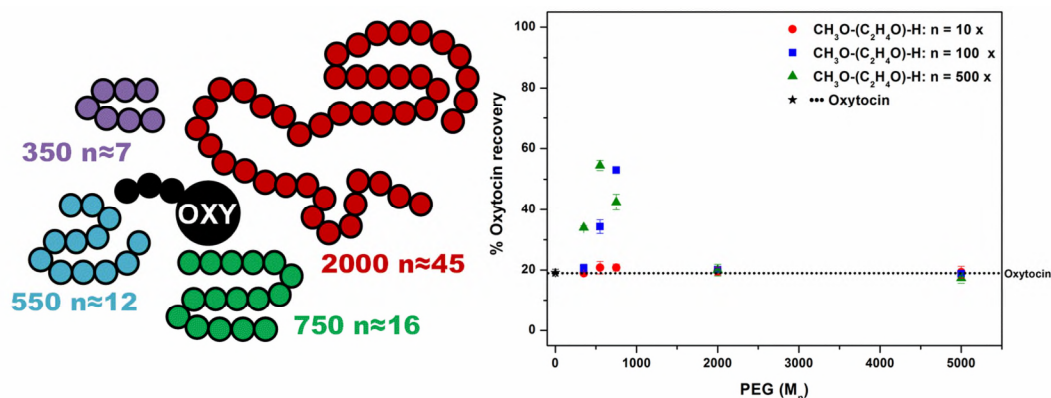


Figure 4.6. Evaluation of % of oxytocin remaining after 24 hours of thermal stressing (80 °C) containing different molecular weights of PEG after taking 'n' into consideration.

The results show that, as observed previously there is no effect on the stability of the peptide by using higher molecular weight PEG (> 1 kDa) as an external additive for oxytocin, however, the effect of low molecular weight PEG on the stability of the peptide is more interesting. At low 'n' ($n = 10$), where there are only a small number of ethylene glycol units per peptide, there is no observed effect on the stability of the peptide, with oxytocin recovery remaining low.

Contrastingly, when 'n' is increased 10- or 50- fold, within these small MW PEGs, the stability of the peptide greatly increases upon thermally stressed storage. In this study, up

to 55 % oxytocin recovery can be attained for PEG₅₅₀ and PEG₇₅₀ upon carefully tuning the amount of PEG added to the peptide solution. This is a stability improvement of almost 3 times that observed for solutions containing no external additives, and highlights the potential of low molar mass PEGs for use in this manner. This is in agreement with the non-conjugated low molar mass PEGs that are used widely within the pharmaceutical industry, but have not yet been applied to improve the stability of this important therapeutic peptide.

These results suggest that there is scope for the use of PEG as an external non-conjugated excipient for oxytocin, with increases in stability observed of more than double that observed for the native peptide alone. More than 50 % recovery can be established for the peptide by the addition of commercially available, inexpensive small polymer additives. The use of polymer excipients in solutions of oxytocin could also be advantageous in that any loss of activity by covalent attachment to the peptide could be prevented. Although these results seem promising, the degradation of the peptide is still evident in all samples, highlighting the need to optimise improvement, further minimising the degradation.

4.1.4. Degradation study on different architectures of oxytocin – PEG conjugates

It was hypothesised that the conjugation of linear and polyPEGs onto oxytocin would improve the thermal stability of the peptide, leading to a decrease in the previously reported degradation (and an increase in the peptide conjugate recovery). The PEGylated oxytocin conjugates synthesised in chapters 2 and 3 were subjected to the same high temperature stability assay and were compared to their non-conjugated counterparts. The thermal stability should highlight the effect that PEG architecture and conjugation position / linkage functionality would have on improvements to stability.

The high thermally stressed conjugate studies were carried out in the same manner as for the excipient (non-conjugated studies), with analysis of stability carried out after 24 hours of heating at 80 °C. For each conjugate a calibration plot was first prepared, so that the concentrations of the remaining conjugates could be calculated in a similar manner to oxytocin. For the majority of the linear conjugates the starting concentration was maintained at 1 mM and for the polyPEG conjugates the concentrations for the thermal stability assay varied between 0.05 and 0.25 mM. Calibration plots were constructed for each conjugate to reflect this (figure 4.7).

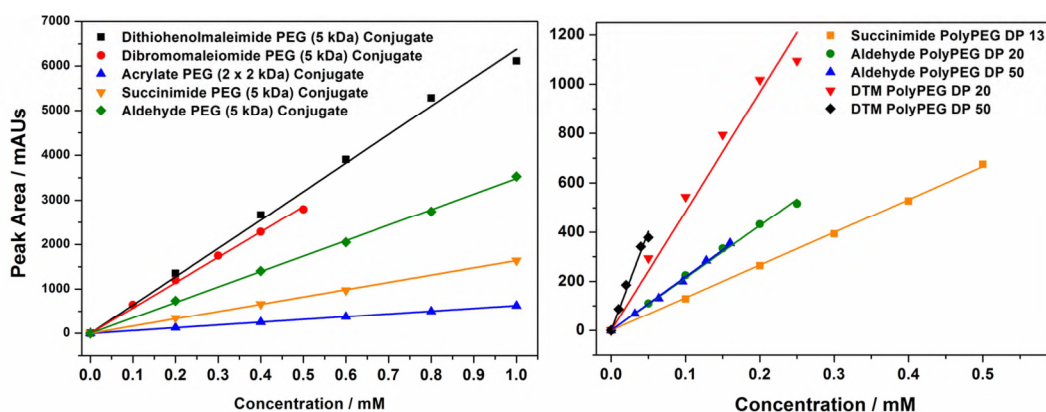


Figure 4.7. Calibration plots of peak areas from RP-HPLC for linear and polyPEG conjugates at concentrations used for thermally stressed stability testing.

The calibration plots also reveal useful information about the molar absorbance of the different conjugates under the RP-HPLC wavelength ($\lambda = 280$ nm), using the peak area (mAU) from the chromatograms. As expected, the maleimide polymers have the highest absorbance of all the linear and polyPEGs. The polyPEGs, in general, have a much lower absorbance than their linear counterparts, but the molecular weights of these are generally higher, therefore the groups with high absorbance's become diluted within the polymers.

4.1.4.1. Stability of linear oxytocin –PEG conjugates

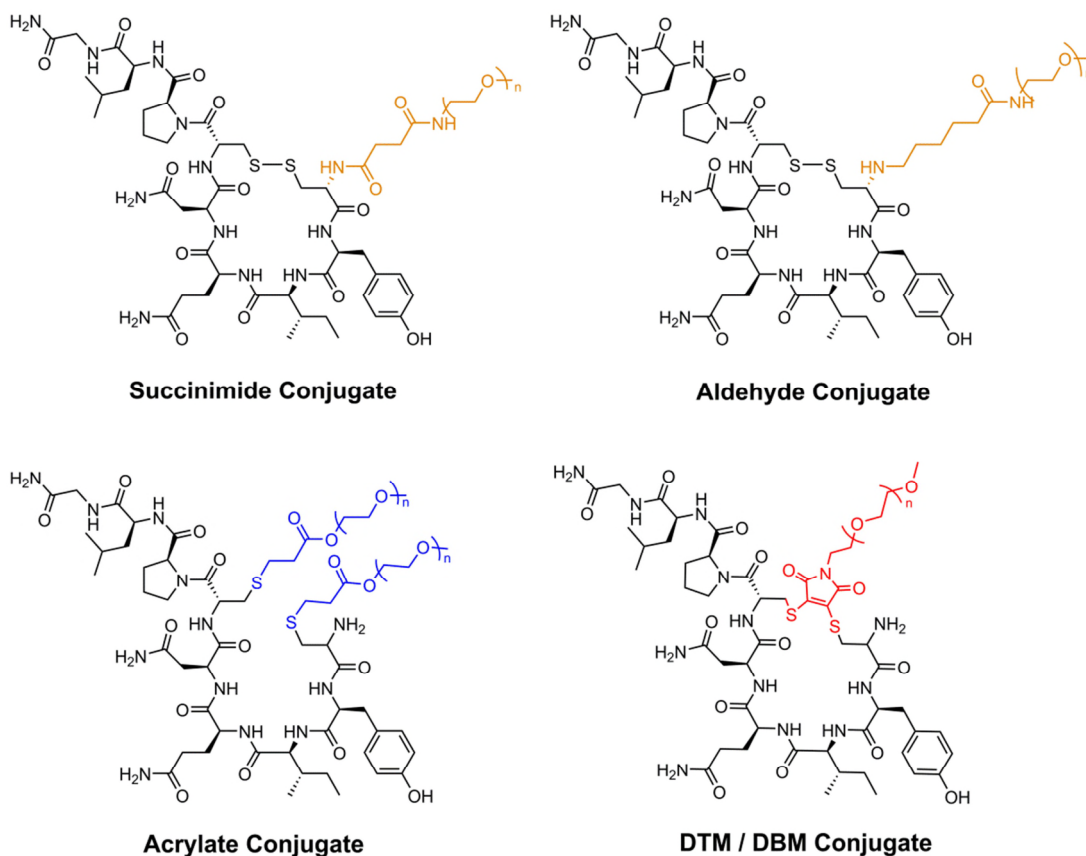


Figure 4.8. Structures of linear PEGylated oxytocin

The linear polymers characterised by this study were investigated using the same molar mass (5 kDa polymer: 6 kDa conjugate) so that comparisons could be made between the different conjugation positions, or conjugation linkage chemistries. The results of the degradation of the linear conjugates under these high temperature conditions show that all of conjugates have a much greater stability (2.5 times to 5 times) compared to that observed for the native peptide under the same conditions. Figure 4.9 shows the stability results for all the linear 6 kDa PEGylated oxytocin conjugates, using 5 different conjugating groups, additional to the previously mentioned 5 kDa PEG additive, which showed no stabilising behaviour.

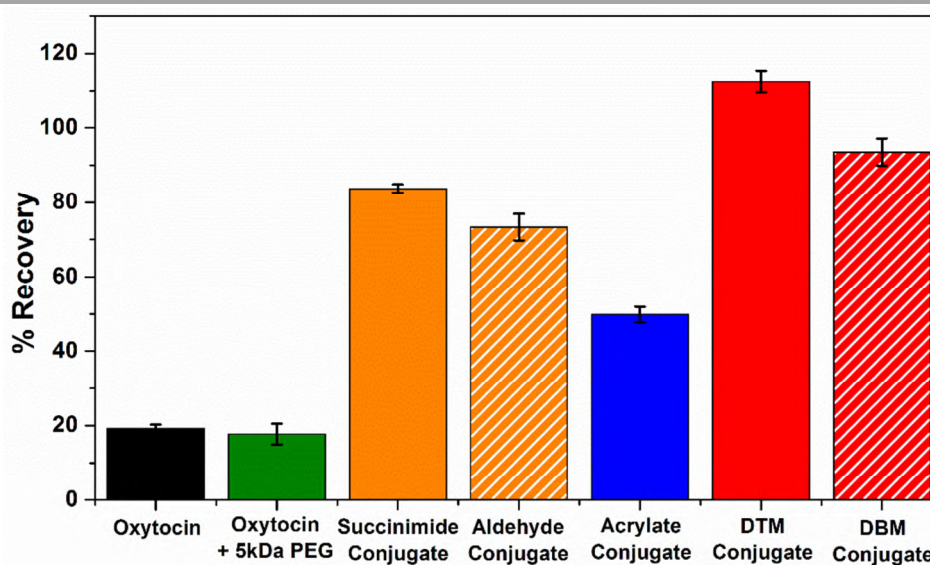


Figure 4.9. Stability results for all linear PEGylated conjugates (6 kDa) compared to native oxytocin and the peptide solution containing 5 kDa PEG as a non-conjugated additive.

The worst performing conjugate that least improved the stability was the thioether conjugate, arising from the double thiol functionalisation of oxytocin using mPEG_{A2000}. This conjugation approach involves the addition of two polymer chains onto oxytocin concurrently, preventing reformation of the 20 membered ring/ cyclic structure. This fundamental change of structure of the native peptide occurs at a position that has already been established as vital in ensuring degradation is kept to a minimum. The disulfide bond is where a large proportion of the degradation products arise; usually occurring as an increase to the ring size or total loss of the ring structure (these include tri/tetrasulfide formation and the formation of oxytocin dimers or larger aggregates). It should, however, be noted with regards to this conjugate that, although this may be the least stable of these linear PEG conjugates it still exhibits a 2.5 times increase in stability compared to the native peptide. This is higher than the majority of stabilising effects observed with the unconjugated polymer additives.

The two *N*-terminally targeted linear conjugates (NHS PEG resulting in amide linked conjugate, and aldehyde PEG resulting in 2° amine linked conjugate) have similar

stabilities, with between 70 -85 % of the conjugate remaining in the native form after 24 hours at 80 °C. This is a prominent increase in stability (3.5 to 4 times that observed for the native peptide), and from the RP-HPLC chromatograms it is clearly evident that there is a decrease in the observed degradation products (figure 4.10).

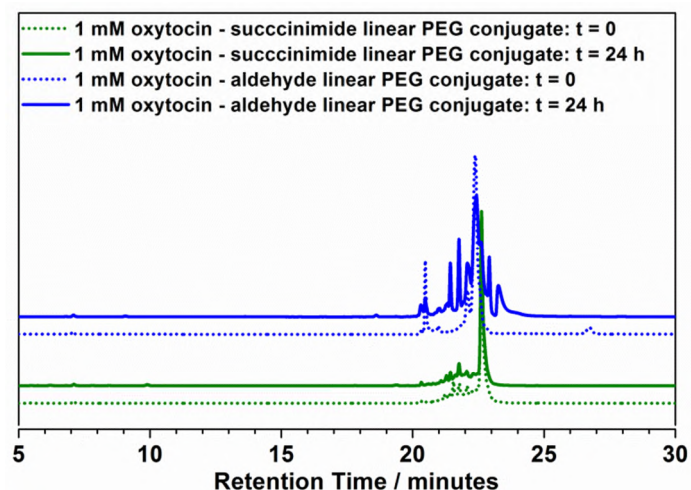


Figure 4.10. RP-HPLC chromatograms of succinimide and aldehyde oxytocin polymer conjugates (6 kDa) after 24 hours of storage at 80 °C.

The two maleimide disulfide bridged conjugates (which have the same conjugate structure post-conjugation) showed the highest stability under this study, with recovery remaining close to 100 %. This is, similarly to the other disulfide bond targeted approach, likely due to suppression of the normally observed degradation products resulting from the disulfide bond. However, in this case the maleimide linkage is adding additional stability to the peptide structure in this position by the addition of a three carbon bridged linkage. This prevents the disulfide bond from breaking, preventing the degradation into the normally observed degradation products, as the 22 membered ring has a higher stability at the Cys¹-Cys⁶ bridging position.

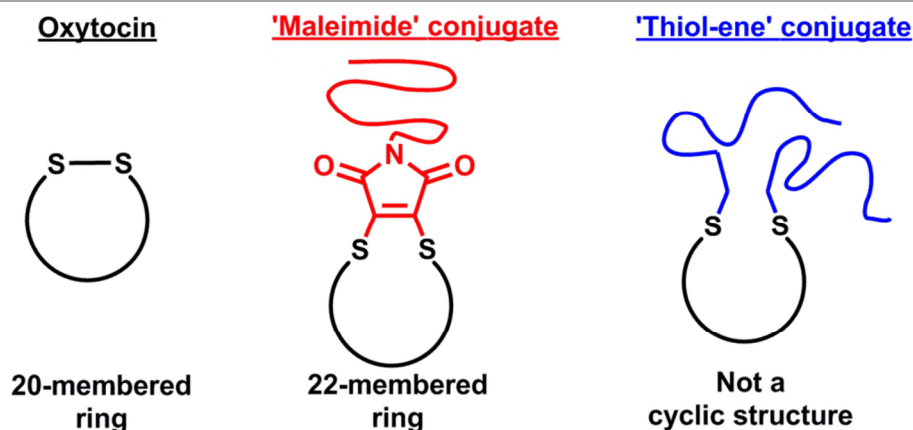


Figure 4.11. Diagrams showing different structures of disulfide conjugated polymers and influence on cyclic ring size within oxytocin.

Table 4.2. Results of thermal degradation study for linear oxytocin-polymer conjugates (6 kDa) after 24 hours storage at 80 °C compared to oxytocin, and non-conjugated PEG (5kDa).

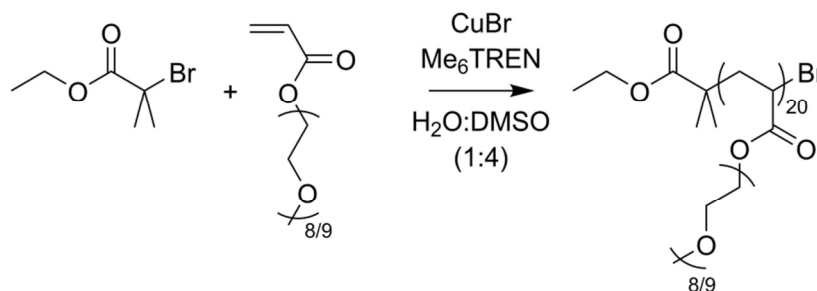
Sample	Sample type	MW (Da)	Conc (mM)	% Recovery
Oxytocin	Peptide	1007	1.0	19.2 (± 1.10)
mPEG 5kDa	Unconjugated linear PEG	5000	1.0	17.7 (± 2.78)
Linear Succinimide	Amide linked linear PEG	6000	1.0	83.7 (± 1.11)
Linear Aldehyde	Secondary amine linked linear PEG	6000	1.0	73.3 (± 3.55)
Linear Acrylate	Thioether linked linear PEG	6000	1.0	49.8 (± 2.08)
Dithiophenolmaleimide	Maleimide linked linear PEG	6000	1.0	112.5 (± 2.92)
Dibromomaleimide	Maleimide linked linear PEG	6000	0.5	93.5 (± 3.65)

Values above 100 % are likely due to concentration errors, arising from the high temperature used for the thermal degradation testing, and the method of data analysis. It is theorised that the degradation of these samples remains minimal, allowing approximately 100 % of conjugate recovery.

4.1.4.2. Stability of polyPEGylated oxytocin

Prior to investigating the stability of the oxytocin polyPEG conjugates under the same thermally accelerated conditions, a non-conjugating polyPEG was synthesised as a comparison. This would be analogous to the linear PEG additives in comparison to the linear PEG conjugates, to discount the effects of non-covalent interactions. This is also important as several of the conjugates contained excess PEG impurities in the solutions, and would highlight the effect that these might have.

Poly(mPEGA₄₈₀) was synthesised by Cu(0)-mediated living radical polymerisation, using ethyl α -bromoisobutyrate (EBiB) as the initiator ([I]:[M]:[Me₆Tren]:[CuBr] = 1:20:0.4:0.4) (scheme 4.1). Cu(I)Br was allowed to disproportionate in water (1 ml) after which EBiB and mPEGA₄₈₀ were added in a solution of DMSO (6 ml) and water (1 ml). After 24 hours samples were removed for ¹H NMR (δ_6 -DMSO; 94 % conversion) and SEC molecular weight (DMF; M_n = 12300, Đ = 1.06) analysis (figure 4.12).



Scheme 4.1. Copper mediated polymerisation of mPEGA₄₈₀ with EBiB initiator in DMSO/H₂O (4:1) ([I]:[CuBr]:[Me₆TREN] = 1:0.4:0.4).

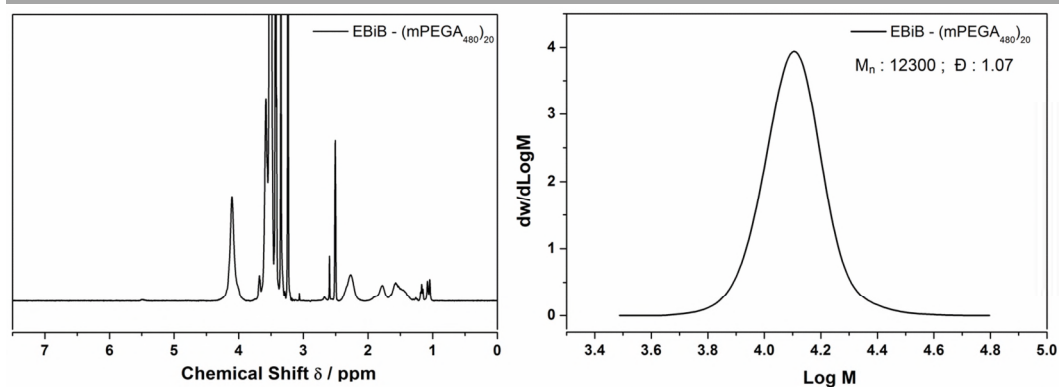


Figure 4.12. NMR and GPC of EBiB initiated polymer used as a non-conjugating polyPEG additive in heat stability testing of oxytocin at 80 °C.

Following purification (dialysis against water, 3.5 kDa MWCO, 3 days), the polymer was added to a solution of oxytocin as 1:1 molar equivalents and heated for 24 hours at 80 °C. Under the conditions of the stability assay, RP-HPLC of oxytocin solutions containing the Poly(mPEGA₄₈₀) additive revealed a small improvement (1.7 times) in the level of remaining oxytocin present in solution after 24 hours. From the RP-HPLC chromatogram the suppression of degradation products appearing at 21-24 minutes retention time is clear in the sample containing the polyPEG additive (figure 4.13). This highlights that the polyPEGs can, without covalent binding to the peptide, exhibit a small amount of protection compared to solutions of oxytocin containing no such additive in the solution. As this polymer was synthesised as 20 repeat units of a small (< 500 Da) PEG monomer, the stability study was also undertaken for oxytocin containing 20 equivalents of a small linear methoxy PEG (350 Da). This, however, revealed no stabilising effect with oxytocin recovery remaining similar to the native peptide containing no excipients (within 1 %).

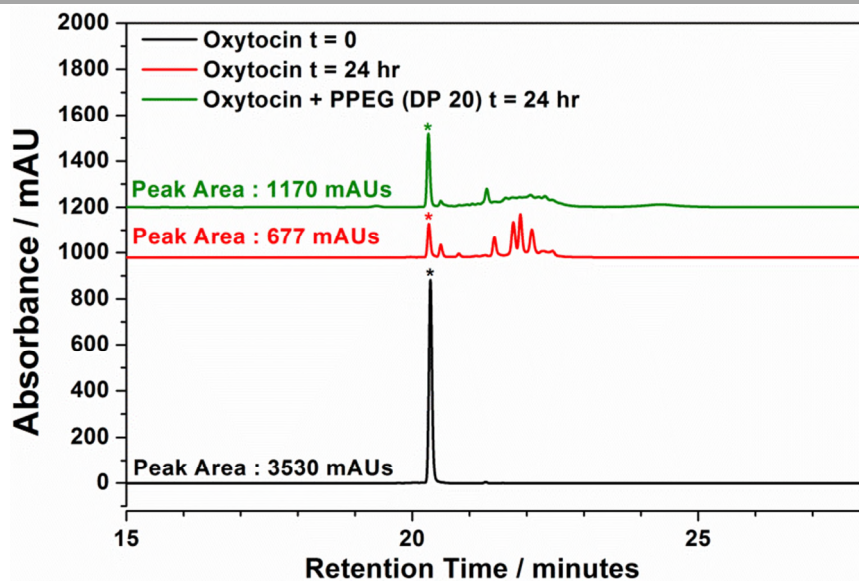


Figure 4.13. RP-HPLC traces of oxytocin at $t = 0$, oxytocin after 80 °C storage ($t = 0$) and oxytocin after 80 °C storage with addition of a polyPEG additive.

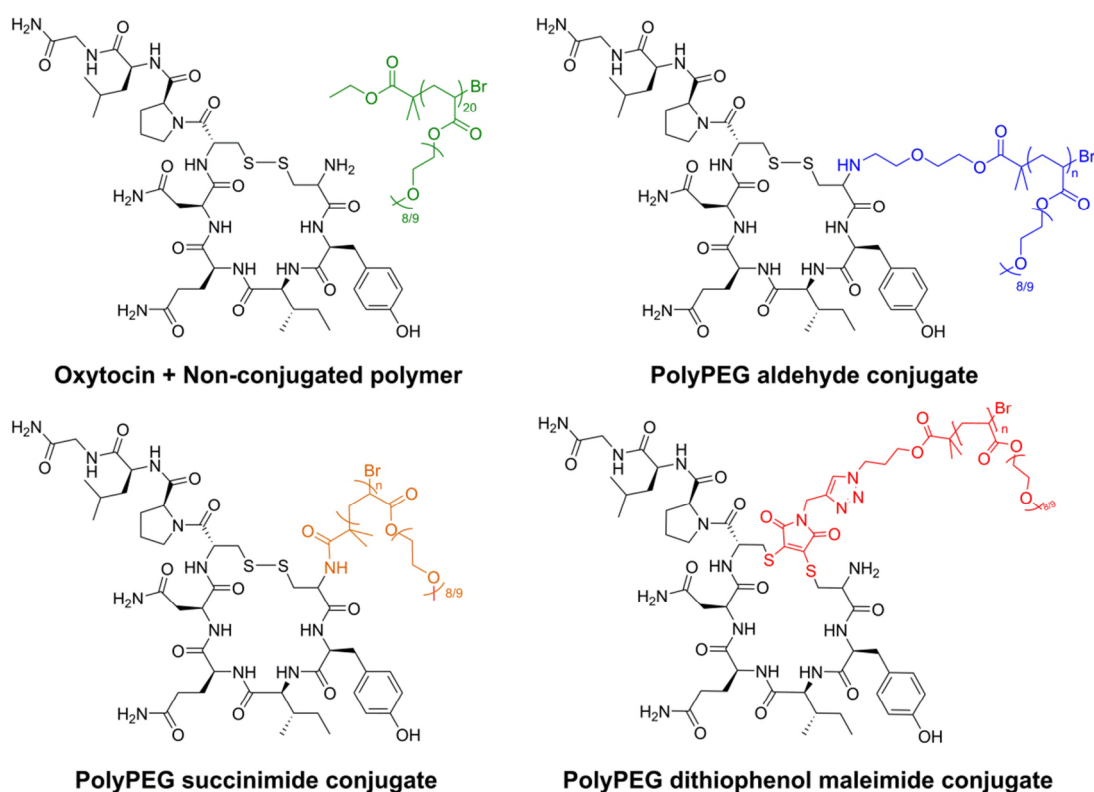


Figure 4.14. Structures of polyPEG oxytocin conjugates, and oxytocin with non-conjugated polymer.

When the polyPEG conjugates (figure 4.14) were subjected to the same stability assay as the non-covalent additives and the linear conjugates, all showed high increases in stability compared to native oxytocin. The product return for the majority of samples was close to 100 %, which is much higher than the stability monitored on addition of any of the external excipients (figure 4.15).

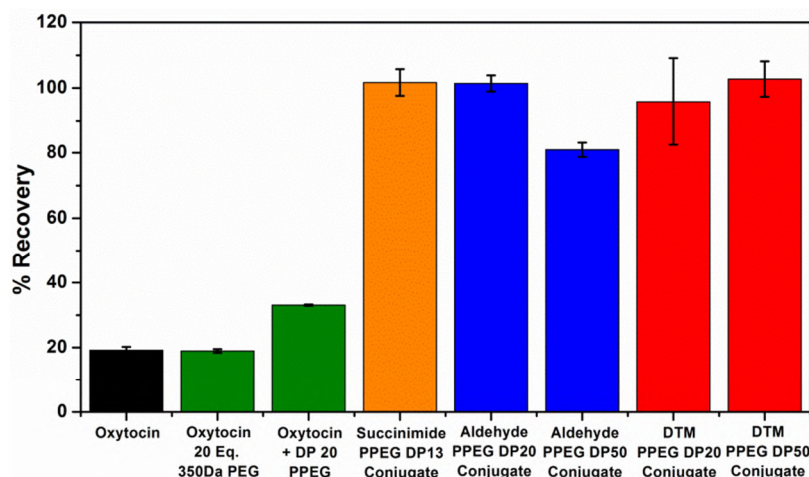


Figure 4.15. Stability results for all polyPEGylated conjugates compared to native oxytocin and the peptide solution containing 20 Eq. 350 Da PEG, and DP_n 20 polyPEG as a non-conjugated additive.

Due to the high stability measured under these conditions it is challenging to recognise if there are differences between the two different conjugation positions (N -terminal, or Cys¹-Cys⁶ disulfide bond) with respect to improved stability (table 4.3). The polyPEG conjugate with the lowest observed stability maintained 81 % of the conjugate structure, which still shows a significant conjugate return, compared to that of the native peptide. The RP-HPLC traces shown in figure 4.16 highlight this, where there is the observation of a small amount of degradation peaks, after 80 °C storage for 24 hours, at a similar retention time to those observed after degradation of the native peptide (between 21 – 24 minutes). The main conjugate peaks are the same shape and size, and appear at similar retention time to the $t = 0$ samples, suggesting that little degradation has occurred.

Chapter 4 – PEGylated oxytocin: Effects of PEGylation on activity and stability

Table 4.3. Results of thermal degradation study for oxytocin-polyPEG conjugates after 24 hours storage at 80 °C, compared to relevant non-conjugated polymers.

Sample	Sample type	MW (Da)	Conc (mM)	% Recovery
Oxytocin	Peptide	1007	1.0	19.2 (± 1.10)
mPEG 350 kDa (20 eq)	Unconjugated linear PEG	350	1.0	19.0 (± 0.56)
PPEG DP_n 20	Non-conjugated polyPEG	10000	1.0	33.1 (± 0.21)
Succinimide PPEG DP_n 13	Amide linked polyPEG conjugate	7500	0.25	101.7 (± 4.06)
Aldehyde PPEG DP_n 20	Secondary amine linked polyPEG	11000	0.25	101.4 (± 2.44)
Aldehyde PPEG DP_n 50	Secondary amine linked polyPEG	25000	0.16	80.9 (± 2.19)
Dithiophenolmaleimide PPEG DP_n 20	Maleimide linked polyPEG	11000	0.25	95.79 (± 13.33)
Dithiophenolmaleimide PPEG DP_n 50	Maleimide linked polyPEG	25000	0.05	102.76 (± 5.40)

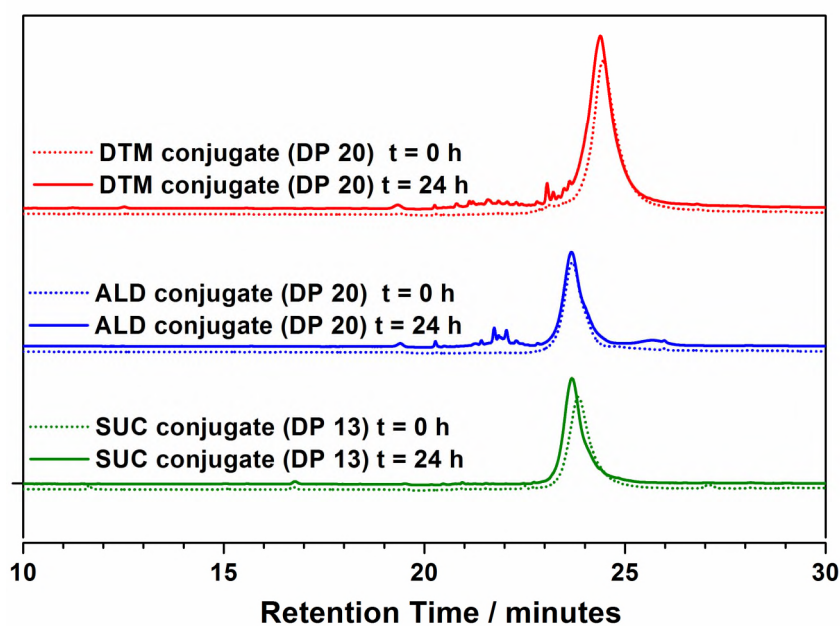


Figure 4.16. HPLC traces of degradation of oxytocin polyPEG conjugates (80 °C, 24h, 25 mM)

4.1.4.3. Additional oxytocin conjugate stability testing

In addition to the high temperature thermally stressed stability assay, additional stability testing was carried out on the polyPEG maleimide bridged conjugates, monitoring the degradation across 28 days (50 °C, 1 mg ml⁻¹) (figure 4.17). Following the degradation at more applicable temperature across several time points gives a more appropriate idea of how the conjugates degrade and how this might compare to the native peptide in a tropical climate. Aliquots of the samples were removed periodically and monitored by RP-HPLC for analysis of remaining concentration of polymer conjugate, in comparison to that observed at t = 0. The largest and smallest polymer conjugates were tested (11 kDa & 50 kDa) to investigate whether the molecular weight had any effects on enhanced stability.

This study found that, as observed after high thermal stressing, the degradation was largely suppressed by the conjugation of dithiophenolmaleimide polymers across the double bond of oxytocin. The amount of oxytocin previously observed to remain after 28 days at 50 °C was 2.5 %, whereas for the polymer conjugates it was 93.5 % and 86.5 % (oxytocin-(mPEGA₄₈₀)₂₀ and oxytocin-(mPEGA₄₈₀)₁₀₀ respectively). The major peaks observed for the conjugates after 28 days coincide with the conjugate peaks observed at t = 0. The minor peaks observed can be attributed to oxytocin or oxytocin degradation products, suggesting very slight instability in the conjugation. The RP-HPLC traces of the conjugate products at t = 0 and t = 28 days show that the major peak remains in the same place, and that peak shape also does not change. This is important in determining that polymer conjugate degradation is not occurring, rather than if degradation products were appearing at a similar retention time.

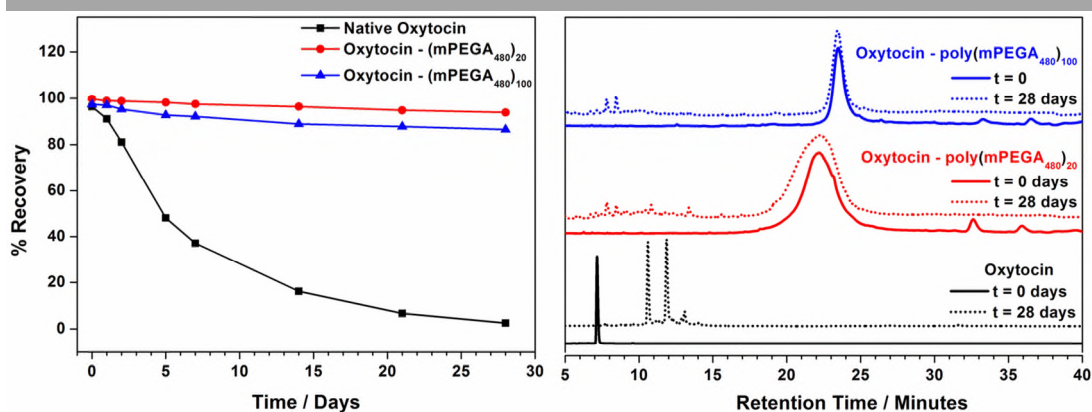


Figure 4.17. Stability of oxytocin polymer conjugates at 50 °C across 28 days.

4.1.5. Stability testing conclusions

The investigation of the thermal stability of the oxytocin conjugated PEG (both linear and polyPEG) shows that polymer conjugation has a strong influence on the stability/degradation properties of oxytocin. Non-conjugated polymers, and small molecules added as external excipients, do not have any strong stability increasing effects, particularly for the larger linear PEGs and all sugars/polyols. There is a potential stabilising effect observed for high concentrations of small PEGs, and upon the addition of non-covalently bound polyPEG, but these are minimal compared to most of the oxytocin-polymer conjugates. These results show that polyPEGs have the highest stability enhancing effect on oxytocin, both conjugated at the disulfide bond and *via* the *N*-terminal amine, where all stabilities were improved by 4 - 5 X that observed for the native peptide. Overall, these results suggest that the PEGylation of oxytocin has high potential benefits with respect to increasing the solution thermal stability.

4.2. Uterotonic Experiments

4.2.1. Introduction

The primary use of oxytocin is for the induction of uterine cell contraction, particularly in relation to pregnancy, either for labour induction, or for prevention of post-partum haemorrhaging (PPH).^{15,16} Therefore, the main analysis measurement used to investigate the retained activity of oxytocin analogues, such as the oxytocin-polymer conjugates synthesised in previous chapters, should be in investigating the level of uterotonic contraction induced by the polymeric oxytocin analogues, and how this compares to the native peptide.

The mechanism by which oxytocin induces contractions within the cells arise from oxytocin binding into the oxytocin binding receptor, on the outside of the cell which activates the G-protein ($G_{\alpha q/11}$) inside the cell. $G_{\alpha q/11}$ causes activation of the voltage induced Ca^{2+} channel allowing Ca^{2+} to enter the cell, whilst also phosphorylating the enzyme phospholipase CB (PLC_{β}). PLC_{β} cleaves phosphatidylinositol 4,5-diphosphate (PIP_2) into diacyl glycerol (DAG) and inositol 1,4,5-triphosphate (IP_3). IP_3 induces the endoplasmic reticulum to release calcium, and is then recycled as free inositol. From DAG, free arachidonic acid (AA) is cleaved by the enzyme phospholipase A_2 (PLA_2), and then converted into prostaglandin $F_{2\alpha}$ by cyclooxygenase (COX_2). The calcium induced within or entering the cell binds to calmodulin, and this Ca^{2+} -calmodulin complex activates MLC Kinase. Together a combination of prostaglandin and MLC Kinase lead to cell contraction (figure 4.18).^{17,18}

The cell contraction mechanism is initially stimulated by the binding of oxytocin into the oxytocin binding receptor, which exists on the surface of many cells within the body (not solely within uterine tissue). Ile³, Gln⁴, Pro⁷ and Leu⁸ are important residues required on

oxytocin for binding into the oxytocin binding receptor, whilst Asn⁵ and Tyr² are important for the activation, which ultimately causes uterine contraction.^{1,19}

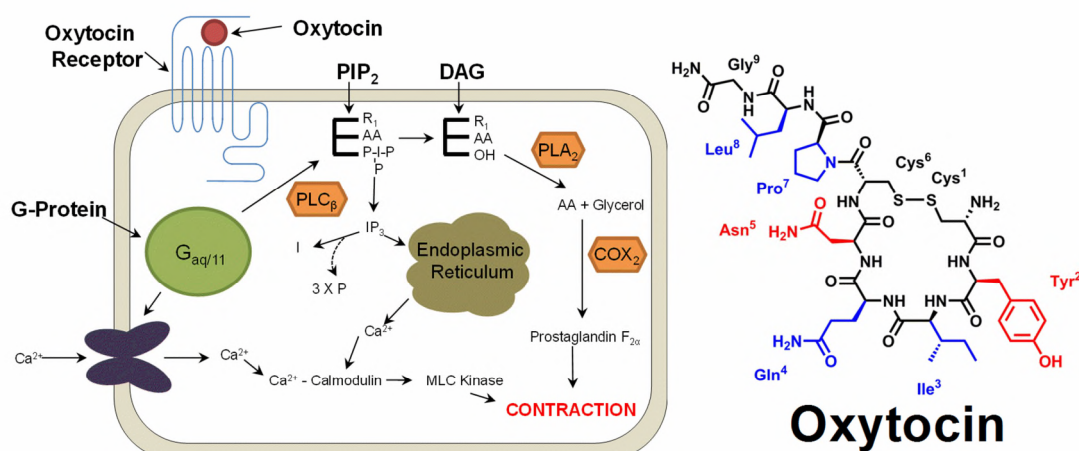


Figure 4.18. Oxytocin mechanism for stimulating contractions and structure of oxytocin highlighting important residues for contraction.

Previous biological evaluations assays, under which oxytocin or oxytocin analogues have been tested for uterotonic activity retention have been undertaken by evaluating the *ex-vivo* contractility of smooth muscle tissue.^{20–23}

In the second part of this chapter, initial uterotonic studies carried out on three different oxytocin-polymer conjugates will be investigated to probe the contractile behaviour compared to the native peptide.

4.2.2. Uterotonic testing of oxytocin polymer conjugates Vs. oxytocin.

The uterotonic studies on oxytocin and the oxytocin peptide conjugates were performed in an organ bath using a force transducer to accurately measure contractions. Tissue was freshly extracted from 3 week old Sprague-Dawley (SD) rats, and used as soon as possible after extraction, with a maximum viability of approximately 12 hours. After the uterine

tissue preparation (trimmed of any connective tissues, approx. 10 mm) was suspended in the organ bath a 10 mN force was applied. The samples were then allowed to rest for 60-90 minutes under constant flow of oxygenated (95% O₂ / 5% CO₂) Krebs buffer (120.0 mM NaCl, 5.9 mM KCl, 25.0 mM NaHCO₃, 1.2 mM NaH₂PO₄, 2.5 mM CaCl₂, 1.2 mM MgCl₂, and 5.5 mM glucose) until stable contractions were reached.

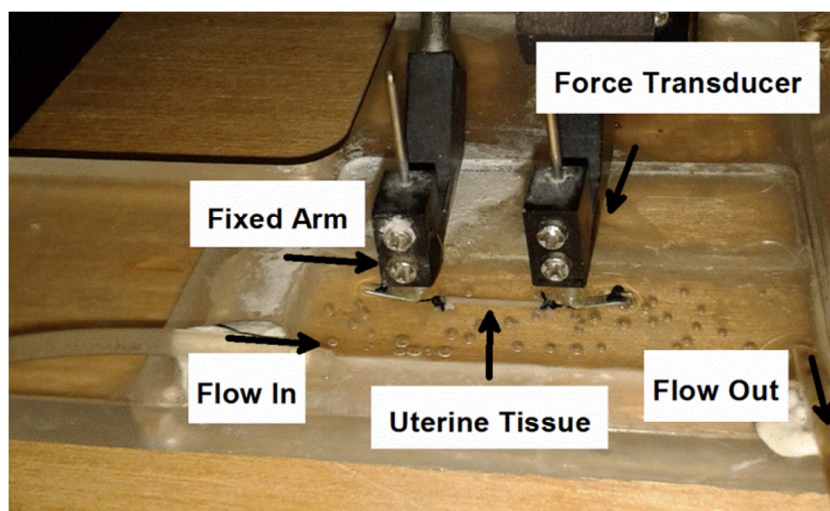


Figure 4.19. Experimental organ bath set-up.

For this particular uterine tissue, spontaneous contractions were evident throughout the study, and stimulated changes in these were monitored. After a stable baseline was achieved, a maximal contractile response was induced by applying HiK (20 mM KCl) to the tissue followed by a wash out with Krebs buffer for 20 minutes. Native oxytocin, oxytocin-polymer conjugate and respective polymers were applied to the same uterine sample (10 minutes) followed by wash outs (20 minutes), for which the order was changed each run and the tensions were constantly recorded. 10⁻⁶ M concentrations of polymer, peptide-polymer conjugate and native oxytocin were applied to uterine tissue extracted from 5 different rats. Using this set-up three of the different oxytocin-polymer conjugates were tested; linear aldehyde PEG –oxytocin conjugate (2 kDa), polyPEG aldehyde conjugate (DP_n 20) and polyPEG maleimide conjugate (DP_n 50).

4.2.2.1. Responses of oxytocin or conjugates upon spontaneous contractile behaviour

Due to the spontaneous nature of the contractions observed within the tissue, complete analysis of induction of contractions is challenging, particularly with the frequency and intensity of these baseline contractions. The highest intensity contractions are those observed upon stimulation with HiK, which causes an ion based mechanism which induces significant cell contractions. This is observed within the tissue as a period of very high frequency contractions, where the peaks are occurring too quickly to return to the baseline. This is used to confirm the viability of the tissue to cell contraction, and in some cases can be used as the maximum contractile response, from which agonists can be compared. Upon addition of oxytocin (10^{-6} M) to the organ bath set-up, it is still relatively easy to observe that this causes a high contractile effect upon the tissue, in terms of frequency and amplitude compared to baseline contractions (figure 4.20).

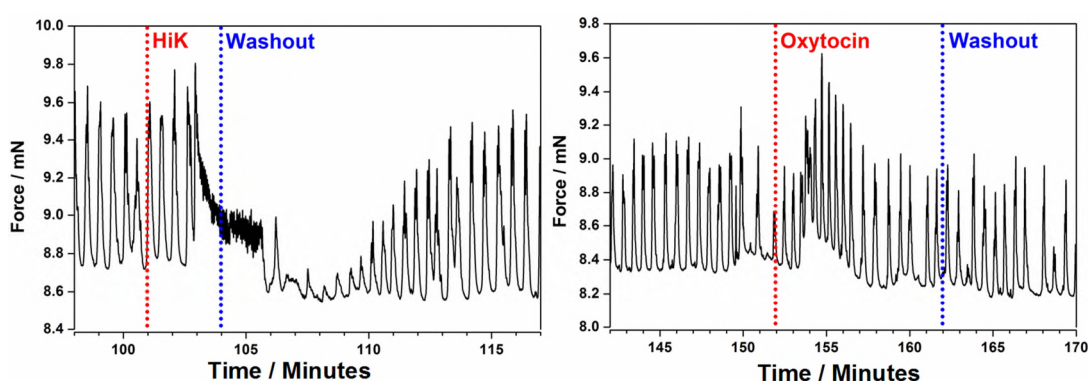


Figure 4.20. Example pictures of HiK and oxytocin induced response in uterine tissue showing effect on spontaneous contractions.

The effect of both of these 'effective' contraction agents can be washed out leading to the return of spontaneous contractions with similar characteristics to before the stimulation was induced. A few minutes after initial onset of contractile behaviour caused by oxytocin

evocation, the contractions become less intense, even before washout had begun, which is theorised to be due to tissue fatigue.

The same observations cannot be made for the conjugate samples, whereby it becomes much more difficult to observe a change in the spontaneous baseline contractions (figure 4.21). It was, however, initially expected that the conjugation of polymers would reduce the oxytocin contraction effect to some degree.

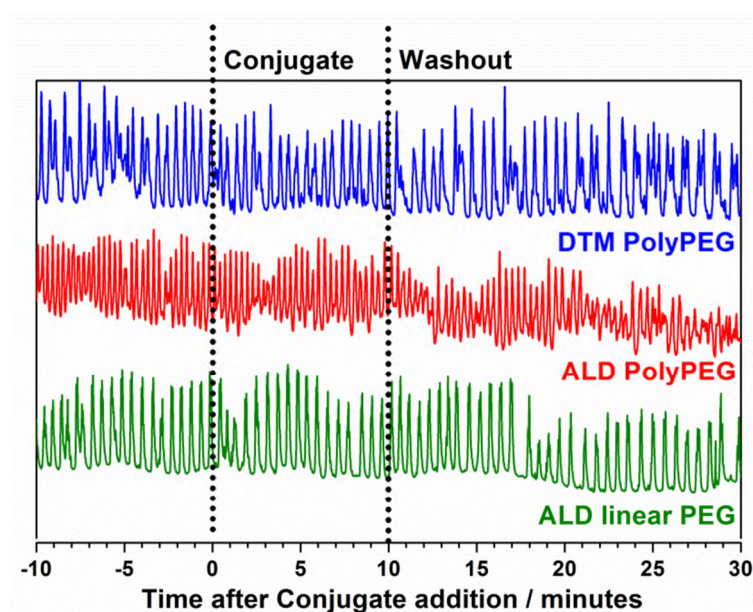


Figure 4.21. Example uterotonic traces for linear aldehyde, polyPEG aldehyde and polyPEG dithiophenolmaleimide conjugates.

This is particularly prominent on observation of a whole tissue run (figure 4.22), where the HiK is observed as the highest contractile response, followed by the oxytocin, with little difference on addition of the conjugate. This could potentially be highlighting that uterotonic activity is severely suppressed by the conjugation of polymers, but further analysis of each contraction is required to make conclusions.

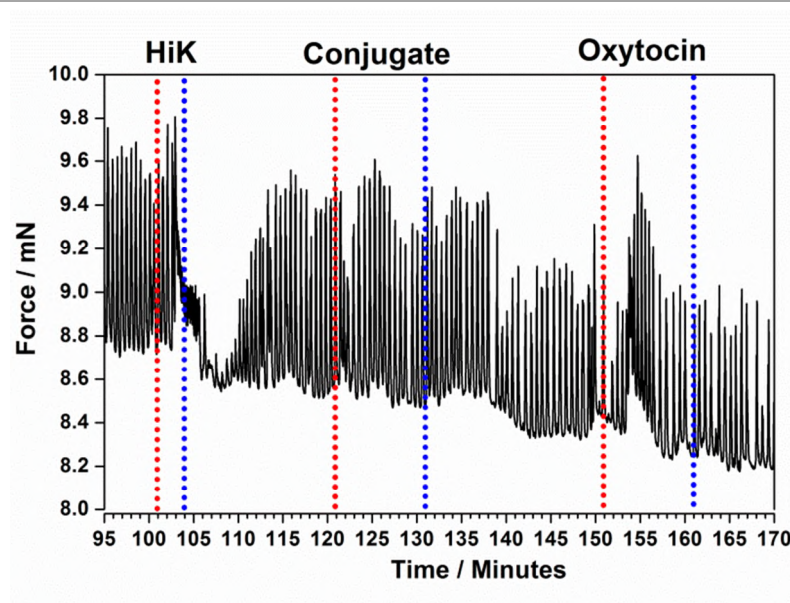


Figure 4.22. Observation of contractile responses for linear aldehyde PEG conjugate monitoring the effect of HiK, oxytocin and conjugate upon spontaneous contractions.

4.2.2.2. Analysis of results of uterotonic testing

For analysis of the effect of each of the conjugates in comparison to oxytocin (using a tissue repeat of $n = 5$) the contractile peaks (from baseline contractions and induced contractions) were monitored across the studies. At each 2 minute interval, contractions were monitored following amplitude, integration, duration and frequency to establish whether there were changes compared to the normal baseline contractions. All peak analysis was carried out with respect to 2 control peaks of the baseline contractions before addition of the samples. After analysis of the data, the most relevant time points were plotted for comparison of the native peptide compared to the oxytocin polymer conjugate (figure 4.23).

Upon analysis of the data from the linear aldehyde oxytocin PEG conjugate, it is clear that oxytocin has a large effect on the amplitude and integration of contractions, with high observed increases after 4 minutes. This effect then dissipates, with smaller contractions

than the baseline response at 10 minutes. The non-conjugated polymer does not show any effect on the baseline contractions, with results remaining within 15 % of the amplitude and integration of the control peaks. The PEGylated oxytocin shows some suppression of spontaneous contractions, particularly after a longer exposure time to the sample (4 minutes: 0.73 X amplitude, 0.75 X integration, 10 minutes: 0.58 X amplitude, 0.50 X integration). There are not notable changes to the frequency and duration of contractions of the polymer or conjugate compared to the baseline control; however, oxytocin does show a slight increase in the time between contractions after 10 minutes. This, alongside the small reduction in integration and amplitude at this time point, is likely due to tissue fatigue, where the oxytocic response causes large contractions initially, before dissipating after extended exposure.

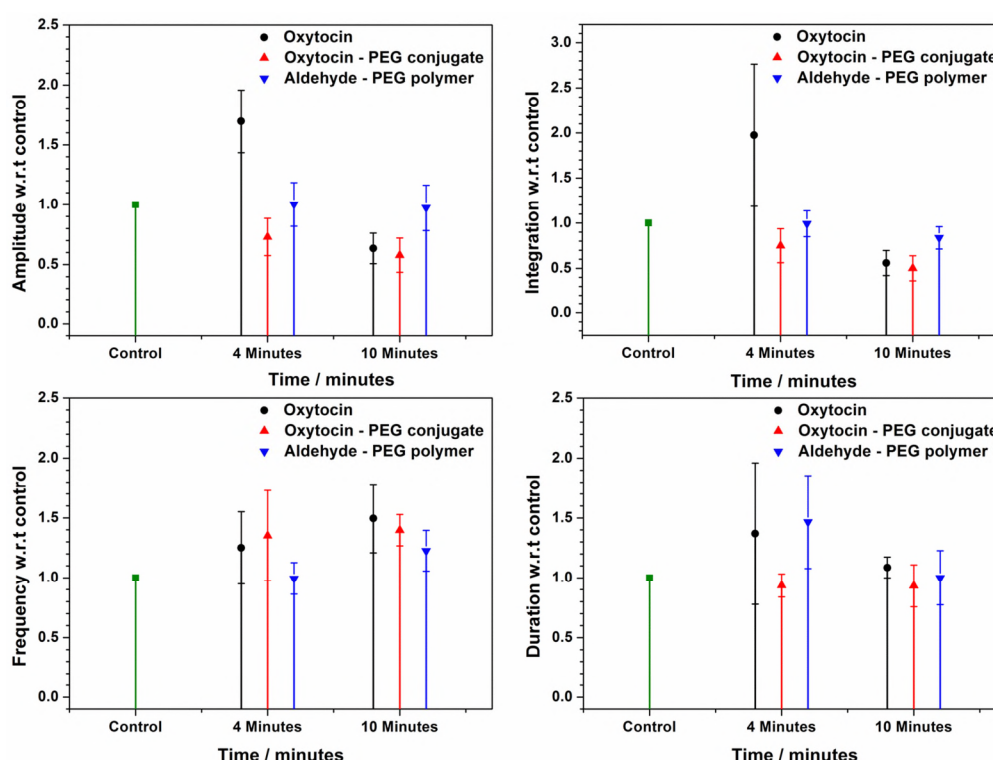


Figure 4.23. Contractile peak response analysis of data for linear aldehyde PEG and oxytocin PEG conjugate with respect to amplitude, integration, frequency and duration.

Overall, for the linear aldehyde conjugate, there is no data that the conjugates are eliciting any contractile response from the tissue. It is likely that a high level of activity has been lost from peptide conjugation.

The data for the aldehyde polyPEG conjugate shows similar results to the linear conjugate, where there is very little observed difference between the polymer induced (conjugated and non-conjugated) and the baseline contractions with respect to amplitude, integration, duration and frequency (figure 4.24). It is still observed that oxytocin exhibits a higher contractile response, as expected for integration and amplitude data shortly after introduction to the tissue, and that the frequency of contractions appears to decrease after a longer exposure. The polymer conjugate potentially shows a higher contractile response (compared to the control contractions and those observed with the polymer) after 4 / 10 minutes, however, this is still below the maximum response observed for the native peptide. This points to some activity being maintained, but not to the level exhibited by the native peptide, and that a longer time is taken for the conjugate to elicit a response. This would likely be due to a longer time for the conjugate to bind into the receptor as, although the residues required for receptor binding were not changed, the addition of a large polymer onto the peptide would likely hinder the accessibility of these required positions to the receptor.

Overall for the polyPEG aldehyde conjugate, it is challenging to elucidate useful information about the level of retained activity of the conjugate compared to native polymer. Initial data suggests that it is likely activity is severely reduced; however, further investigation is required to confirm this.

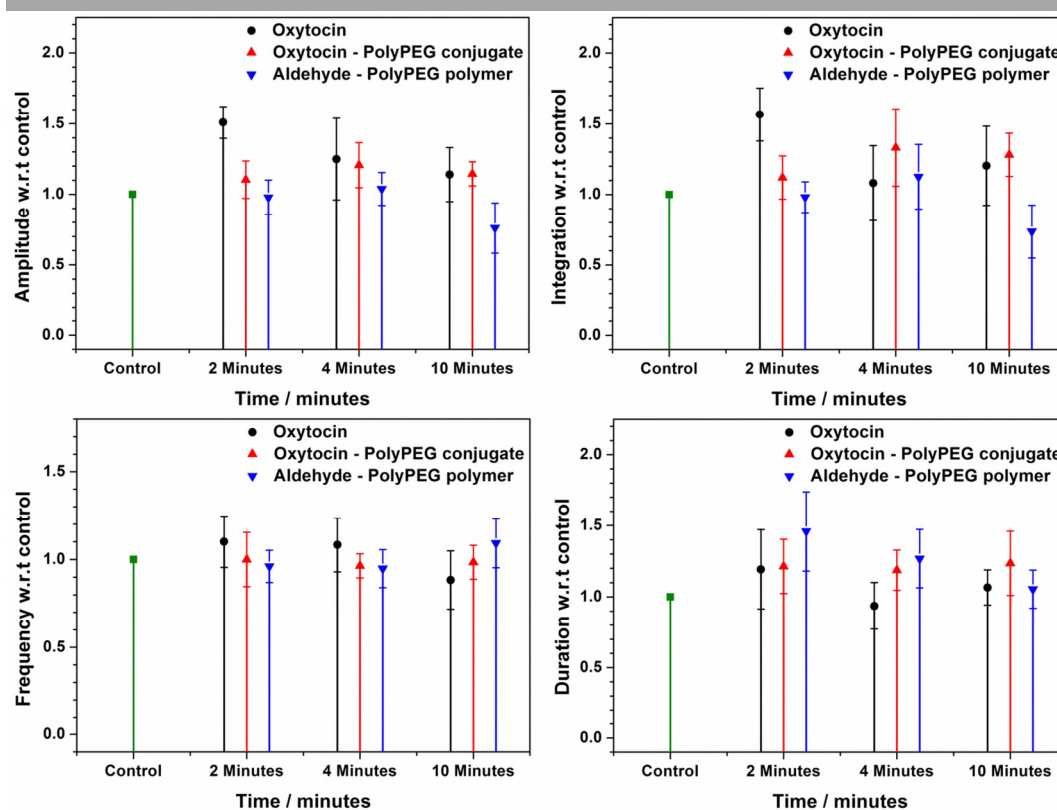


Figure 4.24. Contractile peak response analysis of data for aldehyde polyPEG and oxytocin polyPEG conjugate with respect to amplitude, integration, frequency and duration.

In the maleimide polyPEG sample the results are similar, with few differences between the polymer conjugate induced, polymer induced and control contractile responses (figure 4.25). This was the largest polymer conjugate evaluated, which has a 5-fold increase in molecular weight from the native peptide, which is highly likely to diminish the contractile activity observed for the cells.

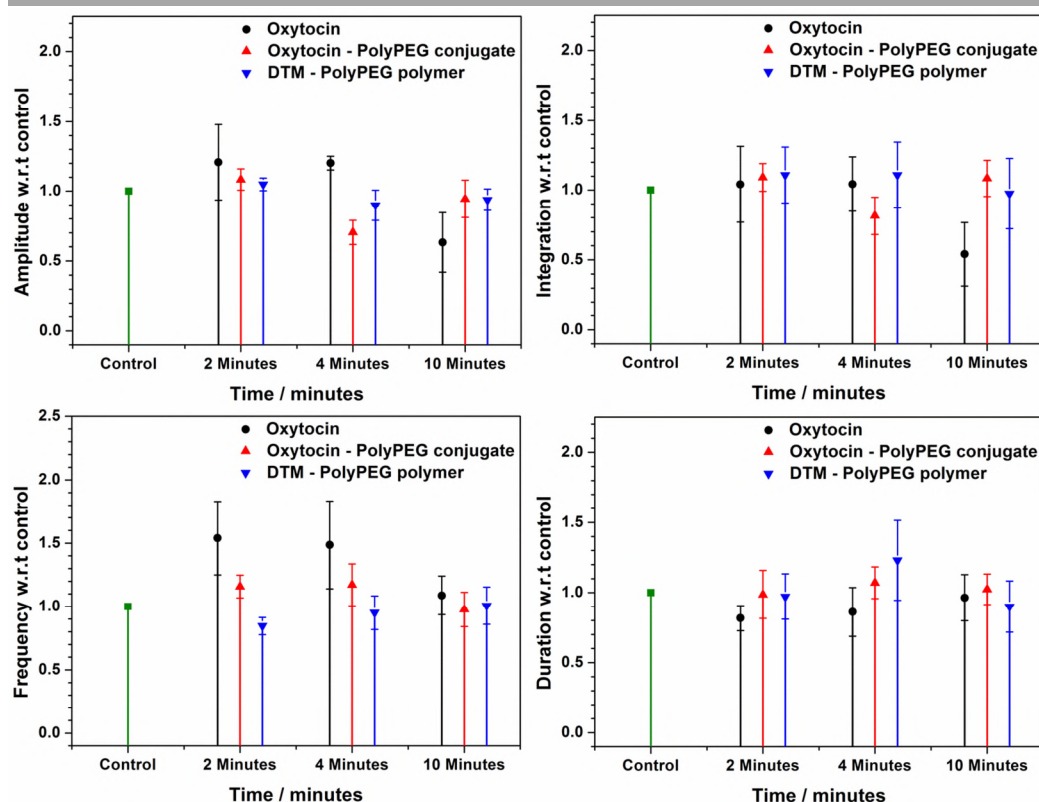


Figure 4.25. Contractile peak response analysis of data for dithiophenolmaleimide polyPEG and oxytocin polyPEG conjugate with respect to amplitude, integration, frequency and duration.

The information elucidated from the organ bath uterine tissue contractility is still unclear of the effect that polymer conjugation has on the oxytocic type activity to the cells. There is little that appears conclusive in terms of PEGylation architecture or conjugation approach, although it generally does point towards some loss of contractile activity of all samples post-conjugation.

4.2.2.2.1. Statistical analysis outcomes of extracted data

Statistical analysis was performed on the results of the uterotonic testing for the oxytocin polymer conjugates (and unconjugated polymers) in comparison to oxytocin with respect to amplitude, integration, frequency and duration. In general, statistically there were no

significant differences between the effects of the conjugates or the polymers to the native peptide.

Differences were, however, observed for the linear aldehyde conjugate (and unconjugated polymer) for contraction amplitude, with both samples showing smaller responses, 4 minutes after introduction of the solutions (conjugate: $49 \pm 14 \%$; polymer: $61 \pm 11\%$ w.r.t oxytocin) ($p < 0.05$). At $t = 4$ minutes is where the oxytocin produces maximal contraction, so it is likely that the reduction observed suggests that no oxytocic effect is observed in these cases. The aldehyde polyPEG oxytocin conjugate and polymer did not show any significant differences to the native peptide across the tissue studies in any of the four criteria.

For the dithiophenolmaleimide polyPEG conjugate there were a couple of points raised upon statistical analysis although overall there were mostly no significant differences evident in comparison to native oxytocin. In terms of the amplitude of contractions after 4 minutes both the polymer and polymer conjugate showed a smaller response in comparison to the native peptide (conjugate: $59 \pm 8 \%$; polymer: $74 \pm 8 \%$) ($p < 0.05$). This is potentially due to similar reasons as suspected for the linear aldehyde PEG, whereby the oxytocin response is strongest at this point.

A major feature raised for this conjugate was that 10 minutes after introduction to the tissue, the conjugate showed a much greater response w.r.t oxytocin ($178 \pm 26 \%$) ($p < 0.05$), with the unconjugated polymer not exhibiting the same behaviour. This potentially highlights that the conjugate does induce a contractile response, but requires additional time. Importantly, this large response could also be washed out in the same way that the oxytocin effects were, meaning that the receptors did not become irreversibly blocked. There is also evidence on analysis of the integration data to support an enhancement in contractions after an additional lag time ($t = 10$ minutes, conjugate: $271 \pm$

49 % w.r.t oxytocin) ($p < 0.05$). Again, no effect was observed in the polymer, highlighting the need for oxytocin within the structure, and contractions quickly returned to baseline responses upon wash out.

These results present potentially useful information in how these particular conjugates might behave as uterotonic agents, although further work is required. At present, little information has been realised on the effect of polymer architecture or conjugation approach through these experiments, due to the challenging nature of the spontaneous contractions observed within the tissue.

4.2.2.3. Oxytocin receptor antagonist: Atosiban

To further investigate the binding mechanism of oxytocin to the receptor, additional uterotonic testing was carried out using a competitive oxytocin receptor antagonist, atosiban (figure 4.26). Atosiban has a similar structure to oxytocin, and acts by causing an inhibition of oxytocin binding thereby preventing uterine contractions and is regularly used as a therapeutic to delay premature labour.

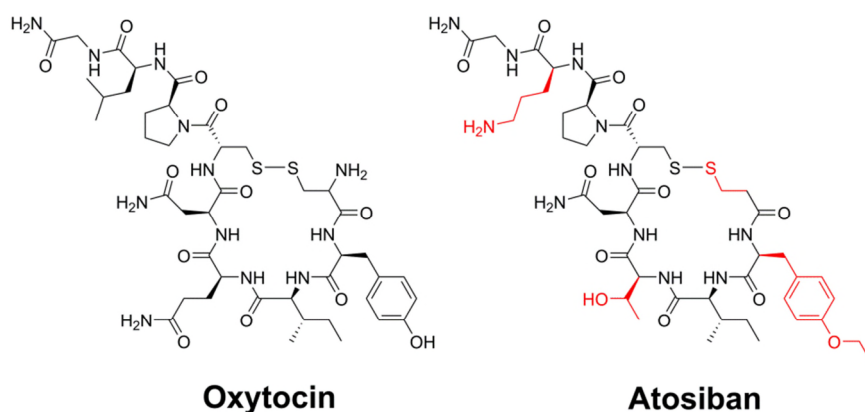


Figure 4.26. Comparison of the structure of oxytocin and oxytocin antagonist atosiban.

The problems encountered on analysis of oxytocin contractility data for the conjugates were also observed whilst comparing the effects of atosiban. The same type of tissue was

used (3 week old SD rats) and differences between oxytocin, atosiban or oxytocin + atosiban added in a competitive mixture did not produce any definitive findings by visual observations or analysis of data. The results with respect to amplitude, frequency, duration and integration all remained within 10 % of those observed for spontaneous contractions.

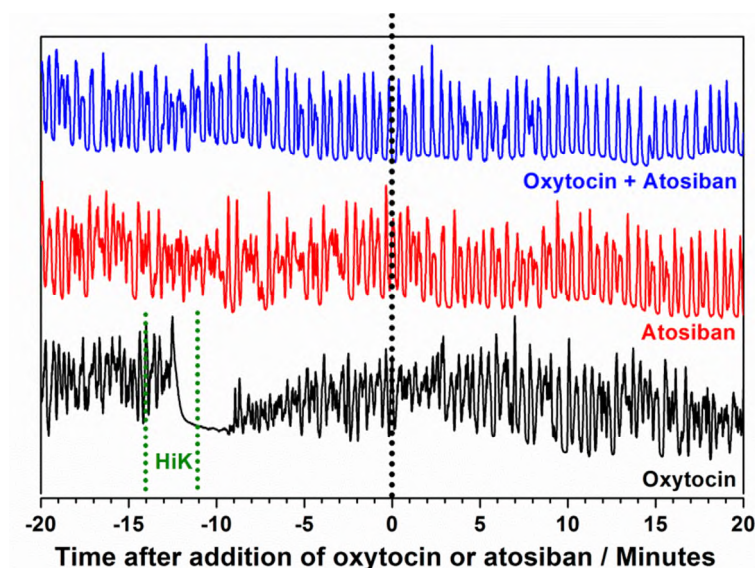


Figure 4.27. Trace of uterotonic contractions showing the effect of atosiban upon oxytocin uterotonic activity, after initial HiK response.

4.2.3. Uterotonic testing conclusions

It is very difficult to make conclusions about to what extent the conjugation of PEG onto oxytocin might have influenced the uterotonic activity, due to the difficulty in observing changes for contractions in the tissue investigated. The results from these studies are inconclusive in establishing whether the synthesised oxytocin conjugates retain any contractile activity. The dithiophenolmaleimide polymer conjugates present a potentially significant find as contractions seem to be evident, but require a longer time before contraction onset.

Another notable point is that the concentrations investigated within this work were fairly high compared to usual oxytocin based contraction studies. Due to the observed spontaneous contractions causing obscuration of the exact data, it was not possible to work with lower concentrations to observe differences between these spontaneous baseline contractions and those induced by oxytocin.

Ideally, all polymer conjugates (and their respective polymers) would be tested to analyse uterotonic activity, in comparison to the native peptide. However, initially a suitable tissue needs to be fully investigated that would allow for more reasonable conclusions to be developed. At this time there is not enough evidence to confirm that the uterotonic activity is completely diminished upon conjugation of polymers to the peptide, however, it is very likely that the action for an effective uterotonic is severely suppressed.

4.3. Cancer cell-line studies

4.3.1. Introduction

Research carried out by Bussolati *et al.* in the 1990s has shown that oxytocin and a synthetic oxytocin-analogue (atosiban, reported in this incidence under the manufacturer code F314) have an inhibitory effect on the cell proliferation of MDA-MB231 human breast cells.^{24–26} F314 has a similar structure to oxytocin (figure 4.28) with 4 main substituent changes, and shows similar results for the reduction of growth of these cancer cells.

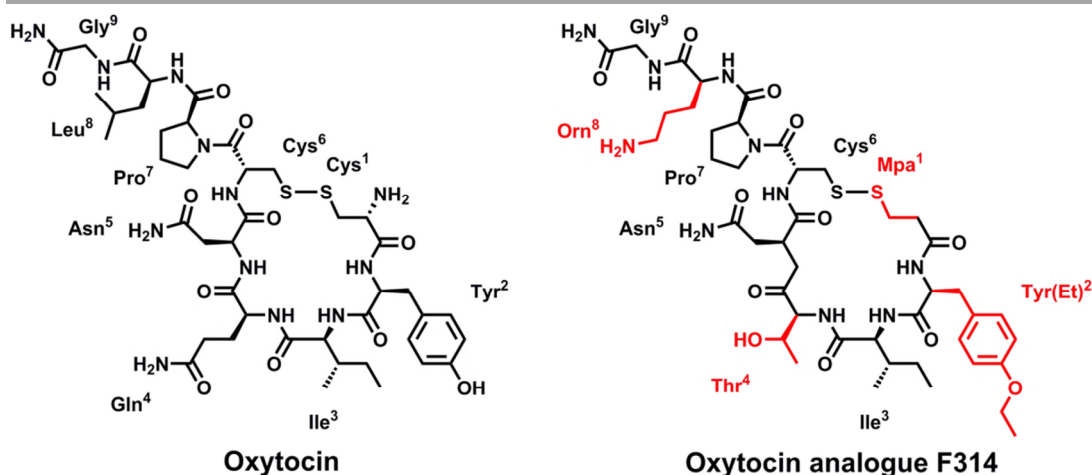


Figure 4.28. Structure of oxytocin and oxytocin analogue F314 (atosiban).

The inhibitory effect was found to be specific to the MDA-MB 231 cell line, with the same studies carried out on a colon cancer cell line (HT29) and two hormone dependant cell lines (MCF7 and T47D), showing that cancer cell growth was not affected by oxytocin treatment.²⁴ After 144 hours 10^{-7} M oxytocin showed a 34 % inhibition of cell growth of MDA-MB 231, with 27 % at 10^{-8} M and no inhibitory effect at 10^{-9} M.

Oxytocin and F314 were also investigated for their *in-vivo* effect on mouse and rat breast cancer tumours, using mouse colon cancer as a control.²⁶ No effect was observed for the colon cancer, however, an inhibitory antiproliferative effect was observed for oxytocin and F314 (10^{-8} M) for both the mouse and rat tissue cell lines. The % volume increase of the rat breast cancer tissue was decreased dramatically for oxytocin (10^{-8} M, 52 %) and F314 (10^{-8} M, 20 %) compared to the control (200 %). Oxytocin receptors have previously been found to be expressed on a variety of different cells, not specifically within the uterus and this was found to be the case for breast cancer cells, highlighting how oxytocin could have an effect on cell proliferation.²⁵

It is clear that oxytocin has many important roles within different branches of biology and physiology, including playing an important role in inhibiting the proliferation of breast

cancer cells. Due to the oxytocin analogue F314 also proving effective for this, an investigation was undertaken as to whether oxytocin-polymer conjugates still had an effect on breast cancer cell growth.

4.3.2. Investigation of oxytocin and polymer conjugates on cancer cell proliferation

The effects of oxytocin and oxytocin polymer conjugates on cell viability were tested for the cancer cell line MDA-MB 231 at concentrations between 10^{-3} M and 10^{-10} M. The cell line study was conducted to investigate if the previously observed decreases in cell proliferation were found for the oxytocin conjugates as with oxytocin, and the high concentrations of polymers and conjugates may also begin to show trends in general cell toxicity. Analysis of the cell lines was carried out with the use of an MTT assay (a colorimetric assay) through which the absorbance of the MTT dye (3-(4,5-dimethylthiazol-2-yl)-2,5-diphenyltetrazolium bromide) is observed at 590 nm, which gives an idea of numbers of live cells.

The effect of oxytocin on the cell proliferation of MDA-MB 231 was tested at 8 different concentrations, with analysis after 6 days (144 hours), as previously investigated in the literature (figure 4.29).²⁴ This revealed that there was no overall effect observed for the concentration of oxytocin on the proliferation of cancer cell lines, with cell growth remaining close to a control cell growth where there was no oxytocin treatment. The concentration that proved the most effective in the literature for inhibiting cell proliferation was 10^{-7} M (34 % inhibitory growth), and this concentration was also found to be the furthest from the control (7 % inhibitory growth). However, this difference is not as significant as within the literature and therefore it is difficult to build conclusions that the

cell proliferation is being affected by the addition of oxytocin, and remains within 10 % of the growth of control cells.

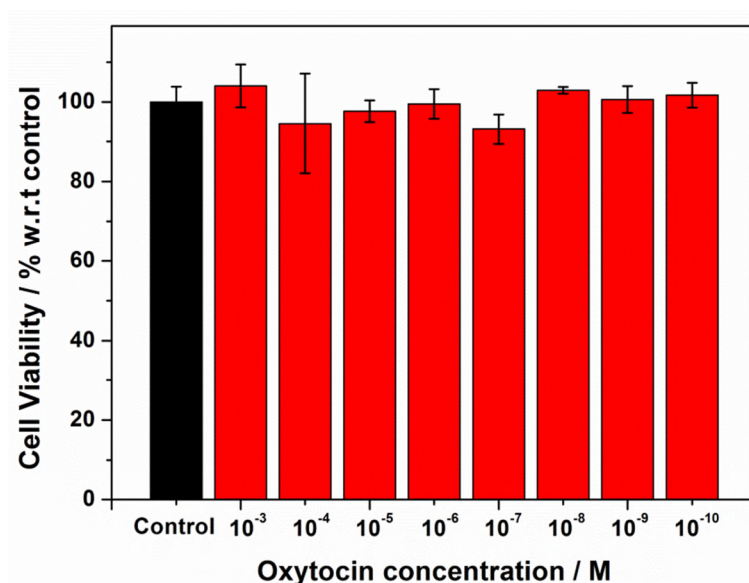


Figure 4.29. Cell viability after treatment with different concentrations of oxytocin compared to untreated control cells after 144 hours.

The oxytocin – polymer conjugates were then tested under the same conditions as the oxytocin study (144 hours) at concentrations between 10^{-6} – 10^{-10} M. Following this another study was undertaken investigating the effect on cell growth of higher concentrations (10^{-3} – 10^{-7}) for all conjugates (both linear and polyPEG) as well as the unconjugated polymers.

Figure 4.30 shows the effect upon cell growth of each variety of oxytocin-polymer conjugate (both architectures, from PEGylation at the *N*-terminal amine and the Cys¹-Cys⁶ disulfide bond) and the native peptide, compared to untreated control cells. The results show that for all the conjugates tested, the cell viability was below that observed for the control cells. Overall cell growth for all samples stayed above 75 % of that observed for the untreated cells, indicating that there wasn't severe cell death associated with the addition of the conjugates, although a cell toxicity of 25 % is still significant.

The results presented here, alongside the above results for the native peptide (a lack of inhibition behaviour) suggest it is unlikely that the values below 100 % are due to inhibitory effects on cell proliferation.

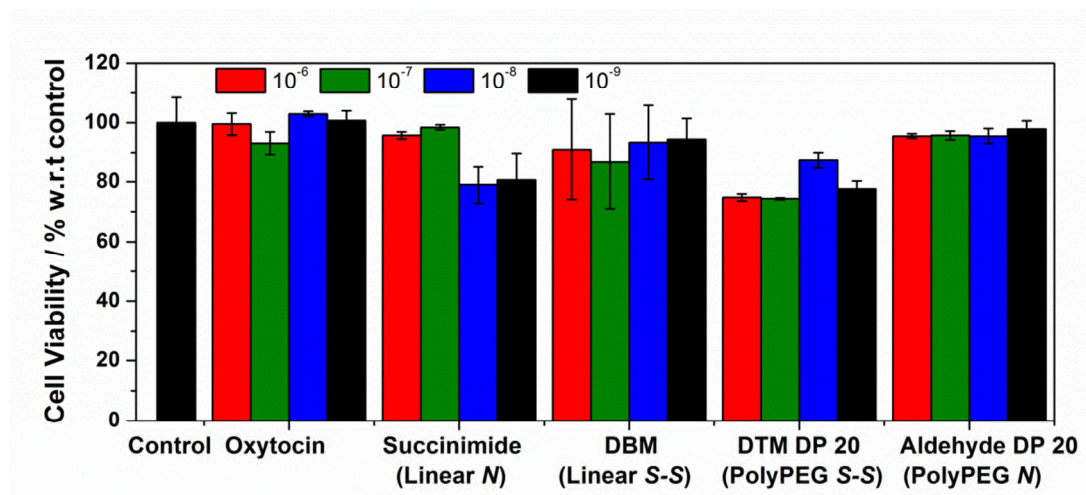


Figure 4.30. Cell viability on treatment with different oxytocin conjugates for 144 hours.

A further cell growth study was undertaken for all the oxytocin-polymer conjugates and their respective polymers, investigating the effect of higher concentrations (up to 10^{-3} , 72 h). The use of higher concentrations can yield useful information about the toxicity of the polymers and conjugates for the cell line being tested (MDA-MB231 in this investigation).

For the majority of the conjugates tested the highest concentration of oxytocin-polymer conjugate (10^{-3}) used to treat the cancer cells showed the least cell viability after 72 hours. This is likely due to cell toxicity, which is known to occur at very high concentrations of polymers. For the linear conjugates (excluding the linear aldehyde conjugate which could only be carried out on a concentration of 10^{-5} or lower) the 10^{-3} samples, although showing the lowest value of cell viability, still remained over 75 % of that observed for control cells indicating that 25 % of the cells had died compared to the control.

In comparison when the high (10^{-3} M) concentrations of the polyPEG conjugates are examined, most of the samples had a cell viability of 65 % or less, with the two higher

molecular weight DTM polyPEG conjugates causing complete cell death. This suggests these DTM polymers are toxic at these concentrations to the MDA-MB231 cells. At concentrations of 10^{-4} or above none of the oxytocin-polymer conjugates were observed to exhibit this level of toxicity with cell viability remaining above 75 % for all other samples.

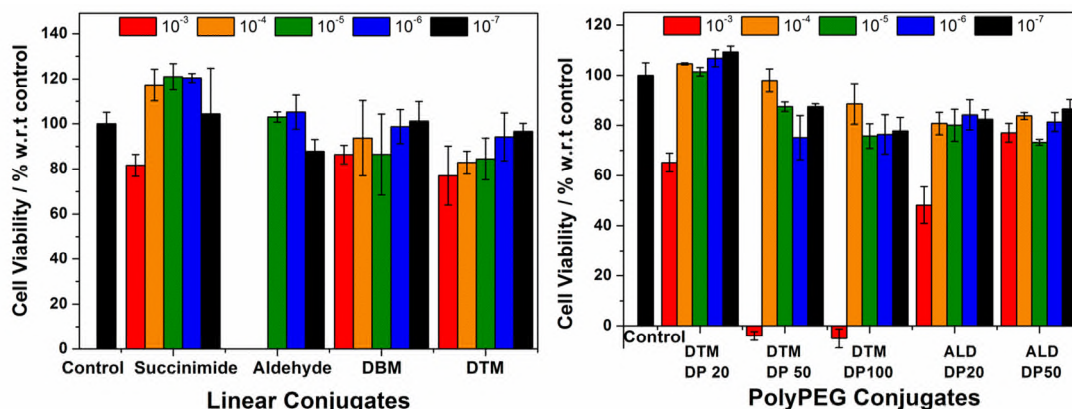


Figure 4.31. Cell viability of all linear and polyPEG oxytocin conjugates w.r.t untreated control after 72 hours of cell growth.

The cell viability on treatment of the cells with the unconjugated polymers was also performed using polymer concentrations from 10^{-3} – 10^{-7} M, which would further provide evidence of the toxicity for the MDA-MB231 cells. This showed similar trends for the 10^{-3} M concentrations observed for these unconjugated polymers compared to the oxytocin polymer conjugates, in that the dithiophenol polyPEGs prove toxic to the cells at a 10^{-3} concentration, independent of the molecular weight (viability < 9 %). As a comparison, the aldehyde functional polyPEGs of the same molecular weights do not have the same extreme toxicity, with the viability remaining about 75 % even at 10^{-3} M. For all the linear polymers the cell viability remained between 65 – 90 % even at high concentrations, suggesting less toxicity of the polymers.

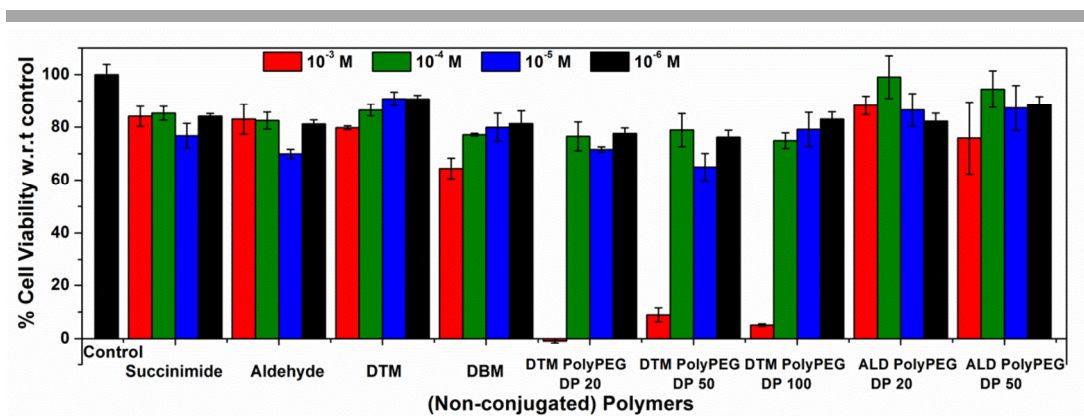


Figure 4.32. Cell viability of all polymers after 72 hours w.r.t untreated control.

4.3.3. Cancer cell line study conclusions

Although the results of the cancer cell line study with oxytocin do not support the same inhibition of proliferation conclusions as to those observed by Bussolati *et al.*, it is difficult to determine what effect oxytocin has on this line of breast cancer cells. Regardless of this unobserved effect, important data is established regarding the overall toxicity trends of the polymers and conjugates. For this cell line the samples synthesised in chapters 2 and 3 show only moderate levels of toxicity (less than 25 %) until concentrations become very high, where total cell death can be observed. It should be noted that toxicity of 25 % however is still fairly significant, and this must be considered.

This is promising data as the toxicity of the conjugates is highly important to the application for providing an oxytocin alternative as a therapeutic. It would be beneficial to run further cell line studies to confirm that the toxicity remains low with a more appropriate classification of cells, but the results from the tested cell line are positive in this respect.

4.4. Chapter 4 Conclusions

Three different methods were utilised to investigate the effect that conjugation has on the properties of oxytocin with regard to enhancements in stability, retained uterotonic activity and any potential inhibitory effect on the cancer cell line MDA-MB-231.

As one of the main aims of the project was to improve the heat stability of oxytocin, high thermal stability assays were carried out on all of the conjugates in comparison to the native peptide. It was found that all of the conjugates were less prone to degradation under the heat stability assay than the native peptide. The polyPEG conjugates were particularly stable with recoveries remaining above 80 % in all cases. The addition of non-covalently bound polymers or other commonly found excipients, for the majority do not have a large effect on improving the stability of the native peptide, although small molecular weight PEGs can show some promising characteristics. These results show that one of the major aims of this project has been achieved and that the PEGylation of oxytocin, respective of the conjugation chemistry used or architecture of the polymer can have a high influence on the thermal stability.

As it has been established that the oxytocin polymer conjugates do have highly increased heat stability, an investigation was undertaken to assess to what degree uterotonic activity was retained. Due to the spontaneous contractile behaviour of the tissue examined, the uterotonic activity testing is so far inconclusive as to whether the peptide retains any activity after the conjugation of linear or polyPEG. The activity shows a reduction when compared to the native peptide in terms of the observation of contractions and on analysis of the contractile data. The maleimide polyPEG conjugate shows that onset to contractions is extended, but that contractions can still be obtained, however, further studies are required to confirm these results.

The cancer cell line studies did not show an inhibitory effect of oxytocin on the proliferation MDA-MB 231 cancer cells. The conjugates compared well to the native peptide by remaining around 100 % cell viability, relative to untreated control cells when low concentrations were used. Upon the addition of high concentrations of polymer or peptide-polymer conjugates, some toxicity can be observed leading to decreases in observed cell growth or potential cell death.

In conclusion oxytocin is a highly important peptide with many different roles within medicine and biology, other than just in those relating to childbirth. The functionalisation of this peptide, and the effect this might have on these various applications, as well as on general oxytocin properties (such as susceptibility to degradation) is therefore of high interest to a range of scientific fields.

4.5. Experimental

4.5.1. High temperature thermal stability tests

4.5.1.1. Materials

Oxytocin (c- [Cys-Tyr-Ile-Gln-Asn-Cys]-Pro-Leu-Gly-NH₂) was gifted from PolyPeptide laboratories (Hillerød, Denmark) and used as received. All additives (PEG / other excipients) were purchased from Sigma Aldrich and used as received.

4.5.1.2. Instrumentation & Analysis

High performance liquid chromatography (HPLC) was performed on Agilent 1260 Infinity series stack equipped with an Agilent 1260 binary pump and degasser. 50 µl samples were

injected using Agilent 1260 autosampler with a flow rate of 1 ml/min. The HPLC was fitted with a Phenomenex Luna C18 column (250 x 4.6 mm) with 5 micron packing (100Å). Detection was achieved using an Agilent 1260 variable wavelength detector monitoring at 280 nm. Mobile phase A consisted of 100 % water containing 0.04 % TFA and mobile Phase B consisted of 100 % acetonitrile containing 0.04 % TFA as an additive. The column was equilibrated by washing with the starting % of mobile phase A for 10 minutes prior to injection for all conditions. The method used was as follows: 95 % mobile phase A decreasing to 80 % mobile phase A after 15 minutes, followed by decreasing to 40 % mobile phase A after a further 7 minutes and remaining at 40 % mobile phase A for 5 minutes before resetting to 95 % mobile phase A in 1 minute.

4.5.1.3. Heat Stability assay procedure

Each of the conjugate samples were run at 5 different concentrations on RP-HPLC (UV: $\lambda=280$ nm) as dilutions of the concentration used for the stability assay of [1.0], [0.8], [0.6], [0.4] & [0.2]. The native peptide was also run at each of these concentrations as well as [0.1], [0.05] & [0.01] for increased reliability of low oxytocin levels. A linear calibration plot was produced from the concentrations vs. the peak area (mAU) for all samples.

Oxytocin and oxytocin polymer conjugates were dissolved in HPLC grade water at the concentrations between 0.05 mM and 1 mM. For the excipient studies the additives (2 mM or 200 mM) were added to solutions of oxytocin (2 mM) giving total concentration of oxytocin as 1 mM with excipients in 1 x or 100 x molar excess.

The solutions were placed in a Thermo Scientific Heratherm oven set to 80 °C and left for 24 hours. After this time the samples were cooled to room temperature before being submitted for RP-HPLC. The % remaining of oxytocin or the oxytocin conjugates was

calculated from the absorbance of oxytocin (or the conjugate) with respect to the calibration curve.

4.5.1.4. Synthesis of non-conjugating poly(mPEGA₄₈₀)₂₀

In an oven dried Schlenk tube, CuBr (3.6 mg, 24.9 μ mol) and water (1 ml) were added and stirred before the addition of tris[2-(dimethylamino)ethyl]amine (6.6 μ l) upon which there was the immediate formation of Cu(0) powder and blue CuBr₂ solution which was degassed by nitrogen bubbling for 30 minutes. In a separate vial, EBiB (9.1 μ l, 62.2 μ mol) and poly(ethylene glycol) methyl ether acrylate (M_w = 480, 0.548 ml, 1.24 mmol) were dissolved in DMSO (6 ml) and water (0.5 ml) and degassed by nitrogen bubbling for 30 minutes. The monomer/initiator solution was then added into the catalyst solution by injection ($t = 0$) and the reaction was stirred at ambient temperature under nitrogen for 20 hours. After this time a sample was removed and diluted with δ_6 -DMSO for ¹H NMR analysis and DMF for GPC molecular weight data. The polymer was purified by dialysis (1 kDa MWCO) for 3 days against water, before lyophilisation.

4.5.2. Uterotonic testing of oxytocin and oxytocin conjugates

N.B. This work was carried out by the author at Monash University, Melbourne, Australia as part of an 11 week research visit.

No animal ethics approval or animal ethics committee (AEC) notification was required for the uterotonic work as the tissues were scavenged post-mortem from rats that were scheduled to be culled from Monash animal research platform (MARF) stocks under their

approved ethics protocol. This is as set out in the guidelines for the conduct of animal ethics committees (Victoria) and Monash University ethical research and approvals policy.

4.5.2.1. Materials

Oxytocin (c- [Cys-Tyr-Ile-Gln-Asn-Cys]-Pro-Leu-Gly-NH₂) was gifted from PolyPeptide laboratories (Hillerød, Denmark) and used as received. Krebs buffer was freshly prepared and consisted of 120.0 mM NaCl, 5.9 mM KCl, 25.0 mM NaHCO₃, 1.2 mM NaH₂PO₄, 2.5 mM CaCl₂, 1.2 mM MgCl₂, and 5.5 mM glucose. The synthesis of peptide-polymer conjugates and unconjugated polymers are described within this thesis in chapters 2 and 3.

4.5.2.2. Experimental Procedures

For the investigation of uterotonic activity of oxytocin and oxytocin-polymer conjugates *ex vivo* organ bath analysis was carried out using uterotonic tissue freshly scavenged from 3 week old Sprague Dawley rats. The right uterine horn was promptly removed post mortem and immediately stored in Krebs solution. The tissue was trimmed to 10 mm and suspended in the organ bath after which a force of 10 mN was applied. The organ bath was perfused at a constant rate of 4 ml/min with Krebs solution whilst the temperature was maintained at 37 °C and the solutions constantly aerated with 95 % O₂/5 % CO₂.

Tensions were constantly recorded and monitored using LabChart software connected to the PowerLab instrument (ADL instruments).

4.5.3. Cancer cell line study

N.B. The cancer cell line study was carried out by Danielle Senyschyn in the presence of the author at Monash University, Melbourne, Australia as part of an 11 week research visit.

4.5.3.1. Materials

Oxytocin (c- [Cys-Tyr-Ile-Gln-Asn-Cys]-Pro-Leu-Gly-NH₂) was gifted from PolyPeptide laboratories (Hillerød, Denmark) and used as received. The synthesis of peptide-polymer conjugates and unconjugated polymers are described within this thesis in chapters 2 and 3. Media formulation consisted of Dulbecco's modified eagle medium (DMEM, high glucose, GlutaMAX™, Gibco), 10% fetal bovine serum (FBS, Life Technologies) and penicillin-streptomycin 100X (10,000 U/mL, Life Technologies) and was kept at 37 °C prior to immediate use and stored at 4 °C.

4.5.3.2. Experimental Procedures

4.5.3.2.1. Cell line preparation

Cells removed from liquid nitrogen and thawed in 37 °C water bath, and added to media (10 % cell solution). Cells spun for 5 minutes at 125 - 130 x g, before removal of media, and repetition of procedure. Pellet suspended in 1 ml media and added to flask containing 4 ml media, for incubation at 37.5 °C / 5 % CO₂ for 3 days.

Media was removed from flask and cells washed with 5 ml PBS before addition of 5 ml Trypsin (0.25 %, Life Technologies) and placed in incubator at 37 °C for a few minutes. 10 ml media was added, and an aliquot removed for cell counting and remainder of solution span in centrifuge for 5 mins at 125 – 130 x g, before removal of media. Fresh media was added so concentration of cells was 50,000 per ml, and 96 well plate seeded with 100 µl of this solution per well. 24 hours after seeding, media removed and replaced with 80 µl fresh media before treating cells with oxytocin, oxytocin-polymer conjugates or unconjugated polymers (10⁻³ – 10⁻⁹ M) and leaving for 72 or 144 hours.

4.5.3.2.2. *MTT assay*

MTT (3-(4,5-dimethylthiazol-2-yl)-2,5-diphenyltetrazolium bromide) was reconstituted in PBS at 5 mg ml⁻¹ and sterile filtered, before dilution in fresh media to 0.5 mg ml⁻¹. Media was removed from cells and 100 µl of MTT solution added to each well. Plate was incubated at 37.5 °C / 5 % CO₂ for 2 hours, before removal of MTT and addition of 100 µl DMSO and plate shaken for 5 – 10 minutes. The absorbance of cells was read with a plate reader at 590 nm.

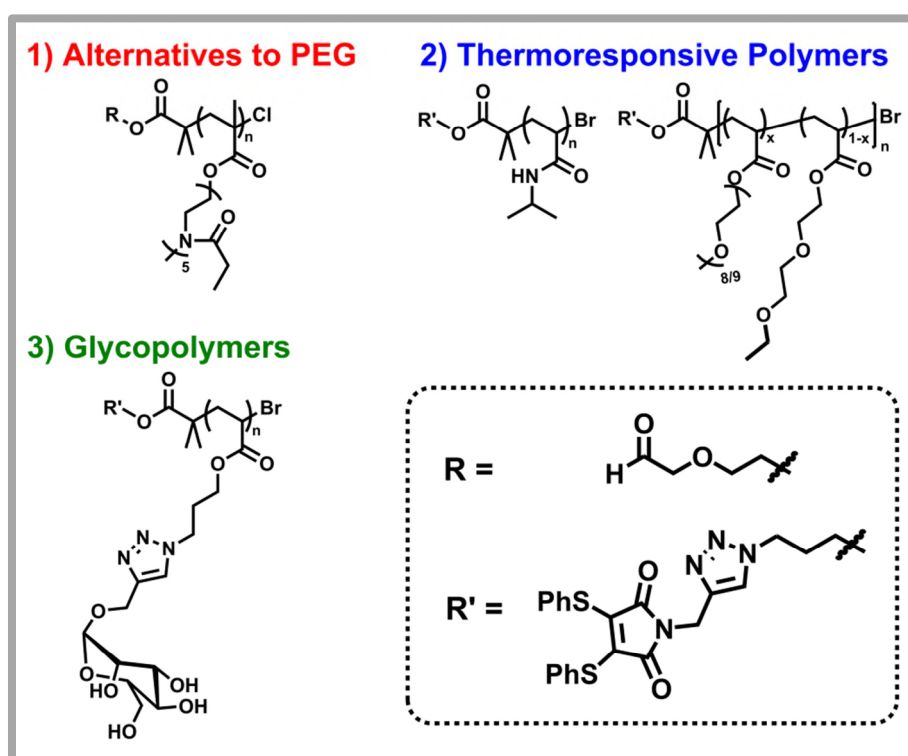
4.6. References

- 1 A. Hawe, R. Poole, S. Romeijn, P. Kasper, R. Van Der Heijden and W. Jiskoot, *Pharm. Res.*, 2009, **26**, 1679–1688.
- 2 K. Wiśniewski, J. Finnman, M. Flipo, R. Galyean and C. D. Schteingart, *Biopolymers*, 2013, **100**, 408–421.
- 3 J.-F. Roy, M. N. Chrétien, B. Woodside and A. M. English, *Nitric Oxide*, 2007, **17**, 82–90.
- 4 C. Avanti, W. L. J. Hinrichs, A. Casini, A. C. Eissens, A. Van Dam, A. Kedrov, A. J. M. Driessen, H. W. Frijlink and H. P. Permentier, *J. Pharm. Sci.*, 2013, **102**, 1734–1741.
- 5 M. Muttenthaler, A. Andersson, A. D. de Araujo, Z. Dekan, R. J. Lewis and P. F. Alewood, *J. Med. Chem.*, 2010, **53**, 8585–8596.
- 6 *Stability of injectable oxytocics in tropical climates*, World Health Organization, Geneva, 1993.
- 7 F. M. Veronese and A. Mero, *BioDrugs*, 2008, **22**, 315–329.
- 8 E. T. Maggio, *J. Excipients food Chem.*, 2010, **1**, 40–49.
- 9 C. Avanti, H. P. Permentier, A. Van Dam, R. Poole, W. Jiskoot, H. W. Frijlink and W. L. J. Hinrichs, *Mol. Pharm.*, 2012, **9**, 554–562.
- 10 A. J. Keefe and S. Jiang, *Nat. Chem.*, 2012, **4**, 59–63.
- 11 P. Bazzacco, K. S. Sharma, G. Durand, F. Giusti, C. Ebel, J. L. Popot and B. Pucci, *Biomacromolecules*, 2009, **10**, 3317–3326.
- 12 K. S. Sharma, G. Durand, F. Giusti, B. Olivier, A. S. Fabiano, P. Bazzacco, T. Dahmane, C. Ebel, J. L. Popot and B. Pucci, *Langmuir*, 2008, **24**, 13581–13590.

-
- 13 R. J. Mancini, J. Lee and H. D. Maynard, *J. Am. Chem. Soc.*, 2012, **134**, 8474–8479.
 - 14 J. Lee, E.-W. Lin, U. Y. Lau, J. L. Hedrick, E. Bat and H. D. Maynard, *Biomacromolecules*, 2013, **14**, 2561–2569.
 - 15 *WHO recommendations for the prevention and treatment of postpartum haemorrhage*, World Health Organization, Geneva, 2012.
 - 16 P. W. Van Dongen, J. Van Roosmalen, C. N. De Boer and J. Van Rooij, *Pharm. Weekbl. Sci.*, 1991, **13**, 238–243.
 - 17 G. Gimpl and F. Fahrenholz, *Physiol. Rev.*, 2001, **81**, 629–683.
 - 18 N. Vrachnis, F. M. Malamas, S. Sifakis, E. Deligeoroglou and Z. Iliodromiti, *Int. J. Endocrinol.*, 2011, **2011**, Article ID 350546.
 - 19 R. Walter, I. L. Schwartz, J. H. Darnell and D. W. Urry, *Proc. Natl. Acad. Sci. U. S. A.*, 1971, **68**, 1355–1359.
 - 20 B. Berde, W. Doepfner and H. Konzett, *Br. J. Pharmacol. Chemother.*, 1957, **12**, 209–214.
 - 21 M. Manturewicz, Z. Grzonka, L. Borovicková and J. Slaninová, *Acta Biochim. Pol.*, 2007, **54**, 805–811.
 - 22 R. J. Prankerd, T.-H. Nguyen, J. P. Ibrahim, R. J. Bischof, G. C. Nassta, L. D. Olerile, A. S. Russell, F. Meiser, H. C. Parkington, H. A. Coleman, D. A. V Morton and M. P. McIntosh, *PLoS One*, 2013, **8**, e82965.
 - 23 P. G. Wyatt, M. J. Allen, J. Chilcott, C. J. Gardner, D. G. Livermore, J. E. Mordaunt, F. Nerozzi, M. Patel, M. J. Perren, G. G. Weingarten, S. Shabbir, P. M. Woollard and P. Zhou, *Bioorg. Med. Chem. Lett.*, 2002, **12**, 1405–1411.
 - 24 P. Cassoni, A. Sapino, F. Negro and G. Bussolati, *Virchows Arch.*, 1994, **425**, 467–472.
 - 25 P. Cassoni, A. Sapino, N. Fortunati, L. Munaron, B. Chini and G. Bussolati, *Int. J. Cancer*, 1997, **72**, 340–344.
 - 26 P. Cassoni, A. Sapino, M. Papotti and G. Bussolati, *Int. J. Cancer*, 2002, **820**, 817–820.

Chapter 5

5. Synthesis and post-polymerisation peptide conjugation of functional polymers



There is considerable scope within polymer synthesis and conjugation chemistry for the incorporation of a wide variety of different polymers for a variety of tailored functions. Using the copper mediated polymer synthesis and post-polymerisation peptide conjugation strategies introduced in chapters 2 & 3; different functional polymers were incorporated site-specifically onto oxytocin and a second small peptide. Three different classes of polymers are described all of which could provide interesting or advantageous properties within the biomedical field of protein / peptide modification and polymer therapeutics.

5.1. Potential alternatives to PEG

PEG is still one of the most popular polymers utilised for a variety of different biomedical applications (including in the pharmaceutical market, where multiple PEG products have achieved FDA approval), and is the gold standard in the field of polymeric drug delivery.^{1–3} A multitude of advantageous properties are evident including stealth behaviour, prolonged blood circulation, which, coupled with a high biocompatibility lead to its success within the biomedical field and on the commercial market.^{4–6} However, the use of PEG is not without disadvantages including a lack of biodegradability leading to potential accumulation within tissues as well as the possibility of interaction with the immune system.^{3,7,8}

Many natural polymers have been utilised in various drug-delivery systems but more recently there has been a substantial amount of research focused on developing synthetic alternative polymers to PEG.⁹ This is with an overall aim to reproducing some of the highly desirable PEG characteristics but with potential suppression of some of these unfavourable side effects. These can generally be placed into two classes: biodegradable and non-biodegradable polymers (figure 5.1). Biodegradable polymers generally contain backbone functionality capable of undergoing the desired degradation and several examples are derived from amino acids, such as poly(glutamic acid), poly(hydroxyethyl-glutamine) and poly(hydroxyethyl-asparagine).^{10,11} These degrade into their amino acid units, which can simply be metabolised within the body, and thus have been utilised as drug-delivery alternatives to PEG.

Non-biodegradable PEG alternatives generally possess similar problems to PEG with respect to accumulation within organs, but can also provide highly desirable PEG-type characteristics. Various non-biodegradable PEGs have been investigated which include similarities to PEG with the inclusion of heteroatoms in the backbone chain such as

polyglycerols,^{12,13} poly(2-methyl-2-oxazoline) and poly(2-ethyl-2-oxazoline).^{14–16} These have proven to have comparable advantages to PEG including good biocompatibility, but some of the disadvantages for PEG are still evident with the potential for bioaccumulation and immune activation.⁹ Other PEG alternatives wherein the use of vinyl monomers creates a polymer backbone with a repeating unit consisting of the side chains are also available, similar to the polyPEGs discussed in previous chapters. These include poly(vinylpyrrolidone),¹⁷ poly(acrylamide),^{17,18} and poly(*N*-(2-hydroxypropyl)methacrylamide)^{19,20} with varying levels of success in biomedical applications. As with PEG, high biocompatibility can be achieved but there are still drawbacks associated with accumulation of polymers and immunological behaviour.

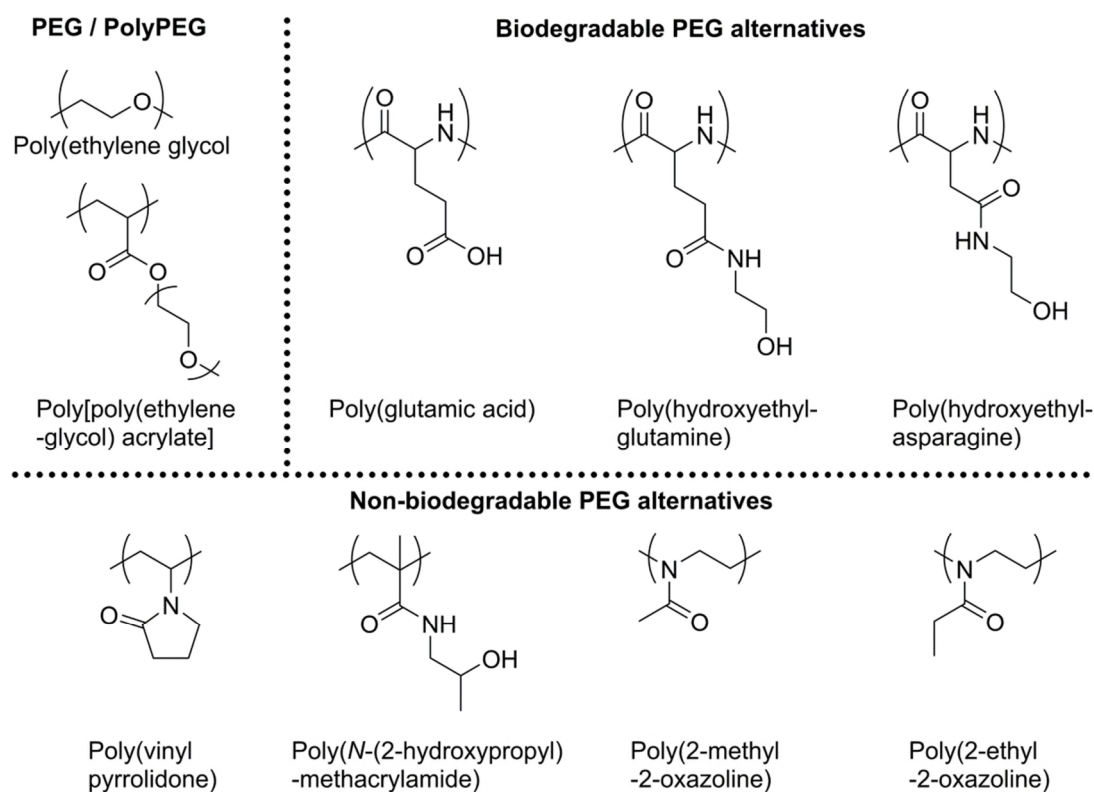


Figure 5.1. PEG, polyPEG and some different biodegradable and non-biodegradable PEG alternatives.

In the first sub-section of this chapter, the synthesis of one other PEG alternative will be explored using copper mediated living radical polymerisation. The post-polymerisation conjugation of this polymer onto the *N*-terminal amine of oxytocin will then be evaluated in comparison to the PEGylation strategies described in chapter 2.

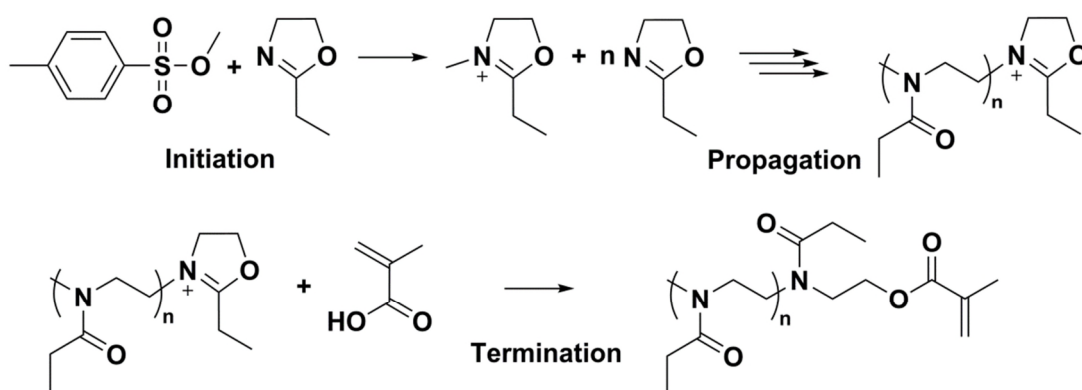
5.1.1. Poly(2-oxazolines): A valuable PEG alternative?

One of these promising PEG alternatives that has received considerable investigation within the literature is poly(2-oxazoline)s (POx), a highly functional class of polymers that are themselves also biocompatible.¹⁶ POx are synthesised by cationic ring opening polymerisation (CROP) of 2-substituted-2-oxazolines, and depending on the 2-substituent functionality, different properties can be obtained. Poly(2-oxazoline)s have previously shown promise as anti-fouling polymers and for ‘stealth’ behaviour and this, coupled with their biocompatibility, has expanded the use of these polymers for a variety of purposes.¹⁴ The structure and functionality of polymers can also be effectively tailored to purpose by careful selection of initiation and termination reagents for the incorporation of a variety of functionalities in the chain.²¹ Linear POx polymers have previously been studied for peptide and protein modifications with successful conjugations reported with carboxylate, alkyne and aldehyde functional polymers, often of ethyl or methyl poly(2-oxazolines).¹⁵

In a similar manner to PEG, as well as proving highly useful as a linear polymer, ‘comb’ type polymers can be synthesised utilising an oxazoline based macromonomer.^{22–24} Upon polymerisation this yields a polymer backbone with short oxazoline based side chain ‘teeth’, the functionality of which is determined by the 2-substituent on the 2-oxazoline monomer. POx macromonomers have previously been used in controlled radical polymerisation techniques, such as reversible addition-fragmentation chain-transfer polymerisation (RAFT) and atom transfer radical polymerisation (ATRP), although synthesis

have previously proved challenging.^{23,25} Little work, however, has been carried out on the functionalisation of peptides or proteins with comb poly(POx) based polymers, using traditional conjugation approaches, even with large amounts of interest generated in the highly successful conjugation of linear POx. There have, however, been some incidences of repeat unit ‘teeth’ functionalisation for the synthesis of glycosylated or antibody conjugated poly(POx), but this was targeted at a general decoration of poly(POx) with biomolecules of interest.^{26,27} This therefore leads to the potential exploitation of this relatively unexplored area within polymeric therapeutic conjugation of the effects that this comb poly(POx) might have upon the biomolecules, particularly in comparison to equivalent poly(PEG)s, which have been well studied. The various methods of polyPEG synthesis and conjugation described in chapters 2 & 3 can be applied to the synthesis and oxytocin conjugation of poly(POx) for the incorporation of a potentially highly valuable, but relatively unexplored PEG alternative.

5.1.1.1. Synthesis of poly(OEtOxMA)



Scheme 5.1. Oligo(2-ethyl-2-oxazoline)methacrylate macromonomer synthesis with initiation by methyl tosylate and termination by methacrylic acid.

Oligo(2-ethyl-2-oxazoline)methacrylate (OEtOxMA) ($DP_n = 5$, $M_n = 600 \text{ g mol}^{-1}$) was synthesised within our group by CROP, with initiation by methyl tosylate and termination

with methacrylic acid, which results in a methacrylic monomer containing a short side chain of oligo(2-ethyl-2-oxazoline) (scheme 5.1).²⁴ This resulted in a macromonomer with a molecular weight of 600 g mol^{-1} (CHCl_3 NMR), whilst maintaining a narrow dispersity ($\bar{D} = 1.21$, CHCl_3 SEC) (figure 5.2).

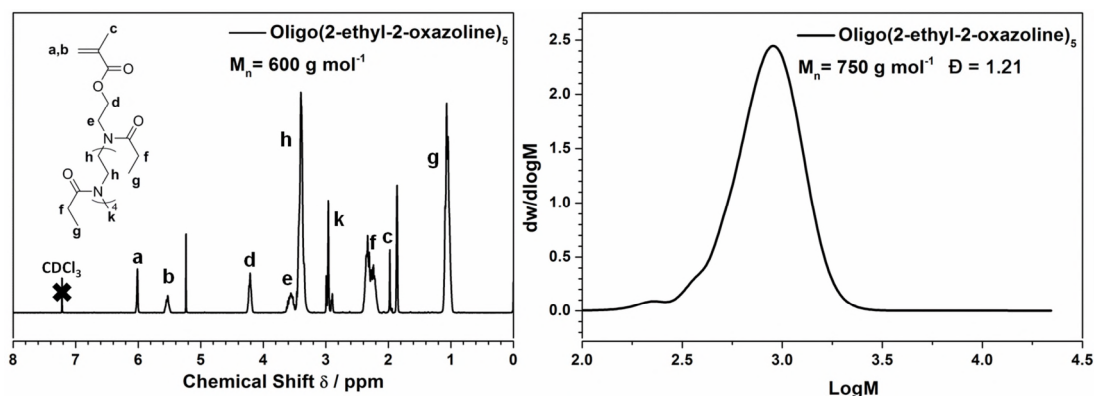
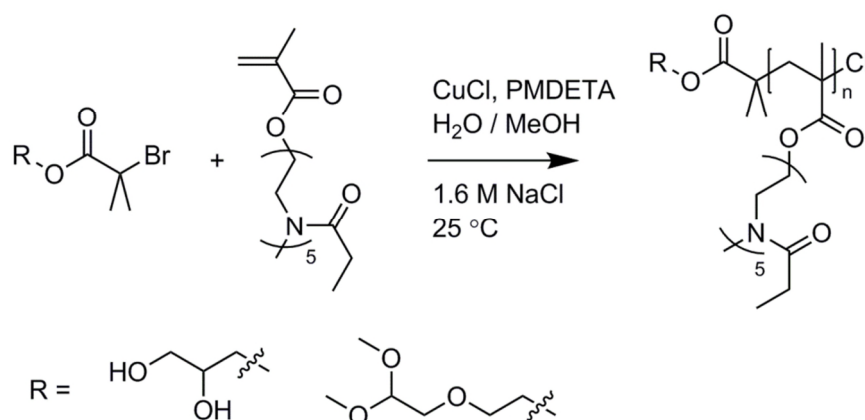


Figure 5.2. ^1H NMR (CDCl_3) and SEC (CHCl_3) of oligo(2-ethyl-2-oxazoline) methacrylate macromonomer.

Previous polymerisations described in chapter 3 utilised the disproportionation of Cu(I)Br with Me_6TREN in aqueous solutions for the controlled synthesis of poly(mPEGA), an acrylic macromonomer.^{28–30} When utilising the disproportionation of copper(I) in aqueous solutions as a polymerisation technique for the synthesis of methacrylates, it has previously been found that for control to be maintained a few adaptations must be made to the polymerisation system.³¹ The replacement of CuBr with CuCl is beneficial in improving polymerisation control. More termination can usually be observed with the polymerisation of methacrylates compared to acrylates (due to a lower k_p) further disadvantaged by the weak nature of the Cu-Br bond. It is also useful to use a less activating ligand for the polymerisation of methacrylates and hence Me_6TREN (which is a very proficient ligand for the synthesis of poly(acrylate)s) was substituted for PMDETA .²⁸ Additionally, the inclusion of a halide salt (NaCl) as an external additive to the polymerisation solutions has been shown to improve the control of polymerisations by

preventing halide dissociation from the copper complex,³² and can influence the ω-Cl end group retention.³¹

OEtOxMA was polymerised at 25 °C in water/methanol (1.5:2) with the addition of 1.6 M NaCl ([I]:[CuCl]:[PMDETA] = 1:0.8:0.8). Two different molecular weight poly(OEtOxMA) polymers were targeted at [M]:[I] ratio of 10 and 20 (target molecular weights of 6 and 12 kDa) using two different initiators, with reaction sampling after 24 hours (scheme 5.2).



Scheme 5.2. Polymerisation of oligo(2-ethyl-2-oxazoline) in water/methanol containing 1.6 M NaCl salt using two different initiators with [I]:[CuCl]:[PMDETA] = 1:0.8:0.8.

Initially a water soluble initiator (WSI, 2,3-dihydroxypropyl 2-bromo-2-methylpropanoate),³³ which has been well established for aqueous Cu(0) mediated polymerisations,²⁹ was utilised using the optimised (CuCl/PMDETA/NaCl) polymerisation conditions. After 24 hours an almost quantitative conversion was attained at both molecular weights. The conversion was calculated by a comparison between the monomer vinyl peaks (δ = 5.6 – 6.0 ppm) and the 10 protons from the CH₂ within the ethyl chain of the macromonomer (δ = 2.29 ppm). Molecular weight distributions were narrow (\mathcal{D} < 1.12) and mono-modal, with molecular weights estimated by SEC as 7.5 and 11 kDa (figure 5.3).

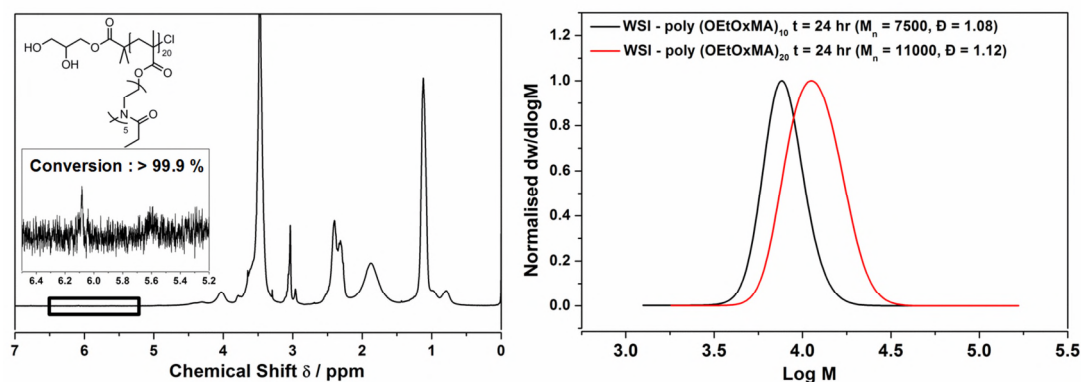


Figure 5.3. ^1H NMR (CHCl₃, 400 MHz) and SEC (CHCl₃) of poly(OEtOxMA) at $t = 24$ hours synthesised with WSI ([I]:[CuCl]:[PMDETA] = 1:0.8:0.8, MeOH/H₂O, 1.6 M NaCl).

5.1.1.2. Synthesis of α -aldehyde functional poly(OEtOxMA)

The protected aldehyde (PALD) initiator^{34,35} utilised for the synthesis and conjugation onto oxytocin of aldehyde α -end group functional poly(mPEGA) in chapter 2 was then applied under the same conditions ([I]:[CuCl]:[PMDETA] = 1:0.8:0.8; [M]:[I] = 10 / 20). As with the polymerisations using the water soluble initiator, quantitative conversions were attained after 24 hours at 25 °C. SEC analysis of the resulting polymers displayed mono-modal peaks with narrow dispersities ($\bar{D} < 1.10$) (figure 5.4).

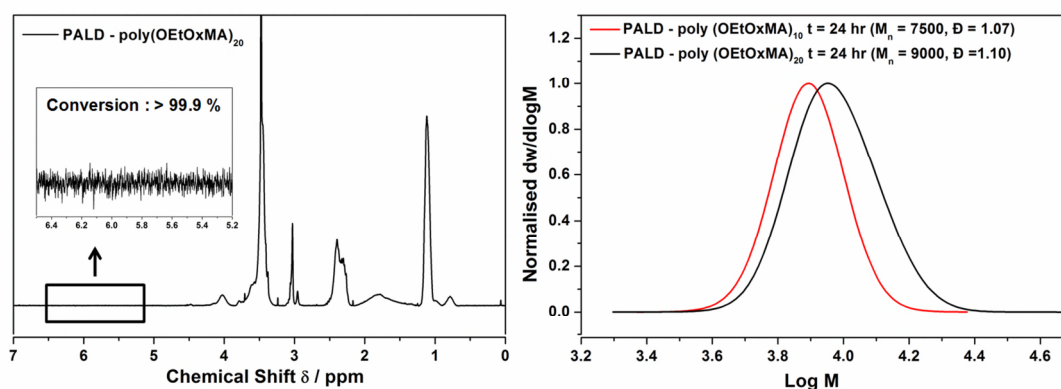


Figure 5.4. ^1H NMR (CHCl₃, 400 MHz) and SEC (CHCl₃) of poly(OEtOxMA) at $t = 24$ hours synthesised with PALD initiator ([I]:[CuCl]:[PMDETA] = 1:0.8:0.8, MeOH/H₂O, 1.6 M NaCl).

The controlled synthesis of these polymers to quantitative conversions under benign conditions present clear advantages over previous polymerisation techniques which have been described for the OEtOxMA monomer. Within the literature, polymerisations have often struggled to achieve full monomer conversions or have required much higher equivalencies of copper salts and ligands.^{23,25}

The molecular weight of the DP_n 20 polymer (particularly for synthesis with PALD initiator) by SEC analysis ($M_n = 8$ kDa) deviated slightly from the theoretical target (12 kDa), this is ascribed to the differences in the hydrodynamic volume of polymers and the SEC PMMA calibration. On further analysis of the purified polymers (dialysis against water, 1 kDa MWCO, 3 days) by ^1H NMR (δ_6 -DMSO) (figure 5.5) the exact molecular weights could be evaluated by a comparison of the $(\text{CH}_3\text{O})_2\text{CH}$ peak ($\delta = 4.42$ ppm) of the initiating group, and the CH_2 group within the macromonomer repeat unit within the polymer ($\delta = 2.9$ ppm). This gave resulting experimental molecular weights of 7.8 kDa and 12.4 kDa for the DP_n 10 and DP_n 20 PALD polymers, which are in agreement with the theoretical values. After purification there was a small increase in the dispersity of polymers, but the molecular weight distributions still remained narrow ($\text{Đ} < 1.25$).

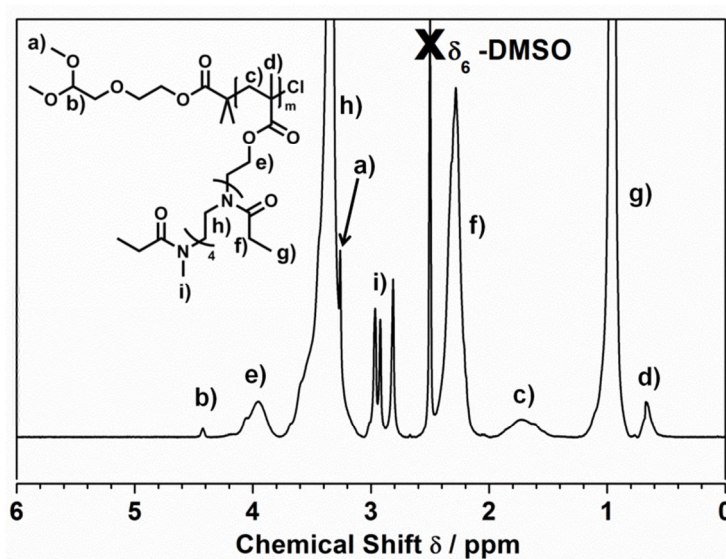


Figure 5.5. ^1H NMR (δ_6 -DMSO, 400 MHz) of PALD-poly(OEtOxMA)₁₀ polymer after purification.

The α -acetal protecting group of the polymer was removed by treatment in aqueous solutions of trifluoroacetic acid (50 % v/v) for 3 days, resulting in α -aldehyde functional polymers (figure 5.6). The end group was confirmed by ^1H NMR, where there was a complete disappearance of the peaks representing the acetal protecting group ($\delta = 4.42$ ppm) with the appearance of characteristic aldehyde peaks ($\delta = 9.57$ ppm).

After deprotection, analysis by SEC confirmed there was no decrease in molecular weight of the polymers, verifying that there was no cleavage of the oligo(2-ethyl-2-oxazoline) side chains from the polymer backbone. This resulted in two different molecular weights of α -end aldehyde functional poly(OEtOxMA), which could subsequently be grafted onto a peptide or protein at an amine group in a ‘grafting-to’ process.³⁴

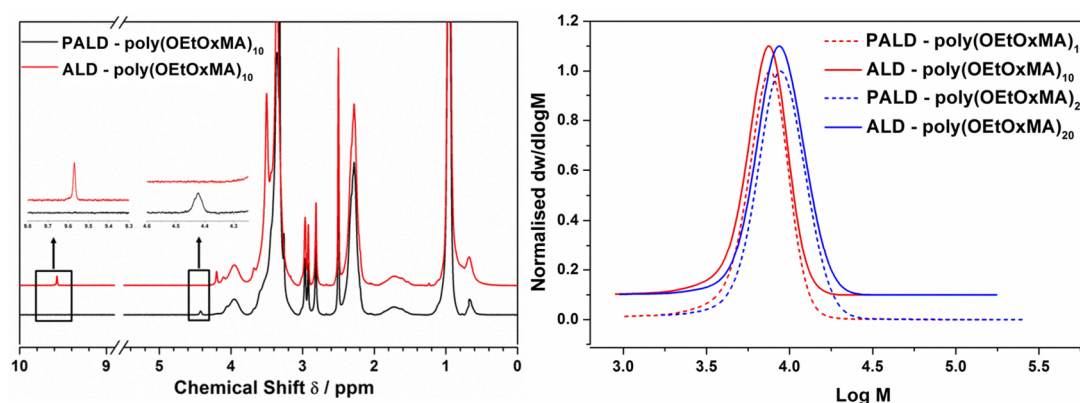


Figure 5.6. ^1H NMR (δ_6 -DMSO) and SEC (CHCl_3) after deprotection of acetal protected aldehyde end group functionality.

Table 5.1. Polymerisation data for the synthesis of poly(OEtOxMA) in MeOH/H₂O (2:1.5) containing 1.6 M NaCl with CuCl and PMDETA.

Initiator	Target DP_n	Target MW (Da)	Conversion % (NMR)	M_n (Da) (SEC)	\bar{D} (SEC)	M_n (Da) (SEC) Deprotected	\bar{D} (SEC) Deprotected
WSI	10	6000	>99.9	7500	1.08	-	-
WSI	20	12000	>99.9	10900	1.12	-	-
PALD	10	6000	>99.9	6000	1.23	6500	1.14
PALD	20	12000	>99.9	8000	1.18	7900	1.15

5.1.1.3. Peptide conjugation reactions of α -aldehyde poly(OEtOxMA)

Initially, a dipeptide (NH₂-Gly-Tyr-COOH) [Gly-Tyr] was used as a model peptide for the reductive amination reaction of α -aldehyde functional poly(OEtOxMA). As with oxytocin [Gly-Tyr] does not contain any amino groups other than that of the *N*-terminal amine of the peptide and thus conjugation would occur in a singular and site-specific manner (figure 5.7).

After 5 days the conjugation reaction was monitored by RP-HPLC which revealed the disappearance of the Gly-Tyr signal alongside the appearance of a broad conjugate peak at a higher retention time to the native peptide. The polymer conjugate was then purified by dialysis to remove any residual dipeptide and ¹H NMR analysis revealed the appearance of aromatic peaks (δ = 6.5 – 7.0 ppm) consistent with the tyrosine signals observed within the dipeptide confirming that the [Gly-Tyr] group was now present on the polymer.

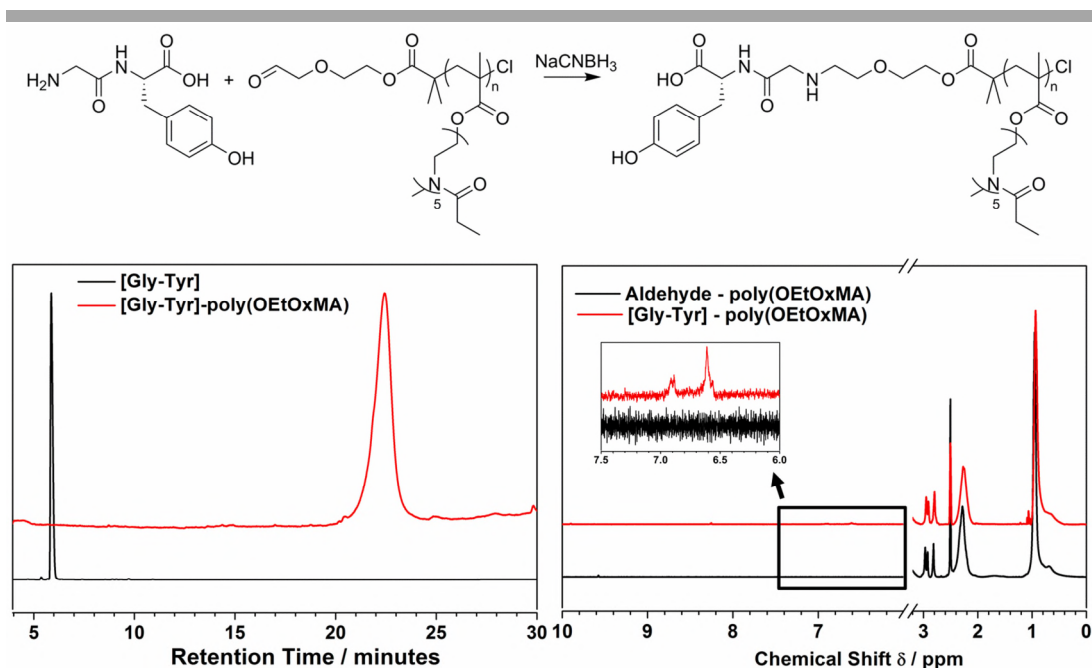
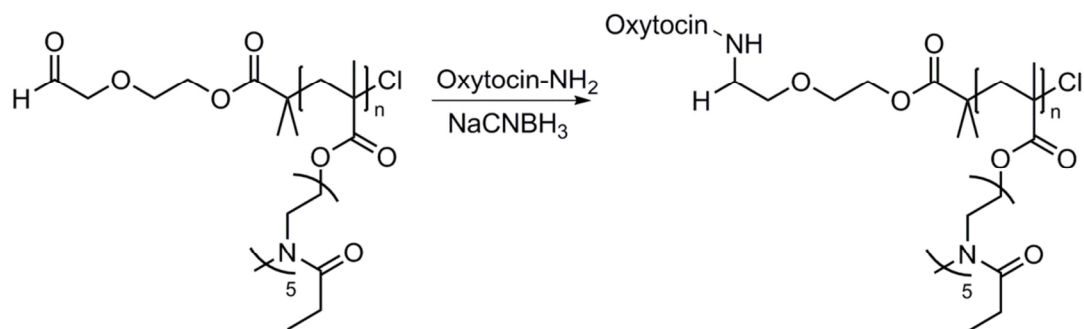


Figure 5.7. Conjugation reaction of [Gly-Tyr] with α-aldehyde poly(OEtOxMA) monitored by RP-HPLC ($\lambda = 280$ nm) and ^1H NMR (δ_6 -DMSO, 300 MHz).

The aldehyde α-end functional poly(OEtOxMA)s were then conjugated onto oxytocin *via* reductive amination, with the addition of NaCNBH₃ as a reducing agent (scheme 5.3).



Scheme 5.3. Reductive amination conjugation of aldehyde poly(OEtOxMA) onto oxytocin with addition of NaCNBH₃.

After 4 days a sample was removed from the reaction and analysed by RP-HPLC which revealed the disappearance of the majority of the native peptide (retention time $t = 12.5$ minutes) and the appearance of a new, broad peak at a higher retention time (DP_n 10: $t = 20.8$ minutes; DP_n 20: $t = 21.4$ minutes) (figure 5.8). As previously explored with the

reductive amination of aldehyde functional linear PEG and polyPEG onto oxytocin, there is only one amino group present at the Cys¹ amino terminus, and therefore polymer conjugation is singular and site-specific. For the conjugation of these polymers onto oxytocin, the reaction was more efficient than with the reductive amination of the α -aldehyde poly(mPEGA)s observed in chapter 2, with less unreacted peptide remaining within the solutions.

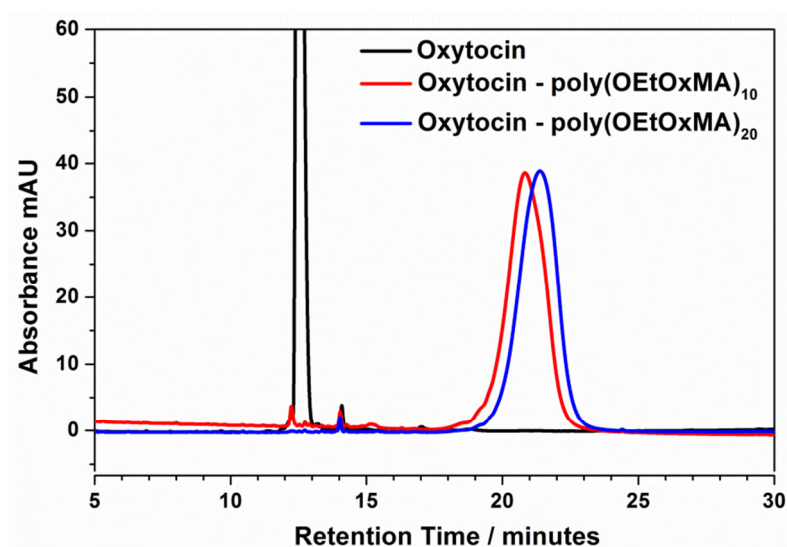


Figure 5.8. RP-HPLC of reductive amination of aldehyde functional poly(OEtOxMA) onto oxytocin after addition of NaCNBH₃.

It must be noted that the polymer, prior to conjugation, shows a small broad peak in a similar region, but when the same concentration of polymer and oxytocin-polymer conjugate were analysed ($\lambda = 280$ nm) the absorbance increased approximately 20 times post conjugation (figure 5.9). There is also a very minor shift in the retention time of the peak from the polymer to the conjugate (DP_n 10: 21.6 to 20.8 minutes; DP_n 20: 21.9 to 21.4 minutes). This, alongside the disappearance of the native peptide observed on RP-HPLC, suggests that polymer conjugation has occurred and that the absorbance of the polymer conjugate RP-HPLC chromatogram is larger due to a change in molar extinction coefficient (most likely due to the high absorbance of the peptide at $\lambda = 280$ nm).

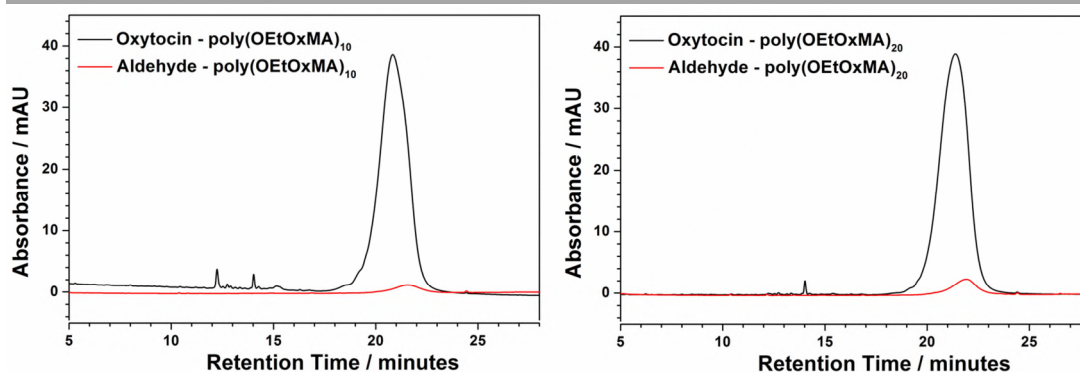
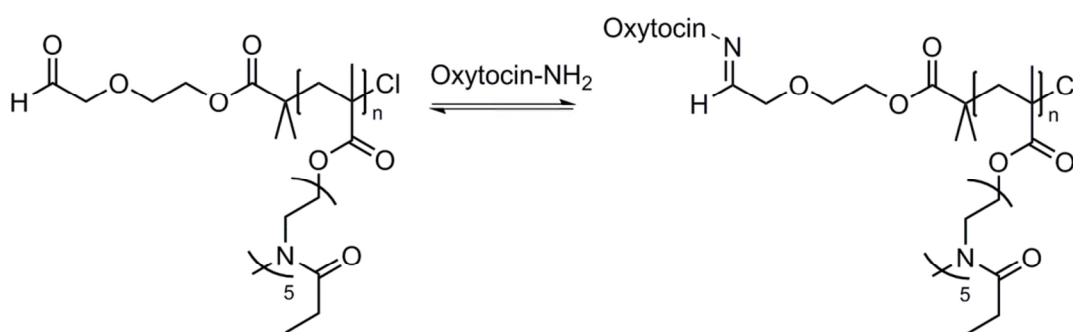


Figure 5.9. RP-HPLC monitoring of aldehyde functional poly(OEtOxMA) (DP_n 10 and 20) before and after conjugation onto oxytocin.

The reversibly linked Schiff base conjugates (without the addition of NaCNBH_3) were synthesised in the same manner as by reductive amination with an exclusion of the reducing agent (scheme 5.4). The conjugation was much slower than for the reductive amination conjugation, but the appearance of broad conjugate peaks can still be observed by RP-HPLC, with a new conjugate peak clearly visible at $t = 4$ days. After 14 days there was a further appreciable decrease in the oxytocin peak (further 66 % decrease compared to $t = 4$ days). Although there is still unreacted peptide remaining within the solution, there is an accompanying (2 X) increase in the amount of conjugate (figure 5.10).



Scheme 5.4. Reversible (Schiff base) conjugation of aldehyde poly(OEtOxMA) onto oxytocin.

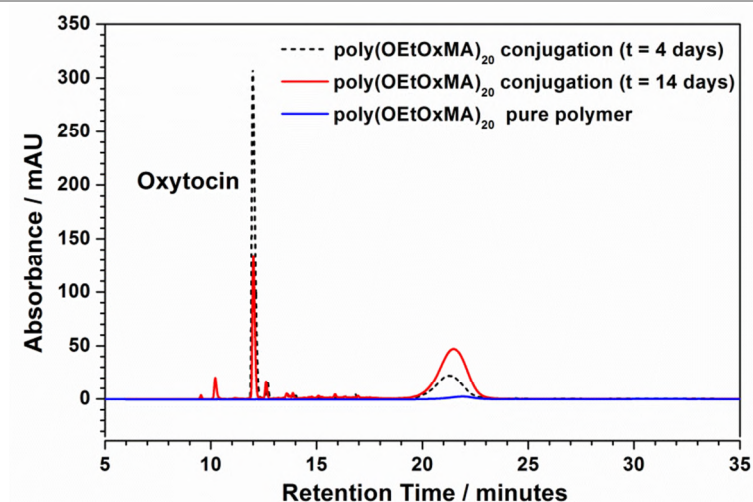


Figure 5.10. RP-HPLC monitoring of the formation of oxytocin-poly(OEtOxMA)₂₀ Schiff base conjugate.

5.1.1.4. Schiff base reversibility studies of oxytocin-poly(OEtOxMA) conjugates

As with the Schiff base linked poly(mPEGA) oxytocin conjugates, described in chapter 2, reversibility studies were undertaken to establish whether the native peptide could be released under stimulated conditions. When the polyPEG Schiff base conjugates were studied these were found not be reversible under the conditions evaluated, whereas similar linear polymers did have reversible characteristics, suggesting that architecture plays an important role. The poly(OEtOxMA) conjugates were analysed to determine whether the different macromonomer behaved differently, which would highlight further details about the stability of this aldehyde linkage.

The reversibility of the DP_n 10 and DP_n 20 polymers were analysed at pH 5 (citrate buffer, 0.1 M) and pH 7.4 (phosphate buffer, 0.1 M) at $t = 4$ days and $t = 14$ days. The experiments were performed at ambient temperature ($T < 20\text{ }^{\circ}\text{C}$) as with the poly(mPEGA) samples and at $T = 37\text{ }^{\circ}\text{C}$, to examine whether temperature played a role in the reversal. This revealed

that there was no significant reversal of the Schiff base linkage for any of the samples, with the conjugate peak remaining in the same position, and peak area not decreasing significantly (figure 5.11).

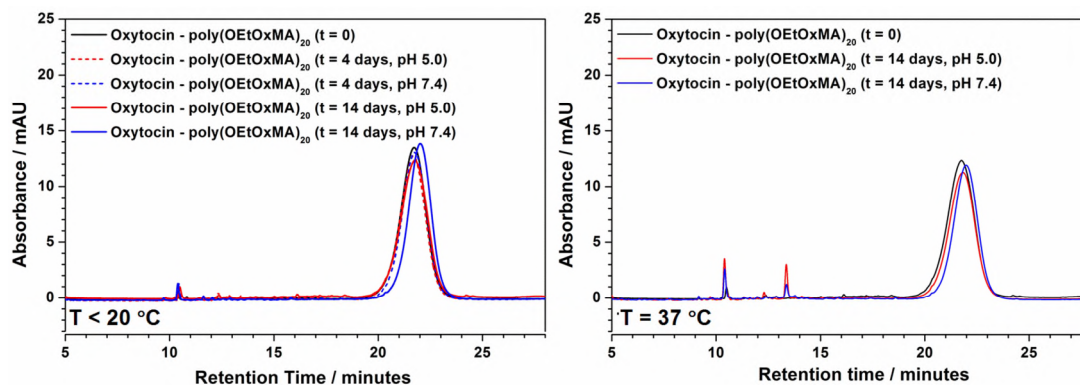


Figure 5.11. RP-HPLC monitoring of reversal of oxytocin-poly(OEtOxMA)₂₀ conjugates at pH 5 and pH 7.4 after 14 days at ambient temperature or at T = 37 °C.

The higher temperature studies showed minor shifts within the conjugate peak, as well as the potential appearance of some other products at retention times $t = 10.4$ minutes and $t = 13.4$ minutes. However, any changes in peak area remain below 15 % of the total conjugate area, which does not suggest that appreciable reversible characteristics were achieved.

This shows very similar characteristics to the attempted reversibility of polyPEG Schiff base linked oxytocin conjugates. It is believed that this is possibly due to the linker length between the aldehyde and highly polymer dense ‘comb’ type structure. In chapter 2 the polymer (or non-polymer) architecture was found to be highly vital in allowing the reversible nature of this linkage to be exploited. As two different polymers synthesised from respective macromonomers (poly(mPEGA) and poly(OEtOxMA)) have both been found to show difficulties in stimulating the reversible nature, from this particular protected aldehyde initiator, it has been shown that the incorporation of these architectures suppresses peptide release.

5.1.1.5. Degradation studies on reduced oxytocin- *poly(OEtOxMA)* conjugates

The degradation of the poly(OEtOxMA) oxytocin conjugates was monitored after 24 hours of storage at 80 °C (figure 5.12). The stability, with respect to retained conjugate peak area remained at close to 100 %, as previously observed for poly(mPEGA) oxytocin conjugates, with little differences between repeats of samples.

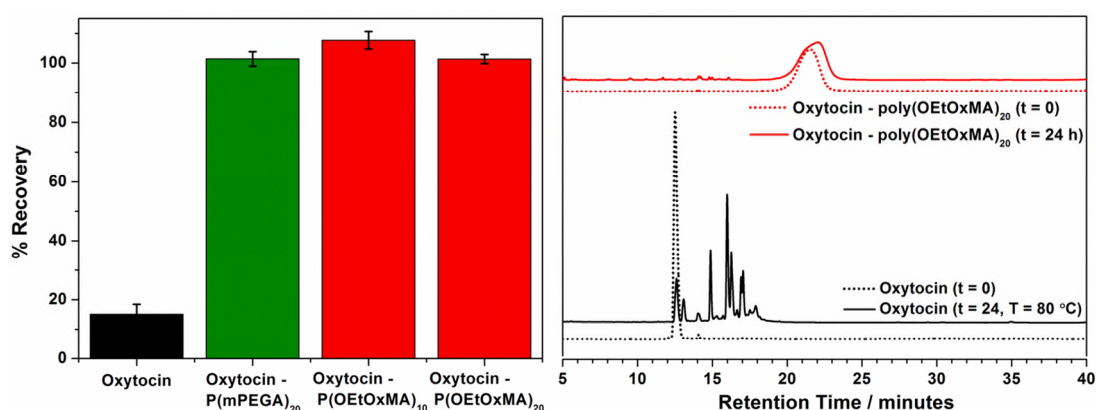


Figure 5.12. Bar chart and RP-HPLC traces showing degradation of oxytocin-poly(OEtOxMA) conjugates in comparison to native peptide after 24 h at 80 °C.

On closer inspection of the RP-HPLC traces, however, there are some differences between the chromatograms at $t = 0$ and after 24 hours of high temperature storage for the polymer conjugates with regard to peak shape and retention time. This could be indicative that there has been some distortion or degradation within the polymer conjugate at this temperature; however, with no loss of oxytocin or diminishment of absorbance it is difficult to confirm. Whilst there is only a minor shift of the peak, this highlights a challenge of this high temperature degradation study as a method of testing the conjugate stability.

Further it must be noted for the synthesis of 2-ethyl-2-oxazoline based polymers that LCST (lower critical solution temperature) transitions can often be observed, whereby cloud

points can be exhibited, particularly for linear polymers of 2-ethyl-2-oxazoline.³⁶ The cloud point temperatures of poly(2-R-2-oxazoline)s vary depending on the R substituent. For linear POx polymers; poly(2-methyl-2-oxazoline) does not have an observed cloud point in aqueous solutions, whereas the cloud points of poly(2-ethyl-2-oxazoline), poly(2-*n*-propyl-2-oxazoline) and poly(2-iso-propyl-2-oxazoline) are all very different. This allows tuning of LCST behaviour to a desired temperature to be achieved by changing the monomer, or allowing the synthesis of a copolymer, where each monomer exhibits different thermally responsive temperatures. The LCST behaviour of poly(POx) ‘comb’ polymers has also previously been evaluated, with large differences observed between different macromonomer sizes and depending on the pH of the solution.²⁵

As the degradation studies are performed at elevated temperatures, this could be reaching close to the cloud point of these polymer conjugate solutions. To investigate this, cloud point measurements were undertaken with the two oxytocin-polymer conjugates monitoring the absorbance at $\lambda = 500$ nm, between 20 °C and 90 °C (figure 5.13).

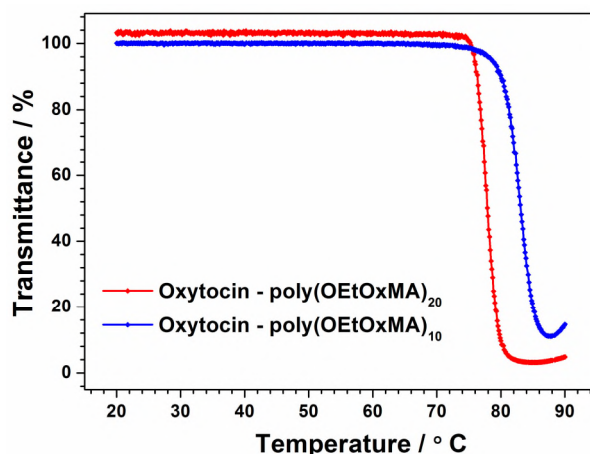


Figure 5.13. Cloud point measurements of oxytocin –poly(OEtOxMA) conjugates in water (5 mg ml⁻¹) at $\lambda = 500$ nm.

By observing the point where the transmission is at 50 % within the third heating run, the cloud points for the oxytocin polymers conjugate solutions (5 mg ml⁻¹) were determined as

83.1 °C (DP_n 10) and 77.8 °C (DP_n 20). These are close to the temperature used for the degradation study, and it is likely that some of this thermoresponsive behaviour is present when measuring the stability of both conjugates in this manner. Previously a DP_n 20 poly(OEtOxMA) prepared by RAFT (33 % conversion, M_n = 7100 Da, \bar{D} = 1.18) of the same size macromonomer (DP_n = 5) was evaluated as having a cloud point as 84.4 °C (5 mg ml⁻¹, H₂O).²⁵ The similarity in value suggests that polymers synthesised in different manners can show similar cloud points, and the end group functionality, regardless of whether this is a peptide or small molecule does not have a large effect on the temperature of non-solubility.

The polyPEGs that were analysed by the same 80 °C degradation study do not show a cloud point around this temperature (previously reported cloud points > 90 °C), therefore the possible thermoresponsive nature does not create similar issues for the thermal stability described in chapter 4. In conclusion, the thermal behaviour of these poly(POx) polymers must be considered when performing high temperature stability studies. This is particularly important when polymers are being evaluated as potential alternatives for PEGylation in respect of prioritising increasing the thermal stability.

5.1.2. Potential alternatives to PEG conclusions

There are many strategies available for the synthesis and conjugation of a variety of polymers that can act as alternatives to PEG for a multitude of purposes. In this chapter so far we have explored the potential use of poly(POx) for the synthesis of peptide polymer conjugates and how these compare to the well-studied poly(PEG)s with regard to improving the degradation profile of a dramatically unstable, but globally well-utilised therapeutic peptide.

In this work these polymers have been synthesised in a controlled manner, utilising an optimised copper mediated polymerisation technique to contain α -aldehyde end group functionality. Succeeding the synthesis, post-polymerisation modification and two subsequent conjugations onto the Cys¹ amino terminus of oxytocin were achieved *via* reductive amination and Schiff base chemistry. The Schiff base reversal studies show similar results to those previously observed for the conjugation of polyPEGs in that the reversible reaction is hard to stimulate under acidic conditions.

It would be beneficial to further synthesise other alternatives to PEG and evaluate the properties that polymer-conjugates may possess, post-conjugation, as a comparison. There is a large library of different polymers that can exhibit PEG-like properties, where the same polymer synthesis and conjugation chemistry could be easily adapted for the investigation of new polymers for conjugation onto therapeutics.

5.2. Thermoresponsive polymers for peptide conjugation

The incorporation of stimuli-responsive functionalities into polymers (such as temperature-, pH-, redox- and light-responsive) is a field that has received large amounts of attention within the literature.^{37,38} Thermoresponsive polymers exhibit a change in properties upon stimulation with temperature, such as a rapid change in solubility in a medium upon reaching a critical temperature (LCST, lower critical solution temperature; UCST, upper critical solution temperature). This behaviour has previously been utilised for a variety of applications, and is particularly notable within the field of polymer therapeutics such as for drug delivery.^{39–42}

The development of living radical polymerisation (LRP) techniques has allowed the synthesis of thermoresponsive polymer bioconjugates to be rapidly developed.⁴³ Different functional monomers are available which, when incorporated into (co)polymers, can exhibit interesting phase transitions at elevated temperatures. A popular example of a monomer regularly utilised in LCST systems is *N*-isopropylacrylamide (NiPAm). Poly(NiPAm) is a useful thermoresponsive polymer with a biologically relevant thermal solubility transition at ~32 °C in aqueous solutions, generally independent of molecular weight and concentration.^{44,45} A coil-to-globule transition is stimulated on heating, which is entropically favourable and driven by the formation of hydrogen bonds and water expulsion.⁴⁶ A second class of polymers that have received a lot of interest are the utilisation of copolymers of monomers exhibiting highly different phase transition temperatures. These prove very useful as these can be specifically tailored as desired by varying the relative component ratios. One of such copolymer mixtures is poly(oligo ethylene glycol)(meth)acrylates.^{47,48} The solubility transitions of shorter (meth)acrylate oligo ethylene glycol monomers are relatively low (MEO₂MA = ~26 °C), whereas for longer PEG monomers this is much higher (8/9 ethylene glycol units < 90 °C). Therefore, by altering the ratio of the monomers, any temperature for an LCST transition can be attained between these two temperatures.

The attachment of thermoresponsive (or other stimuli-reactive polymers) onto biomolecules, including proteins and peptides, can provide an interesting class of bioconjugates.⁴³ The properties of the attached polymers can be lent to the biomolecules, and due to the large library of thermoresponsive polymers available, this can be tailored to a suited purpose. Stimuli responsive conjugates have previously been reported wherein conjugation was performed utilising a *grafting-from* or *grafting-to* approach, with biomolecule targeting including both amino and thiol routes. Stimuli responsive protein-

polymer conjugates can prove useful in allowing tuning or control of biomolecular processes, by using external changes to alter function for a range of applications. One example of a thermally induced biomolecule response, described in the 1990s by Hoffman, was a thermoresponsive enzyme conjugate which had the ability to mask the active site, altering enzyme activity and thereby preventing or allowing active site binding.^{49,50}

Within this next sub-chapter the synthesis of dithiophenolmaleimide α -end functional thermoresponsive polymers is presented which could be utilised for disulfide rebridging conjugation *via* a post-polymerisation conjugation ('grafting-to') type technique. This would result in more thermally resistant peptide polymer conjugates, which should retain some of the thermoresponsive behaviour of the post-conjugation polymers.

5.2.1. Optimisation of reaction conditions and synthesis of thermoresponsive polymers

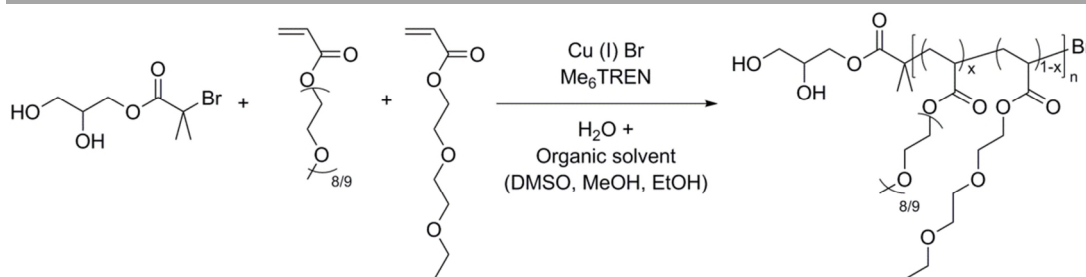
The copper mediated living radical polymerisation method utilising the prior disproportionation of Cu(I)Br with Me₆TREN in aqueous solvents was used to prepare thermoresponsive dithiophenolmaleimide polymers. Due to the insolubility of the initiator in aqueous solutions a reasonable cosolvent system had to be developed which could be used in a similar manner to the DMSO/H₂O polymerisation described for the synthesis of DTM polyPEGs in chapter 3, for the controlled synthesis of thermoresponsive polymers.

Firstly, the solubility of the initiator was investigated in various organic solvents and found to remain soluble as long as the water content remained below 25 % in DMSO, 35 % in MeOH and 45 % in EtOH. As a cosolvent is required, the solvent conditions were initially optimised for the polymerisation, and this optimisation was performed using the

completely water soluble initiator (WSI) mentioned previously, which has been well reported for these types of polymerisations.²⁹ As a starting point polymerisations were conducted in a DMSO/H₂O system using a similar method to that described in chapter 3 for the synthesis of DTM α -end functional poly(mPEGA).

Two different classes of polymers exhibiting potentially biologically relevant LCSTs were investigated, *N*-isopropylacrylamide (NiPAm), and a copolymer of poly(ethylene glycol) methyl ether acrylate (mPEGA) and di(ethylene glycol)ethyl ether acrylate (eDEGA). The cloud point observed for the poly[(mPEGA)_x(eDEGA)_{1-x}] copolymer is entirely tuneable by changing the ratio between the monomers. Homopolymers of poly(mPEGA) generally exhibit high cloud points (> 90 °C), whereas homopolymers of DEGA are lower (\approx 10 °C), therefore copolymers can be synthesised which have a desired cloud point within this range, by changing the monomer ratio.⁴⁷ Copolymerisations varying the ratios of these monomers with evaluation of resultant cloud point temperatures have previously been reported by Lutz *et al.* using copper mediated polymerisation (ATRP)⁵¹⁻⁵³ and by Davis *et al.* using RAFT.^{54,55} For the cloud point to be biologically relevant at approximately 32 - 37 °C, (a similar temperature to that observed for poly(NiPAm) \sim 32 °C) the ratio required is between 5 – 20 % of the PEGA macromonomer.

An important step in the polymerisation is the initial disproportionation of Cu(I)Br with Me₆TREN forming a blue Cu(II) solution and Cu(0) particles, before the addition of the initiator or monomer. This step was carried out in pure water to ensure full disproportionation was achieved, as organic solvents dramatically affect the extent of disproportionation,³⁰ after which the monomer and initiator could be added in the cosolvent. The resulting solution was 80 % DMSO, which is within the range of solubility deemed suitable for the dithiophenolmaleimide initiator.



Scheme 5.5. Polymerisation of mPEGA and DEGA with WSI in water – organic solvents.

For the polymerisations in DMSO, a molar mass of 7500 Da was targeted for homopolymers of eDEGA, mPEGA and NiPAm as well as two random copolymers of eDEGA/mPEGA containing 10 % and 5 % of the PEG monomer (scheme 5.5). CuBr and Me₆TREN were allowed to disproportionate fully in 0.75 ml water, and the solution degassed under nitrogen bubbling, after which a degassed solution of the monomer and initiator in 4 ml DMSO and 0.25 ml water were added under the flow of nitrogen ([I]:[CuBr]:[Me₆TREN] = 1:0.4:0.4). After 24 hours a sample was removed and diluted with D₂O for ¹H NMR conversion and DMF for SEC molecular weight analysis (table 5.2).

Table 5.2. Polymerisation data for synthesis of eDEGA, mPEGA, NiPAm and copolymers of mPEGA and eDEGA using WSI in DMSO/H₂O (5:1) using [I]:[CuBr]:[Me₆TREN] = 1:0.4:0.4,

Monomer(s)	Target MW (Da)	Conversion % (NMR)	M _n (Da) (SEC)	Đ (SEC)
mPEGA ₄₈₀	7500	100	10200	1.08
mPEGA ₄₈₀ : eDEGA (1:9) (10 % PEGA)	7500	98	10500	1.22
mPEGA ₄₈₀ : eDEGA (1:19) (5 % PEGA)	7500	99	10900	1.31
eDEGA	7500	99	11400	1.37
NiPAm	7500	17	3230	1.91

The polymerisations for eDEGA and mPEGA₄₈₀ (and copolymers of the two) showed quantitative or almost quantitative conversions, with analysis by SEC showing symmetrical and monomodal peaks (figure 5.14). The SEC molecular weight distributions although starting to approach $\bar{D} = 1.4$, remained acceptably narrow, showing some control over the polymerisation. It is, however, evident that upon higher ratios of eDEGA within the copolymer (and for the eDEGA homopolymers) the molecular weight distribution is broadening. The polymerisation of NiPAm was not as successful, with ^1H NMR analysis showing less than 20 % conversion attained after 24 hours, although some presence of polymer peaks was evident within the spectra. SEC analysis shows a bimolecular peak with high molecular weight tailing, theorised to be due to the presence of termination events and a lack of control.

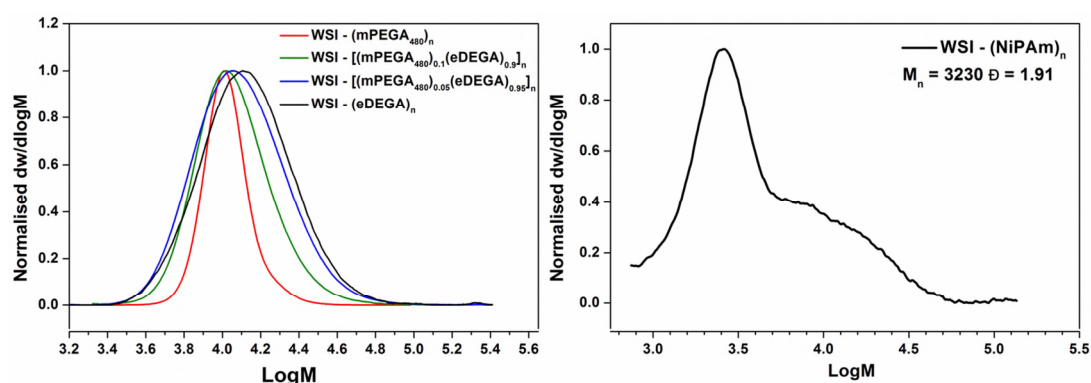


Figure 5.14. SEC analysis of poly[(mPEGA)_x(eDEGA)_{1-x}] for $x = 1, 0.1, 0.05$ & 0 and SEC analysis of synthesis of poly(NiPAm) in DMSO/H₂O.

Acrylamides have previously been successfully synthesised in a controlled manner by utilising the prior disproportionation of Cu(I)Br with *N*-donor aliphatic ligands (such as Me₆TREN) in purely aqueous, mixed aqueous/alcoholic solutions and biologically relevant conditions.^{29,56–58} It would be beneficial to devise a polymerisation system that allows the synthesis of these two different classes of thermoresponsive polymers, which could also utilise a non-water soluble initiator such as the dithiophenolmaleimide initiator.

As a result, the cosolvent in the reaction was changed from DMSO to methanol for the monomer / initiator solution. Again, it is important that full disproportionation was allowed to occur under purely aqueous conditions, prior to the addition of monomer/initiator. Methanol as a cosolvent showed promising behaviour in the polymerisations of OEtOxMA described earlier in this chapter. For all polymerisations [M]:[I] ratios (targeted degrees of polymerisation) were set to 50, and polymerisations were performed on homopolymers of eDEGA and NiPAm and one copolymer of eDEGA and mPEGA.

Table 5.3. Polymerisation data for synthesis of eDEGA, NiPAm and one copolymer of mPEGA and eDEGA using WSI in MeOH/H₂O (5:1) using [I]:[CuBr]:[Me₆TREN] = 1:0.4:0.4.

Monomer(s)	Target MW (Da)	Conversion % (NMR)	M _n (Da) (SEC)	Đ (SEC)
mPEGA ₄₈₀ : DEGA (1:9) (10 % PEGA)	11000	65	7600	1.06
eDEGA	10000	0	-	-
NiPAm	6000	39	3500	1.10

The polymerisations in methanol were not successful and after 24 hours zero conversion was observed for the polymerisation of eDEGA. The addition of an mPEGA monomer improves the polymerisation, resulting in a narrow molecular weight distribution, although the conversion was still much below quantitative. The polymerisation of NiPAm proved more successful than for the analogous polymerisation using DMSO as a cosolvent, with a higher molecular weight attained, and dispersity remaining low (Đ = 1.10), however, the conversion attained was still low (≈ 40 %).

As high conversions are not achieved using methanol as a cosolvent, and due to these unsatisfactory conversions for the synthesis of either of the desired thermoresponsive polymers of poly((mPEGA₄₈₀)(eDEGA)) or polyNiPAm, the solvent system was changed again, this time to ethanol. An alternative initiator ethyl 2-bromoisobutyrate (EBiB) was investigated for polymerisation under these conditions as EBiB has a comparable solubility in ethanol-water solutions to the dithiophenolmaleimide initiator ($\approx 50\%$ water content). The homopolymer of eDEGA was first polymerised, as this has proven challenging under the previous two cosolvent conditions investigated. A targeted DP_n of 50 (9.5 kDa) was synthesised, and after 24 a sample submitted for ^1H NMR showed that the polymerisation had reached 95 % conversion. SEC analysis (DMF) revealed a peak with a narrow dispersity and M_n close to the targeted molecular weight, although there is some evidence of high molecular weight tailing upon inspection of the SEC chromatogram (figure 5.15).

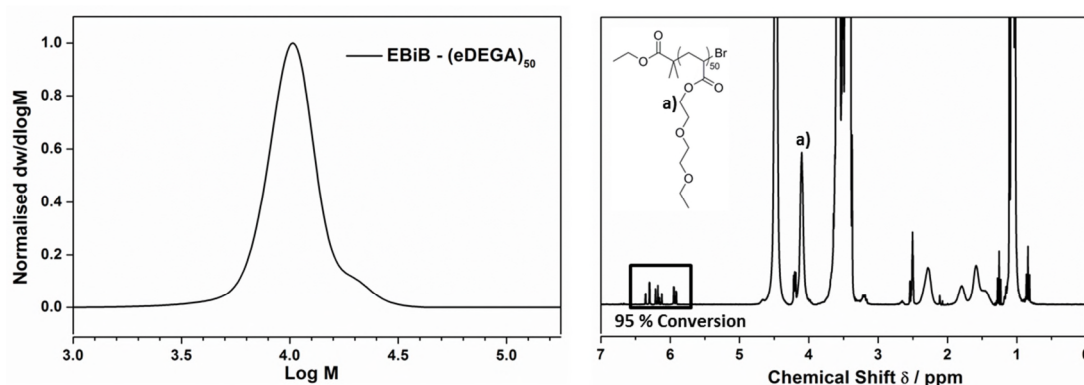
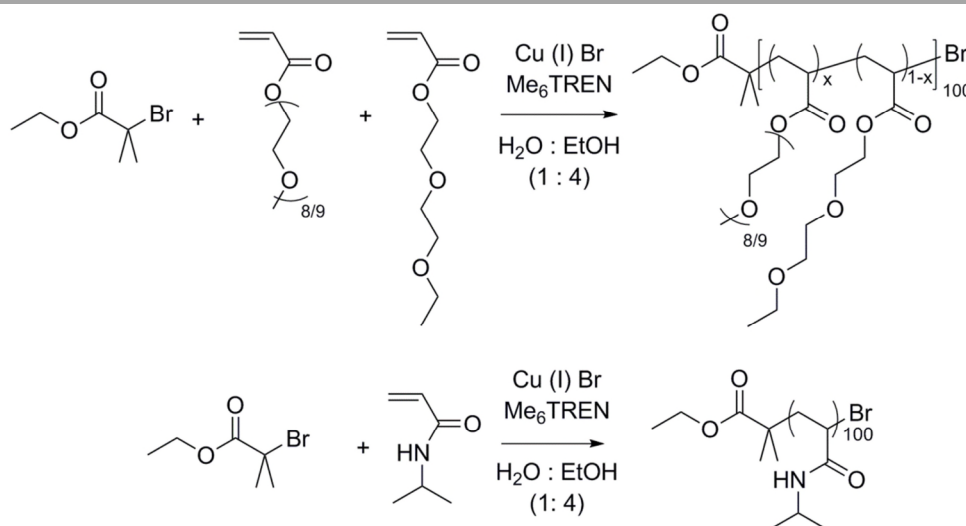


Figure 5.15. SEC (DMF) and ^1H NMR (δ_6 -DMSO) at $t = 24$ hours for homopolymerisation of eDEGA in ethanol/water (4:1).

After a successful polymerisation of eDEGA had been achieved, three different copolymers of eDEGA and mPEGA were synthesised alongside a homopolymer of NiPAm (scheme 5.6). All polymers were synthesised using a monomer: initiator ratios of 100: 1, with samples removed after 24 hours for ^1H NMR conversion and SEC molecular weight analysis data.



Scheme 5.6. Copolymerisation of mPEGA /eDEGA and homopolymerisation of NiPAm in ethanol/water (4:1) using EBiB as initiator ([I]:[M]:[CuBr]:[Me₆TREN] = 1:100:0.4:0.4)

Table 5.4. Polymerisation data for the synthesis of thermoresponsive polymers in ethanol / water (4:1) using EBiB as initiator

Monomer(s)	Target MW (Da)	Conversion % (NMR)	M _n (Da) (SEC)	Đ (SEC)
eDEGA	9500	95	9800	1.12
mPEGA ₄₈₀ : eDEGA (1:4) (20 % PEGA)	24800	97	22100	1.18
mPEGA ₄₈₀ : eDEGA (15 % PEGA)	23400	94	21800	1.12
mPEGA ₄₈₀ : eDEGA (1:9) (10 % PEGA)	21900	95	20100	1.15
NiPAm	11300	97	11400	1.08

For all polymerisations high conversions were attained (> 94 % conversion), including for the polymerisation of NiPAm, the first cosolvent condition to achieve a conversion higher than 50 %. On analysis of SEC data, all molecular weight distributions were narrow (Đ <

1.18) and mono-modal, although there is the presence of some high molecular weight peak tailing for the poly[(mPEGA)_x(eDEGA)_{1-x}] copolymers (figure 5.16).

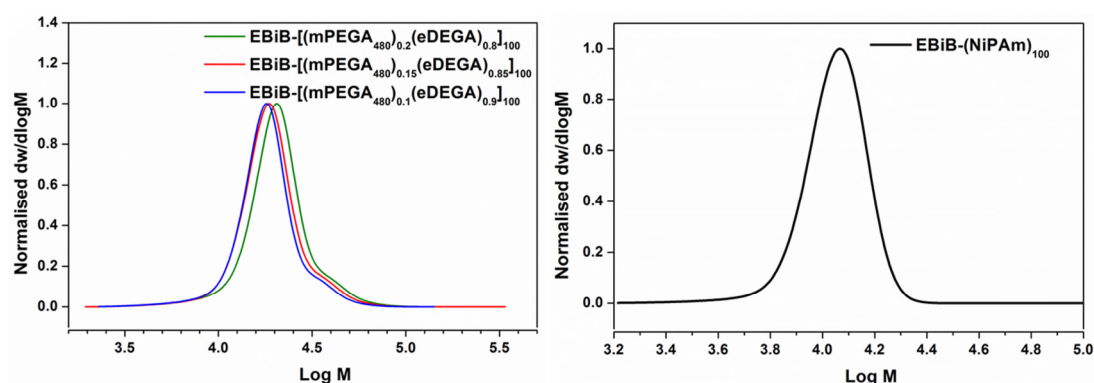


Figure 5.16. SEC analysis of different copolymers of mPEGA and eDEGA, and a NiPAm homopolymer synthesised with EBiB in ethanol/water (4:1).

5.2.1.1. Cloud point measurements

These polymers were then purified by dialysis against water (1 kDa MWCO), and after lyophilisation resulted in colourless oils (poly[(mPEGA)₄₈₀]_x(DEGA)_{1-x}] copolymers) and a white powder (poly(NiPAm)). The polymers were dissolved at a concentration of 1 mg ml⁻¹ in phosphate buffered saline (PBS) and investigated for their cloud point behaviour, by monitoring the absorbance at $\lambda = 500$ nm between 20 °C and 80 °C .

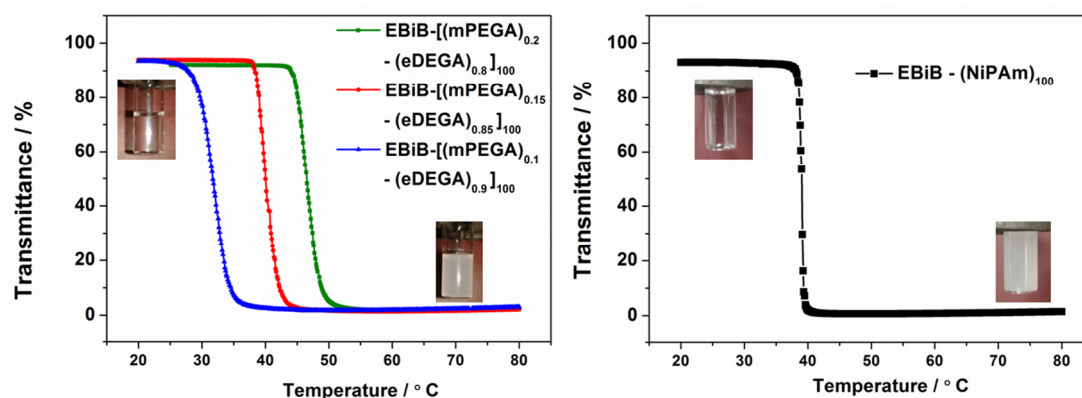


Figure 5.17. Transmittance responses of ethyl end functional thermoresponsive polymers in PBS between 20 °C and 80 °C.

The cloud point was measured as the temperature where the polymer showed a 50 % transmission response on the third heating cycle, where this revealed that all 4 polymers had cloud points within expected regions with all measurements occurring between 30 – 50 °C (figure 5.17). Importantly, the trend for the poly[(mPEGA)_x(eDEGA)_{1-x}] copolymers showed that, as expected, the higher concentration of PEG within the polymer, the higher the observed cloud point. This can be used to tailor polymers for targeting a specific temperature for thermoresponsive behaviour to be observed.

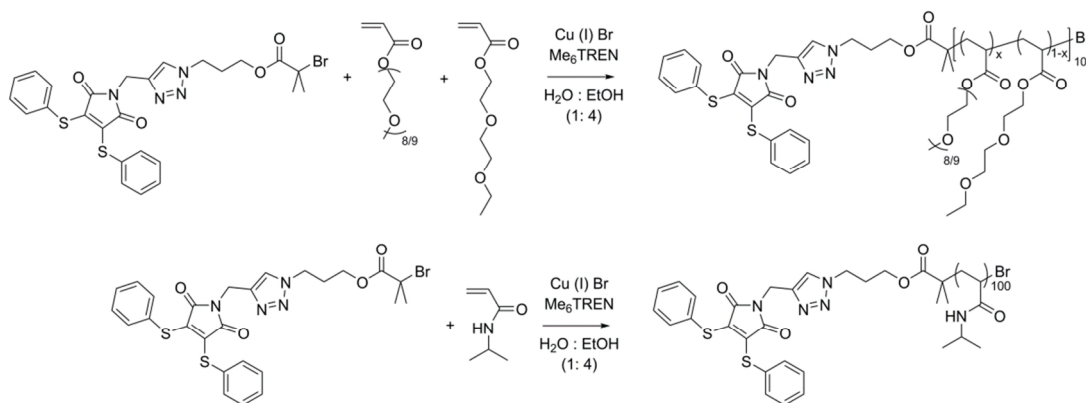
Table 5.5. Molecular weight data and cloud point measurements for 1 mg ml⁻¹ solutions of copolymers of eDEGA and mPEGA and polyNiPAm.

Polymer	M _n (Da) (SEC)	Đ (SEC)	Cloud Point (°C)
EBiB – [(mPEGA ₄₈₀) _{0.2} -(eDEGA) _{0.8}] ₁₀₀	22100	1.18	46.5
EBiB – [(mPEGA ₄₈₀) _{0.15} -(eDEGA) _{0.85}] ₁₀₀	21800	1.12	40.1
EBiB – [(mPEGA ₄₈₀) _{0.1} -(eDEGA) _{0.9}] ₁₀₀	20100	1.15	31.7
EBiB – (NiPAm) ₁₀₀	11400	1.08	39.0

5.2.2. Dithiophenolmaleimide α -end functional polymers with thermoresponsive behaviour

After successful polymerisations of both poly[(mPEGA₄₈₀)(DEGA)] and (poly(NiPAm)) being achieved *via* copper mediated polymerisation in water ethanol mixtures using EBiB as an initiator, the reactions were carried out using the dithiophenolmaleimide initiator for post-polymerisation conjugation. Three different polymers were synthesised, polyNiPAm and two copolymers of mPEGA and eDEGA, containing 10 and 20 % mPEGA respectively. The

degree of polymerisation was targeted at 100, using 0.4 eq. of CuBr and Me₆TREN and approx. 80 wt % of the mixed solvents, with the polymerisations carried out at 25 °C (scheme 5.7).



Scheme 5.7. Polymerisation reactions for synthesis of copolymers of eDGA and mPEGA and a homopolymer of NiPAm using dithiophenolmaleimide initiator in EtOH/H₂O (4:1).

After 24 hours the reactions were sampled for ¹H NMR (δ₆-DMSO) conversion analysis which highlighted that the majority of the monomer(s) had disappeared with high conversions (> 95 %) for all three polymerisations. SEC analysis (DMF) revealed the synthesis of controlled polymers maintaining narrow and mono-modal molecular weight distributions (Đ < 1.25) (figure 5.18). The nature of this initiator gives rise to highly coloured (yellow-orange) polymerisation solutions and resulting polymers, signifying the incorporation of dithiophenolmaleimide α-end group functionality. This is evident by analysis of the SEC UV detector chromatogram where, a coincidental peak is observed to the RI detector, suggesting a highly UV active polymer at this molecular weight.

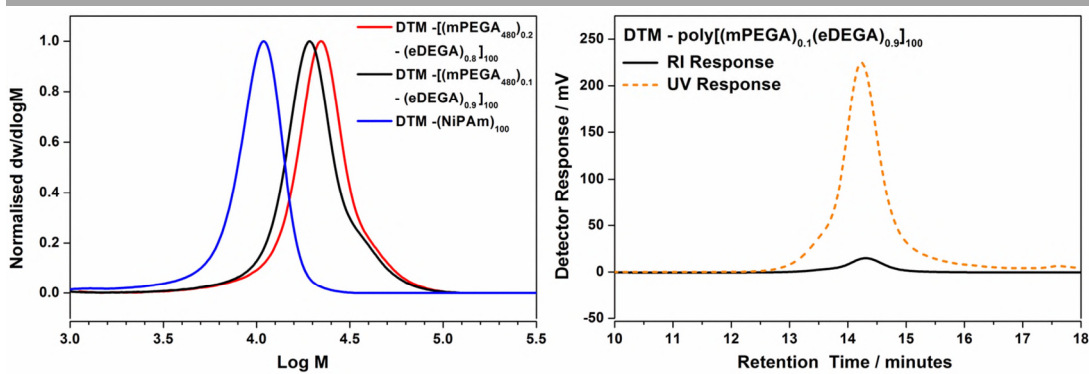


Figure 5.18. SEC (DMF) analysis of DTM functional thermoresponsive polymers synthesised in EtOH/H₂O (4:1).

Table 5.6. Polymerisation data for synthesis of thermoresponsive dithiophenolmaleimide polymers

Monomer(s)	Target MW (Da)	Conversion % (NMR)	M _n (Da) (SEC)	Đ (SEC)
mPEGA ₄₈₀ : eDEGA (1:4) (20 % PEGA)	24800	88	19800	1.19
mPEGA ₄₈₀ : eDEGA (1:9) (10 % PEGA)	21900	90	18500	1.23
NiPAm	11300	98	9200	1.12

The polymers were purified by dialysis against water (3.5 kDa MWCO, 3 days) and after lyophilisation this resulted in two strongly coloured yellow oils (mPEGA₄₈₀-eDEGA copolymers) and a yellow powder (polyNiPAm). NMR analysis of the polymers revealed that the dithiophenolmaleimide end group was still present, where the aromatic peaks of the phenol groups and the triazole within the end group are clearly identifiable (figure 5.19). This confirms that the polymer still retains the conjugatable functionality required for the post-polymerisation disulfide bridging conjugation of the peptide.

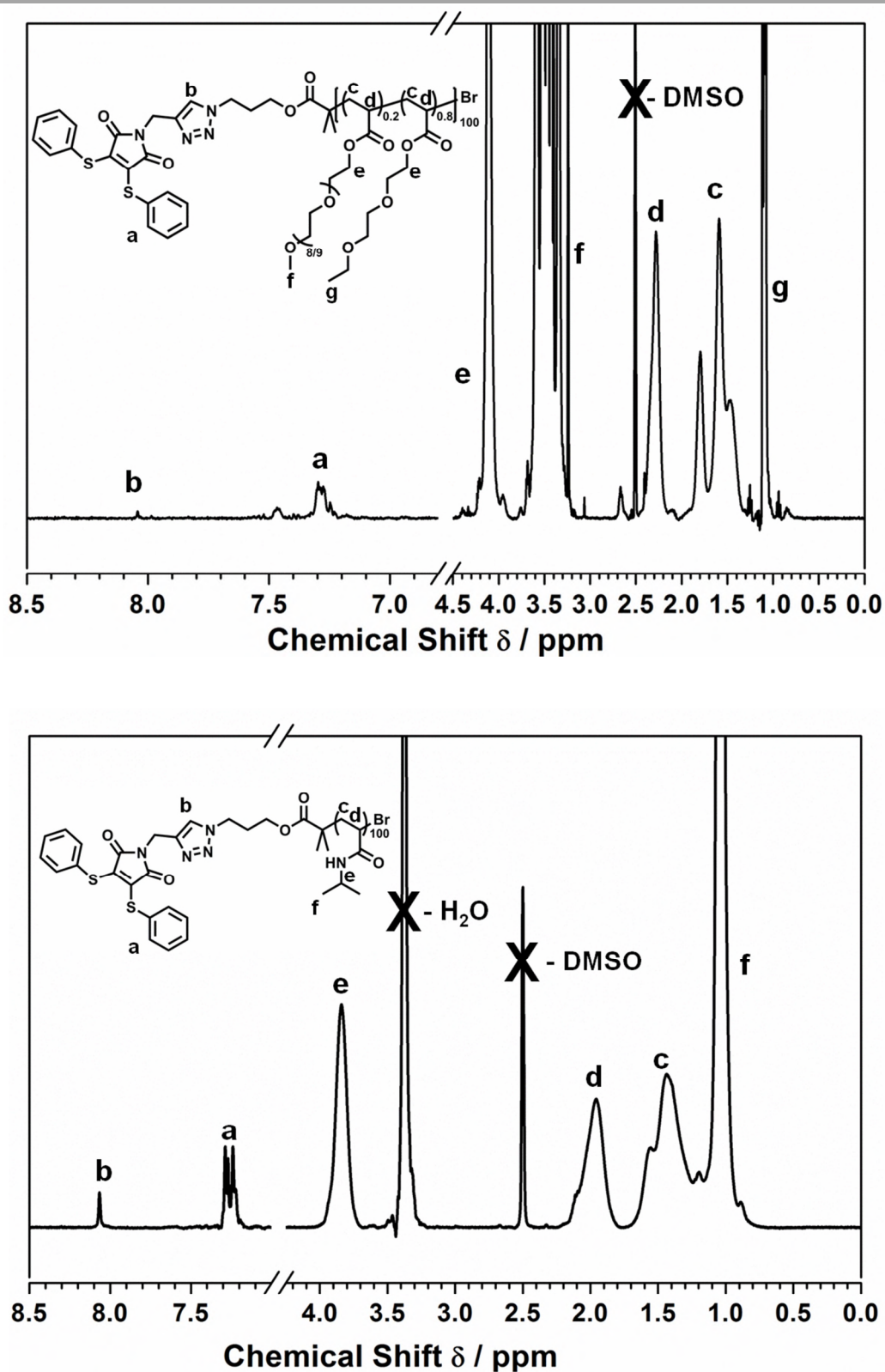


Figure 5.19. ^1H NMR (δ_6 - DMSO) of purified DTM- poly[(mPEGA)_{0.2}(eDEGA)_{0.8}] and DTM- poly(NiPAm)₁₀₀ showing presence of α -DTM functionality.

5.2.2.1. Cloud point measurement of dithiophenolmaleimide polymers

Similar cloud point measurements were undertaken for the dithiophenolmaleimide end functional thermoresponsive polymers as for the polymers initiated with EBiB, where similar behaviour was observed (figure 5.20). For the dithiophenolmaleimide functional poly(NiPAm)₁₀₀ the transmittance does not initially start at 100 %, but at 72 % in the cloud point measurements. This relates to a starting absorbance of 0.14, suggesting that the polymer was not entirely soluble, although there is still the observation of LCST behaviour for which a cloud point can be evaluated.

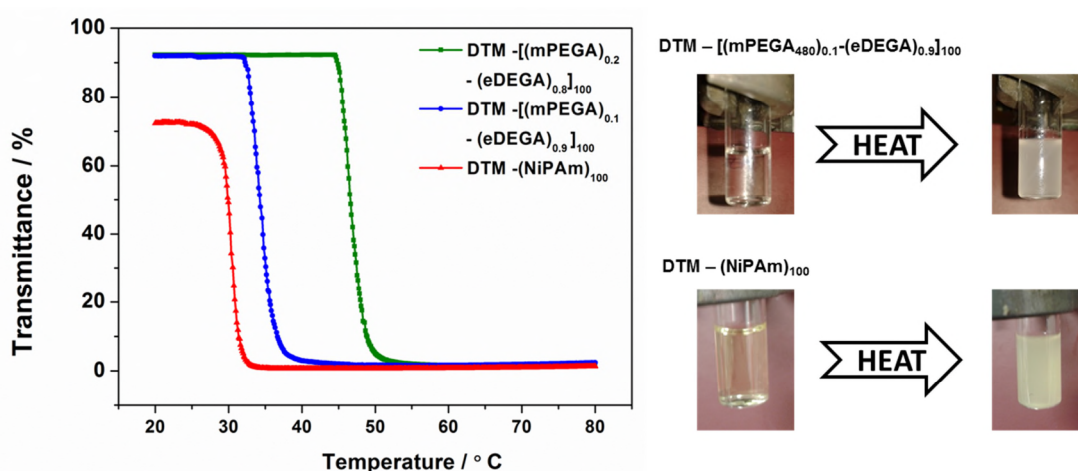


Figure 5.20. Transmittance of thermoresponsive DTM functional polymers between 20 °C and 80 °C, and photographs of polymer solutions below and above cloud point.

The cloud point measurements of the α -end functional dithiophenolmaleimide polymers are similar to those measured for those same polymers initiated with EBiB. The expected trend was observed where the cloud point measured increased on increasing the amount of mPEGA in the PEG-DEG copolymers, and all results are within 30 °C – 50 °C. The cloud point measured for poly(NiPAm) differs by the highest margin from 39.0 °C (EBiB) to 30.0 °C (DTM), likely due to an increase in the hydrophobicity of the polymer after addition of

the DTM α -end group functionality. However, results for these and for the 9:1 ratio of eDEGA:mPEGA are both consistent with a bio relevant region cloud point temperature (approximately 37 °C).

Table 5.7. Cloud point measurements of DTM α -end functional thermoresponsive polymers.

Polymer	M_n (SEC, Da)	\bar{D} (SEC)	Cloud Point (°C)
DTM – [(mPEGA ₄₈₀) _{0.2} -(eDEGA) _{0.8}] ₁₀₀	19800	1.19	46.6
DTM – [(mPEGA ₄₈₀) _{0.1} -(eDEGA) _{0.9}] ₁₀₀	18500	1.23	34.3
DTM – (NiPAm) ₁₀₀	9200	1.12	30.0

5.2.3. Disulfide bridging conjugation of thermoresponsive polymers onto oxytocin

The conjugation reaction of the synthesised dithiophenolmaleimide end functional poly[(mPEGA₄₈₀)(eDEGA)] and poly(NiPAm) were carried out in the same manner as for the poly(PEG) conjugations described in chapter 3. Initially the conjugations were performed using the ‘without purification/*in-situ*’ method through which, after firstly reducing the disulfide bond of oxytocin using TCEP, an aliquot of the polymerisation solution is added to rebridge the two sulfhydryl residues with the unpurified polymer. After 24 hours the reactions were analysed by RP-HPLC, although there was no appearance of a conjugate peak by either UV or fluorescence. The experiments were repeated again using the same polymers, but with prior purification, before addition to the reduced peptide solution. Analysis by RP-HPLC again showed no appearance of conjugate peaks, or corresponding fluorescence as expected within these conjugations. Analysis of the non-

conjugated polymer under the same conditions also did not show any obvious polymer peaks, possibly indicating that it could be due to the thermoresponsive nature of the polymers (figure 5.21). The standard HPLC conditions used for analysis of the conjugates involve the use of a column oven heated to 25 °C. To counter any potential heat effects, RP-HPLC analysis was instead performed where the column was cooled to 10 °C. At this temperature, there was no change to the chromatogram, and there was still no observation of peaks in the UV or fluorescence that might be related to either the dithiophenolmaleimide polymer or the oxytocin-polymer conjugate.

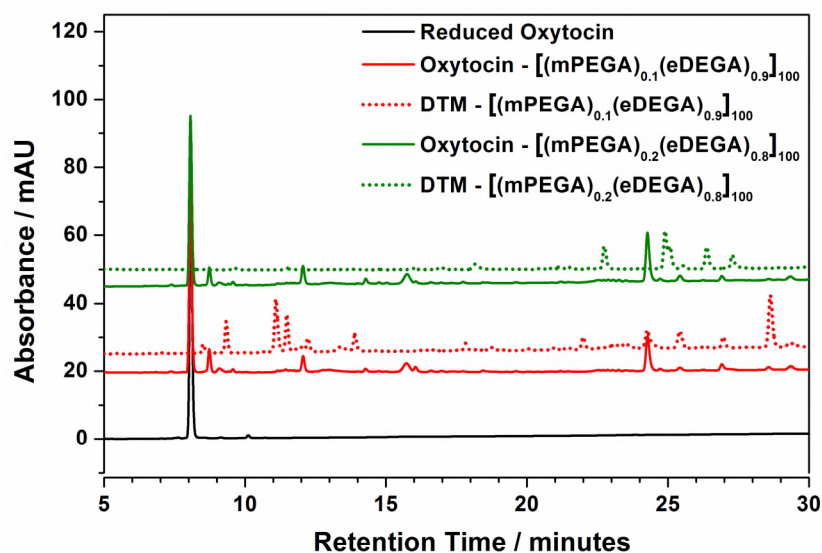


Figure 5.21. RP-HPLC analysis (UV, $\lambda = 280$ nm) of oxytocin conjugation of purified DTM-poly[(mPEGA)_x(eDEGA)_{1-x}]₁₀₀.

A different approach was then pursued where the native peptide and polymer are added together, before adding the reducing agent, hence the disulfide bond is still maintained in the structure. It was hoped that once the reducing agent is added, as the disulfide bond breaks, there is a very large excess of the dithiophenolmaleimide functional polymer and disulfide bridging should occur immediately. This method has previously been utilised in the disulfide bridging of Somatostatin, and prevents potential negative effects on peptide structure by limiting the amount of time the cysteine residues are free.⁵⁹ The solution was

then allowed to stir for 24 hours before sampling for RP-HPLC analysis, which did not show the appearance of any conjugate peaks or any corresponding fluorescence. The chromatograms were very similar to those observed by conjugation with prior reduction of the disulfide bond and made confirmation of conjugation very difficult.

The poly[(mPEGA₄₈₀)_x(eDEGA)_{1-x}] conjugation reactions with pre-reduction of the disulfide bond were repeated, focusing on the concentration of samples for RP-HPLC, paying particular attention to the native peptide. This showed that upon conjugation there is a significant decrease in the concentration of oxytocin after addition of the polymers (poly[(mPEGA₄₈₀)_x(eDEGA)_{1-x}] : 72 % reduction of oxytocin remaining in reaction solution, independent of comonomer ratio) (figure 5.22). This suggests that some form of peptide reaction is taking place, as the native peptide has largely been consumed, perhaps from the conjugation of polymers across the disulfide bond.

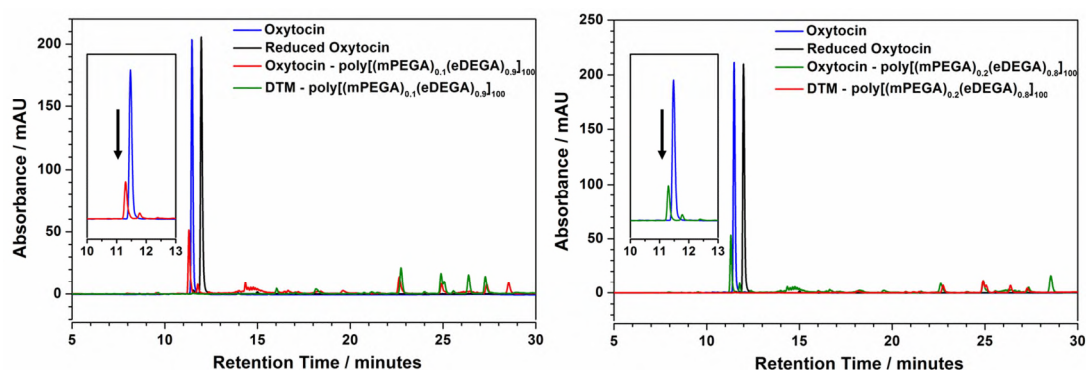


Figure 5.22. RP-HPLC analysis of oxytocin conjugation of DTM-poly[(mPEG)_x(eDEGA)_{1-x}], specifically focussing on consumption of peptide.

5.2.3.1. Conjugation of statistical copolymers of mPEGA₄₈₀ – eDEGA onto a different peptide: Salmon calcitonin

Following on from the uncertainty and limitations of the RP-HPLC data as to the extent of polymer conjugation onto oxytocin, an alternative small peptide, salmon calcitonin (sCT),

was investigated as a conjugation target. sCT is a 32 amino acid hormone currently used in the treatment of some bone conditions, including osteoporosis and hypocalcaemia. Both dithiophenolmaleimide and dibromomaleimide small molecules and polymers have previously been efficiently conjugated onto sCT.^{60,61} Similarly to oxytocin, sCT contains one disulfide bridge (Cys¹ – Cys⁷) although, due to the increased size of the polypeptide, it also contains an alpha helix chain that adds structural rigidity.

After complete reduction of the disulfide bond with TCEP, as observed by RP-HPLC, the two different ratio DTM-[(mPEGA₄₈₀)_x(eDEGA)_{1-x}] polymers were added to the peptide in pH 6.2 phosphate buffer (100 mM). Analysis of the reaction mixtures after 24 hours and after 5 days revealed that there was no observed presence of a new conjugate peak, or any corresponding fluorescence, as observed for the conjugation with oxytocin. There was, however, also a significant decrease in the peak representative of the native peptide in both samples, suggesting some consumption of the native peptide (figure 5.23). This decrease in sCT was represented by a peptide concentration change of 35 – 40 % which, although less than observed for the conjugation with oxytocin, still represents a significant disappearance of native peptide.

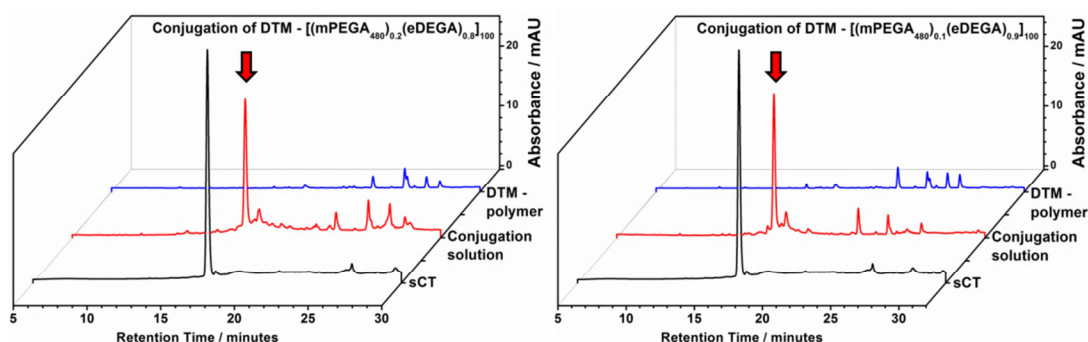


Figure 5.23. RP-HPLC analysis of disulfide bridging conjugation of DTM-[(mPEGA)_x(eDEGA)_{1-x}] onto sCT.

5.2.3.2. Further characterisation of oxytocin conjugated thermoresponsive polymers.

As the disulfide bridging peptide conjugations of the thermoresponsive polymers did not show any obvious peak appearances signifying conjugation by RP-HPLC analysis under any of the conditions tested to either of the peptides investigated, further methods of characterisation had to be developed. The disappearance of the peptide peak observed by RP-HPLC for both oxytocin and salmon calcitonin suggests that some reaction has taken place, consuming the peptide in its native form; however, this cannot be confirmed using the usual HPLC analysis methods.

A close inspection of the conjugation reaction revealed that a moderate colour change could be observed within the first few minutes of addition of the yellow polymer to the reduced peptide (figure 5.24). The DTM polymer has a high intensity yellow colour, which can be observed before addition to the reduced peptide. On stirring at ambient temperature for a few minutes this colour starts to disappear significantly, leaving a solution that is still yellow, but with a less intense colour.

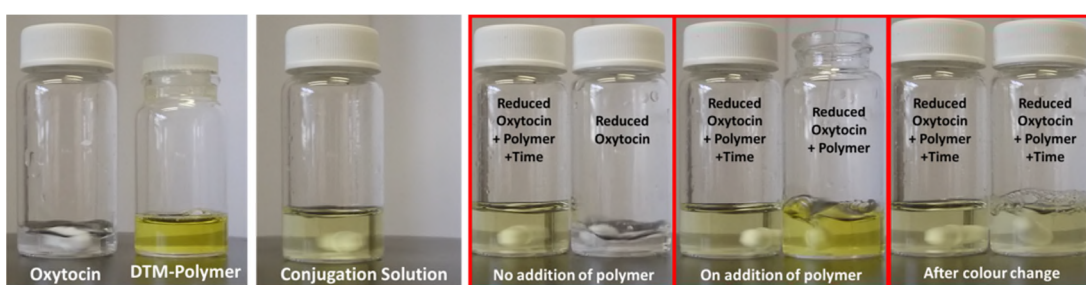


Figure 5.24. Images showing colour change from the bright yellow of the dithiophenolmaleimide polymer to a less intense colour, observed during the conjugation reaction.

Another characterisation method for the conjugation of disubstituted maleimide polymers is UV-vis spectroscopy.⁶² The UV absorption of the maleimide unit is known to change wavelength depending on the thiol functionality, and this was observed in chapter 3 for the characterisation of dibromo- and dithiophenolmaleimide PEGs upon conjugation to oxytocin. When the polymer contains the dithiophenolmaleimide end group a characteristic peak is observed at $\lambda \approx 420$ nm whereas this peak shifts to $\lambda \approx 390$ nm upon conjugation, due to loss of the aromatic functionality. The UV absorbance within this region was investigated for the two DTM-[(mPEGA)₄₈₀]_x – (eDEGA)_{1-x}] polymers, upon addition to disulfide bridged solutions of both oxytocin and salmon calcitonin, where similar behaviour was observed for each (figure 5.25).

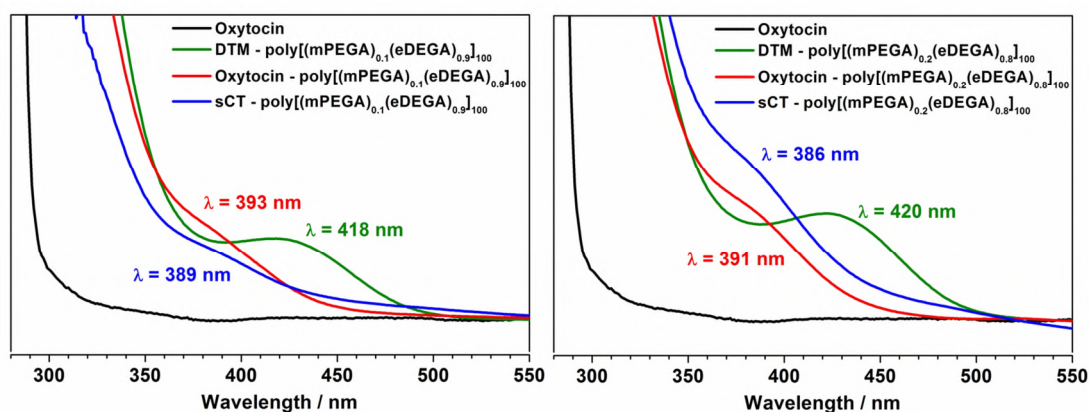


Figure 5.25. UV shifts of DTM functional poly[(mPEGA)_x(eDEGA)_{1-x}] and upon addition to reduced sCT and oxytocin.

This highlights that the α -end group functionality of the polymers is changing from that of the dithiophenolmaleimide, and this potentially indicates that the peptide has successfully undergone polymer conjugation. The same result being observed for both peptides suggests that the disulfide bridge has been reacted in the same manner, as the UV wavelength after conjugation would be expected to be similar for both.

Another possible method of analysis for the confirmation of conjugation of the dithiophenolmaleimide polymers onto oxytocin is the use of SEC, to observe changes in the average molecular weight, or molecular weight distributions, of the polymers before and after conjugation. For the conjugation of polymers onto oxytocin the increase in molecular weight of the polymer upon conjugation is only anticipated to be 1007 Da (the molar mass of oxytocin), as conjugation is singular and site specific. During the reaction, however, there was an excess of polymer added, and this combined with the reaction not going to 100 % completion would result in the presence of the dithiophenolmaleimide polymer alongside any potential peptide conjugate. On SEC analysis of the native peptide, a higher molecular weight distribution is observed than anticipated (theoretical: 1 kDa; SEC: 1.6 kDa) due to the differences between the hydrodynamic volume of oxytocin and the PMMA calibrants.

SEC analysis of the conjugation of both DTM α -end functional NIPAm and poly[(mPEGA)-co-(eDEGA)] reveals an increase in molecular weight after the conjugation reaction has been undertaken (figure 5.26). The chromatogram of the 'conjugate' shows the appearance of bimodal behaviour, which would suggest a peak of larger molecular weight, alongside the remaining unconjugated polymer. It is known that these reactions are not 100 % efficient, as some peptide can still be observed by RP-HPLC and therefore a significant amount of the DTM functional polymer remains in the solution. The appearance of the higher molecular weight species in the solution, however, is significant in proving the formation of peptide polymer conjugate. Overall this appears to further confirm that some conjugation has occurred, leading to a higher molecular weight species.

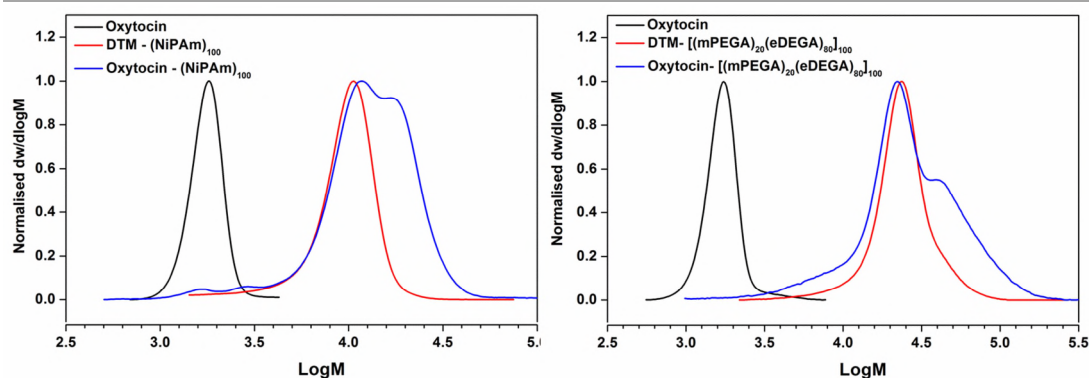


Figure 5.26. SEC analysis of DTM functional thermoresponsive polymers before and after disulfide bridging conjugation of oxytocin.

5.2.4. Thermoresponsive polymer conjugates

conclusions

Several polymers with thermoresponsive properties can be synthesised by copper mediated polymerisations with functionality capable of undergoing post-polymerisation conjugation. The aqueous disproportionation of Cu(I)Br is tolerant of aromatic end groups and the use of co-solvents, (even at 80 % organic) allowing the controlled synthesis of the desired thermoresponsive polymers. The cloud point behaviour for copolymers of mPEGA₄₈₀ and eDEGA can be tuned by altering the ratio between the comonomers to achieve a specific temperature range under which a soluble to non-soluble transition may occur.

Although the traditional characterisation method used throughout this thesis for the conjugation of polymers onto peptides has been through the observance of conjugate peaks on RP-HPLC, for these polymers, no conjugate peaks were observed. Instead a variety of different characterisation techniques have been evaluated for providing evidence of potential conjugation onto the peptide. Visual observances of the solutions,

and peak shifts by UV spectroscopy suggest that the maleimide functionality at the α -end of the polymer chain has undergone some substitution. There is a large consumption of peptide observed by RP-HPLC suggesting that a reaction has taken place, whether by conjugation or otherwise, and this was observed for two different small disulfide bond containing peptides. Increases in molecular weights observed by SEC analysis also suggest that some conjugation has occurred, leading to higher molecular weight species, although there is still evidence of high amounts of unreacted polymers.

5.3. Glycopolymers

The synthesis of polymers featuring carbohydrate functionalities is an ever-expanding area within polymer science, which consistently generates high interest within various biological, biomedical and biomaterials fields. The tailored, well-defined incorporation of saccharide functionalities, such as in glycopolymers or glyconanomaterials, can be prepared with an aim to mimic nature for the use in a variety of bio-related applications, particularly with regards to biomolecular recognition.

The ability to prepare precision glycopolymers containing pendant carbohydrate functionalities has been particularly accessible since the development of controlled polymerisation methods. A variety of different carbohydrate based monomers (consisting of acetylated or deprotected functionality) are available incorporating acrylate, methacrylate, acrylamide and vinyl ester groups as required. These have previously been successfully polymerised by NMP, RAFT, ATRP and SET-LRP, resulting in a variety of saccharide containing polymers of different compositions and architectures.

The attachment of glycopolymers onto peptides or proteins allows the synthesis of new types of biomolecules to be prepared, usually with a particular application or function

targeted. The usual method for synthesis of biomolecule conjugates of glycopolymers is first the synthesis of the polymer to contain desired saccharide functionality followed by post-polymerisation modification with the biomolecule, resulting in polymer attachment. Glycopolymer-biomolecule conjugates have previously been prepared by utilisation of a variety of different pendant saccharide functionalities (including monosaccharide, disaccharide and trisaccharides) with a variety of different biomolecule conjugation targets. Biotin terminated glycopolymers have been prepared *via* different polymerisation techniques (including controlled polymerisation techniques RAFT & ATRP), which, post-polymerisation, could be used to conjugate to streptavidin alongside other proteins or surfaces.^{63–67} Maynard *et al.* prepared glycopolymer conjugates by RAFT which utilised pendant trehalose functionalities that, when conjugated onto lysozyme, were proven successful in improving protein stability to thermally stressing and lyophilisation cycles.^{68,69} Glycopolymer conjugates utilising different sugar functionalities have also been synthesised which have induced or amplified immune responses.^{70,71} The conjugation of glycopolymers onto small peptides have also been described, including the synthesis of pyridyldisulfide end functional glycopolymers by RAFT polymerisation followed by subsequent conjugation onto the tripeptide glutathione. After peptide conjugation, specific carbohydrate - protein recognition is achieved to the protein Concanavalin A alongside the incorporation of antioxidant activity.⁷²

Within this final sub-chapter the synthesis and subsequent copper mediated polymerisation of a previously utilised mannose containing macromonomer is described. Dithiophenolmaleimide α -end group functionality can be easily incorporated as previously described in this thesis, and used to rebridge an internal disulfide bond within a peptide (in this case the model peptide salmon calcitonin). The relatively simple and controlled polymer synthesis and conjugation show a facile route to the synthesis of peptide-

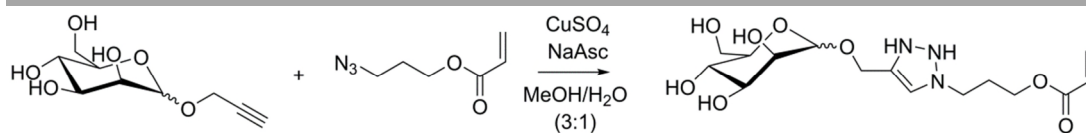
glycopolymer conjugates, which after conjugation also exhibit fluorescence as a smart labelling tool for confirmation of carbohydrate functional maleimide bridging.

5.3.1. Synthesis of α -end functional glycopolymers

5.3.1.1. Synthesis of sugar monomers

The synthesis of acrylate functional monosaccharide monomers have previously been described and used directly for copper mediated controlled radical polymerisation.⁷³ Utilising monomers without the requirement for protecting groups on the sugar can be beneficial as controlled polymerisations can occur without extensive post-polymerisation functionalisation. This results in a polymer that has pendant carbohydrate functionality along the (non-carbohydrate) backbone chain, where the saccharides along the chain can be designed and selected to suit the purpose or application, maintaining some of the sugar-specific binding characteristics.

For the synthesis of mannose functional acrylate monomers the monosaccharide was firstly functionalised to contain an alkyne group using Fischer-glycosylation (utilising H_2SO_4 immobilised on silica gel as a highly effective catalyst for the reaction).⁷⁴ The reaction was performed neat using a five-fold excess of propargyl alcohol which specifically and singularly functionalises the hydroxyl at the anomeric position, although this does lead to a mixture of the α and β product. The exact ratio can be calculated, and the two anomers separated, if desired, by carrying out hydroxyl protection chemistry and separation. Following sugar functionalisation the glycomonomer is synthesised by the copper(I) catalysed azide alkyne ‘click’ reaction (CuAAC) between this alkyne functional mannose and an azide functional acrylate monomer, which has previously been reported for direct polymerisation by ATRP.⁷⁵



Scheme 5.8. Synthesis of mannose glycomonomer.

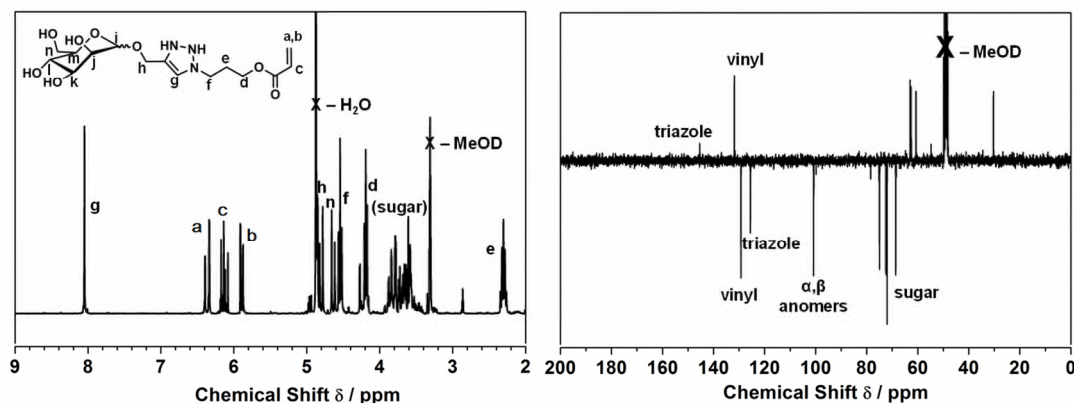


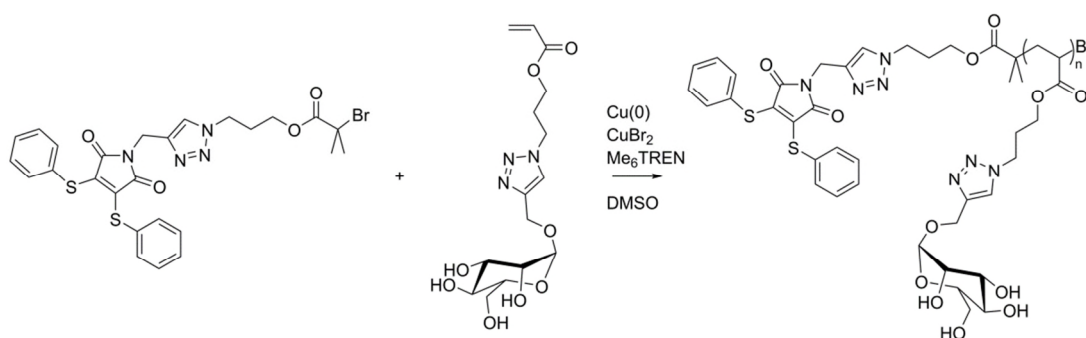
Figure 5.27. ^1H and ^{13}C NMR (MeOD) of mannose functional glycomonomer.

^1H NMR (MeOD) clearly shows the appearance of vinyl peaks ($\delta = 5.8 - 6.5$) associated with the acrylate functional monomer, additional to the mannose sugar peaks ($\delta \approx 3.5 - 4.0$ ppm) and the characteristic peak of the triazole ring ($\delta = 8.05$ ppm) (figure 5.27). The monomer synthesis results in an excess of the α -anomer with respect to the β -anomer, although both products are still present.

5.3.1.2. SET-LRP of glycopolymers

Previously these mannose functional glycomonomers have successfully undergone copper mediated living radical polymerisation, resulting in the controlled formation of polymers containing pendant sugar functionalities. Haddleton *et al.* utilised this for the synthesis of copolymers, wherein the sugar unit within each block could be tailored with the addition of different glycomonomers (in this case mannose, glucose or fucose), resulting in a degree of sequence control within the polymers.⁷³

Using the dithiophenolmaleimide initiator previously described in chapter 3, and earlier within this chapter, the direct copper mediated polymerisation of the described mannose glycomonomer resulting in α -end functionality capable of undergoing disulfide bridging peptide conjugation was performed. These reactions were carried out in DMSO using Cu(II)Br_2 , Cu(0) wire and Me_6TREN as ligand ($[\text{I}]:[\text{Me}_6\text{TREN}]:[\text{CuBr}_2] = 1:0.18:0.1$). As with the other DTM polymer syntheses described previously, the solutions during polymerisation remained a bright orange-yellow colour throughout due to the presence of the dithiophenolmaleimide initiator. Two different $[\text{M}]:[\text{I}]$ ratios were used for the synthesis of two different molecular weights of polymer: 7.5 kDa (DP_n 20) and 15 kDa (DP_n 40).



Scheme 5.9. Polymerisation of mannose monomer with DTM initiator in DMSO ($[\text{I}]:[\text{Cu(II)Br}_2]:[\text{Me}_6\text{TREN}] = 1:0.1:0.18$, 5 cm Cu(0) wire).

After 24 hours the polymerisations were sampled for ^1H NMR conversion analysis (δ_6 -DMSO) and SEC molecular weight data (DMF) (figure 5.28). Conversions were calculated by comparing the vinyl groups ($\delta = 5.5 - 6.5$ ppm) with the peak from the triazole ring ($\delta = 8.1$ ppm) on the monomer or alternatively the first CH_2 group in the monomer next to the acrylate polymer backbone ($\delta = 4.0$ ppm). Although full monomer consumption was not attained (DP_n 20 = 87 %; DP_n 40 = 95 %), high conversions were reached with the appearance of characteristic polymer peaks in the NMR spectrum. SEC analysis of the polymers showed mono-modal molecular weight distributions with low dispersities

attained ($\bar{D} < 1.15$) suggesting that the polymer synthesis remained controlled. The molecular weights (M_n) given by SEC were slightly different from those targeted, particularly for the low molecular weight polymer, but this is largely due to the differences in the structure between the glycopolymer, and the PMMA calibrants. This results in a large difference observed for the hydrodynamic volume within the DMF solvent, potentially due to the hydrophilic nature of the glycopolymer resulting from the large number of hydroxyl groups present.

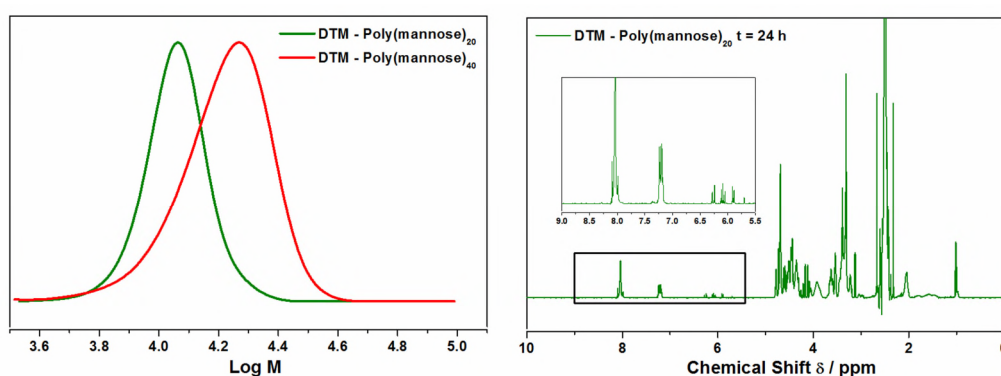


Figure 5.28. SEC (DMF) chromatograms and ^1H NMR analysis of polymerisation of mannose glycomonomers with dithiophenolmaleimide initiator after 24 hours.

Table 5.8. Molecular weight and conversion data for dithiophenolmaleimide end functional poly(mannose)

Entry	Target MW (Da)	Conversion (NMR)	M_n (Da) (NMR)	M_n (Da) (SEC)	\bar{D} (SEC)
Glycopolymer 1 DP_n 20	7500	87 %	6600	10200	1.09
Glycopolymer 2 DP_n 40	15000	95 %	15000	15500	1.14

The polymers were purified by dialysis against water (1 kDa MWCO, 3 days) and after lyophilisation the products were obtained as yellow powders. ^1H NMR analysis of the

polymer confirmed the presence of the dithiophenolmaleimide end groups with aromatic peaks in the region ($\delta = 7.20 - 7.35$ ppm), with a small peak representing the triazole peak from the initiator ($\delta = 8.05$ ppm) appearing next to the larger triazole peak of the monomer ($\delta = 8.10$ ppm) (figure 5.29). By comparison of these aromatic thiophenol peaks with the triazole peak of the monomer (taking into consideration this triazole peak on the initiator) the average DP_n for each polymer were calculated as 16 and 39 respectively. This yielded experimental molecular weights of 6.6 kDa and 15 kDa, which were consistent with the molecular weights targeted.

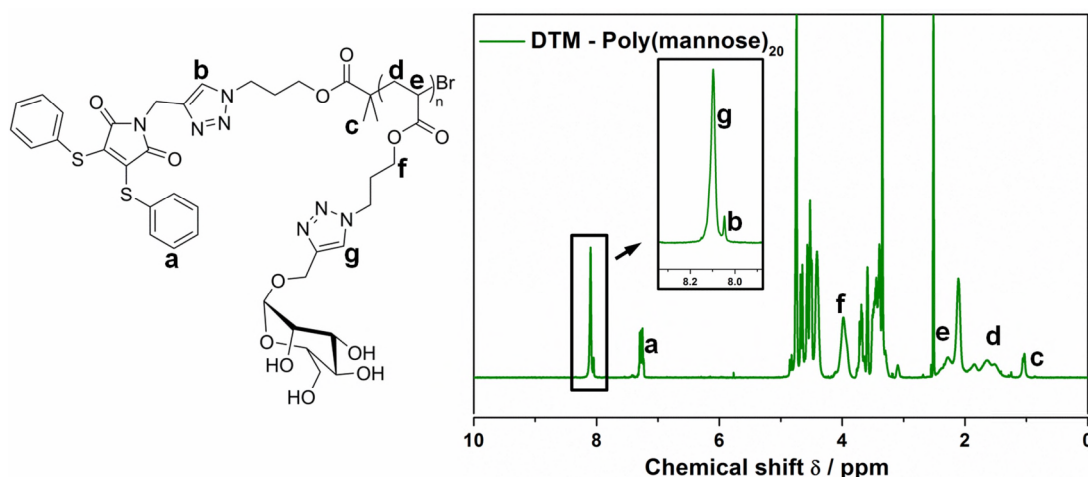


Figure 5.29. ¹H NMR analysis (δ_6 -DMSO) of purified dithiophenolmaleimide α -end functional poly(mannose).

As a comparison, poly(mPEGA₄₈₀) (DP_n 50) was synthesised under the same conditions with the DTM initiator (DMSO with 5 cm Cu(0) wire, [I]:[M]:[Cu(II)Br₂][Me₆TREN]: 1:50:0.1:0.18). After 24 hours the conversion by ¹H NMR was 87 % and analysis by SEC revealed an M_n of 21000 and dispersity of 1.18. The conversion is less than in previously described work (the conditions used here are different to those previously described for the synthesis of DTM-poly(mPEGA₄₈₀) in chapter 3), but a controlled synthesis was still attained, with narrow and mono-modal molecular weight distribution. The triazole peak

and aromatic peaks of the DTM initiator can still be observed on the α -end of the polymer, therefore it is available for post-polymerisation disulfide bridging conjugation (figure 5.30).

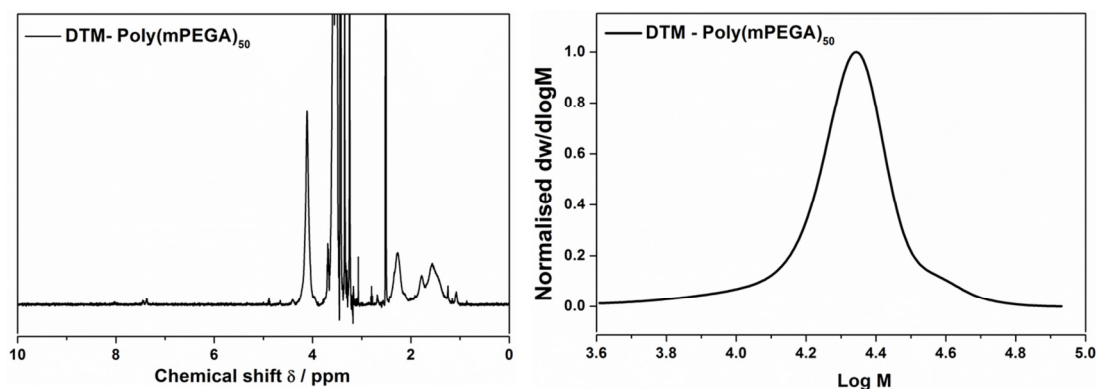
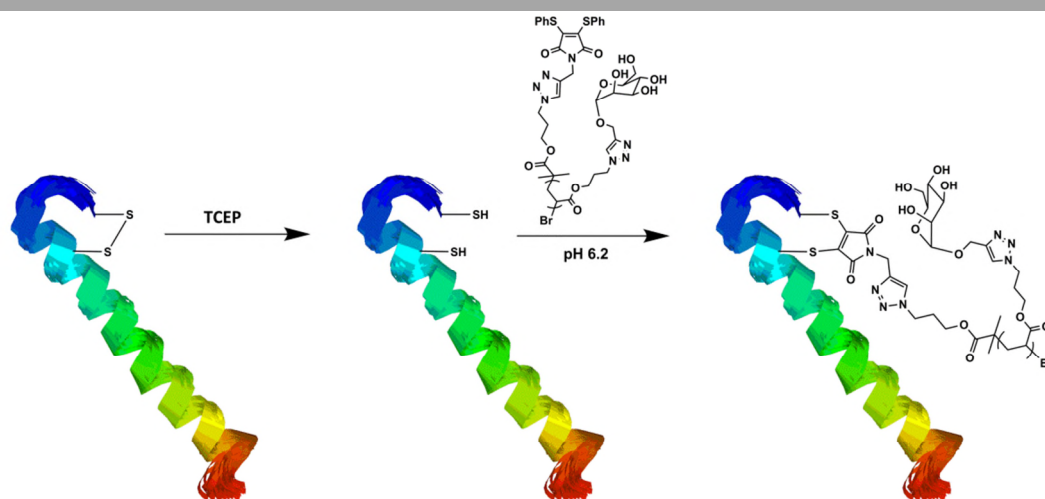


Figure 5.30. ^1H NMR (δ_6 DMSO) and SEC (DMF) of purified dithiophenolmaleimide α -end functional poly(mPEGA₄₈₀)₅₀.

5.3.2. DTM-poly(mannose) and DTM-poly(mPEGA) disulfide bridging conjugation

A model peptide (salmon calcitonin, sCT) was utilised to evaluate the success of conjugation of glycopolymers using dithiophenolmaleimide disulfide bridging chemistry, as sCT has previously been reported for polymers synthesised with a similar initiator by ATRP.⁶¹ This was performed in a very similar manner to the disulfide bridging conjugations described for the PEGylation of oxytocin in chapter 3 and the synthesis of thermoresponsive conjugates of oxytocin or sCT described earlier in this chapter. The reduction of the disulfide bridge to yield two free sulfhydryl groups was achieved using TCEP, with complete reduction within 30 minutes, as monitored by RP-HPLC. After this reduction was observed, the pH of the solution was adjusted using phosphate buffer (pH 6.2, 100 mM) and the glycopolymer was added.



Scheme 5.10. Disulfide bridging conjugation of DTM glycopolymer onto sCT.

The conjugation reaction was allowed to proceed overnight at ambient temperature after which a sample was removed for analysis by RP-HPLC. This revealed a shift in the retention time of the broad polymer peak as well as the appearance of coincidental fluorescence which was not present in the unconjugated polymer. As observed in previous work, as the maleimide functionality on the end group of the polymer changes from dithiophenol to dithioalkyl (where the peptide is acting as a long alkyl chain), fluorescence is induced within the conjugate structure which had previously been quenched by the presence of the aromatic groups.⁷⁶ Also observed in the RP-HPLC spectrum is the appearance of a new sharp peak at retention time $t = 25.4$ minutes, which is attributable to the thiophenol that is substituted away from the maleimide and released during the conjugation.

In comparison to the sCT-polyPEG conjugate the sCT-poly(mannose) conjugates have much smaller retention times by RP-HPLC analysis due to the hydrophilic nature of the multiple hydroxyl groups on sugars being much less likely to interact with the long alkyl chain substituents within the HPLC column. From the chromatogram the unconjugated polymer appears at retention time $t = 9.8$ minutes (DP_n 20) / 8.4 minutes (DP_n 40) shifting by a few

minutes to a slightly longer retention time after conjugation onto sCT (DP_n 20: $t = 10.9$ minutes / DP_n 40 $t = 10.6$ minutes) (figure 5.31).

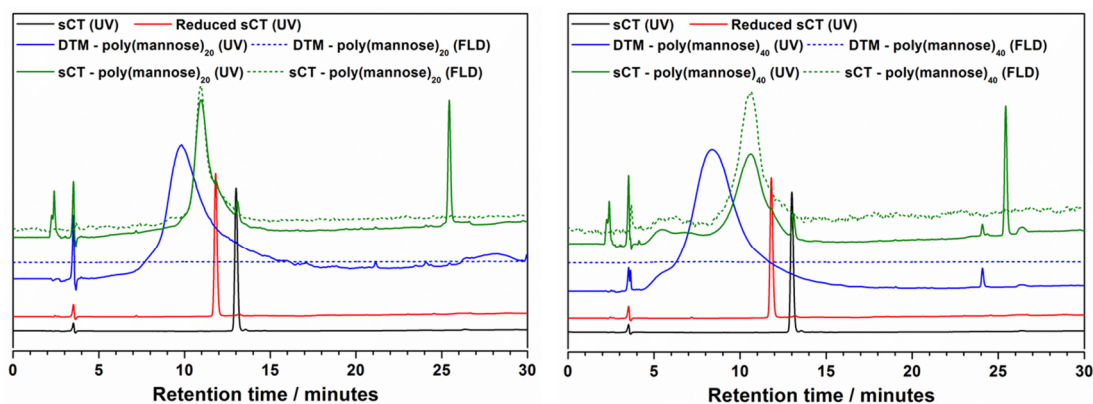


Figure 5.31. RP-HPLC analysis of conjugation of dithiophenolmaleimide poly(mannose) onto salmon calcitonin (UV $\lambda = 280$ nm; FLD λ_{ex} : 341 nm, λ_{em} : 502 nm).

The conjugation of polyPEG onto sCT occurred in a very similar manner, with a shift in retention time of the broad peak relating to the polymer after conjugation and the appearance of coincidental fluorescence (figure 5.32). These results were also very comparable to the conjugation of polyPEG onto oxytocin described in chapter 3, showing that this procedure is applicable to more than one disulfide bond containing peptide, with the polymers and conjugates appearing at similar positions in the RP-HPLC spectrum.

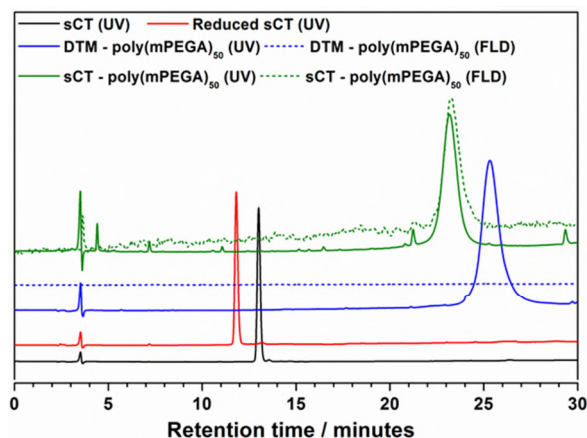


Figure 5.32. RP-HPLC analysis of conjugation of dithiophenolmaleimide poly(mPEGA₄₈₀)₅₀ onto salmon calcitonin.

The conjugation of these polymers onto sCT has much higher reaction efficiency than the reactions previously observed for the disulfide bridging of oxytocin, and after 24 hours there was a severe reduction in the native peptide peak. This is likely due to the structural differences between the two peptides, in oxytocin a reduction of the disulfide bond loses all structure for the small (9 amino acid) peptide, whereas in sCT the presence of the α helix maintains some of the structural integrity, allowing for easier disulfide bridging conjugation. The sCT-glycopolymer and sCT-PEG conjugates were purified by dialysis (water, 3 days, 1 kDa MWCO), and after lyophilisation the resulting products were a much lighter yellow colour compared to the intense yellow unconjugated polymers. Fluorescence spectroscopy was carried out on all three of the conjugates revealing the excitation and emission wavelengths post conjugation. Initially the excitation wavelength was set to that of the fluorescence detector on the HPLC (λ_{ex} : 341 nm), as this showed a highly increased level of fluorescence post conjugation in comparison to the native polymer (figure 5.33).

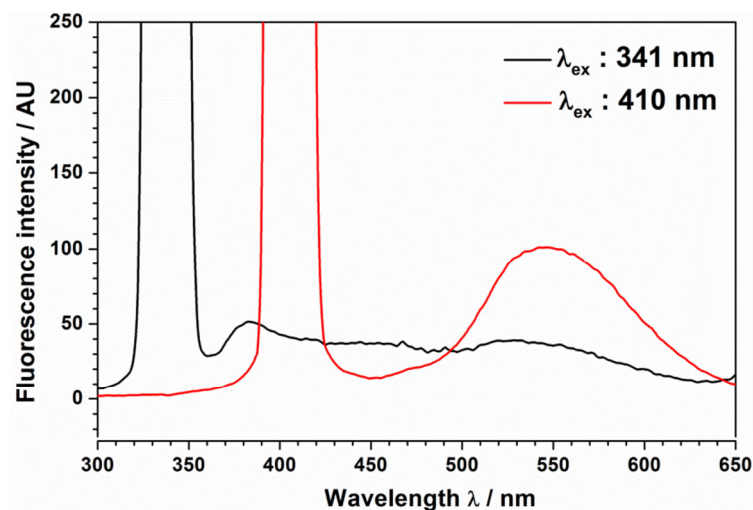


Figure 5.33. Fluorescence spectra of sCT-poly(mannose)₂₀ with excitation at λ_{ex} = 341 nm and λ_{ex} = 410 nm.

Although a minor peak was observed in the region expected (500 -550 nm), the intensity of fluorescence emitted was not particularly prominent, and thus some different excitation

wavelengths were investigated. When the excitation wavelength was $\lambda_{\text{ex}} = 410$ nm this trebled the observed emitted fluorescence, further clarifying that the polymer conjugates do exhibit the fluorescent behaviour previously described for maleimide insertions into the disulfide bond for sCT. The emission spectra were run for the three polymer conjugate (two glycopolymers and polyPEG) with this excitation wavelength ($\lambda_{\text{ex}} : 410$ nm), which revealed different maximal emissions (but within the same region) for the polymer conjugates. Excitation spectra performed using the wavelengths revealed maximal excitation wavelengths between 410 - 415 nm, highlighting that the fluorescence behaviour was similar for the polymer conjugates regardless of the monomer (figure 5.34).

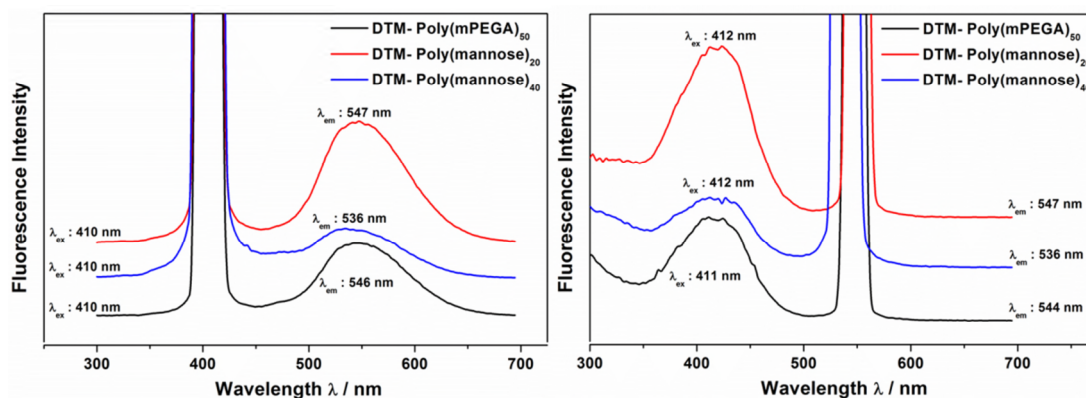


Figure 5.34. Emission ($\lambda_{\text{ex}} = 410$ nm) and excitation ($\lambda_{\text{em}} = 536 - 547$ nm) spectra of sCT polymer conjugates.

5.3.3. Glycopolymer conjugates conclusions

An acrylate monomer containing mannose functionality was synthesised and could be directly polymerised using copper mediated controlled radical polymerisation in DMSO utilising an initiator capable of efficient conjugation. This resulted in α -end dithiophenolmaleimide functionality on the polymer capable of undergoing post polymerisation disulfide bridging peptide conjugation, with pendant sugar functionality along the polymer. The polymers were conjugated onto a model peptide, salmon

calcitonin, using disulfide targeted maleimide bridging chemistry, resulting in glycopolymer- peptide conjugates. The conjugations were monitored by RP-HPLC which confirmed the appearance of fluorescence post conjugation, which was further monitored by fluorescence spectroscopy and provides a smart labelling tool and confirmation of conjugation.

5.4. Chapter 5 conclusions

Various different monomers are available that can be used in the synthesis of polymers with a wide variety of properties or functions. The α -end group functionality can be easily designated with desired functionality able to undergo post-polymerisation grafting onto a desired protein or peptide. This chapter has described the synthesis of three different classes of polymers that can have benefits in pharmaceuticals for therapeutics. Whether the targeted function is for PEG alternatives in the use of similar (and biocompatible) macromonomers, in drug delivery or nanoparticle type assemblies, or for specific targeting with a more biological function in mind, different approaches can be designed.

Using the polymer synthesis and conjugation approaches introduced in chapters 2 & 3, any of these polymers can easily be incorporated with α -end group functionality for the specific targeting of amine groups at the *N*-terminus or on lysine groups and thiol targeting of cysteine residues, whether native or with first the reduction of the disulfide bond. All polymer synthesis remained controlled, leading to narrow molecular weight distributions for polymers, although sometimes polymerisation system optimisation is required. This leads to polymers of targeted molecular weights, with α -end functionality and repeat units designed with targeted functions and applications. After conjugation various techniques are available for characterisation of peptide polymer conjugates, when certain analyses may not be accessible.

5.5. Experimental

5.5.1. Materials

Oxytocin (c-[Cys-Tyr-Ile-Gln-Asn-Cys]-Pro-Leu-Gly-NH₂) was gifted from PolyPeptide laboratories (Hillerød, Denmark) and used as received.

Copper(0) wire was pre-treated by washing in hydrochloric acid (35%) for 20 min, then rinsed with water and dried under nitrogen immediately prior to use. *N,N,N',N',N'',N''*-Hexamethyl-[tris(aminoethyl)amine] (Me₆-TREN) and *N,N,N',N',N'',N''*-pentamethyldiethylenetriamine (PMDETA) were synthesised according to a previously reported procedure and stored at -18 °C prior to use.⁷⁷ Cu(I)Br and Cu(I)Cl were purified according to the method of Keller.⁷⁸ WSI was synthesised according to a literature procedure.³³ Oligo(2-ethyl-2-oxazoline)methacrylate monomer (OEtOxMA) ($DP_n = 5$, $M_n = 600 \text{ g mol}^{-1}$, $\bar{D} = 1.21$) was synthesised within our group by CROP, by Dr Kristian Kempe according to a literature procedure.²² Protected aldehyde initiator and dithiophenolmaleimide initiator were synthesised as described in earlier chapters. Alkyne mannose was synthesised within our group according to a previously reported procedure.⁷³

5.5.2. Instrumentation & Analysis

Nuclear magnetic resonance (NMR) spectra were acquired with a Bruker DPX-300, Bruker DPX-400, Bruker HD-300 and Bruker HD-400 spectrometers with samples prepared in deuterated solvents (CDCl₃, δ₆-DMSO, or D₂O) and chemical shifts were reported in parts per million (ppm) with reference to solvent residual peaks.

Size exclusion chromatography (SEC) was performed on either 1) Agilent Polymer Laboratories GPC50 eluting with DMF (0.1 w/v % LiBr) at 50°C, 1 ml min⁻¹ flow rate, fitted with differential refractive index and UV detectors, 2 x PLgel 5 mm mixed D columns (300 x 7.5 mm), 1 x PLgel 5 mm guard column (50 x 7.5 mm) and autosampler; 2) Varian 390-LC system using DMF (5 mM NH₄BH₄) eluent at 50 °C, 1 ml min⁻¹ flow rate, equipped with RI, UV, light scattering and viscometry detectors, 2 x PLgel 5 mm mixed D columns (300 x 7.5 mm), 1 x PLgel 5 mm guard column (50 x 7.5 mm) and autosampler DMF 3) Varian 390-LC system eluting with CHCl₃ (2 % TEA v/v) at 30 °C, 1 ml min⁻¹ flow rate, equipped with refractive index, UV, viscometry and light scattering detectors, 2 x PLgel 5 mm mixed C columns (300 x 7.5 mm), 1 x PLgel 5mm guard column (50 x 7.5 mm) and autosampler. All molecular weights were calculated relative to narrow PMMA standards (550 – 955,000 g mol⁻¹) and fitted with a 3rd order polynomial. All samples were passed through 0.2 µm filters prior to analysis.

Infrared absorption spectra were recorded on a Bruker VECTOR-22 FTIR spectrometer using a Golden Gate diamond attenuated total reflection cell.

UV/Vis spectra were recorded on Agilent Technologies Cary 60 UV-Vis using a quartz cuvette with 10 mm optical length within the range 200 nm – 600 nm. Cloud point temperature measurements were recorded on Agilent Technologies Cary 60 UV-Vis at a wavelength of 500nm using a quartz cuvette with a 1 cm path length. The polymers were dissolved in PBS or water at concentrations of 5 mg ml⁻¹ or 1 mg ml⁻¹ and were heated and cooled between 20 – 90 °C at a rate of 1 °C min⁻¹ while stirring at 1200 rpm. The cloud point was determined as the temperature at 50 % transmittance on the third heating cycle. Fluorescence spectra were collected on a PerkinElmer LS 55 Fluorescence Spectrometer.

Analytical high performance liquid chromatography (HPLC) was performed on Agilent 1260 infinity series stack equipped with an Agilent 1260 binary pump and degasser. 50 µl

samples were injected using Agilent 1260 autosampler with a flow rate of 1 ml/min. The HPLC was fitted with a Phenomenex Luna C18 column (250 x 4.6 mm) with 5 micron packing (100Å). Detection was achieved using an Agilent 1260 variable wavelength detector monitoring at 280 nm. Mobile phase A consisted of either 100 % water containing 0.04 % TFA as an additive or 90 % water, 10 % acetonitrile containing 0.04 % TFA as an additive. Mobile Phase B consisted of 100 % acetonitrile containing 0.04 % TFA as an additive. The column was equilibrated by washing with the starting % of mobile phase A for 10 minutes prior to injection for all conditions. The method gradient (1) HPLC analysis: 90 % mobile phase A decreasing to 40 % mobile phase A over 27 minutes, and remaining at 40% mobile phase A for 8 minutes, before resetting to the starting conditions in 1 minute, and remaining in these conditions for at least 10 minutes to re-equilibrate the column before subsequent injections. The method gradient (2) HPLC analysis: 95 % mobile phase A decreasing to 80 % mobile phase A across 15 minutes, and to 40 % mobile phase A at 22 minutes and remaining at 40% mobile phase A for 5 minutes, before resetting to the starting conditions in 1 minute, and remaining in these conditions for at least 10 minutes to re-equilibrate the column before subsequent injections.

5.5.3. Synthetic Procedures

5.5.3.1. Poly(ethylene glycol) alternatives

Polymerisation of OEtOxMA with WSI or PALD initiator

To an oven dried Schlenk tube fitted with a magnetic stirring bar and rubber septum was added Cu(I)Cl (0.8 eq.), PMDETA (0.8 eq.), NaCl (0.234 g, 4 mmol) and H₂O (0.5 ml). Separately to a vial fitted with a rubber septum was added initiator (1 eq.), OEtOxMA monomer (400 mg, DP_n eq.), MeOH (1 ml) and H₂O (1 ml). Both solutions were allowed to

deoxygenate with nitrogen for 20 minutes, before the monomer/initiator solution was cannulated into the Schlenk tube and the reaction left to polymerise at 25 °C. After 24 hours samples were removed, and the solvent allowed to evaporate before dilution with CDCl₃ for ¹H NMR analysis and CHCl₃ for SEC analysis. Polymers were purified by dialysis against water (1 kDa MWCO, 3 days).

Deprotection of PALD poly(OEtOxMA)

Acetal functional polymers (250 mg) were deprotected by stirring in aqueous solutions of trifluoroacetic acid (50 % v/v, 15 ml) for 3 days. Polymers were purified by dialysis against water (1 kDa MWCO, 3 days).

Reductive amination conjugation onto oxytocin of poly(OEtOxMA)

Reductive amination conjugation was performed by separately dissolving aldehyde functional polymer (e.g. poly(OEtOxMA)₂₀, 71.5 mg, 6.0 μmol, 1.5 Eq.) and oxytocin (4 mg, 4.0 μmol, 1 Eq.) in phosphate buffer (pH 6.2, 0.1 M) and adding the solutions together at 25 °C, with a freshly prepared solution of NaCNBH₃ (0.25 ml, 40 mM, 2.5 Eq.) (for an overall oxytocin concentration of 2 mM). After 4 days a sample was removed for RP-HPLC monitoring. Following conjugation samples were purified by dialysis against water (1 kDa MWCO, 3 days).

Schiff base conjugation onto oxytocin of poly(OEtOxMA)

Schiff base conjugation was performed by separately dissolving aldehyde functional polymer (e.g. poly(OEtOxMA)₂₀, 71.5 mg, 6.0 μmol, 1.5 Eq.) and oxytocin (4 mg, 4.0 μmol, 1 Eq.) in phosphate buffer (pH 6.2, 0.1 M) and adding the solutions together at 25 °C. After 1 and 4 days a sample was removed for RP-HPLC monitoring. Following conjugation samples were purified by dialysis against water (1 kDa MWCO, 3 days).

Reversibility studies of Schiff base linked oxytocin-poly(OEtOxMA)

Schiff base conjugates were dissolved in buffer (pH 5 citrate buffer or pH 7.4 phosphate buffer, 5 mg ml⁻¹) and left stirring (ambient temperature or 37 °C) before RP-HPLC monitoring at t = 4 days and t = 14 days.

Thermal degradation of oxytocin-poly(OEtOxMA)

The conjugates alongside native oxytocin were separately dissolved in water (in triplicate) before placing in an oven at 80 °C for 24 hours. The samples were monitored by RP-HPLC for changes in concentration compared to a t = 0 sample.

5.5.3.2. Thermoresponsive polymers for peptide conjugation

Example thermoresponsive polymer synthesis in cosolvent system

Cu(I)Br and Me₆TREN were added to H₂O (0.75 ml) and degassed under nitrogen flow. Monomer(s) and initiator (WSI, EBiB or DTM) were added to an organic cosolvent (4 ml) with H₂O (0.25 ml) and degassed under nitrogen flow. After 20 minutes the two solutions were added together and allowed to polymerise at room temperature. After 24 hours samples were removed for ¹H NMR conversion analysis and SEC molecular weight data. Polymers were purified by dialysis against water (3 days, 1 kDa MWCO).

Example polymer conjugation without purification onto disulfide containing peptide

To the native peptide (5 mg, 5 μmol) in water was added TCEP (1.8 mg, 7.5 μmol), and the solution allowed to stir for 2.5 hours. After complete disulfide bond reduction was observed (by RP-HPLC) the dithiophenolmaleimide polymers were added directly as an aliquot of polymerisation solution (1.5 equivalents). After 24 hours an aliquot was removed for RP-HPLC analysis of UV and fluorescence.

Example polymer conjugation onto disulfide containing peptide

To the native peptide (5 mg, 5 μ mol) in water was added TCEP (1.8 mg, 7.5 μ mol), and the solution allowed to stir for 2.5 hours. After complete disulfide bond reduction was observed (by RP-HPLC) the dithiophenolmaleimide polymers were added (1.5 equivalents). After 24 hours an aliquot was removed for RP-HPLC analysis of UV and fluorescence.

Example 'in-situ' polymer conjugation onto disulfide containing peptide

To the native peptide (5 mg, 5 μ mol) in water was added the purified dithiophenolmaleimide polymer (1.5 eq.), and the solution allowed to stir 10 minutes. TCEP(1.8 mg, 7.5 μ mol) was then added and after 24 hours an aliquot was removed for RP-HPLC analysis of UV and fluorescence.

5.5.3.3. Glycopolymers

Mannose glycomonomer

To a mixture of alkyne sugar (2.33 g, 10.7 mmol) and 3-azidopropyl acrylate (2 g, 12.9 mmol) in H₂O:MeOH (1:2, 75 ml), CuSO₄·5H₂O (0.201 g, 8.1 g) and sodium L-ascorbate (0.212 g, 10.7 mmol) were sequentially added. The mixture was stirred for 24 hours at ambient temperature after which the methanol was removed under reduced pressure and the mixture freeze dried for removal of water. The resulting green compound was dissolved in methanol and purified by silica column chromatography (methanol: dichloromethane 1:10). The volatiles were removed under reduced pressure resulting in an off-white solid (2.28g, 6.11 mmol, 57%).

^1H NMR (MeOD, 300.1 MHz) δ (ppm): 2.30 (2H, m, $\text{N}_3\text{-CH}_2\text{CH}_2$), 3.50 – 3.78 (5H, overlapped mannose CH), 4.19 (2H, t, $J = 6.0$ Hz, $\text{N}_3\text{CH}_2\text{CH}_2\text{CH}_2$), 4.54 (2H, t, $J = 6.8$ Hz, N_3CH_2), 4.64–4.80 (2 H, overlap H_2O , CH_2O), 5.90 (1 H, dd, $J = 1.5, 9.0$ Hz, HC=CH_2), 6.13 (1 H, q, $J = 7.2, 10.2$ Hz, HC=CH_2), 6.37 (1H, dd, $J = 1.9, 15.4$ Hz, HC=CH_2), 8.05 (1H, s, NCH=C); ^{13}C NMR (75.4 MHz, MeOD): 30.5 ($\text{N}_3\text{-CH}_2\text{CH}_2$), 54.9 ($\text{N}_3\text{-CH}_2\text{CH}_2$), 60.8 ($\text{N}_3\text{-CH}_2\text{CH}_2\text{CH}_2$), 62.8 (CH_2OH), 63.1 (OCH_2CHN_3), 68.8, 72.2, 72.6, 75.1 (mannose), 100.8, 100.9 (α , β anomers of mannose), 125.7 (N-CH=C), 129.4 ($\text{CH}_2=\text{C}$), 132.0 ($\text{CH}_2=\text{C}$), 145.5 (N-CH=C), 167.6 (C=O);

FT-IR (cm^{-1}): 3335 (ν_{OH}), 2890 ($\nu_{\text{C-H}}$), 1717 ($\nu_{\text{C=O}}$), 1194 ($\nu_{\text{C-O}}$); ESI-MS m/z : calculated for $\text{C}_{15}\text{H}_{23}\text{N}_3\text{O}_8$ ($\text{M} + \text{Na}$) $^+$ 396.1, found 396.1;

Synthesis of DTM functional poly(mannose) or polyPEG

Mannose glycomonomer (373 mg, 1 mmol) was dissolved in 1 ml DMSO and dithiophenolmaleimide initiator (30 mg, 50 μmol), CuBr_2 (1.12 mg, 5 μmol) and Me6TREN (2.4 μl , 9 μmol) were sequentially added. The solution was degassed with nitrogen for 30 minutes and stayed an orange-yellow colour. A stirrer bar wrapped with activated copper wire was added to initiate polymerisation and the flask sealed. The reaction was allowed to run overnight before a sample was taken *via* degassed syringe and dissolved in δ -DMSO for NMR analysis and DMF for SEC molecular weight data. The resultant polymer was dialysed (MWCO, 1 kDa) against water for 3 days, before the solution was freeze dried yielding a yellow powder.

Conjugation of glycopolymers and PEG onto salmon calcitonin

Salmon Calcitonin (sCT) (2 mg, 0.58 μmol) was dissolved in 300 μl of H_2O along with *tris*(2-carboxyethyl)phosphine (TCEP) (0.2 mg, 0.64 μmol). Upon reduction of disulfide bond (30 minutes) monitored by RP-HPLC, phosphate buffer (2 ml, pH 6.2, 100 mM) was added to the solution followed by the dithiophenolmaleimide functional polymer ($M_n = 6.5$ kDa) (4.2 mg, 0.64 μmol) dissolved in 1 ml of the same buffer. The solution was left to stir for 20

minutes before a sample was taken for RP-HPLC, which showed the formation of a new product, as well as showing a fluorescence response.

5.6. References

- 1 S. N. S. Alconcel, A. S. Baas and H. D. Maynard, *Polym. Chem.*, 2011, **2**, 1442–1448.
- 2 R. B. Greenwald, Y. H. Choe, J. McGuire and C. D. Conover, *Adv. Drug Deliv. Rev.*, 2003, **55**, 217–250.
- 3 F. M. Veronese and A. Mero, *BioDrugs*, 2008, **22**, 315–329.
- 4 A. Bendele, J. Seely, C. Richey, G. Sennello and G. Shopp, *Toxicol. Sci.*, 1998, **42**, 152–157.
- 5 P. Caliceti and F. M. Veronese, *Adv. Drug Deliv. Rev.*, 2003, **55**, 1261–1277.
- 6 O. B. Kinstler, D. N. Brems, S. L. Lauren, A. G. Paige, J. B. Hamburger and M. J. Treuheit, *Pharm. Res.*, 1996, **13**, 996–1002.
- 7 F. M. Veronese, *Biomaterials*, 2001, **22**, 405–417.
- 8 A. P. Chapman, *Adv. Drug Deliv. Rev.*, 2002, **54**, 531–545.
- 9 K. Knop, R. Hoogenboom, D. Fischer and U. S. Schubert, *Angew. Chemie*, 2010, **49**, 6288–6308.
- 10 C. Li and S. Wallace, *Adv. Drug Deliv. Rev.*, 2008, **60**, 886–898.
- 11 B. Romberg, J. M. Metselaar, L. Baranyi, C. J. Snel, R. Bünger, W. E. Hennink, J. Szebeni and G. Storm, *Int. J. Pharm.*, 2007, **331**, 186–189.
- 12 R. K. Kainthan and D. E. Brooks, *Bioconjug. Chem.*, 2008, **19**, 2231–2238.
- 13 K. Maruyama, S. Okuizumi, O. Ishida, H. Yamauchi, H. Kikuchi and M. Iwatsuru, *Int. J. Pharm.*, 1994, **111**, 103–107.
- 14 R. Hoogenboom, *Angew. Chemie*, 2009, **48**, 7978–7994.
- 15 R. Luxenhofer, Y. Han, A. Schulz, J. Tong, Z. He, A. V Kabanov and R. Jordan, *Macromol. Rapid Commun.*, 2012, **33**, 1613–1631.
- 16 O. Sedlacek, B. D. Monnery, S. K. Filippov, R. Hoogenboom and M. Hruby, *Macromol. Rapid Commun.*, 2012, **33**, 1648–1662.
- 17 V. P. Torchilin, M. I. Shtilman, V. S. Trubetskoy, K. Whiteman and A. M. Milstein, *BBA - Biomembr.*, 1994, **1195**, 181–184.
- 18 M. Sairam, V. R. Babu, B. V. K. Naidu and T. M. Aminabhavi, *Int. J. Pharm.*, 2006, **320**, 131–136.

- 19 Z.-B. Zheng, G. Zhu, H. Tak, E. Joseph, J. L. Eiseman and D. J. Creighton, *Bioconjug. Chem.*, 2005, **16**, 598–607.
- 20 R. Duncan, *Nat. Rev. Cancer*, 2006, **6**, 688–701.
- 21 K. Aoi and M. Okada, *Prog. Polym. Sci.*, 1996, **21**, 151–208.
- 22 S. Kobayashi, E. Masuda, S. Shoda and Y. Shimano, *Macromolecules*, 1989, **22**, 2878–2884.
- 23 D. Gieseler and R. Jordan, *Polym. Chem.*, 2015, **6**, 4678–4689.
- 24 C. Weber, C. R. Becer, A. Baumgaertel, R. Hoogenboom and U. S. Schubert, *Des. Monomers Polym.*, 2009, **12**, 149–165.
- 25 C. Weber, C. R. Becer, R. Hoogenboom and U. S. Schubert, *Macromolecules*, 2009, **42**, 2965–2971.
- 26 J. Bühler, S. Gietzen, A. Reuter, C. Kappel, K. Fischer, S. Decker, D. Schäffel, K. Koynov, M. Bros, I. Tubbe, S. Grabbe and M. Schmidt, *Chem. Eur. J.*, 2014, **20**, 12405–12410.
- 27 C. Weber, J. A. Czaplewska, A. Baumgaertel, E. Altuntas, M. Gottschaldt, R. Hoogenboom and U. S. Schubert, *Macromolecules*, 2012, **45**, 46–55.
- 28 A. Simula, V. Nikolaou, F. Alsubaie, A. Anastasaki and D. M. Haddleton, *Polym. Chem.*, 2015, **6**, 5940–5950.
- 29 Q. Zhang, P. Wilson, Z. Li, R. Mchale, J. Godfrey, A. Anastasaki, C. Waldron and D. M. Haddleton, *J. Am. Chem. Soc.*, 2013, **135**, 7355–7363.
- 30 F. Alsubaie, A. Anastasaki, V. Nikolaou, A. Simula, G. Nurumbetov, P. Wilson, K. Kempe and D. M. Haddleton, *Macromolecules*, 2015, **48**, 6421–6432.
- 31 A. Simula, A. Anastasaki and D. M. Haddleton, *Macromol. Rapid Commun.*, 2015, **37**, 356–361.
- 32 N. V. Tsarevsky, T. Pintauer and K. Matyjaszewski, *Macromolecules*, 2004, **37**, 9768–9778.
- 33 S. Perrier, S. P. Armes, X. S. Wang, F. Malet and D. M. Haddleton, *J. Polym. Sci. Part A Polym. Chem.*, 2001, **39**, 1696–1707.
- 34 L. Tao, G. Mantovani, F. Lecolley and D. M. Haddleton, *J. Am. Chem. Soc.*, 2004, **126**, 13220–13221.
- 35 B. Podobnik, B. Helk, V. Smilović, S. Škrajnar, K. Fidler, S. Jevševar, A. Godwin and P. Williams, *Bioconjug. Chem.*, 2015, **26**, 452–459.
- 36 C. Weber, R. Hoogenboom and U. S. Schubert, *Prog. Polym. Sci.*, 2012, **37**, 686–714.
- 37 E. Cabane, X. Zhang, K. Langowska, C. G. Palivan and W. Meier, *Biointerphases*, 2012, **7**, 1–27.
- 38 D. Roy, J. N. Cambre and B. S. Sumerlin, *Prog. Polym. Sci.*, 2010, **35**, 278–301.
- 39 A. S. Hoffman, *Adv. Drug Deliv. Rev.*, 2013, **65**, 10–16.

- 40 M. A. C. Stuart, W. T. S. Huck, J. Genzer, M. Müller, C. Ober, M. Stamm, G. B. Sukhorukov, I. Szleifer, V. V Tsukruk, M. Urban, F. Winnik, S. Zauscher, I. Luzinov and S. Minko, *Nat. Mater.*, 2010, **9**, 101–113.
- 41 A. Gandhi, A. Paul, S. O. Sen and K. K. Sen, *Asian J. Pharm. Sci.*, 2015, **10**, 99–107.
- 42 M. A. Ward and T. K. Georgiou, *Polymers (Basel)*, 2011, **3**, 1215–1242.
- 43 I. Cobo, M. Li, B. S. Sumerlin and S. Perrier, *Nat. Mater.*, 2015, **14**, 143–159.
- 44 S. Fujishige, K. Kubota and I. Ando, *J. Phys. Chem.*, 1989, **93**, 3311–3313.
- 45 H. G. Schild, *Prog. Polym. Sci.*, 1992, **17**, 163–249.
- 46 M. Heskins and J. E. Guillet, *J. Macromol. Sci. Part A - Chem.*, 1968, **2**, 1441–1455.
- 47 G. Vancoillie, D. Frank and R. Hoogenboom, *Prog. Polym. Sci.*, 2014, **39**, 1074–1095.
- 48 J.-F. Lutz, O. Akdemir and A. Hoth, *J. Am. Chem. Soc.*, 2006, **128**, 13046–13047.
- 49 Z. Ding, R. B. Fong, C. J. Long, P. S. Stayton and A. S. Hoffman, *Nature*, 2001, **411**, 59–62.
- 50 G. Chen and A. S. Hoffman, *Bioconjug. Chem.*, 1993, **4**, 509–514.
- 51 J.-F. Lutz, S. Pfeifer and Z. Zarafshani, *QSAR Comb. Sci.*, 2007, **26**, 1151–1158.
- 52 J.-F. Lutz and A. Hoth, *Macromolecules*, 2006, 893–896.
- 53 K. Skrabania, J. Kristen, A. Laschewsky, O. Akdemir, A. Hoth and J.-F. Lutz, *Langmuir*, 2007, **23**, 84–93.
- 54 C. Boyer, M. R. Whittaker, M. Luzon and T. P. Davis, *Macromolecules*, 2009, **42**, 6917–6926.
- 55 C. Boyer, M. R. Whittaker, K. Chuah, J. Liu and T. P. Davis, *Langmuir*, 2010, **22**, 2721–2730.
- 56 C. Waldron, Q. Zhang, Z. Li, V. Nikolaou, G. Nurumbetov, J. Godfrey, R. McHale, G. Yilmaz, R. K. Randev, M. Girault, K. McEwan, D. M. Haddleton, M. Driesbeke, A. J. Haddleton, P. Wilson, A. Simula, J. Collins, D. J. Lloyd, J. A. Burns, C. Summers, C. Houben, A. Anastasaki, M. Li, C. R. Becer, J. K. Kiviahio and N. Risangud, *Polym. Chem.*, 2014, **5**, 57–61.
- 57 F. Alsubaie, A. Anastasaki, P. Wilson and D. M. Haddleton, *Polym. Chem.*, 2015, **6**, 406–417.
- 58 Q. Zhang, Z. Li, P. Wilson and D. M. Haddleton, *Chem. Commun.*, 2013, **49**, 6608–6610.
- 59 F. F. Schumacher, M. Nobles, C. P. Ryan, M. E. B. Smith, A. Tinker, S. Caddick and J. R. Baker, *Bioconjug. Chem.*, 2011, **22**, 132–136.
- 60 M. W. Jones, R. A. Strickland, F. F. Schumacher, S. Caddick, J. R. Baker, M. I. Gibson and D. M. Haddleton, *J. Am. Chem. Soc.*, 2012, **134**, 1847–1852.
- 61 M. W. Jones, R. A. Strickland, F. F. Schumacher, S. Caddick, J. R. Baker, M. I.

-
- Gibson and D. M. Haddleton, *Chem. Commun.*, 2012, **48**, 4064–4066.
- 62 L. M. Tedaldi, A. E. Aliev and J. R. Baker, *Chem. Commun.*, 2012, **48**, 4725–4727.
- 63 D. Bontempo and H. D. Maynard, *J. Am. Chem. Soc.*, 2005, **127**, 6508–6509.
- 64 R. Narain, A. Housni, G. Gody, P. Boullanger, M. T. Charreyre and T. Delair, *Langmuir*, 2007, **23**, 12835–12841.
- 65 V. Vázquez-Dorbatt and H. D. Maynard, *Biomacromolecules*, 2006, **7**, 2297–2302.
- 66 X. L. Sun, K. M. Faucher, M. Houston, D. Grande and E. L. Chaikof, *J. Am. Chem. Soc.*, 2002, **124**, 7258–7259.
- 67 S.-G. Lee, J. M. Brown, C. J. Rogers, J. B. Matson, C. Krishnamurthy, M. Rawat and L. C. Hsieh-Wilson, *Chem. Sci.*, 2010, **1**, 322–325.
- 68 J. Lee, E.-W. Lin, U. Y. Lau, J. L. Hedrick, E. Bat and H. D. Maynard, *Biomacromolecules*, 2013, **14**, 2561–2569.
- 69 R. J. Mancini, J. Lee and H. D. Maynard, *J. Am. Chem. Soc.*, 2012, **134**, 8474–8479.
- 70 J. Geng, G. Mantovani, L. Tao, J. Nicolas, G. Chen, R. Wallis, D. A. Mitchell, B. R. G. Johnson, S. D. Evans and D. M. Haddleton, *J. Am. Chem. Soc.*, 2007, **129**, 15156–15163.
- 71 T. Lipinski, P. I. Kitov, A. Szpacenko, E. Paszkiewicz and D. R. Bundle, *Bioconjug. Chem.*, 2011, **22**, 274–281.
- 72 H. Shi, L. Liu, X. Wang and J. Li, *Polym. Chem.*, 2012, **3**, 1182–1188.
- 73 Q. Zhang, J. Collins, A. Anastasaki, R. Wallis, D. A. Mitchell, C. R. Becer and D. M. Haddleton, *Angew. Chemie Int. Ed.*, 2013, **52**, 4435–4439.
- 74 B. Roy and B. Mukhopadhyay, *Tetrahedron Lett.*, 2007, **48**, 3783–3787.
- 75 B. S. Sumerlin, N. V. Tsarevsky, G. Louche, R. Y. Lee and K. Matyjaszewski, *Macromolecules*, 2005, **38**, 7540–7545.
- 76 M. P. Robin, P. Wilson, A. B. Mabire, J. K. Kiviaho, J. E. Raymond, D. M. Haddleton and R. K. O'Reilly, *J. Am. Chem. Soc.*, 2013, **135**, 2875–2878.
- 77 M. Ciampolini and N. Nardi, *Inorg. Chem.*, 1966, **5**, 41–44.
- 78 R. N. Keller, H. D. Wycoff and L. E. Marchi, in *Inorganic Syntheses*, McGraw-Hill Book Company, Inc, 1946, vol. 2, pp. 1–4.
-

6. *Overview and outlook*

Throughout this thesis the general theme has been on the synthesis of peptide-polymer conjugates, utilising a variety of the different conjugation chemistries that have previously been described. The overall aim was to influence the properties (and specifically the shelf-life stability) of the small peptide therapeutic oxytocin. The conjugation techniques described have utilised the reactions at both amino (in this case found specifically at the *N*-terminal amine) and thiol (from a reduction of the disulfide bond) functionalities in a site-specific manner. Very little polymer modification research has previously been applied to oxytocin, particularly with an aim to improving the stability of aqueous formulations and as such these previously well-reported strategies were employed with investigations of the conjugation chemistries and effect this might have on enhancements in stability.

Throughout this work, in general the focus has been on the PEGylation of oxytocin, due to the multitude of advantages that PEG exhibits, which has previously led to PEGylated products being FDA approved. There are two different architectures of polymers described throughout this thesis, which allow easy comparisons between the effect that the PEG density may have on the conjugation efficiency and on the conjugate characteristics. A variety of linear PEGs are easily, and at relatively low cost, available commercially (or from simple synthesis procedures), which allow the attachment of polymers onto the peptide using straightforward conjugation chemistries.

Comb polymers can be synthesised by copper mediated polymerisation under various conditions (specifically using different (co)solvents and copper sources) resulting in polymers with narrow dispersity and tuned molecular weights. By utilising a PEG acrylate monomer the resulting 'comb' PEG polymers, are comparable to their linear counterparts.

Depending on the desired site of conjugation (amino or thiol), the initiator can be modified to allow the simple incorporation of the α -end functionality capable of undertaking the conjugation approaches utilised in the linear polymers.

Following on from the synthesis of a variety of oxytocin-PEG conjugates, the effect of conjugation was assessed in terms of thermal stability of aqueous solutions, uterotonic testing and effect on cell proliferation of cancer cells. Overall the stability improvements post-conjugation surpassed expectations, with the 'comb' PEG conjugates showing very limited degradations under the highly thermally stressed stability assay. The addition of a variety of different non-conjugated excipients into the solutions, although showing some improvements in stability did not show near the level of promise exhibited by the conjugates, promoting the covalent attachment as important in enhancing stability.

A lack of valid and definitive biological activity is disappointing, as the retained uterotonic activity of the conjugates compared to the native peptide is vital in confirming the applicability of this chemistry. If any activity was remaining post-conjugation this would be a large improvement over the native degraded peptide, which shows a complete absence of activity.

Following on from the successful conjugations of PEG and polyPEG at two different positions on oxytocin the scope of the project was again widened. The development of suitable polymerisation conditions with different initiators/solvents the systems could easily be adapted for the synthesis of a variety of different monomers to suit certain purposes or applications. This can further be expanded to a wider range of functional monomers or different initiators, for the synthesis of a larger library of different oxytocin conjugates, altering the peptide properties although attaining biological data is of vital importance for the expansion of this work.

Publications of results in this thesis

1. In Situ Conjugation of Dithiophenol Maleimide Polymers and Oxytocin for Stable and Reversible Polymer–Peptide Conjugates
Jennifer Collins, Joji Tanaka, Paul Wilson, Kristian Kempe, Thomas P. Davis, Michelle P. McIntosh, Michael R. Whittaker, and David M. Haddleton.
Bioconjugate Chemistry, 2015, **26**, 633-638
2. Stability Enhancing N -Terminal PEGylation of Oxytocin Exploiting Different Polymer Architectures and Conjugation Approaches
Jennifer Collins, Kristian Kempe, Paul Wilson, Claudia A. Blindauer, Michelle P. McIntosh, Thomas P. Davis, Michael R. Whittaker, and David M. Haddleton.
Biomacromolecules, 2016, **17**, 2755-2766
3. Comb Poly(Oligo(2-Ethyl-2-Oxazoline)Methacrylate)-Peptide Conjugates Prepared by Aqueous Cu(0)-Mediated Polymerization and Reductive Amination
Jennifer Collins, Sacha J. Wallis, Alexandre Simula, Michael R. Whittaker, Michelle P. McIntosh, Paul Wilson, Thomas P. Davis, David M. Haddleton and Kristian Kempe.
Macromolecular Rapid Communications, 2016, DOI:10.1002/marc.201600534